NASA TECHNICAL
TRANSLATION
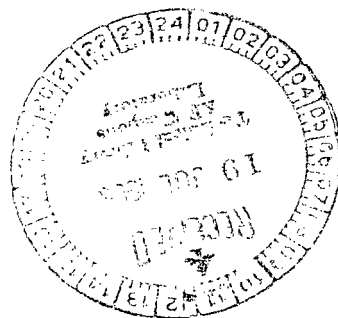
OBSERVATIONS OF THE MOON,
MARS, URANUS, AND THE STARS

OPTICAL PROPERTIES OF PLANTS

G. A. Tikhov, Editor

NASA TT F-419

OBSERVATIONS OF THE MOON, MARS, URANUS, AND THE STARS

OPTICAL PROPERTIES OF PLANTS

G. A. Tikhov, Editor

Translation of "Nablyudeniya Luny, Marsa, Urana i zvezd.
Opticheskiye svoystva rasteniy".
Trudy sektora astrobotaniki, Vol. 8, Izdatel'stvo Akademii
Nauk Kazakhskoy SSR, Alma-Ata, 1960.

NATIONAL AERONAUTICS AND SPACE ADMINISTRATION

TRANSACTIONS OF THE ASTROBOTANY SECTOR, ACADEMY
OF SCIENCES KAZAKH SSR

VOLUME 8

OBSERVATIONS OF THE MOON, MARS, URANUS, AND THE STARS
OPTICAL PROPERTIES OF PLANTS

TABLE OF CONTENTS

Page

iii

OBSERVATIONS OF THE MOON, MARS, URANUS, AND THE STARS
OPTICAL PROPERTIES OF PLANTS

G.A.Tikhov, Editor

A collection of papers comprises: investigations on the in-
fluence of environmental factors, such as temperature, humidi-
ty, and light, on the photosynthesis, spectral transmittance
and reflectance of lower and higher plants; color spectro-
photometry of the surface of Mars, Uranus, the moon, various
asteroids, and magnetic stars; variations in telluric lines
of O_2 at various altitudes; philosophical theories on the
origin of life; etc. Conclusions of the various articles in-
clude: speculative theories on plant life on Mars, based on
the absence of the chlorophyll absorption band and the Wood
effect in terrestrial plants under austere climates and change
in optical properties of plants with change in environmental
conditions; theories on intelligent life on Mars, from rapid
changes in light and dark regions of the surface; presence
of biologically highly developed plants on Mars, from the
materialistic theory of biogenesis; composition of the lunar
surface, from color excess and color indices of craters.

This collection gives an account of the results of visual observations of
the planet Mars during the 1958 opposition and of the cartographic plotting of
the photographic observations of Mars by G.A.Tikhov during the favorable 1909
opposition.

A number of articles are devoted to spectral investigations of the moon,
Uranus, magnetic and variable stars, and the asteroids Vesta and Eunomia; to
electrophotometric investigations of the moon and Mars; to a study of twilight
phenomena in the earth's atmosphere and to results of spectrophotometric in-
vestigations of cultivated and wild plants.

The book is intended for specialists studying problems of astrobotany,
astrophysics, and geophysics.

Editorial Board

G.A.Tikhov (deceased) (Editor-in-Chief), N.I.Suvorov (Assistant Editor-in-
Chief), and A.K.Suslov (Secretary)

---

* Numbers in the margin indicate pagination in the original foreign text.

PROBLEM OF INVESTIGATING THE TOTAL ABSORPTION OF LIGHT
BY PLANT LEAVES UNDER FIELD CONDITIONS

G.A.Tikhov, Deceased

The study of the spectral properties of plants in the Astrobotany Sector of the Kazakh Academy of Sciences began with an investigation of their spectral reflectance. This was followed by research on the spectral transmittance of plants. Presently, this has been supplemented by studies on the light absorption by plants at different wavelengths. All these investigations were carried out on the basis of a scale made from a white baryta plate, illuminated - just as plants - by direct solar rays. In first approximation, the brightness of the baryte plate in all regions of the spectrum is taken as unity.

We will denote the brightness of the light scattered by a plant leaf at the wavelength λ by R_λ, the light transmitted through it by T_λ, and the sum of both by S_λ. Thus, $S_\lambda = R_\lambda + T_\lambda$. Then, for the brightness of the light absorbed by the plant A we obtain the expression

$$A_\lambda = 1 - S_\lambda, \tag{1}$$

where the incident light from the sun is taken as 1.

Next, we will find the total absorption of light for the entire spectrum.

Let us separate the entire measured spectrum, within the limits λ_1 and λ_2, into n regions identical in the number of millimicrons so that the length of

each region $\delta_\lambda = \dfrac{\lambda_2 - \lambda_1}{n}$. We will construct a curve by plotting the wave-

length λ on the axis of abscissas and S_λ on the axis of ordinates. Then, the area between the abscissa of this curve and the two adjacent ordinates, with the center at λ, will represent the mean value of S_λ for this λ. All reflected and

transmitted light for the entire spectrum is equal to $S = \sum\limits_{1}^{n} S$, while the absorbed

light will be $\overset{n}{\underset{1}{A}} = n - \sum\limits_{1}^{n} S_\lambda$; if we take all light that fell on the plant as 1,

then the total coefficient of absorption for the entire spectrum will be expressed by the formula

$$A = 1 - \frac{1}{n} \sum\limits_{1}^{n} S_\lambda. \tag{2}$$

The greater the value of n, the more accurate will be A.

The greatest accuracy will be obtained upon substituting $\sum\limits_{1}^{n} S_\lambda$ by the area

between the axis of abscissas, the extreme axes of ordinates, and the curve S_λ.

Then, n is replaced by the area between these ordinates and a straight line parallel to the abscissa and having an ordinate equal to 1.

The first area can be determined by a planimeter.   <u>/4</u>

Tables 1 - 9 and Figs.1 - 8 show examples for a determination of A, on the basis of observations by V.P.Bedenko, graduate student of the Sector, which he carried out in Uzbekistan, on the Kola Peninsula, in the Crimea, and in the mountains of Zailiyskiy Alatau, and also of the observations by A.P.Kutyreva in the Pamirs.

On the basis of their values of S_λ, smooth curves were plotted from which, every 10 mμ, the values of S_λ were recorded; these are shown in Tables 1 - 9.

Below the columns of S_λ, we entered the calculated sums of S, divided into n numbers. These values were subtracted from unity thus yielding the values of A.

Originally, certain coworkers of the Sector determined A from eq.(1); at the wavelengths at which S_λ was greater than unity, they obtained a negative value for A which they gave the completely obscure designation of "negative absorption".

Actually, for these regions of the spectrum, the light due to self-emission of the plant under solar radiation is added to the incident light from the sun. There is no doubt that in any region of the spectrum the incident sunlight can be taken as unity, but the plant distributes this light over various regions of the spectrum in conformity with its vital requirements, and only on the average for the entire spectrum can we take the total flux of solar irradiation as unity.

To study the absorption of light by a plant in individual spectrum regions, we must determine the self-emission of the plant or, more broadly speaking, the reaction of plants to a light flux in different rays.

This investigation is planned as the next step.

TABLE 1   APPENDIX

TEA SHRUB.   LEAF OF THE THIRD LEVEL.   TASHKENT OBLAST'.   S.SIDZHAK.
October 3, 1957, Noon, t = 35°C.   Observations by V.P.Bedenko

λ	R_λ	T_λ	S_λ		1	2	3	4
1	2	3	4		710	0,400	0,246	0,646
					720	,480	,350	0,830
520 mμ	0,150	0,040	0,190		730	,652	,301	0,953
530	,160	,050	,210		740	,846	,481	1,327
540	,160	,050	,210		750	,912	,395	1,307
550	,150	,053	,203		760	,642	,764	1,406
560	,160	,046	,206		770	,655	,795	1,450
570	,160	,032	,192		780	,655	,785	1,440
580	,137	,024	,161		790	,655	,745	1,400
590	,130	,014	,144		800	,655	,700	1,355
600	,130	,014	,144					
					810	,700	,620	1,320
610	,120	,011	,131		820	,700	,600	1,300
620	,120	,009	,129		830	,570	,740	1,310
630	,106	,009	,115		840	,604	,743	1,347
640	,106	,009	,115		850	,585	,812	1,397
650	,095	,013	,108		860	,570	,830	1,400
660	,103	,014	,117		870	,560	,953	1,513
670	,120	,030	,150		880	,565	,957	1,522
680	,151	,060	,211		890	,565	,550	1,115
690	,237	,156	,393					
700	,294	,180	,474					$S=27,941$
								$1/38\ S=0,735$
								$A=0,265$

TABLE 2   /5

CABBAGE.   PETROZAVODSK, AGRICULTURAL SECTION OF THE
KARELIA BRANCH OF THE USSR ACADEMY OF SCIENCES.
June 20, 1958, 12:20, t = 20°C.   Observations by V.P.Bedenko

λ	R_λ	T_λ	S_λ		1	2	3	4
1	2	3	4		610	0,162	0,074	0,236
					620	,170	,070	,240
450 mμ	0,115	0,009	0,124		630	,157	,060	,217
460	,101	,009	,110		640	,135	,010	,145
470	,131	,009	,140		650	,124	,020	,144
480	,132	,012	,144		660	,125	,018	,143
490	,145	,010	,155		670	,166	,026	,192
500	,148	,015	,163		680	,258	,188	,446
					690	,352	,297	,649
510	,129	,043	,172		700	,436	,380	,816
520	,162	,078	,240					
530	,207	,114	,321		710	,580	,565	1,145
540	,214	,123	,337		720	,650	,690	1,340
550	,217	,128	,345		730	,630	,700	1,330
560	,209	,120	,329		740	,590	,789	1,379
570	,194	,110	,304		750	=,656	,712	1,368
580	,197	,105	,302		760	,596	,451	1,047
590	,178	,086	,264		770	,622	,409	1,031
600	,178	,086	,264		780	,554	,344	0,898
					790	,521	,307	0,828
					800	,487	,307	0,794
								$S=18,102$
								$1/36 S=0,503$
								$A=0,497$

TABLE 3

POTATOES. PETROZAVODSK, AGRICULTURAL SECTION OF THE
KARELIA BRANCH OF THE USSR ACADEMY OF SCIENCES.
June 20, 1958, 12:20, t = 20° C. Observations by V.P.Bedenko

λ	R_λ	T_λ	S_λ	1	2	3	4
1	2	3	4				
				610	0,096	0,102	0,198
400 mμ	0,093	0,016	0,109	620	,093	,097	,190
410	,093	,016	,109	630	,082	,074	,156
420	,085	,016	,101	640	,083	,042	,125
430	,093	,017	,110	650	,076	,035	,111
440	,093	,017	,110	660	,079	,030	,109
450	,085	,024	,109	670	,098	,065	,163
460	,081	,024	,105	680	,170	,202	,372
470	,079	,028	,107	690	,225	,325	,550
480	,082	,029	,111	700	,333	,424	,757
490	,095	,035	,130				
500	,089	,055	,144	710	,483	,597	1,080
				720	,605	,634	1,239
510	,083	,047	,130	730	,592	,640	1,232
520	,104	,104	,208	740	,485	,558	1,043
530	,147	,169	,316	750	,617	,664	1,281
540	,155	,182	,377	760	,520	,576	1,096
550	,155	,185	,340	770	,499	,578	1,077
560	,142	,165	,307	780	,427	,512	0,939
570	,129	,159	,288	790	,374	,480	0,854
580	,123	,142	,265	800	,355	,428	0,783
590	,109	,121	,230				
600	,109	,121	,230				$S=17,291$
							$1/41\ S=0,422$
							$A=0,578$

TABLE 4

LINDEN. CRIMEA RESERVATION.
August 20, 1958, 12:00-12:07, t = +28° C. Observations by V.P.Bedenko

λ	R_λ	T_λ	S_λ	1	2	3	4
1	2	3	4				
				540	0,086	0,195	0,281
330 mμ	0,041	—	0,041	550	,094	,202	,296
340	,040	—	0,040	560	,085	,225	,310
350	,058	—	,058	570	,083	,258	,341
360	,019	—	,019	580	,062	,253	,315
370	,049	0,049	,098	590	,062	,230	,292
380	,049	,049	,098	600	,063	,223	,286
390	,050	,038	,088				
400	,050	,050	,100	610	,058	,214	,272
				620	,056	,217	,272
410	,050	,060	,110	630	,050	,188	,238
420	,050	,086	,136	640	,047	,172	,219
430	,050	,080	,130	650	,049	,166	,215
440	,049	,080	,129	660	,044	,122	,166
450	,050	,098	,148	670	,013	,108	,151
460	,045	,106	,151	680	,052	,129	,180
470	,044	,096	,140	690	,067	,187	,254
480	,045	,106	,151	700	,116	,308	,424
490	,045	,110	,155				
500	,046	,123	,169	710	,207	,599	0,806
				720	,369	,855	1,224
510	,059	,133	,192	730	,472	,855	1,327
520	,071	,176	,247	740	,855	,855	1,710
530	,084	,202	,286	750	,855	,855	1,710
				760	,855	,855	1,710
				770	,605	,855	1,460
							$S=17,145$
							$1/45\ S=0,381$
							$A=0,619$

TABLE 5

LINDEN. POLAR-ALPINE BOTANICAL GARDEN (KOLA PENINSULA).
July 30, 1958, 12:05-12:12, t = +22°C. Observations by V.P.Bedenko

λ	R,	T_λ	S_λ		1	2	3	4
1	2	3	4					
					560	,096	,242	,338
330 mμ	0,042	—	0,042		570	,096	,227	,323
340	,043	—	,043		580	,073	,216	,289
350	,039	—	,039		590	,070	,200	,270
360	,040	—	,010		600	,065	,195	,260
370	,040	0,010	,050					
380	,040	,010	,050		610	,056	,175	,231
390	,038	,011	,049		620	,057	,182	,239
400	,040	,030	,070		630	,050	,137	,187
					640	,040	,121	,161
410	,040	,040	,080		650	,038	,080	,118
420	,043	,053	,096		660	,069	,083	,152
430	,045	,055	,100		670	,043	,144	,187
440	,046	,055	,101		680	,091	,281	,372
450	,044	,057	,101		690	,182	,341	,523
460	,044	,063	,107		700	,232	,310	,542
470	,042	,066	,108					
480	,042	,058	,100		710	,292	,467	,759
490	,045	,063	,108		720	,382	,492	,874
500	,047	,077	,124		730	,344	,395	,739
					740	,344	,342	,686
510	0,044	0,094	0,148		750	,293	,374	,667
520	,067	,155	,222		760	,202	,374	,576
530	,083	,274	,357		770	,147	,293	,440
540	,098	,249	,347					
550	,102	,235	,337					$S=11,752$
								$1\ 45\ S=0,261$
								$A=0,739$

TABLE 6

FILBERT. CRIMEA RESERVATION.
August 20, 1958, 12:00-12:07, t = +28°C, Observations by V.P.Bedenko

λ	R_λ	T_λ	S_λ		1	2	3	4
1	2	3	4					
					570	,073	,170	,243
330 mμ	—	—	—		580	,053	,153	,206
340	—	—	—		590	,053	,150	,203
350	0,052	—	0,052		600	,054	,147	,201
360	,024	—	,024					
370	,030	0,010	,040		610	,049	,119	,168
380	,030	,010	,040		620	,049	,127	,176
390	,033	,013	,046		630	,046	,114	,160
400	,040	,020	,060		640	,043	,097	,140
					650	,042	,080	,122
410	,040	,020	,060		660	,037	,060	,097
420	,043	,033	,076		670	,038	,051	,089
430	,041	,035	,076		680	,043	,068	,112
440	,040	,037	,077		690	,052	,142	,194
450	,042	,042	,084		700	,085	,243	,328
460	,038	,042	,080					
470	,039	,045	,084		710	,153	,664	0,817
480	,041	,047	,088		720	,304	,855	1,159
490	,042	,052	,094		730	,520	,855	1,375
500	,043	,068	,111		740	,855	,855	1,710
					750	,855	,855	1,710
510	0,051	0,087	0,138		760	,855	,855	1,710
520	,056	,117	,173		770	,855	,855	1,710
530	,076	,161	,237					
540	,075	,163	,238					$S=14,910$
550	,083	,172	,255					$1\ 45\ S=0,331$
560	,079	,170	,249					$A=0,669$

TABLE 7

FILBERT.   POLAR-ALPINE BOTANICAL GARDEN (KOLA PENINSULA).
July 30, 1958, 12:05-12:12, t = +22°C. Observations by V.P.Bedenko .   /7

λ	R_λ	T_λ	S_λ	λ	R_λ	T_λ	S_λ
330mμ	0.036	—	0.036	580	0.094	0.155	0.249
340	.034	—	.034	590	.080	.140	.220
350	.033	—	.033	600	.072	.137	.209
360	.033	—	.033	610	.062	.121	.183
370	.033	—	.033	620	.057	.097	.154
380	.033	—	.033	630	.048	.069	.117
390	.032	—	.032	640	.038	.051	.089
400	.033	—	.033	650	.033	.033	.066
410	.033	0.009	.042	660	.069	.041	.110
420	.033	.009	.042	670	.048	.091	.139
430	.035	.020	.055	680	.126	.209	.335
440	.037	.036	.073	690	.220	.279	.499
450	.037	.020	.057	700	.266	.290	.556
460	.037	.020	.057	710	.314	.376	.699
470	.035	.021	.056	720	.374	.352	.726
480	.032	.020	.052	730	.316	.268	.604
490	.040	.030	.070	740	.301	.202	.503
500	0.046	0.048	0.094	750	0.261	0.255	0.516
510	.057	.073	.130				
520	.079	.092	.171	760	.213	.202	.415
530	.121	.188	.309				
540	.109	.194	.303	770	.183	.155	.343
550	.118	.188	.306				
560	.109	.176	.285				$S = 9.356$
570	.088	.176	.264			1/45	$S = 0.208$
							$A = 0.792$

TABLE 8

**SOLENANTHUS STYLOSUS LIPSKY (A ROSETTE OF BROAD LEAVES HAVING A DULL
DARK BLUISH-GREEN COLOR WAS REMOVED).   EASTERN PAMIRS, CHECHEKTY LAND-
MARK, IN THE VICINITY OF THE PAMIR BIOLOGICAL STATION.**   /8
Height 3860 m above Sea Level, August 23, 1951, 16:40, t = 15°C,
Humidity about 10%, Completely Cloudless, Calm; Dark Blue Sky,
Visibility more than 50 km, Observations by A.P.Kutyreva.

$\lambda_{m\mu}$	R_λ	T_λ	S_λ	$\lambda_{m\mu}$	R_λ	T_λ	S_λ
310mμ	0.018	0.000	0.018	610mμ	0.074	0.004	0.078
320	.017	.000	.017	620	.063	.003	.066
330	.016	.000	.016	630	.063	.003	.066
340	.014	.000	.014	640	.068	.004	.072
350	.015	.000	.015	650	.068	.006	.074
360	.008	.000	.008	660	.059	.005	.064
370	.009	.000	.009	670	.061	.004	.065
380	.011	.000	.011	680	.056	.004	.060
390	.012	.000	.012	690	.058	.005	.063
400	.011	.000	.011	700	.088	.006	.094
410	.011	.000	.011	710	.129	.011	.140
420	.025	.000	.025	720	.185	.030	.215
430	.032	.000	.032	730	.429	.057	.486
440	.048	.000	.048	740	.650	.090	.740
450	.047	.000	.047	750	.700	.127	.727
460	.060	.000	.060	770	.788	.142	.930
470	.069	.000	.069	760	.797	.119	.916
480	.063	.000	.063	780	.655	.043	.698
490	.068	.000	.068	790	.678	.116	.794
500	.072	.000	.072	800	.711	.160	.871
510	.080	.000	.080	810	.754	.177	.931
520	.075	.002	.078	820	.790	.185	.975
530	.070	.006	.076				
540	.086	.005	.091				
550	.106	.006	.112				
560	.116	.006	.122				$S = 10.738$
570	.121	.005	.126			1/52	$S = 0.206$
580	.117	.004	.221				$A = 0.794$
590	.104	.004	.108				
600	.062	.007	.068				

TABLE 9 /9

HORSE SORREL (RUMEX CONFERTUS W.). CHIMBULAK LANDMARK, NORTHWESTERN SLOPE OF THE ZAILIYSKIY ALATAU MOUNTAINS, HEIGHT 2980 m ABOVE SEA LEVEL (VICINITY OF ALMA-ATA).

The survey was Performed by V.P.Bedenko on July 20-29, 1955 during the Midday Hours. Temperature Conditions during the Photographic Period: 1. Air Temperature: Maximum 24.6°, Minimum 7.6°, Amplitude of Variation 17.0°. 2. Temperature at Soil Surface: Maximum +64.0°, Minimum 7.8°, Amplitude of Variation 56.2°. Humidity 72%, Cloudless.

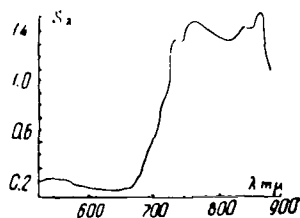| λ	R_λ	T_λ	S_λ	λ	R_λ	T_λ	S_λ
390$m\mu$	0,020	0,000	0,020	610$m\mu$	0,092	0,026	0,118
400	,040	,000	,040	620	,094	,033	,127
410	,035	,000	,035	630	,090	,040	,130
420	,031	,000	,031	640	,040	,035	,075
430	,030	,000	,030	650	,020	,026	,046
440	,030	,000	,030	660	,020	,026	,046
450	,030	,000	,030	670	,030	,031	,061
460	,030	,000	,030	680	,039	,032	,071
470	,030	,000	,030	690	,079	,060	,139
480	,037	,000	,037	700	,168	,300	,468
490	,045	,000	,045	710	,290	,359	,578
500	,050	,000	,050	720	240	,400	,640
510	,047	,009	,056	730	,240	,360	,600
520	,042	,017	,059	740	,240	,360	,600
530	,040	,025	,065	750	,230	,360	,590
540	,048	,049	,097	760	,230	,360	,590
550	,055	,060	,115				
560	,073	,047	,120				$S = 6,278$
570	,090	,031	,121			1/38	$S = 0,165$
580	,093	,028	,121				$A = 0,835$
590	,093	,027	,120				
600	,092	,024	,116				

Fig.1 Tea Shrub (Observations by V.P.Bedenko)
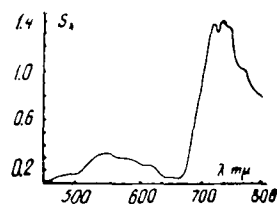

Fig.2 Cabbage (Observations by V.P.Bedenko)
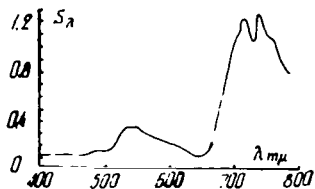
8

Fig.3 Fotatoes (Observations by
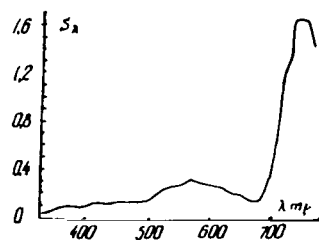   V.P.Bedenko)

Fig.4 Linden. Crimea Reservation
       (Observations by V.P.Bedenko)

Fig.5 Linden. Polar-Alpine Botanical
Garden (Observations by V.P.Bedenko)
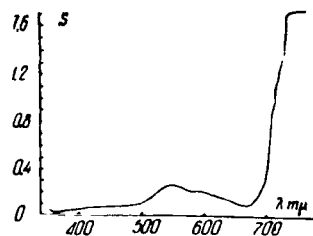

Fig.6 Filbert. Crimea Reservation
       (Observations by V.P.Bedenko)

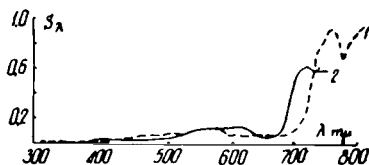Fig.7 Filbert. Polar-Alpine Botanical
Garden (Observations by V.P.Bedenko)

Fig.8 Solenanthus (1). Data by
A.P.Kutyreva. Horse Sorrel (2).
      Data by V.P.Bedenko

9

REGULARITIES IN THE OPTICAL PROPERTIES OF LEAVES AND PETALS OF IRIS OF DIFFERENT COLORS

V.S.Sokolova

1. Introduction

It is known that the color of a flower is produced by the presence of some pigment in the cell sap. Such pigments include: a) anthocyanins - blue, violet, red and b) flavones - yellow.

Investigations of the chemical composition of the cell sap have shown that anthocyanins in the cells are usually formed on an excess of sugar and at a low temperature and also on acid reaction of the cell sap. Anthocyanins and flavones, under suitable conditions, are interdependent. For example, under the effect of light the oxygen-rich flavones are reduced to anthocyanins (Bibl.1, 2, 6).

At present, considerable emphasis is placed on an investigation of the role of anthocyanins in photochemical reactions of plants. No doubt, an investigation of the optical properties of anthocyanins, flavones, and chlorophyll will help to define the role of anthocyanins in the metabolism and, furthermore, reveal the correlation between anthocyanins and chlorophyll.

Laboratory investigations have demonstrated that the absorption spectra of anthocyanins have higher values in the wavelength region from 200 to 600 mμ, with the maximum depending on their color.

Up to 650 mμ, the red pigments fully transmit red rays, in the orange region they transmit 10%, while in the yellow region the absorption increases, reaching a maximum in the green region at 550 mμ. In the blue region, the absorption drops off markedly: yellow flowers have their absorption maximum in the blue region.

Investigations of the optical properties of flowers under natural conditions have confirmed this regularity. Nevertheless, laboratory results cannot be entirely reliable with respect to the quantitative aspect of spectral reflection and transmission. Spectral reflection and transmission of light by plants under natural conditions, as will be shown below, is a function of many factors, whose main variable is the environment - air temperature, humidity, etc.

2. Working Method

The investigated objects were recorded by a quartz spectrograph with a set of attachments. The attachments were needed for spectrographic analysis of the objects, both in reflected and in transmitted light, and for obtaining the /12 characteristic indicatrix in these rays. To determine the coefficient of reflection and transmission of light, the investigated object was spectrophoto-

graphed in reflected and transmitted rays by means of an attachment consisting of two small metal tubes welded together at an angle of 45°. The dimensions were selected by calculating the solid angles of the diaphragms of the spectrograph so that the entire solid angle was filled by the light emitted by the investigated object. The welded tubes formed an attachment with three openings. A wide ring with a glued-on velvet piece was attached to the opening, formed by welding the two tubes. To this the test specimen was tightly superposed on the velvet wedge and covered, at the opposite side, by a disk of black paper; this assembly was then fastened by special clamps.

After spectrographing, the object was removed and replaced by plaster of Paris, enclosed in a special round holder. The other two openings of the attachment had a different function. One of them was used for setting the attachment on the slit of the spectrograph collimator and the other was aimed at the sun. These orifices could be interchanged, depending on the angle to the incident solar rays at which the specimen was to be placed: normal, or at an angle of 45°. The disk of black paper was removed from the object when spectrographing in transmitted light, and the specimen, together with the tube, was aimed directly at the sun. With this arrangement, the other two orifices were reversed; the aperture that had been aimed at the sun was placed on the slit, and the other was covered with a black cap to exclude extraneous light. Aiming of the aperture with the test specimen toward the sun was monitored by a scanner or by projection of the slit screw onto a recording drum with diaphragms.

To obtain the characteristic indicatrix, the spectra of reflected and transmitted rays were recorded by special attachments, a detailed description of which was given in the Vol. VII of the Transactions of the Astrobotany Sector (Bibl.3). It should be recalled that, to obtain the characteristic indicatrix of reflected rays, an attachment in the form of a small cylinder 6 cm in diameter with an average height of 5 cm was used. The upper part of the cylinder was truncated at an angle of 45° to the base. The cut area was used as working platform on which the specimen was placed. By means of a special small rod, this attachment was screwed to the collimator of the spectrograph, the center of the cut area and the slit being on the optical axis of the collimator. A small cylinder in the stand made it possible to turn the device through any angle to the incident light. The angle of turn is recorded on a dial mounted to the side of the support.

The specimen is placed on the working platform of the cylinder and is attached by special clamps, after which the small cylinder with the object is rotated normal to the incident light. The small cylinder is turned by means of a special sunseeker placed on the side of the working platform.

The characteristic indicatrix in reflected radiation was investigated in a plane close to the plane of the incident light; the angle between these planes was 17°. This angle can be obtained experimentally only by means of an inverted spectrograph.

To obtain the characteristic indicatrix of the transmitted rays, an accordion-type attachment was used (Bibl.3), one side of which was hermetically screwed to the collimator of the spectrograph while the specimen was inserted on the other side, by means of a special frame. The frame with the specimen must be

11

perpendicular to the incident light, when in working position. The slit of the collimator, together with the spectrograph, is turned at any angle to the normal of the leaf. Sighting on the sun and turning of the collimator to the necessary angle are accomplished by a sunseeker and dial, mounted above the attachment. /13 The latter makes it possible to investigate the indicatrix of transmitted rays in the plane of the incident light.

The energy flux of reflected and transmitted rays is expressed in terms of the energy flux reflected from the plaster-of-Paris screen, which subsequently is reduced to baryta. The plaster-of-Paris screen is spectrographed under the same conditions as the specimen, i.e., with the same exposure and slit width. The slit width was 0.02 mm. Pan-infra photographic plates with the smallest interval in the green region were used. In this case pan-infra plates with 1056 emulsion, sensitive to 760 mμ proved to have the highest transmittance. The negatives were photometered on a MF-4 recording microphotometer. To determine the reflection and transmission coefficients, each spectrum was measured at no less than 32 wavelengths, and to plot the indicatrix the minimum was 7 - 8 wavelengths. When determining the albedo of the reflected and transmitted light it was first assumed that the specimen represented an ideal ground-glass diffuser with indicatrices of a spherical shape. This assumption reduced the determination of the albedo of diffusely reflected and transmitted rays to simple calculations, namely, to a multiplication of the brightness coefficient of the diffusely reflected and transmitted rays k' and k'' by the brightness coefficient of baryta k. The values of k' and k'' were determined by the usual method of relative spectrophotometry, with a sufficiently high accuracy (see Bibl.4). The brightness coefficient of baryta k was determined under laboratory conditions and, for all subsequent investigations, was kept constant.

Actually, the specimens generally were not ideally dull surfaces, so that their indicatrices were not spherical (4:5). Therefore, it was necessary to introduce into the reflection and transmission coefficients a correction coefficient, i.e., the coefficient k_0 of the deviation of the given indicatrix from a spherical shape. This coefficient was mathematically determined as the quotient of the division of the numerical value of the real indicatrix by the numerical value of the spherical indicatrix, the radius of the spherical indicatrix = k' or k'' in the direction toward 0^0.

To eliminate an error in calculating the correction coefficient k_0, it had to be determined with a higher accuracy than the albedo. For example, if the albedo A was calculated with an accuracy up to the second significant figure, i.e., to 0.01, then k_0 had to be calculated with an accuracy to the third significant figure, namely, 0.001. Consequently, one had to know beforehand into what number of elementary figures the spatial indicatrix had to be divided so that this difference did not exceed the required accuracy. The number of elementary figures was determined by means of a control sphere. It was found that this sphere had to be divided into truncated cones whose generatrix would be a straight line and correspond to 2^0.

The sphere was divided into degrees at the point of tangency of the sphere with the plane. Truncated cones were constructed through the points of intersection of the sphere with the planes drawn through the point of tangency and every 2^0 from the normal to the tangent plane, and segments were plotted at the

12

point of tangency of the sphere with the plane and at the opposite point. Then, the value of k' was taken as the distance from the point of tangency to the middle of the generatrix of the corresponding cone. The angle ϵ was read from the normal to the tangent plane. The solid angle $d\omega$ was determined as the quotient of the division of the area of the lateral surface of the truncated /14

cone $\dfrac{2\pi r_1 + 2\pi r_2}{2}$ ds = $\pi r ds$, where r_1, r_2 are the radii of the base of the

truncated cone, $r = r_1 + r_2$, by the square of the distance ρ from the point of tangency to the middle of the generatrix. In this case, $k' = \rho$. Then, $d\omega$ was multiplied successively by k' cos ϵ. The resultant values were added. The difference was $\Sigma k'$ cos $\epsilon \Delta\omega - \int k'$ cos $\epsilon d\omega = 0.004$, where ϵ is the angle between the normal of the area of the specimen and the direction of the light flux passing from it into the collimator of the spectrograph; $d\omega$ is the solid angle.

This difference is negligible within the limits of the required accuracy. Consequently, when calculating the correction coefficient, the given spatial indicatrix should be divided into the same number of elementary figures as the control sphere, i.e., into 45. Then, the obtained sum should be divided by the value $k \cdot k'$. The resultant correction coefficients are multiplied by the brightness coefficient of the diffusely reflected and transmitted rays. When plotting the spatial indicatrices it was assumed that, in other planes, the indicatrices behave in a corresponding manner, i.e., in such a manner that the spatial indicatrix becomes a symmetrical figure.

3. Results

The specimens used were irises of various species, grown in the Botanical Garden of the Kazakh Academy of Sciences, Yakutsk, and Zhigansk. The blossom of the iris was represented by different colors: ultraviolet, blue, azure, yellow, red, and infrared. The petals of the flower and the first leaf from the flower were spectrographed both in reflected and in transmitted rays.

The iris in Yakutsk and Zhigansk was spectrographed in 1957 by Z.S.Parshina who was there on an expedition. The iris in the Botanical Garden of the Kazakh Academy of Sciences was spectrographed by us in June 1958. Irises of only one color, blue, were found in Zhigansk and Yakutsk and irises with colors of the entire visible region of the spectrum were in the Botanical Garden of the Kazakh Academy of Sciences. Simultaneously with spectrographing, we determined the relative humidity by means of an aspiration psychrometer, GOST 6353-52. In all, we obtained 38 negatives with an average of 23 spectra on each; of these, 13 negatives were for determining the reflection and transmission coefficients of light and 25 for determining the indicatrices of diffusely reflected and transmitted rays.

For each object we plotted the indicatrices in 7 - 8 wavelengths, both for diffusely reflected and transmitted light.

To determine the brightness coefficient, we first made the assumption that the surface of all specimens was absolutely dull and had a spherical indicatrix;

13

this reduced the calculation of the reflection and transmission coefficient, as already indicated, to a very simple process.

Next, the indicatrices were investigated. For this purpose, all plotted indicatrices were divided into groups: 1) spherical; 2) those extended in an equatorial direction; 3) those extended in a polar direction; 4) intermediate.

We determined the correction coefficient for each group. /15

A spherical indicatrix is exhibited by:

a) Leaf of blue iris in reflected light for λ = 358; 377; 427; 475; 570; 642 mμ.

b) Flower of dark-red iris in reflected light at λ = 358; 427; 642: 720; 738 mμ and for transmitted rays at λ = 377; 475; 758 mμ.

c) Flower of blue iris in reflected light at λ = 358; 377; 570: 642 mμ and for transmitted light at λ = 358; 377; 427; 475; 570: and 642 mμ.

d) Flower of yellow iris in transmitted light at λ = 358; 577; 720 mμ.

e) Flower of azure iris at λ = 570; 642 mμ.
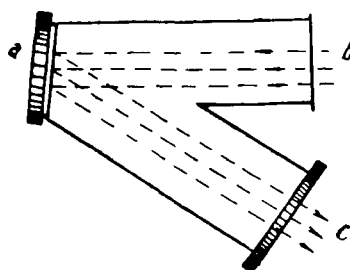
Fig.1   Attachment for Determining Brightness
Coefficient of Specimen
a - Object; b - In transmitted rays; c - In reflected rays

Indicatrices close to spherical with correction coefficient k_o = 1.167 were exhibited by:

a) Flower of blue iris in reflected light at λ = 475; 720 mμ.

b) Flower of yellow iris in reflected light at λ = 358; 377; 570 mμ.

c) Flower of red iris in reflected light at λ = 358; 377; 427; 475; 570; 642 mμ.

d) Flower of white iris in reflected light at λ = 358; 377; 475; 570; 642; 720 mμ.

14

e) <u>Leaf of red</u> iris in reflected light at λ = 358; 377; 427; 475 mμ. In transmitted light at λ = 720; 738 mμ.

f) <u>Leaf of yellow</u> iris in reflected light at λ = 358; 377; 427; 475; and 57C mμ. In transmitted light at λ = 738 mμ.

g) <u>Leaf of white</u> iris in reflected light at λ = 358; 427; 720 mμ.

Indicatrices extended in a polar direction:

a) With correction coefficient k_o = 0.785 were exhibited by flower of red iris in transmitted light at λ = 358; 377; 427; 738 and flower of white iris at λ = 427; 642 mμ.

b) With correction coefficient k_o = 0.830, by flower of azure iris in transmitted light at λ = 427; 475; 720; 738 mμ.
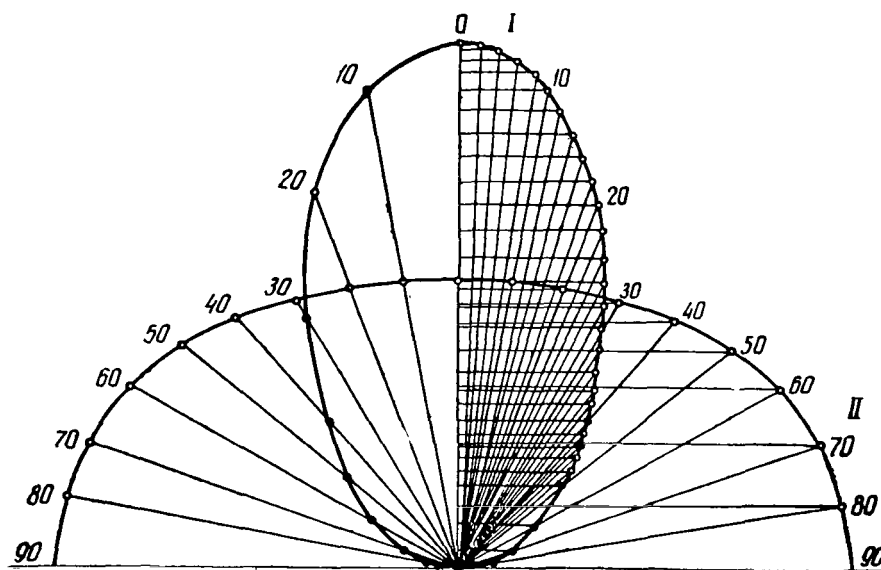
Fig.1a   Indicatrices
1 – Extended in polar direction; 2 – Extended in
equatorial direction

Indicatrices extended in an equatorial direction:

a) With correction coefficient k_o = 1.203 were exhibited by flower of yellow iris in reflected light at λ = 427; 475 mμ.

b) With correction coefficient k_o = 1.294, by flower of yellow iris in re-flected light at λ = 642; 720 and by flower of white iris in reflected light at λ = 427; 428; 475; and 642 mμ.

c) With correction coefficient k_o = 1.318, by leaf of dark-red iris in

15

transmitted light at λ = 358; 377; 427; 570; and 642 mμ. As a typical example, we are giving two characteristic indicatrices: 1) extended in a polar direction and 2) in an equatorial direction (Fig.1a). After determining the correction coefficients, all the obtained brightness coefficients of the object in re-   /16 flected and transmitted light were corrected. Certain plants were spectrographed twice under different conditions. All flowers were divided into groups based on their color: dark-blue, blue, azure, yellow, red, dark-red, and white. We will analyze each group separately:

1. Dark-blue iris (Iris hybrid.hort., variety unknown) (Fig.2). Air temperature t = +22.0°C with relative humidity of 55%, time of photographing the petal 17:25 - 17:50, of the leaf 17:58 - 17:03 (June 1, 1958).

Fig.2 Curves of Spectral Brightness k of Dark-Red Iris
1 - Petal in reflected light; 2 - Petal in transmitted light;
3 - Leaf in reflected light; 4 - Leaf in transmitted light

The spectral brightness curves of the petal in reflected and transmitted light have two maxima and two minima.

Petal   /17

Maxima: a) from 400 to 500 mμ,with a highest value of 18 and 5%; b) from 720 to 800 mμ, 78 and 70%.

Minima: a) from 320 to 400 mμ, with a lowest value of 0 and 2%.

The spectral brightness curves of the petal in reflected and transmitted light have two maxima and two minima.

Maxima: a) from 500 to 600 mμ, with a highest value of 5 and 15%: b) from 800 to 850 mμ, 60 and 58%.

Minima: a) from 320 to 570 mμ, with a lowest value of 0 and 3%; b) from 660 to 725 mμ, 2 and 3%.

2. **Blue iris** (Iris sibirica L., "Perry's Blue") (Fig.3). Spectrographed at Alma-Ata at the Botanical Garden of the Kazakh Academy of Sciences. Air temperature t = +19.5° C; relative humidity 54%; time of photographing the petal and leaf 11:00 - 11:20 (June 12, 1958).
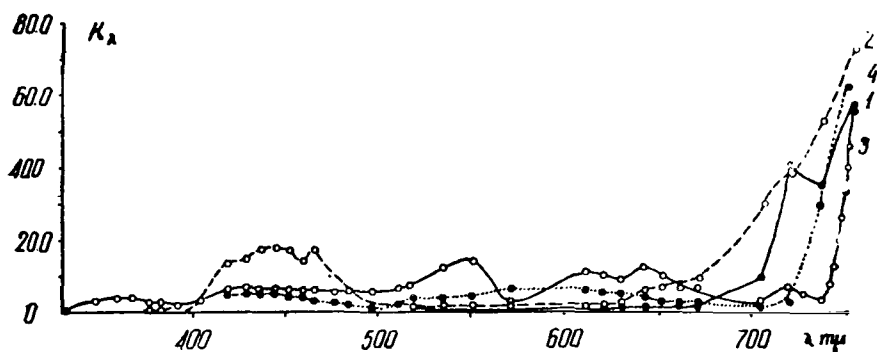

Fig.3 Curves of Spectral Brightness k of Blue Iris
1 - Petal in reflected light; 2 - Petal in transmitted light;
3 - Leaf in reflected light; 4 - Leaf in transmitted light

The spectral brightness curves of the petal in reflected and transmitted light have two maxima and two minima.

Petal

Maxima: a) from 390 to 510 mμ, with a highest value of 20 and 64%; b) from 700 mμ and beyond, 36 and 73%.

Minima: a) up to 380 mμ, with a lowest value of 0 and 8%; b) from 660 to 720 mμ, 3 and 8%.

Leaf

Maxima: a) from 530 to 570 mμ, with a highest value of 25 and 30%; b) from 700 to 730 mμ, 45%.

Minima: a) from 330 to 400 mμ, with a lowest value of 0 and 5% and b) from 650 to 720 mμ, 3 and 8%.

3. **Blue iris** (Iris hybrid. sibirica, variety unknown) (Fig.4). Spectrographed at Yakutsk. Air temperature t = +31.2° C, relative humidity 24%, time of photographing 14:00 - 14:59 (July 5, 1957).

Petal /18

Maxima: a) from 410 to 480 mμ, with a highest value of 30 and 50%; b) from 660 to 720 mμ, 84 and 48%.

Minima: a) from·500 to 530 mμ, with a lowest value of 12 and 13%.

Fig.4 Curves of Spectral Brightness k of Blue Iris (Yakutsk)
1 - Petal in reflected light; 2 - Petal in transmitted light;
3 - Leaf in reflected light; 4 - Leaf in transmitted light

Leaf

Maxima: a) from 510 to 640 mμ, with a highest value of 23 and 25%;
b) from 680 to 720 mμ, 42 and 60%.

Minima: a) from 400 to 500 mμ, with a lowest value of 0 and 11%; b) from 640 to 680 mμ, 8 and 13%.
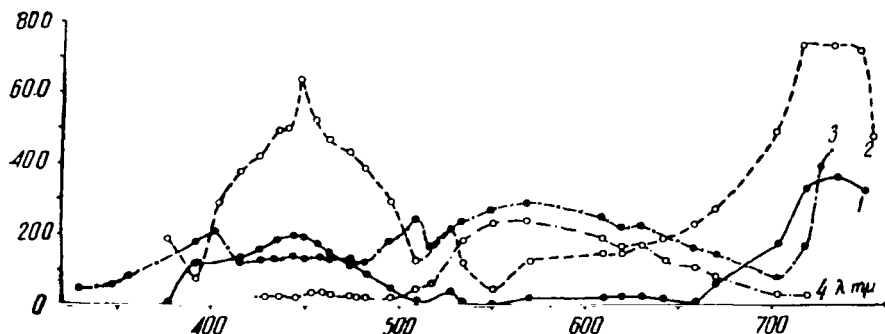

Fig.5 Curves of Spectral Brightness k of Blue Iris (Zhigansk)
1 - Petal in reflected light; 2 - Petal in transmitted light;
3 - Leaf in reflected light; 4 - Leaf in transmitted light

4. **Blue iris** (Iris hybrid. sibirica, variety unknown) (Fig.5). Spectrographed in Zhigansk. Air temperature t = +18.0° C, time of photographing 16:00 - 16:27, July 28, 1957.

The spectral brightness curves of the petal in reflected and transmitted light have two maxima and two minima and of the leaf, three maxima and two minima.

18

Maxima: a) from 410 to 500 mμ, with a highest value of 22 and 24%; b) from 650 to 720 mμ, 28 and 52%.

Minima: a) from 680 to 560 mμ, with a lowest value of 0 and 3%; b) from 710 to 560 mμ, 25%.

Leaf

Maxima: a) from 480 to 560 mμ, with a highest value of 76 and 25%; b) from 660 to 720 mμ, 52 and 28%.

Minima: a) from 400 to 470 mμ, with a lowest value of 0 and 3%; b) from 640 to 680 mμ, 2 and 6%.
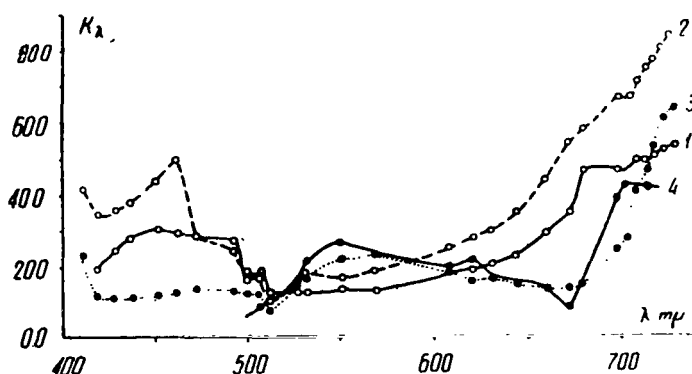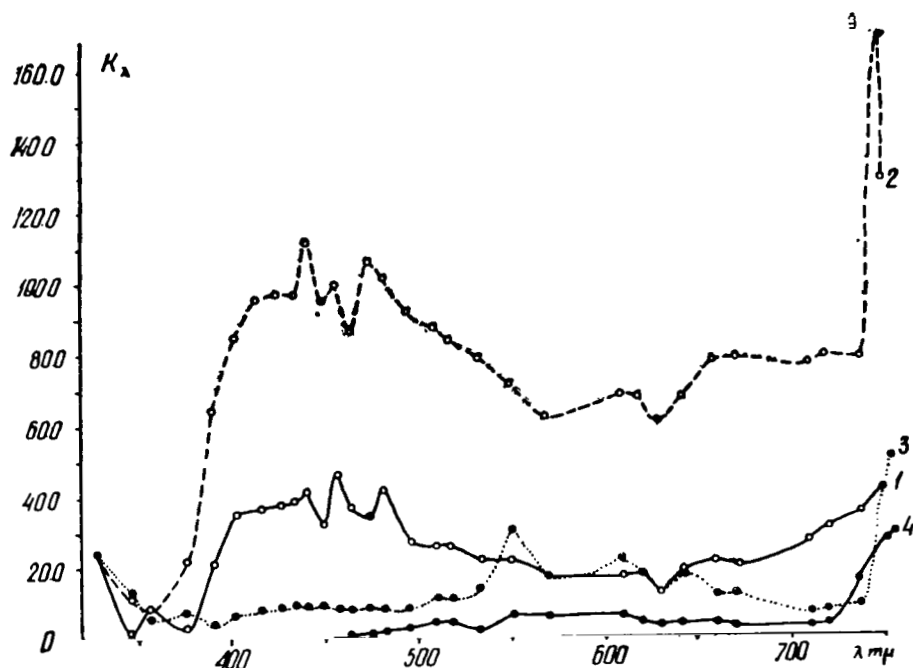
Fig.6 Curves of Spectral Brightness k of Azure Iris
1 - Fetal in reflected light; 2 - Petal in transmitted light;
3 - Leaf in reflected light; 4 - Leaf in transmitted light

5. Azure Iris (Iris hybrid., variety "Darwin") (Fig.6). Spectrographed at the Botanical Gardens of the Kazakh Academy of Sciences, Alma-Ata. Air temperature t = +21.0°C, relative humidity 55.0%, time of photographing was 18:30 - 18:50 for the petal and 18:50 - 18:58 for the leaf, June 1, 1958. The curves of the spectral brightness of the petal in reflected and transmitted light have two maxima and two minima.

The spectral brightness curves of the leaf in reflected and transmitted

light have two maxima and two minima.

<div align="center">Petal</div>

Maxima: a) from 490 to 520 mµ, with a highest value of 110 and 45%; b) from 730 to 860 mµ, 170 and 50%.

Minima: a) from 330 to 380 mµ, with a lowest value of 3 and 8%; b) from 610 to 660 mµ, 12 and 60%.   /20

<div align="center">Leaf</div>

Maxima: a) from 540 to 570 mµ, with a highest value of 30 and 8%; b) from 760 to 830 mµ, 50 and 30%.

Minima: a) from 340 to 400 mµ, with a lowest value of 0 and 9%; b) from 660 to 720 mµ, 6 and 3%.
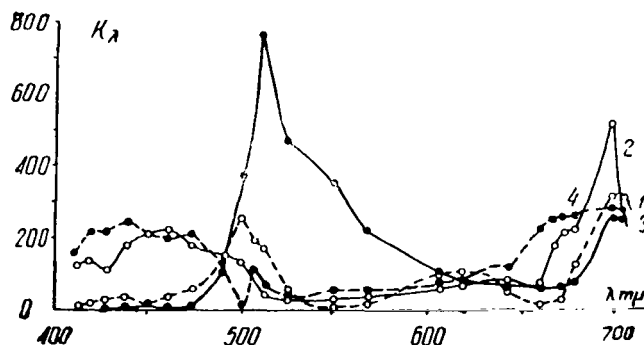

Fig.7 Curves of Spectral Brightness k of Yellow Iris
1 - Petal in reflected light; 2 - Petal in transmitted light;
3 - Leaf in reflected light; 4 - Leaf in transmitted light

6. Yellow iris (Iris pseudoacorus L.) (Fig.7). Air temperature t = = +20.0° C, relative humidity 58%, time of photographing 12:10 - 12:30 for the petal and 12:39 - 12:45 for the leaf, June 1, 1958, Botanical Garden, Alma-Ata.

The spectral brightness curves of the petal in reflected and transmitted light have three maxima and two minima.

The spectral brightness curves of the leaf in reflected and transmitted light have two maxima and two minima.

<div align="center">20</div>

<center>Petal</center>

Maxima: a) from 320 to 370 mμ, with a highest value of 10 and 55%; b) from 520 to 640 mμ, 98 and 53%; c) from 720 to 760 mμ, 38 and 50%.

Minima: a) from 360 to 520 mμ, with a lowest value of 2 and 8%; b) from 630 to 730 mμ, 27 and 30%.

<center>Leaf</center>

Maxima: a) from 540 to 620 mμ, with a highest value of 53 and 12%; b) from 720 to 760 mμ, 130 and 82%.

Minima: a) from 360 to 480 mμ, with a lowest value of 0 and 4%; b) from 680 to 720 mμ, 2 and 3%.

Fig.8 Curves of Spectral Brightness k of Yellow Iris
1 - Petal in reflected light; 2 - Petal in transmitted light;
3 - Leaf in reflected light; 4 - Leaf in transmitted light

7. Yellow iris (Iris pseudoacorus L.) (Fig.8). Air temperature t = +17.2° C, relative humidity 64%, time of photographing 08:40 - 09:15 for the petal and /21 09:43 - 09:53 for the leaf, June 12, 1958. The spectral brightness curves of the petal and leaf in reflected and transmitted light have two maxima and two minima.

<center>Petal</center>

Maxima: a) from 550 to 640 mμ, with a highest value of 35 and 30%; b) at 760 mμ, 55%.

Minima: a) from 330 to 500 mμ, with a lowest value of 1 and 3%; b) from 660 to 720 mμ, with a smallest value of 28 and 31%.

<center>Leaf</center>

Maxima: a) from 500 to 630 mμ, with a highest value of 14 and 4%; b) from 630 to 720 mμ, 0 and 5%.

Minima: a) from·500 to 640 mμ, with a lowest value of 14 and 3%; b) at

<center>21</center>

750 mμ, 40 and 57%.

8. <u>Red iris</u> (Iris hybrid.hort.L.) (Fig.9). Air temperature t = +20° C, <u>/22</u>
relative humidity 63%. Time of photographing the petal 13:13 - 13:30, June 1,
1958.
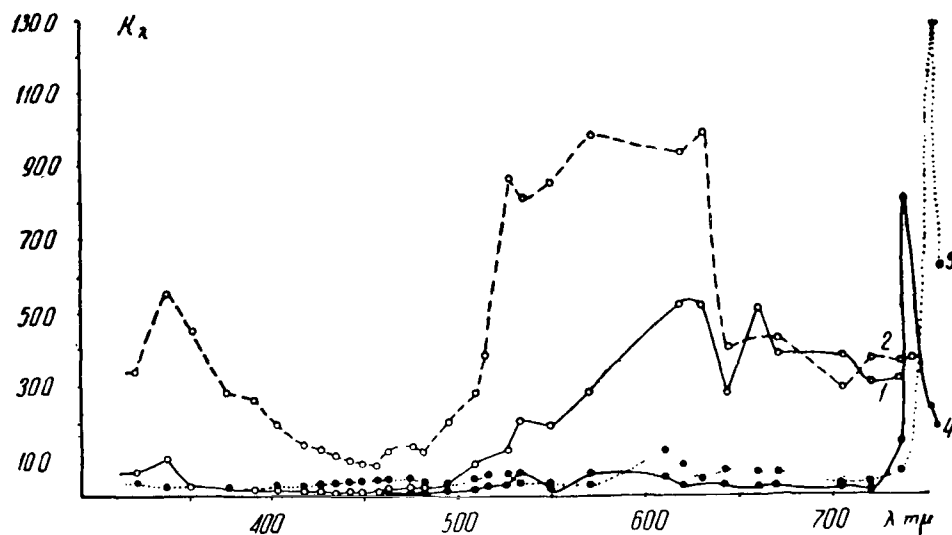

Fig.9 Curves of Spectral Brightness k of Red Iris
1 - Petal in reflected light; 2 - Petal in transmitted light;
3 - Leaf in reflected light; 4 - Leaf in transmitted light

The spectral brightness curves of the petal and leaf in reflected and
transmitted light have two maxima and two minima.

Petal

Maxima: a) from 350 to 470 mμ, with a highest value of 28 and 4%;
b) from 630 to 740 mμ, 113 and 74%.

Minima: a) from 480 to 620 mμ, with a lowest value of 1 and 7%; b) at
750 mμ, 30 and 50%.

Leaf

Maxima: a) from 520 to 620 mμ, with a highest value of 13 and 7%;
b) from 720 to 760 mμ, 50 and 56%.

Minima: a) from 320 to 500 mμ, with a lowest value of 0 and 5%; b) from
610 to 720 mμ, 1 and 5%.

9. <u>Dark-red iris</u> (Iris hybrid. arabasador) (Fig.10). Air temperature t =
= +23.0° C, relative humidity 53.5%, time of photographing 16:25 - 16:40 for the
petal and 16:45 - 16:55 for the leaf, June 1, 1958.

The spectral brightness curves of the petal in reflected and transmitted
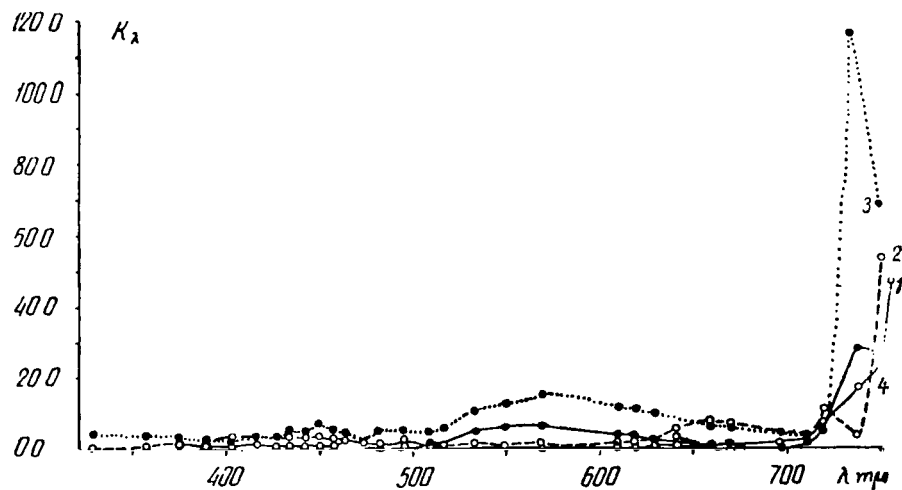
Fig.10 Curves of Spectral Brightness k of Dark-Red Iris
1 - Petal in reflected light; 2 - Petal in transmitted light;
3 - Leaf in reflected light; 4 - Leaf in transmitted light

light have one maximum and one minimum. The curves of the leaf have two maxima and two minima.

Petal

Maxima: a) from 720 to 760 mμ, with a highest value of 50%.

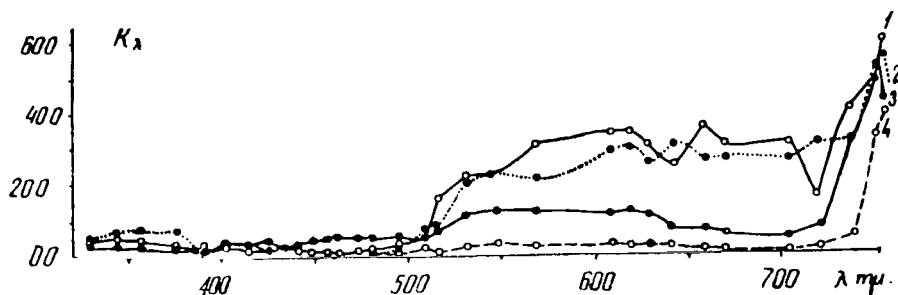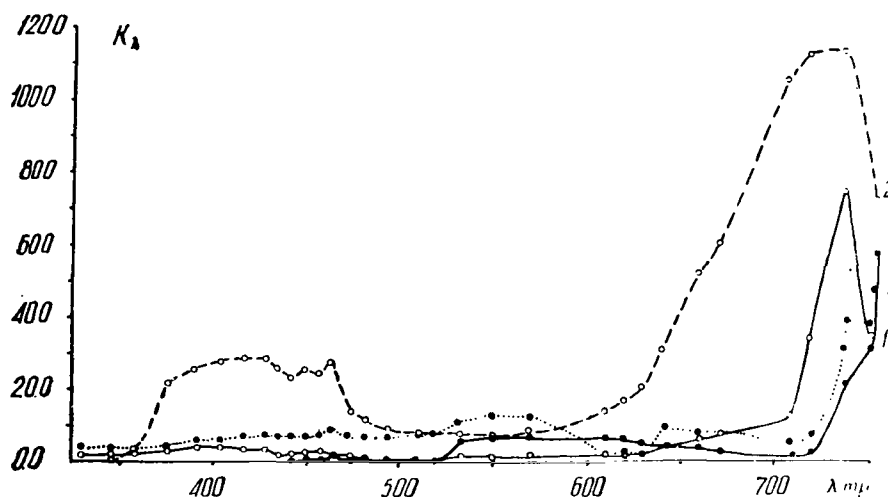Minima: a) from 330 to 720 mu, with a lowest value of 1 and 2%.
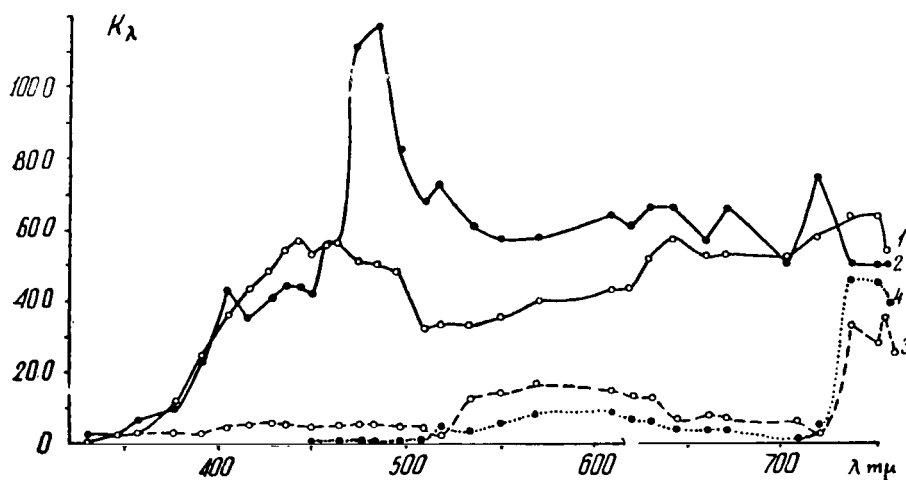
Fig.11 Curves of Spectral Brightness k of White Iris
1 - Petal in reflected light; 2 - Petal in transmitted light;
3 - Leaf in reflected light; 4 - Leaf in transmitted light

23

Maxima: a) from 520 to 640 mμ, with a highest value of 16 and 7%; b) from 720 to 760 mμ, 118 and 55%.

Minima: a) from 330 to 520 mμ, with a lowest value of 1 and 4%; b) from 660 to 720 mμ, 0 and 4.5.

10. White iris (Iris hybrid. hort., variety "Darwin") (Fig.11). Air temperature t = +19.5° C, relative humidity 54.0%, time of photographing 10:25 to 10:55, June 1, 1958.

The spectral brightness curves of the petal and leaf in reflected light and transmitted light have two maxima and two minima.

Petal

Maxima: a) from 350 to 500 mμ, with a highest value of 116 and 58%; b) from 610 to 720 mu, 75 and 64%.

Minima: a) from 320 to 360 mμ, with a lowest value of 3 and 2%; b) from 520 to 620 mμ, with a lowest value of 33 and 57%.

Leaf

Maxima: a) from 520 to 640 mμ, with a highest value of 16 and 10%; b) from 720 to 780 mμ, 45 and 33%.

Minima: a) from 330 to 520 mμ, with a lowest value of 0 and 5%; b) from 640 to 720 mμ, 1 and 6%.

4. Conclusions

1) The reflection and transmission of light for petals and leaves depends on the environment, namely, on air temperature and relative humidity. The higher the temperature and the lower the humidity, the greater will be the reflection and transmission of light.

2) The value of reflection and transmission of light, for both petal and /24 leaf depends on the time of day. In all probability, this is associated with photosynthesis.

3) Flowers of all colors have two maxima in the spectral brightness curves of the petal in reflected and transmitted light. The range of the former depends on the color of the flower, while the range of the latter is not a function of color and is located in the red and infrared regions of the visible portion of the spectrum.

4) The zone of the first maximum in the curves of spectral brightness of the petal in reflected and transmitted light coincides with the color of the flower.

For example, a yellow flower has a maximum in the yellow spectrum region, a red flower in the red, a blue flower in the blue.

5) Under suitable environmental conditions (temperature, humidity, and time of day) the above objects exhibit transmittance and strong complementary light in both zones of the maxima.

6) The nature of the maxima in the curves of spectral brightness of petals (anthocyanins and flavones) in reflected and transmitted light most likely is identical with the nature of the infrared effect of chlorophyll. Therefore, we will call the maxima, by analogy with the infrared effect, the red, yellow, and blue effects.

7) The spectral brightness curves of leaves in reflected and transmitted light are quite similar in slope to those of petals of the same color. This similarity can be explained apparently by the presence of chlorophyll in latent form in petals.

8) The magnitude of the maxima in the spectral brightness curves of leaves in reflected and transmitted light depends on the time of day. During the evening and morning hours, these maxima are appreciably broader and higher in the green region of the spectrum than at midday. Apparently this phenomenon is intimately connected with some kind of physiological process.

9) The nature of the complementary light of anthocyanins and flavones is apparently analogous to the nature of the infrared effect of chlorophyll. The physical meaning of these effects has not yet been explained.

BIBLIOGRAPHY

1. Lyubimenko, V.N. and Brilliant, V.A.: Plant Colors (Okraska rasteniy). Gosizdat, 1924 (Chapters V, VI, and VII).
2. Gudvin (Goodwin), T.: Comparative Biochemistry of Carotenoids (Sravnitel'naya biokhimiya karotinoidov). Moscow, Izd. Inostro Lit., 1954.
3. Sokolova, V.S.: Spectral Method of Determining Light Absorption by the Living Leaf (Spektral'nyy metod opredeleniya pogloshcheniya sveta zhivym listom). Trudy Sekt. Astrobotan., Vol.V, Alma-Ata, Izd. Akad. Nauk KazSSR, 1957.
4. Tikhov, G.A.: Principles of Visual and Photographic Photometry (Osnovy vizual'noy i fotograficheskoy fotometrii). Alma-Ata, Izd. Akad. Nauk KazSSR, 1950.
5. Sytinskaya, N.N.: Absolute Photometry of Extended Celestial Objects (Absolyutnaya fotometriya protyazhennykh nebesnykh ob"yektov). Leningrad, Izd. Leningrad. univers. im. A.A.Zhdanova, 1948.
6. Rubin, B.A.: Plant Physiology (Fiziologiya rasteniy). Moscow, Sovets. Nauka, 1954.

V.S.Sokolova

Several authors (Bibl.1) have de..o..⸱crated that the optical properties of plants do not always reflect basic chemical changes occurring within the organism. This is due to the fact that a change in optical properties is not directly related to a change in chemical composition. Extensive chemical conversions may only negligibly, or not at all, affect the chromophore group of atoms and thus cannot cause marked changes in the spectra of light reflection and transmission. However, also the reverse may be true: An insignificant (for chemical processes) regrouping or change of atoms in the chromophore group might markedly change the optical properties. The members of the Astrobotany Sector have found that the optical properties of plants change with the height of their habitat (Bibl.3, 4). This characteristic of plants was explained by environmental conditions, without penetrating into the physical essence of the organism.

This article is to confirm this phenomenon and give certain bases for its explanation.

1. Working Method

The specimens were photographed by a superhigh-transmission spectrograph on Ilford Special plates. To obtain the spectra in reflected and transmitted light and the indicatrix in the same rays, the objects were photographed with suitable attachments. A detailed description of the latter is given in our preceding article.

The coefficients of spectral brightness of both reflected and transmitted rays were obtained by the usual method of spectrophotometry (Bibl.2).

2. Results

The objects investigated were the geranium (Geranium collinum Steph.) and the yellow poppy (Papaver alpinum L.). These plants were spectrographed in 1956 in the mountains of Zailiyskiy Alatau at three points:

1) Ust'-Gorel'nik near the hydroelectric power plant. The elevation of the site was 1850 m above sea level.

2) Vorota - Camp Lokomotiv. Elevation, 2100 m above sea level.

3) Myn-Zhilki. Elevation, 3000 m above sea level.

In all, we obtained 18 negatives, of which 11 with 20 spectra on each   /26
were intended for obtaining spectra in reflected and transmitted light, while the other seven with 40 spectra on each were for obtaining the indicatrix in

reflected and transmitted light.

For each object, we plotted the indicatrix at nine wavelengths, both for diffusely reflected and for transmitted light.

The brightness coefficients of the petal and leaf in reflected and transmitted light were determined with consideration of the indicatrix. All plotted indicatrices were divided into the following groups:

1) Those extended in an equatorial direction;
2) Those extended in a polar direction;
3) Intermediate.

For each group, we determined the correction coefficient. The flowers and leaves of the geranium and the flowers and leaves of the yellow poppy had indicatrices close to a spherical indicatrix in reflected light.
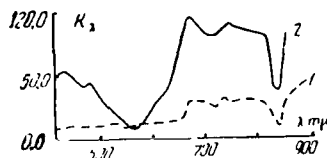
Fig.1 Myn–Zhilki.   Curves of Spectral Brightness
of the Geranium Petal
1 – In reflected light; 2 – In transmitted light

In transmitted light, the yellow poppy had an indicatrix extended in a polar direction.

Geranium (Geranium collinum Steph.)

1. Myn–Zhilki.

Air temperature $t = +27.0°$ C; time of photographing 17:30 – 17:50, July 22, 1956.

The spectral brightness curve of the petal in reflected light has two maxima and two minima (Fig.1).

Maxima: a) from 670 to 820 mμ, with a highest value of 37%; b) from 860 to 890 mμ, 54%.

Minima: a) from 400 to 660 mμ, with a lowest value of 16%; b) from 830 to 860 mμ, 12%.

The spectral brightness curve of the petal in transmitted light has three maxima and two minima.

27

Maxima: a) from 400 to 520 mμ, with a highest value of 68%; b) from 640 to 820 mμ, 120%; c) from 820 to 860 mμ, 105%.

Minima: a) from 520 to 640 mμ, with a lowest value of 9%; b) from 830 to 850 mμ, 46%.

Both curves are almost everywhere smooth.

2. Vorota.

Air temperature t = +25.0°C, time of photographing 12:40 - 12:40.

The spectral brightness curve of the petal in reflected light has two maxima and two minima (Fig.2).

Fig.2 Vorota - Camp Lokomotiv. Curves of Spectral
Brightness of Geranium
1 - Petal in reflected light; 2 - In transmitted
light; 3 - Leaf in reflected light; 4 - Leaf in
transmitted light

Maxima: a) from 500 to 560 mμ, with a highest value of 21%; b) from 720 to 820 mμ, 35%.

Minima: a) from 400 to 490 mμ, with a lowest value of 12%; b) from 570 to 610 mμ, 15%.

The spectral brightness curve of the petal in transmitted light has two maxima and two minima.

Maxima: a) from 400 to 500 mμ, with a highest value of 118%; b) from 630 to 840 mμ, 170%.

Minima: a) 400 mμ, with a lowest value of 25%; b) from 500 to 600 mμ, 22%.

The spectral brightness curve of the leaf in reflected light has one maximum and one minimum.

Maximum: a) from 720 to 860 mμ, with a highest value of 35%.

Minimum: a) from 400 to 700 mμ, with a lowest value of 6%.

28

The spectral brightness curve of the leaf in transmitted light has two maxima and two minima.

Maxima: a) from 510 to 640 mµ, with a highest value of 57%; b) from 690 to 840 mµ, 180%.

Minima: a) from 450 to 510 mµ, with a lowest value of 7%; b) from 640 to 680 mµ, 7%.

The spectral brightness curves of the petal and leaf in reflected and transmitted light are not smooth and have sharp projections over the entire spectrum with a maximal value in the blue and red regions.
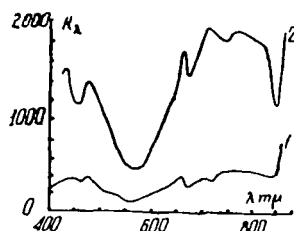
Fig.3 Ust'–Gorel'nik. Curves of Spectral Brightness
of the Geranium Petal
1 – In reflected light; 2 – In transmitted light

3. Ust'–Gorel'nik.

Air temperature t = +32.0°C; time of photographing 16:15.

The spectral brightness curve of the petal in reflected light has two maxima and one minimum (Fig.3).

Maxima: a) from 400 to 500 mµ, with a highest value of 40%; b) from 660 to 850 mµ, 46%.

Minimum: a) from 520 to 620 mµ, with a lowest value of 12%.

The spectral brightness curve of the petal in transmitted light has three maxima and two minima.

Maxima: a) from 400 to 520 mµ, with a highest value of 150%; b) from 620 to 820 mµ, 195%; c) at 860, 190%.

Minima: a) from 500 to 630 mµ, with a lowest value of 50%; b) at 850 mµ, 115%.

The spectral brightness curves in reflected and in transmitted light are not smooth and have sharper projections in the blue and red regions than such curves for geranium growing at Lokomotiv.

29

Yellow Poppy (Papaver alpinum L.)

1. Myn-Zhilki.

Elevation 3000 m above sea level, air temperature t = +27.0°C; time of photographing 17:15 - 17:25.

The spectral brightness curve of the petal in reflected light has two maxima and two minima (Fig.4).
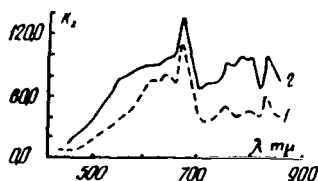
Fig.4 Myn-Zhilki. Curves of Spectral Brightness
of Yellow Poppy Petal
1 - In reflected light; 2 - In transmitted light

Maxima: a) from 510 to 690 mμ, with a highest value of 110%; b) from 820 to 850 mμ, 62%.

Minima: a) from 420 to 510 mμ, with a lowest value of 5%; b) from 670 to 740 mμ, 35%.

In transmitted light, three maxima and three minima.

Maxima: a) from 510 to 700 mμ, with a highest value of 140%; b) from 740 to 810 mμ, 100%; c) from 820 to 860 mμ, 100%.

Minima: a) from 420 to 480 mμ, with a lowest value of 12%; b) from 620 to 740 mμ, 66%; c) at 820 mμ, 70%.

The spectral brightness curves both in reflected and transmitted light are not smooth, have sharp projections, and very high values in the yellow, red, and infrared regions of the visible portion of the spectrum.

2. Vorota - Camp Lokomotiv.

Elevation 3000 m above sea level, air temperature t = +29.0°C, time of photographing 15:35 - 15:50.

The spectral brightness curve of the yellow poppy petal in reflected light has two maxima and two minima (Fig.5).

Maxima: a) from 550 to 750 mμ, with a highest value of 49%; b) from 820 to 850 mμ, 59%.

30

Minima: a) from 400 to 520 mμ, with a lowest value of 9%; b) from 750 to 810 mμ, 22%.

The spectral brightness curve of the petal in transmitted light has one maximum and one minimum.

Maximum: from 510 to 850 mμ, with a highest value of 220%.

Minimum: from 420 to 460 mμ, with a lowest value of 20%.

The spectral brightness curve of the leaf in reflected light has two maxima and two minima.

Maxima: a) from 510 to 540 mμ, with a highest value of 18%; b) from 700 to 840 mμ, 30%.

Minima: a) from 400 to 500 mμ, with a lowest value of 2%; b) from 600 to 690 mμ, 0.5%.

Fig.5 Vorota – Camp Lokomotiv. Curves of Spectral Brightness of Yellow Poppy
1 – Petal in reflected light; 2 – Petal in trans-mitted light; 3 – Leaf in reflected light; 4 – Leaf in transmitted light

The spectral brightness curve of the leaf in transmitted light has two maxima and two minima (Fig.5).

Maxima: a) from 510 to 650 mμ, with a highest value of 33%; b) from 690 to 850 mμ, 180%.

Minima: a) from 400 to 690 mμ, with a lowest value of 5%; b) from 650 to 690 mμ, 8%.

The spectral brightness curves of the petal and leaf both in reflected   /29
and in transmitted light have very high maxima and very deep minima.

The maximum of the petal belongs to the yellow region and, to an appreciably smaller extent, to the red and infrared region of the visible portion of the spectrum. The maxima of the spectral brightness curve of the leaf are located in the red and infrared regions and appreciably less in the yellow region.

3. Ust'-Gorel'nik.

Height 1850 m above sea level, air temperature ‘ = +32.0°C; time of photographing 13:17 – 13:32.

The spectral brightness curve of the petal of the yellow poppy in reflected light has one maximum and one minimum (Fig.6).

Maximum: from 510 to 780 mμ, with a highest value of 62%.

Minimum: from 400 to 490 mμ, with a lowest value of 8%.

The spectral brightness curve of the petal in transmitted light has one maximum with two values and one minimum.

Maximum: from 480 to 760 mμ, with a highest value of 168 and 280%.

Minimum: from 400 to 480 mμ, with a lowest value of 20%.

The spectral brightness curves of the leaf both in reflected and transmitted light have two maxima each and two minima each.
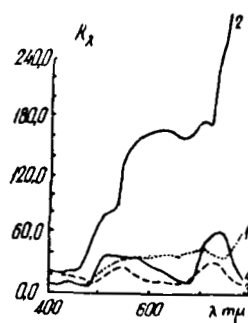
Fig.6 Ust'-Gorel'nik. Curves of Spectral Brightness
of the Yellow Poppy
1 – Petal in reflected light; 2 – Petal in transmitted
light; 3 – Leaf in reflected light; 4 – Leaf in trans-
mitted light

In Reflected Light:

Maxima: a) from 490 to 630 mμ, with a highest value of 25%; b) from 700 to 770 mμ, 33%.

Minima: a) from 420 to 500 mμ, with a lowest value of 8%; b) from 640 to 690 mμ, 10%.

In Transmitted Light:

Maxima: a) from 490 to 630 mμ, with a highest value of 35%; b) from 700

32

to 780 mμ, 63%.

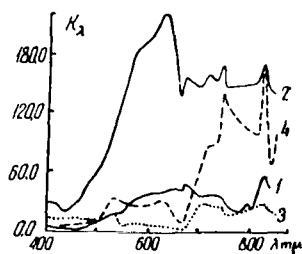Minima: a) from 440 to 480 mμ, with a lowest value of 7%; b) from 640 to 690 mμ, 10%.

The spectral brightness curves of the petal in reflected and transmitted light have very high maxima and deep minima. The maxima of the leaf are less high. The minima of the petal are located in the yellow, red, and infrared regions. It is interesting to note that the maxima and minima of the leaf coincide with respect to regions with the maxima and minima of the petal.

3. Conclusions

1. The flowers of the geranium and yellow poppy, like the flowers of the iris, have two maxima in the spectral brightness curves of the petal in reflected and transmitted light. The region of the first maximum depends on /30 the color of the flower and coincides in color with that of the petal, i.e., for a red flower the maximum is located in the red region of the spectrum, for a yellow flower in the yellow region, etc.

The second maximum is similar for all these flowers with respect to location in the spectrum and is in the red and infrared regions.

2. At these maxima, the mentioned objects show complete transmittance plus a strong complementary light.

3. The spectral brightness curves of the petal and leaf, for the same flower in reflected and transmitted light, are very similar.

4. The maxima of the spectral brightness curves for the same flower change with elevation above sea level of the habitat of the object, i.e., the maximum diminishes with increasing elevation.

It should be noted that such a comparison can be made only if similar conditions of temperature, time of spectrographing, and humidity are maintained. In our case, strict fulfillment of the requirement was impossible because of climatic conditions; nevertheless, a comparison can be made between Figs.1 and 3 and Figs.4 and 5.

5. The optical properties of the chromophore group depend less on the chemical processes than on the physiological processes associated with assimilation of light energy and organic substances, this being a function of the environment.

BIBLIOGRAPHY

1. Lyubimenko, V.N. and Brilliant, V.A.: Plant Colors (Okraska rasteniy). Leningrad, Gosizdat, 1924.
2. Tikhov, G.A.: Principles of Visual and Photographic Photometry (Osnovy

vizual'noy i fotograficheskoy fotometrii). Alma-Ata, Izd. Akad. Nauk
  KazSSR, 1950.
3. Sokolova, V.S.: Trudy Sektora astrobotaniki, Vol.II, Alma-Ata, Izd. Akad.
  Nauk KazSSR, 1953.
4. Kozlova, K.I.: Spectrophotometry of Plants of Various Climatic Zones in
  Reflected Rays (Spektrofotometriya rasteniy razlichnykh klimaticheskikh
  zon v otrazhennykh luchakh). Alma-Ata, Izd. Akad. Nauk KazSSR, 1956.

OPTICAL PROPERTIES AND PHOTOSYNTHESIS OF CERTAIN SPECIES
OF CULTIVATED AND WILD PLANTS IN RELATION TO
ECOLOGICAL CONDITIONS

G.S.Gorbunova, Z.S.Parshina, and V.P.Bedenko

The purpose of the work reported here was to define the characteristics of the optical properties of plants and photosynthesis in relation to the conditions of the geographical latitude of the locale, i.e., the various ecological zones.

The observations were carried out in the territory of the Soviet Union along a meridian starting from the high North and ending in the deep South. The northern point of this line was Tiksi Bay ($73^{\circ}35'$ N), the southern point Blagoveshchensk (50° N), and the intermediate point Yakutsk (62° N). Thus, the total length from North to South was 21°, or about 2500 km.

The investigations were carried out from June to September 1957. The optical properties of the plants were studied by the method of relative spectrophotometry (Bibl.15 - 21). Photosynthesis was determined by the half-leaf method 24 hours a day at 3-hour intervals with calculations in dry weight per unit surface of leaves per hour and per 24-hour period. The productivity during the entire growing season was calculated for certain plants (at two points, Yakutsk and Blagoveshchensk).

1. Objects of the Investigations

For the investigations, we used two representatives of wild plants which are common along the above geographical line. Because of the impossibility to select their widespread species, the investigations were carried out within one genus (Betula, Salix). At all points the cultivated cosmopolitan plants were sown in soil by the same farming method: Viner barley, white-tipped rose radish, Khibin Chinese cabbage, and early rose potatoes (with the exception of Tiksi). All the seeds of the crop plants were of Yakutsk reproduction.

In view of the various climatic conditions, the plants at all points were sown at different periods, but the investigations of the physiological processes and optical properties of the plants were carried out at the same developmental stages, mainly three times during the growing season: 1) at the vegetation stage (tillering); 2) at the blooming stage (heading); 3) at the mature stage (milk ripeness).

Sowing of the crop plants and investigation of the physiological processes were carried out by the staff of the Laboratory of Plant Physiology, Yakutsk branch of the USSR Academy of Sciences. The optical properties of the plants were studied by members of the Astrobotany Sector of the Kazakh Academy of Sciences.

Tiksi Bay, on the shore of the Laptev Sea, is in the tundra zone. The relief of this region is monticulate. The temperature during the winter drops to $-40^{\circ}C$ and, during the summer, does not rise above $+15^{\circ}C$. Rainfall is scanty, but as a consequence of the scarcity of sunny days and the short summer, evaporation is negligible; consequently, there is an excess of moisture. The soils which freeze during the winter do not have time to thaw in the summer, and the layer of permafrost is close to the surface. The harsh climate of this region excessively limits the growing season and the constitution of the species.

Vegetation is represented mainly by various species of mosses and lichens; dwarf willows, birches, and blueberries are encountered rather frequently. Aside from the small vegetable plots of the Tiksi Experimental Station, no vegetable crops are raised.

The vicinity of Yakutsk on the left bank of the Lena River is in the taiga region. The continentality of the climate at Yakutsk reaches its most extreme degree: very low temperatures in the winter dropping on the average to $-40^{\circ}C$ and excessively high summer temperatures. There is very little rainfall, about 200 mm in all during the year; the largest amount usually falls during August. Owing to the dearth of precipitation, there is an abundance of sunny days during the year. These conditions nevertheless permit the development of vegetable plants.

The region is rich in a diversity of species of woody and, especially, herbaceous forms. The most characteristic are larch, pine, willow, and birch. Alder is sometimes found. Blueberries, cowberries, cloudberries, and frequently mosses and lichens grow in the underbrush.

The herbaceous cover is represented by members of the sedge family and grass family.

The region of Blagoveshchensk on the left bank of the Amur River is a forest-steppe zone. The climate here is quite unique. The amount of heat which this region receives does not correspond to its geographical location, since the proximity of the Asiatic Continent with its heavy winter frosts has a great influence on the climate. The winter is cold, dry, clear, with little snow; the spring is late, drawn out, cold, arid; the summer is hot, rains are abundant, and the fall is dry and warm. The winter temperatures on the average drop to $-24^{\circ}C$ and the summer temperatures reach $+40^{\circ}C$. The growing season is about 170 days. The abundant precipitation in the second half of the summer (July-August), in combination with the high humidity and high temperatures, create the atmosphere of a "hothouse". The high relative moisture content of the soils, which, after rains, reaches 100%, causes the presence of capillary water in the soil profile. Fragments of Far-Eastern flora wedge into the vegetation of the transition zone from the steppes to the forests.

Measurements of the air temperature, relative humidity, soil temperature at the surface and at a depth of 10 and 20 cm were taken during observations of

TABLE 1

METEOROLOGICAL DATA OF 1957

Index	Tiksi					Yakutsk					Blagoveshchensk				
	May	June	July	August	Average for Growing Season	May	June	July	August	Average for Growing Season	May	June	July	August	Average for Growing Season
Air temperature	−6.7	+4.1	+7.2	+7.7	+3.3	13.4	16.8	20.3	17.4	17.2	11.9	18.1	19.7	18.4	17.8
Relative humidity, %	88	84	77	77	82	—	—	—	—	54	56	61	83	82	70
Soil temperature at surface (minimal)	−17.7	−0.7	+1.2	−1.2	−4.9	0.1	4.1	8.3	7.6	6.7	5.4	9.9	12.7	10.3	9.5
Soil temperature at depth of 10 cm	—	—	—	—	—	11.9	17.1	18.5	13.9	15.3	13.8	19.7	21.0	20.1	18.7
Soil temperature at depth of 20 cm	—	—	—	—	—	8.5	14.4	15.7	12.6	12.8	11.0	16.9	18.6	18.8	16.4
Precipitation, mm	23.9	45.4	—	22.4	81.6	35	12.5	14.0	16.9	78.4	13.8	33.9	122	102.2	271.9

TABLE 2

PHENOLOGICAL OBSERVATIONS, 1957

Developmental Stages	Tiksi				Yakutsk				Blagoveshchensk		
	Barley	Radishes	Chinese Cabbage	Potatoes	Barley	Radishes	Chinese Cabbage	Potatoes	Barley	Radishes	Potatoes
Sowing	21 June	22 June	22 June	22 June	24 May	24 May	24 May	26 May	16 May	16 May	16 May
Germination	24 June	28 June	29 June	17 July 10 Aug.	31 May	29 May	30 May	16 June	23 May	23 May	11 June
Third leaf (tillering)	22 July	25 July	25 July	(Winter-killed)	10 June	15 June	—	—	5 June	3 June	—
Fifth leaf	5 Aug.	24 Aug.	27 Aug.	—	12 June	27 June	—	—	9 June	18 June	—
Shooting	—	—	—	—	16 June	—	—	—	20 July	—	—
Heading (budding)	—	—	—	—	2 July	8 July	10 July	28 June	8 July	6 July	1 July
Flowering	—	—	—	—	10 July	29 July	9 July	31 July	11 July	28 July	9 July
Ripeness (milky-wax, complete)	—	—	—	–	22 July 2 Aug. 8 Aug.	25 July	—	2 Sept.	22 July 1 Aug. 10 Aug.	25 June	10 Aug.

both the physiological processes and optical properties. The average meteorological data for the summer of 1957 are given by months in Table 1. In view of the different climatic conditions the stages of plant development occurred at different times, but the observations of the physiological properties and optical properties of the plants were timed to certain developmental stages. The data of the phenological observations of the plants at various points on the meridian are given in Table 2.

3. Optical Properties and Photosynthesis of Plants

An organism and its environment are one – this is the basic law of the Michurin biology. Organisms, during their development, adapt to various environmental conditions.

Thus, representatives of the plant world can be found in different habitats: in deserts, humid subtropics, cold antarctic, on solonchak soil, in sands, hot springs, etc. Everywhere one meets with the surprising adaptability of plants to the environmental conditions, expressed in various degrees and forms. For example, plants in the desert adapt to less evaporation of moisture by reducing their evaporating surface, by reducing the number of stomata, and by thickening of the cuticle (in succulents), by growing a thick layer of hairs on the leaves and a waxy coat (sagebrush, etc.), and so on. In cold habitats, plants are short and have a high metabolic rate. Growing on various soils, they exhibit numerous morphological adaptations and various physiological properties.

The variability of organisms ensures their extensive adaptability, resulting a broad distribution of vegetation. However, another noteworthy aspect of variability is the conservation of heredity. As is known, mutations caused by environment can be inherited, when reinforced by the same environmental conditions year after year. An organism which chances to exist under conditions not characteristic for it, will conserve, during the first year of life, the inherent properties of its former habitat.

The optical properties of plants, which are an external manifestation of physiological processes, in particular of photosynthesis, may either change under the effect of environmental conditions or remain conservative (under certain conditions).

Various members of the Astrobotany Sector (Bibl.19, 20, 23) detected changes in the optical properties of plants, in relation to seasons and zonal-ecological conditions. Our investigations, which were carried out with cultivated plants along the meridian at the points indicated above, showed that their optical properties during the first year of sowing (seeds of the same Yakutsk reproduction) in different ecological regions did not change in the visible region of the spectrum (Figs.1 – 3). The spectral brightness curves in reflected and transmitted light for radishes, potatoes, and barley are shown in the accompanying diagrams.

These show that the reflection curves for all investigated plants are the same for different areas in the visible spectrum region. Only slight differ-

39

Fig.1 Curves of Spectral Brightness of
Radish Leaves (Raphanus sativus var.
minor) in Reflected (A) and Transmitted
(B) Light
1 - Blagoveshchensk; 2 - Yakutsk;
3 - Tiksi

Fig.2 Curves of Spectral Brightness of
Potato Leaves (Solanum tuberosum) in
Reflected (A) and Transmitted (B) Light
1 - Blagoveshchensk; 2 - Yakutsk;
3 - Tiksi
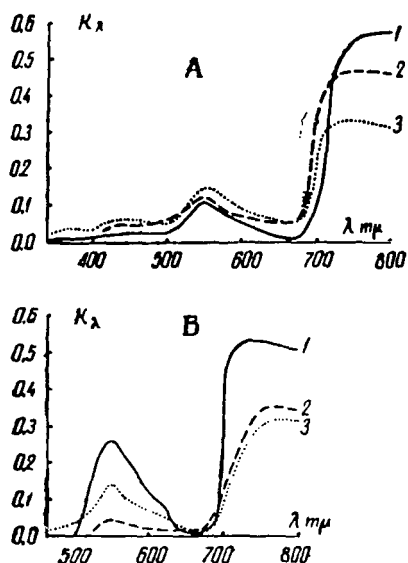
Fig.3 Curves of Spectral Brightness of
Barley Leaves (Hordeum sativum) in Re-
flected (A) and Transmitted (B) Light
1 - Blagoveshchensk; 2 - Yakutsk;
3 - Tiksi
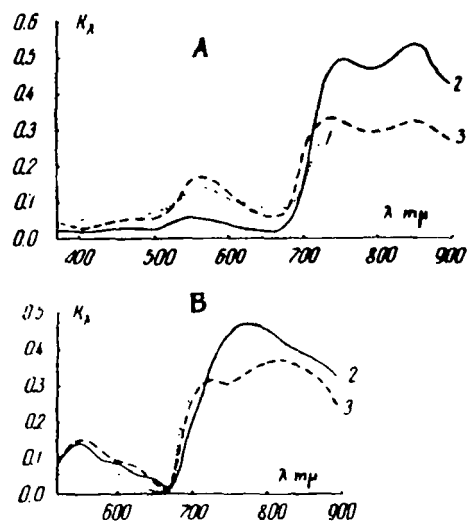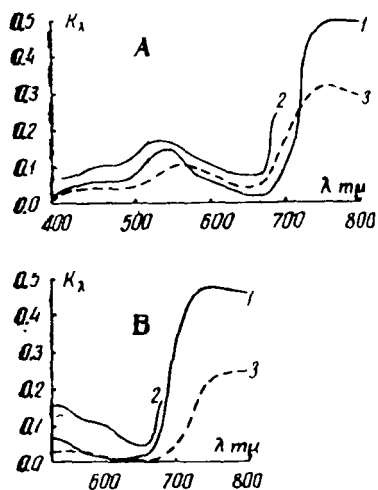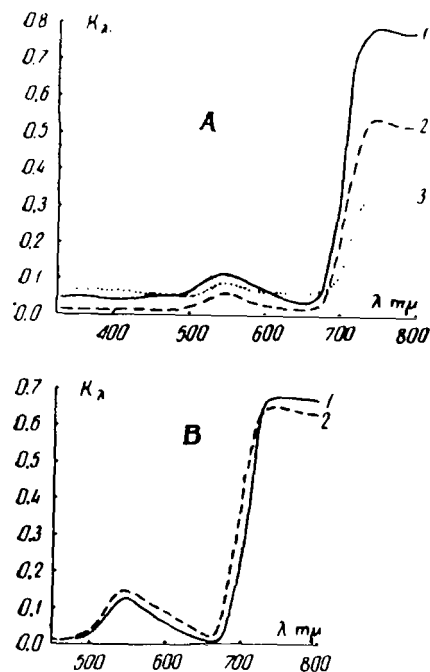
Fig.4 Curves of Spectral Brightness of
Goat-Willow Leaves (Salix caprea) in
Reflected (A) and Transmitted (B) Light
1 - Blagoveshchensk; 2 - Yakutsk;
3 - Gray-leaved willow (Salix glauca),
Tiksi

TABLE 3

SPECTRAL BRIGHTNESS COEFFICIENTS OF THE LEAVES OF RADISHES, BARLEY, AND POTATOES IN REFLECTED AND TRANSMITTED LIGHT

| Wave-length | Blagoveshchensk | | | | Yakutsk | | | | Tiksi | | | |
| | Radish | | Barley | | Radish | | Potato | | Barley | | Potato | |
	Re-flected	Trans-mitted	Re-flected	Trans-mitted	Re-flected	Trans-mitted	Re-flected	Trans-mitted	Re-flected	Trans-mitted	Re-flected	Trans-mitted
340	0.009	—	—	—	—	—	—	—	—	—	—	—
348	0.0115	—	—	—	—	—	—	—	—	—	—	—
362	0.0168	—	—	—	—	—	—	—	—	—	0.0391	—
391	0.0115	—	0.0149	—	—	—	0.0486	—	0.0198	—	0.0306	—
415	0.0235	—	0.0434	—	0.0373	—	0.0656	—	0.0353	--	0.0365	—
420	0.0225	—	0.0456	—	0.0495	—	0.0672	—	0.0373	—	0.0413	—
440	0.0252	—	0.0510	—	0.0527	—	0.0663	—	0.0403	—	0.0492	-
449	0.0263	—	0.0547	—	0.0192	—	0.0687	—	0.0407	—	0.0492	—
459	0.0286	—	0.0527	—	0.0558	—	0.0695	—	0.0451	—	0.0481	--
468	0.0310	—	0.0566	—	0.0605	—	0.0970	—	0.0458	—	0.0515	—
478	0.0265	—	0.0618	—	0.0495	—	0.0727	—	0.0463	—	0.0508	—
498	0.0260	—	0.0705	—	0.0592	—	0.0798	—	0.0470	—	0.0539	—
510	0.0310	0.0311	0.0843	—	0.0835	—	0.0907	—	0.0533	—	0.0799	—
522	0.0600	0.146	0.132	—	0.0982	—	0.104	—	0.9736	—	0.110	0.0865
534	0.096	0.255	0.140	—	0.0592	0.0470	0.1208	0.1142	0.0930	—	0.154	0.1295
554	0.114	0.244	0.141	0.0639	0.118	0.0503	0.187	0.142	0.105	—	0.1527	0.1487
560	0.096	0.258	0.128	0.0539	0.0982	0.0317	0.137	0.118	0.105	—	0.165	0.1475
571	0.0778	0.202	0.0924	0.0282	0.078	0.0365	0.118	0.0960	0.104	—	0.140	0.131
581	0.0720	0.170	0.0769	0.0272	0.0982	—	0.105	0.0938	0.0855	—	0.130	0.123
601	0.0545	0.112	0.0701	0.0184	0.0640	—	0.117	0.0855	0.0769	—	0.103	0.105
620	0.0460	0.088	0.0345	—	0.0865	0.0240	0.1003	0.0703	0.0682	—	0.0855	0.0413
612	0.0428	0.0730	0.0504	—	0.0711	0.0240	0.1114	0.0648	0.0688	—	0.0807	0.0790
617	0.0396	0.0738	0.0424	—	0.0679	—	0.0980	0.0663	0.0663	—	0.0842	0.0835
621	0.0422	0.0715	0.0475	—	0.0679	—	0.0960	0.0578	0.0592	—	0.0790	0.0817
625	0.0342	0.0348	0.0434	—	0.0663	—	0.0960	0.0508	0.0648	—	0.0865	0.0760
629	0.0260	0.0237	0.0398	—	0.0817	—	0.1064	0.0565	0.0604	—	0.0835	0.0662
632	0.0235	0.0148	0.0341	—	0.0727	—	0.0855	0.0198	0.0552	—	0.0744	0.0578
637	0.0231	—	0.0267	—	0.0619	—	0.0865	0.0456	0.0515	—	0.0610	0.0454
648	0.0185	—	0.0225	—	0.0865	—	0.0938	—	0.0476	—	0.0671	0.0294
652	0.0187	—	0.0261	—	0.0663	--	0.0938	—	0.0448	--	0.0592	0.0255
654	0.0222	—	0.0284	—	0.0649	—	0.0760	—	0.0448	—	0.0688	0.0290
659	0.0244	—	0.0318	—	0.0641	0.0344	0.0817	—	0.0412	—	0.0572	0.0163
662	0.0349	0.0410	0.0330	—	0.0687	0.0565	0.0807	—	0.0410	—	0.0652	—
666	0.0527	0.117	0.0345	—	0.0835	0.0770	0.0917	—	0.0433	—	0.0633	0.0209
671	0.094	0.258	0.0655	0.0149	0.0786	0.084	0.0744	0.0244	0.0509	—	0.0865	0.0137
677	0.144	0.352	0.1115	0.0374	0.1295	0.104	0.0895	0.0419	0.0695	—	0.147	0.0968
680	0.163	0.386	0.149	0.0560	0.1668	0.0938	0.110	0.0616	0.0695	.01486	0.161	0.118
685	0.202	0.402	0.196	0.122	0.2094	0.0770	0.140	0.110	0.104	0.0213	0.217	0.185
691	0.214	0.382	0.274	0.208	0.253	0.0817	0.1748	0.154	0.1324	0.0329	0.266	0.235
698	0.234	0.410	0.322	0.286	0.348	0.1126	0.246	0.214	0.168	0.0391	0.278	0.255
705	0.246	0.433	0.348	0.280	0.438	0.1064	0.293	0.268	0.202	0.0528	0.307	0.283
710	0.368	0.566	0.378	0.328	0.382	0.0907	0.397	0.308	0.214	0.0727	0.330	0.277
715	0.277	0.462	0.493	0.415	0.438	0.0884	0.419	0.297	0.315	0.104	0.449	0.369
730	0.244	0.405	0.429	0.470	0.398	0.0454	0.501	0.348	0.310	0.135	0.344	0.297
735	—	—	—	—	0.356	—	0.499	0.350	0.322	0.1293	0.310	0.290
741	—	—	--	—	0.386	—	0.518	0.286	0.318	0.1215	0.334	0.300
748	—	—	—	—	0.481	—	0.664	0.336	0.359	0.133	0.308	0.282
760	..	—	—	—		—	0.344	0.258	0.279	0.300	0.280	0.235
770	—	—	—	—	0.341	0.409	0.419	0.401	0.317	0.294	0.274	0.341
800	—	—	—	—	0.459	0.352	0.492	0.267	0.286	0.246	0.307	0.365
830	—	—	—	—	0.520	0.352	0.537	0.393	0.279	0.260	0.323	0.389
840	—	—	—	—	0.499	0.290	0.537	0.333	0.281	0.261	0.322	0.395
850	—	—	—	—	0.283	0.258	0.503	0.314	0.279	0.261	0.312	0.396
855	—	—	—	—	0.459	0.231	0.487	0.308	0.291	0.258	0.296	0.356
860	—	—	—	—	0.503	0.212	0.470	0.216	0.290	0.253	0.293	0.323
865	—	—	—	—	0.492	0.253	0.470	0.272	0.266	0.238	0.277	0.305
870	—	—	—	—	0.481	—	0.438	0.246	0.267	0.241	0.258	0.283
880	—	—	—	—	0.270	0.241	0.322	0.322	0.280	0.230	0.217	0.241
885	—	--	—	—	0.400	0.332	0.268	—	0.249	—	—	—

ences are observed in the value of the brightness coefficients for different wavelengths (Table 3).

The same pattern is observed on examining the transmission curves. In the infrared spectrum region, there is a certain drop in the reflection and transmission of infrared radiation as these plants move North,which apparently ensures an increase of the vegatative mass during the short growing period of these plants in the North.
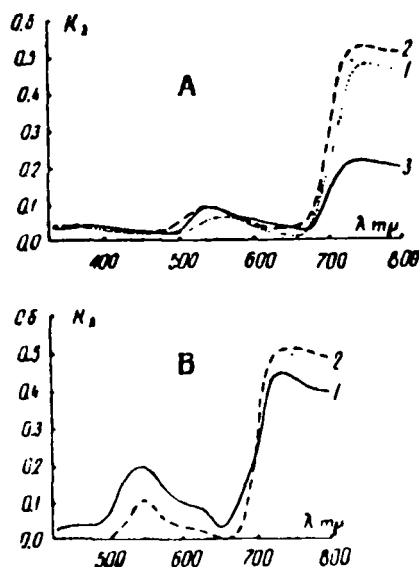
Fig.5 Curves of Spectral Brightness of White-Birch Leaves
(Betula verrucosa) in Reflected (A) and Transmitted
(B) Light
1 - Blagoveshchensk; 2 - Yakutsk; 3 - Dwarf Arctic birch
(Betula nana), Tiksi

The observations of wild plants (willow and birch, Figs.4 - 5, Table 4) showed that reflection and transmission drop slightly over the entire spectrum, with higher geographic latitude of the locale (i.e., from South to North).

We also studied the optical properties of plants at various developmental stages and in relation to leaf age.   /39

Figure 6 (Table 5)shows the spectral reflectance and transmittance curves of barley, recorded at Yakutsk at the stages of incipient heading and blossoming. It is apparent from the diagrams that the lowest reflection and transmission in the region of the main absorption band of chlorophyll is observed at the beginning of the tillering stage and that the profile of the main absorption band of chlorophyll is quite distinct on the spectral curves. At the flowering stage we observe a broadening of the profile of the main absorption band of chlorophyll owing to a decrease in reflection and transmission of orange, yellow, and green rays; a general drop of the brightness coefficients at the other wavelengths is also observed. Figure 7 (Table 5) shows the spectral reflectance

TABLE 4 /38

SPECTRAL BRIGHTNESS COEFFICIENTS OF WILLOW AND BIRCH LEAVES IN REFLECTED AND TRANSMITTED LIGHT

| Wavelength | Yakutsk | | | | Tiksi | | Blagoveshchensk | | | |
| | Birch | | Willow | | Birch | Willow | Birch | | Willow | |
	Reflected	Transmitted	Reflected	Transmitted	Reflected	Reflected	Reflected	Transmitted	Reflected	Transmitted
414	0,050	—	0,033	—	0,020	0,048	—	—	—	—
420	051	—	033	—	022	047	0,031	—	—	—
427	052	—	032	0,03(	—	—	—	—	—	—
439	056	—	035	033	025	055	012	),023	0,006	0,016
451	056	0,028	035	042	027	056	028	027	004	018
463	055	032	034	047	028	056	027	026	002	017
474	062	039	038	058	027	054	026	029	001	018
494	052	052	033	148	—	—	—	—	—	—
506	038	059	054	678	031	061	027	043	019	042
512	—	063	058	118	032	058	026	079	—	039
521	—	085	063	135	056	069	080	148	028	152
533	079	144	089	204	048	077	095	208	023	159
544	100	178	100	234	068	097	096	188	029	192
550	105	169	102	229	060	094	028	158	023	174
562	120	186	107	234	062	089	095	165	022	147
568	120	195	100	157	062	082	066	133	016	127
573	120	191	096	251	—	—	—	—	—	—
579	107	178	089	229	254	072	059	114	014	099
597	076	129	066	182	—	—	—	—	—	—
602	076	126	068	186	060	069	039	100	012	080
608	078	126	0-6	178	054	066	030	079	004	063
614	078	126	065	169	050	064	033	095	002	071
620	076	115	060	155	052	065	032	097	003	061
626	071	115	055	151	052	065	032	084	—	057
631	069	107	054	144	050	063	028	073	—	048
637	071	107	054	144	046	063	029	066	—	042
643	071	107	050	138	043	060	025	056	—	032
649	072	100	046	123	043	064	022	038	—	021
652	071	091	045	110	038	059	019	033	—	015
660	063	074	041	093	037	058	022	034	—	016
664	063	072	041	085	034	053	020	038	—	017
667	059	058	039	076	—	—	—	—	—	—
671	059	051	039	069	034	055	022	062	—	027
675	059	048	039	065	034	058	034	113	—	074
679	059	047	042	065	042	062	062	177	052	148
683	063	054	047	068	059	070	108	208	037	233
691	069	079	081	102	085	086	140	227	051	291
695	096	138	118	162	—	—	—	—	—	—
699	141	223	141	245	121	119	162	220	073	287
703	199	316	182	302	148	150	149	202	068	269
707	257	—	174	324	156	194	219	251	123	292

and transmittance curves of barley, recorded at Blagoveshchensk at the tillering and heading stages. It is also apparent that, in the earliest phase of de- /41 velopment (tillering), the profile of the main absorption band of chlorophyll is quite pronounced, i.e., reflection and transmission of the red spectrum rays is lowest. At the heading stage, the main absorption band smoothes out, due to a decrease in reflection and transmission of orange and yellow rays.

TABLE 5

/39

SPECTRAL BRIGHTNESS COEFFICIENTS OF BARLEY LEAVES IN REFLECTED AND TRANSMITTED LIGHT

Wave-length	Yakutsk				Blagoveshchensk			
	Heading Stage		Flowering Stage		Tillering Stage		Heading Stage	
	Re-flected	Trans-mitted	Re-flected	Trans-mitted	Re-flected	Trans-mitted	Re-flected	Trans-mitted
414	0.046	—	0.056	0.036	0.043	—	0.020	—
420	046	—	058	037	045	—	015	—
427	047	—	056	037	—	—	—	—
439	048	—	055	038	051	—	028	—
451	047	—	058	047	054	—	—	—
463	044	—	056	051	056	—	029	—
474	045	—	054	051	062	—	020	—
494	043	—	059	064	070	—	016	—
506	044	0.058	—	—	—	—	—	—
512	045	072	060	085	094	—	028	—
521	060	087	068	151	132	—	039	—
533	083	118	126	209	140	—	048	—
544	077	118	126	229	—	—	—	—
550	081	123	141	239	141	0.064	063	—
562	081	115	129	224	128	054	051	—
568	077	112	123	214	—	—	—	—
573	074	102	118	209	092	028	043	—
579	072	098	112	204	077	027	042	—
597	063	083	087	159	—	—	—	—
602	063	083	085	148	070	018	031	—
608	063	081	085	162	034	—	025	—
614	057	076	081	155	050	—	020	—
620	055	069	074	135	042	—	022	—
626	051	063	069	132	013	—	022	—
631	054	064	064	120	034	—	018	—
637	051	059	064	100	026	—	014	—
643	044	047	060	120	—	—	—	—
649	031	031	052	102	022	—	011	—
652	023	023	049	039	026	—	013	—
660	012	010	048	083	032	—	017	—
664	011	008	047	078	033	—	018	—
667	008	011	045	069	034	—	028	—
671	—	—	045	051	065	149	054	012
675	—	—	045	063	112	037	076	019
679	—	—	046	076	149	056	093	029
683	—	—	051	076	196	122	111	040
691	064	089	068	115	274	208	136	074
695	085	138	110	214	—	—	—	—
699	102	174	144	246	322	286	156	107
703	118	199	186	288	348	280	162	135
707	132	219	—	—	378	328	188	159
715	—	—	—	—	483	415	187	144
730	—	—	—	—	429	470	188	127

Hence, we can conclude that, on transition of the plants from the vegetative stage to the reproductive stage, a decrease in reflection and transmission of solar radiation takes place over the entire investigated region of the spectrum, which apparently ensures optimum supply of plastic substances to the reproductive organs.

The observations carried out on different-age leaves of cabbage, birch, and willow showed that a decrease in reflection and transmission of solar energy takes place with progressing leaf development (Figs.8, 9, 10; Table 6). On the
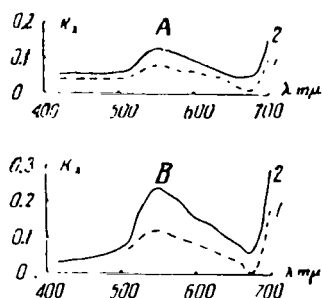
Fig.6 Curves of Spectral Brightness of Barley Leaves
(Hordeum sativum) in Reflected (A) and Trans-
mitted (B) Rays
1 - Heading stage; 2 - Flowering stage
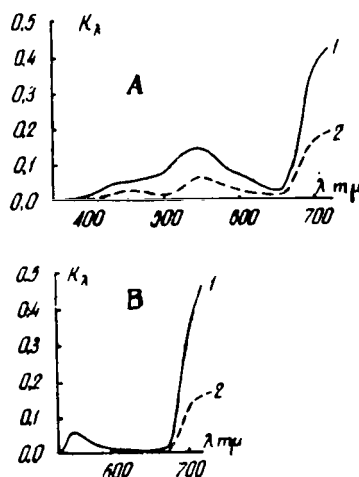
Fig.7 Curves of Spectral Brightness of Barley Leaves
(Hordeum sativum) in Reflected (A) and Transmitted (B)
Light
1 - Tillering stage; 2 - Heading stage

spectral reflectance and transmittance curves, the profile of the main absorption band of chlorophyll for young leaves is quite distinct, due to the lowest reflection and transmission mainly of the red rays of the spectrum at wavelengths of 660 - 680 mμ. In more mature leaves, there is a smoothing out of the profile of the main absorption band of chlorophyll owing to a decrease in reflection and transmission of orange and, partially, of yellow rays. Consequently, as the leaf develops from young to mature, a change occurs in the profile of

the main absorption band of chlorophyll, associated with a decrease in reflection and transmission of various rays of the solar spectrum.
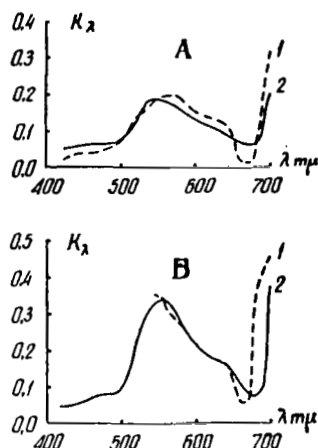
Fig.8 Curves of Spectral Brightness of Different-Age
Leaves of Cabbage (Brassica oleracea v. capitata f.
alba) in Reflected (A) and Transmitted (B) Light
1 - Young; 2 - Mature
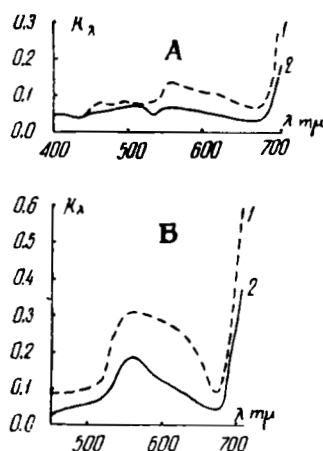
Fig.9 Curves of Spectral Brightness of
Different-Age Leaves of White Birch
(Betula verrucosa) in Reflected (A) and
Transmitted (B) Rays
1 - Young; 2 - Mature
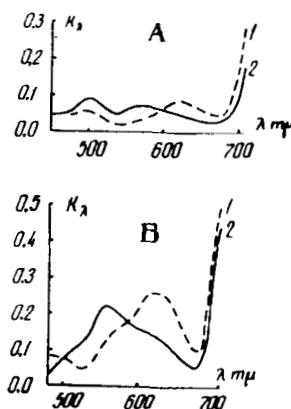
Fig.10 Curves of Spectral Brightness
of Different-Age Leaves of the Goat
Willow (Salix caprea) in Reflected (A)
and Transmitted (B) Light
1 - Young; 2 - Mature

Simultaneously with investigating the optical properties of the plants at all points on the meridian, we calculated the assimilation of these plants. Preliminary investigations (Bibl.14, 15, 16) carried out in 1956 at Tiksi Bay and Yakutsk showed an appreciably greater total absorption of solar energy by the plants at Tiksi than by those at Yakutsk. Corresponding to this, the daily

46

TABLE 6 /42

SPECTRAL BRIGHTNESS COEFFICIENTS OF DIFFERENT-AGE LEAVES OF BIRCH, WILLOW, AND CABBAGE IN REFLECTED AND TRANSMITTED LIGHT

Wavelength	Birch Mature Leaf		Birch Young Leaf		Willow Mature Leaf		Willow Young Leaf		Cabbage Mature Leaf		Cabbage Young Leaf	
	Reflected	Transmitted	Reflected	Transmitted	Reflected	Transmitted	Reflected	Transmitted	Reflected	Transmitted	Reflected	Transmitted
414	0,045	—	—	—	—	—	—	—	0,047	0,046	0,056	—
420	042	—	—	—	—	—	—	—	050	047	020	—
427	047	—	—	—	—	—	—	—	052	049	030	—
439	033	—	—	--	—	—	—	—	059	050	—	—
451	049	0,026	0,056	0,091	—	—	—	—	060	065	—	—
463	049	032	089	091	—	—	—	—	060	071	—	—
474	052	049	076	093	0,063	0,031	0,047	0,084	062	074	—	—
494	059	052	089	098	096	—	062	093	074	091	059	—
506	074	063	079	110	093	—	062	076	—	--	—	—
512	084	084	033	123	096	105	—	085	081	115	121	—
521	—	059	—	132	042	105	—	050	120	214	174	0,128
533	033	076	058	235	027	128	022	048	178	302	174	347
544	048	148	107	275	044	174	022	093	186	324	199	347
550	057	182	123	289	052	204	024	107	195	355	195	324
562	073	191	151	309	074	229	—	145	191	339	195	309
568	065	178	138	317	077	229	033	151	182	363	195	302
573	059	174	132	302	073	224	033	159	174	302	121	283
579	059	183	120	302	068	204	042	174	169	182	144	224
597	049	120	118	296	058	163	066	191	132	229	138	229
602	050	118	118	296	056	169	074	224	126	224	141	214
608	049	118	118	179	054	151	077	229	126	246	132	199
614	049	118	118	179	054	155	085	252	123	246	126	187
620	044	103	110	275	050	148	085	264	115	224	126	182
626	044	084	105	257	048	144	079	283	110	209	132	187
631	042	087	103	257	047	135	079	251	102	195	109	187
637	046	087	093	240	045	126	077	251	100	182	091	155
643	039	076	091	224	039	118	068	224	096	182	604	121
649	035	065	085	199	035	103	069	224	083	162	004	080
652	033	061	079	182	035	096	052	199	078	148	004	089
660	033	055	076	144	027	079	049	162	071	110	003	056
664	033	052	072	135	027	069	059	141	068	098	—	003
667	031	052	072	118	027	065	058	138	065	091	007	091
671	031	059	074	103	027	057	042	118	062	083	087	182
675	036	050	072	098	029	057	046	097	060	081	112	381
679	042	050	072	096	033	060	047	098	059	078	228	408
683	042	052	074	107	039	060	047	120	068	081	283	447
691	055	150	091	178	058	100	091	138	085	107	339	450
695	073	151	118	264	076	148	126	186	120	347	—	—
699	100	252	145	399	107	229	174	263	174	347	—	—
703	126	289	199	447	141	324	216	347	224	407	—	—
707	186	372	276	603	178	437	283	526	—	—	—	—

yield of dry substance in the Tiksi plants exceeded by more than a factor of 1.5 the yield of the Yakutsk plants.

Our present investigations confirmed this assumption, which was indicated by the above data on the optical characteristics of the plants. With respect /43 to photosynthesis, we found that, as the plants advance from South to North, both their mean diurnal rate of photosynthesis and the daily yield of dry sub-

stance increase (Table 7).

The high rate of photosynthesis and of several other biochemical and physiological processes under austere growing conditions has been noted by a number of authors (Bibl.1, 2, 3, 7, 9, 10, 11).

TABLE 7

RATE OF PHOTOSYNTHESIS AND DAILY YIELD OF DRY SUBSTANCE
(in gm per 1 m² per 1 hr)

Plants	Tiksi			Yakutsk			Blagoveshchensk		
	Mean Diurnal Rate	Maximal Rate	Daily Yield	Mean Diurnal Rate	Maximal Rate	Daily Yield	Mean Diurnal Rate	Maximal Rate	Daily Yield
Barley	1,17	2,56	28,18	1,69	4,35	40,17	1,62	3,76	38,88
	1,37	3,01	32,94	1,67	3,69	40,06			
	1,24	2,02	29,82	1,55	3,67	37,26			
Potatoes				1,00	1,96	24,09	0,93	2,93	22,41
				1,71	3,09	41,10			
				0,82	2,02	19,74			
Radish	1,60	3,21	38,40	0,74	2,21	17,76	1,02	2,82	24,63
	1,93	3,95	46,23	1,34	3,16	32,23	0,77	1,71	18,58
	1,37	2,54	33,06	1,12	1,39	26,91			
Chinese cabbage	1,89	3,91	43,35	0,87	2,48	20,97			
	1,72	4,76	41,93	1,06	2,39	25,53			
	0,88	1,96	20,22	1,41	3,03	33,84			
Birch	1,38	2,95	33,30	1,37	3,32	33,04	1,24	2,88	29,97
	1,72	3,85	41,55	1,57	4,48	37,87	1,00	3,05	24,00
Willow	2,67	4,85	64,05	1,28	2,88	30,80	0,89	2,43	21,58
	3,74	5,60	69,70	1,09	2,08	26,25	0,98	3,78	23,53
	1,14	3,05	27,45	0,68	1,69	19,32			

Thus, the high rate of photosynthesis of cabbage and potatoes under transpolar conditions was explained by M.N.Goncharik (Bibl.9) by the high "intensity of phototrophy".

Our data on the optical adaptability of plants indicate that the relative utilization of light by plants increases with higher geographic latitude of the locale, i.e., as the plants move from South to North. Since the relative utilization of light increases in the North, we are justified to expect, under these conditions, an increase in the intensity of this process which is based on the assimilation of light, i.e., photosynthesis.

The data of recent investigations (Bibl.15, 16, 17, 18) and our own observations show that the plants of the high North utilize more fully solar energy, including its infrared portion which is used either directly in the

process of photosynthesis, as indicated by A.N.Danilov (Bibl.4, 5, 6), or for heating of the plants to supply heat for the photosynthetic process, as was proposed by G.A.Tikhov (Bibl.24). It is also possible that thermal infrared radiation, under the environmental conditions of the North, can be utilized for other physiological processes (associated with heat expenditure) such as transpiration, freeing the entire visible spectrum region directly for photosynthesis.

4. Conclusions /44

1. The spectral properties of crop plants, growing under different ecological conditions, change little in the visible spectrum region during the first year of life, which can be explained by the conservation of the heredity of optical properties of plants.

2. As cultivated plants advance toward North, their reflection and transmission of light in the infrared spectrum region decreases, which leads to enhanced increment of the vegetative mass during the comparatively short growing season in the North.

3. As plants change from the vegetative stage to the reproductive stage, a decrease in reflection and transmission of solar rays of various spectral distribution is observed, which apparently provides optimum supply of the reproductive organs with plastic substances.

4. In young leaves, a distinct profile of the main absorption band of chlorophyll is observed, associated with the lowest reflection and transmission of the red rays of the spectrum. In mature leaves, there is a decrease in reflection and transmission of light energy in other spectrum regions, causing a slight smoothing of the profile of the main absorption band of chlorophyll.

5. As plants progress from South to North, there is an increase in the average daily rate of photosynthesis and the diurnal yield of dry substance, apparently associated with the greater absorption of solar radiation by plants in the North.

<div align="center">BIBLIOGRAPHY</div>

1. Sveshnikova, V.M.: Osmotic Pressure in Alpine Plants (Osmoticheskoye davleniye u vysokogornykh rasteniy). Trudy Inst. Botan., Akad. Nauk Tadzh. SSR, Vol.XIV, Stalinabad, Izd. Akad. Nauk Tadzh. SSR, 1956.
2. Tyurina, M.M.: Investigations of the Frost Resistance of Plants under the Alpine Conditions of Pamir (Issledovaniye morozostoykosti rasteniy v usloviyakh vysokogoriy Pamira). Trudy Inst. Botan., Akad. Nauk Tadzh. SSR, Vol.VII, Stalinabad, Izd. Akad. Nauk Tadzh. SSR, 1957.
3. Trebinskiy, S.O.: Physiological and Biochemical Characteristics of Mountain Plants (Fiziologo-biokhimicheskiye osobennosti gornykh rasteniy). Uspekhi Sovrem. Biol., Vol.18, 1944.
4. Danilov, A.N.: Light Quality as a Factor Determining the Pathways of Radiant

Energy Utilization in Photosynthesis (Kachestvo sveta kak faktor, opredelyayushchiy puti ispol'zovaniya luchistoy energii v protesse fotosinteza). Sovets. Botan., No.4, 1935.

5. Danilov, A.N.: Peculiarity of the Biological Effect of Light Rays of Different Wavelength (Svoyeobraziye biologicheskogo deystviya svetovykh luchey raznoy dliny). Arkhiv Biol. Nauk, Vol.43, No.2-3, 1936.

6. Danilov, A.N.: Mechanism of Radiant Energy Utilization in Photosynthesis (Mekhanizm ispol'zovaniya luchistoy energii v protsesse fotosinteza). Trudy Botan. Inst., Akad. Nauk SSSR, Seriya IV, No.2, Leningrad, Izd. Akad. Nauk SSSR, 1936.

7. Danilov, A.N. and Miromanyan, V.A.: Photosynthesis of Transpolar Plants under Natural Conditions (Fotosintez rasteniy Zapolyar'ya v prirodnykh usloviyakh). Trudy Botan. Inst., Akad. Nauk SSSR, Seriya IV, No.6, Leningrad, Izd. Akad. Nauk SSSR, 1943.

8. Begishev, A.N.: The Work of Leaves of Various Agricultural Plants (Rabota list'yev raznykh sel'skokhozyaystvennykh kul'tur). Trudy Inst. Fiz. Rast. Akad. Nauk SSSR, Vol.VIII, No.1, Moscow-Leningrad, Izd. Akad. Nauk SSSR, 1953.

9. Goncharik, M.N.: Rate of Photosynthesis and Activity of Biochemical Processes in Potatoes and Cabbage under Transpolar Conditions (Intensivnost' fotosinteza i aktivnost' biokhimicheskikh protsessov u kartofelya i kapusty v usloviyakh Zapolyar'ya). In the Collection: "Biokhimiya plodov i ovoshchey" (Biochemistry of Fruits and Vegetables). No.3, Moscow, Izd. Akad. Nauk SSSR, 1955.

10. Semikhatova, O.A.: Certain Characteristics of Oxygen Respiration in Plants of the Pamir Highlands (O nekotorykh osobennostyakh kislorodnogo dykhaniya u rasteniy vysokogoriy Pamira). Trudy Botan. Inst., Akad. Nauk SSSR, Seriya IV, No.9, Leningrad, Izd. Akad. Nauk SSSR, 1953.

11. Zalenskiy, O.V.: Photosynthesis of Plants under Natural Conditions (Fotosintez rasteniy v yestestvennykh usloviyakh). Vopr. Botan., Vol.1, Moscow-Leningrad, Izd. Akad. Nauk SSSR, 1954.

12. Moshkov, B.S.: The Value of Individual Portions of the Spectrum of the Physiological Region of Radiation for the Growth and Development of Certain Plants (Znacheniye otdel'nykh uchastkov spektra fiziologicheskoy oblasti izlucheniya dlya rosta i razvitiya nekotorykh rasteniy). Dokl. Akad. Nauk SSSR, Vol.21, No.1, Moscow, 1950.

13. Moshkov, B.S.: Cultivation of Plants in Artificial Light (Vyrashchivaniye rasteniy na iskusstvennom svete). Sel'khozgiz, Moscow-Leningrad, 1953.

14. Gorbunova, G.S.: On the Problem of Photosynthesis of Plants under Conditions of Central Yakutia (K voprosu o fotosinteze rasteniy v usloviyakh Tsentral'noy Yakutii). Izv. Vost. Filialov Akad. Nauk SSSR, No.1, 1957.

15. Dadykin, V.P., Stanko, S.A., Gorbunova, G.S., and Igumnova, Z.S.: Assimi-/45 lation of Light by Plants at Yakutsk and Tiksi (Ob usvoyenii sveta rasteniyami v Yakutske i Tiksi). Dokl. Akad. Nauk SSSR, Vol.115, No.1, Moscow, 1957.

16. Dadykin, V.P. and Stanko, S.A.: Environmental Conditions and the Assimilation of Light by Plants (Vneshniye usloviya i usvoyeniye sveta rasteniyami). Izv. Vost. Filialov Akad. Nauk SSSR, No.1, 1957.

17. Dadykin, V.P. and Bedenko, V.P.: On Ways of Adaptation of Plants to Life under Conditions of the Far North (O putyakh prisposobleniya rasteniy k zhizni v usloviyakh kraynego Severa). Tezisy dokladov, konferentsii po fiziologii ustoychivosti rasteniy 3-7 marta 1959 g. (Summary of Reports

to the Conference on the Physiology of Plant Resistance on March 3-7,
1959), Moscow, Izd. Akad. Nauk SSSR, 1959.

18. Shakhov, A.A. and Semenenko, A.D.: Absorption of Light by Plants in the
    Transpolar Region (O pogloshchenii sveta rasteniyami v Zapolyar'ye).
    Zh. Obshch. Biol., Vol.XIX, No.6, 1958.

19. Kozlova, K.I.: Spectrophotometry of Plants of Various Climatic Zones in
    Reflected Light (Spektrofotometriya rasteniy raznykh klimaticheskikh zon
    v otrazhennykh luchakh). Alma-Ata, Izd. Akad. Nauk KazSSR, 1955.

20. Stanko, S.A., Bedenko, V.P., and Nebogatikova, M.S.: Radiant Energy Utiliza-
    tion by Plants (Ispol'zovaniye rasteniyami luchistoy energii). Trudy
    Sekt. Astrobotan., Vol.VI, Alma-Ata, Izd. Akad. Nauk KazSSR, 1958.

21. Parshina, Z.S.: Phylogenetic Characteristics of the Spectral Brightness of
    Plants in Reflected Rays (Filogeneticheskiye osobennosti spektral'noy
    yarkosti rasteniy v otrazhennykh luchakh). Trudy Sekt. Astrobotan.,
    Vol.VI, Alma-Ata, Izd. Akad. Nauk KazSSR, 1958.

22. Lyubimenko, V.N.: An Approach to the Theory of Light Adaptation of Plants
    (K teorii prisposobleniya rasteniy k svetu). Sovets. Botan., No.6, 1935.

23. Tikhomirov, V.S.: Seasonal Changes of Certain Reflective Properties of
    Plants and the Problem of Vegetation on Mars (Sezonnyye izmeneniya neko-
    torykh otrazhatel'nykh svoystv rasteniy i vopros o rastitel'nosti na
    Marse). Alma-Ata, Izd. Akad. Nauk KazSSR, 1951.

24. Tikhov, G.A.: Astrobiology (Astrobiologiya). Moscow, Izd-vo "Molodaya
    gvardiya", 1935.

OPTICAL PROPERTIES OF VARIOUS SPECIES OF WHEAT

A.D.Semenenko

Illumination conditions play a basic role in the formation of plants, both in ontogeny and during evolutional development. Therefore, the light status of plants is determined by their nature. Plants apparently assimilate light energy in relation to the type of nutrition and metabolism. Consequently, they have a different assimilation apparatus, resulting in the fact that different plants will show a different relation between the pigments and the protein-lipid complex and differing ratios of atoms in the chromophore groups.

Even in the same plant, the optical properties may vary during the course of a day, since the fluctuations in illumination, temperature, and other factors cause changes in the regrouping of atoms in the chromophore groups, phototaxis, and phototropism.

To study the characteristics of the optical properties of plants, spectrophotometric investigations were carried out on various species of wheat at the Alma-Ata State Selection Station.

The experimental plants, sown at the same time in adjacent plots, grew and developed under similar conditions.

The spectrograms of all investigated plants and of the plaster-of-Paris screen were obtained on July 12 at 14:00 - 14:15 by means of a quartz spectrograph on the same "Pan Infra" photographic plate (experimental). The wheat was

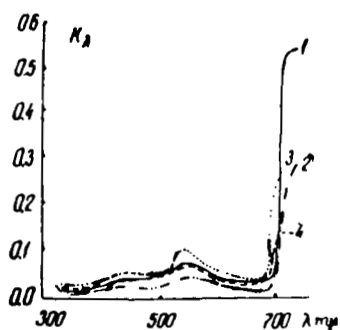Fig.1 Curves of the Spectral Brightness of Wheat
in Reflected Light
1 – Spelt; 2 – Triticum monococcum; 3 – Tr. milturum;
4 – Tr. melanopus

spectrographed at the same developmental stage and at the same angle of illumination in three replications.

The results of the spectrophotometric studies showed that different wheats absorb light energy differently, particularly rays of the extreme red, depending on their heredity traits.
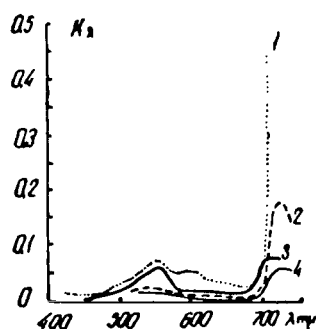

Fig.2 Curves of Spectral Brightness of Wheat in
Transmitted Light
1 – Spelt; 2 – Tr. monococcum; 3 – Tr.milturum; 4 – Tr. melanopus

Low brightness coefficients in the visible spectrum region are a common characteristic feature of the optical properties of the investigated wheats in the South (Table 1). Their spectral brightness curves are smoothed out (see Figs.1, 2). The principal absorption band of chlorophyll is wide and merges with other absorption bands. The rise of the maximal brightness in the green region is only faint. A maximum of light absorption is noted in ultraviolet and red rays.

TABLE 1

SPECTRAL CHARACTERISTICS OF WHEAT VARIETIES IN
THE FAR–RED REGION

Wheat Variety	K_{max}	$K_{740 m\mu}$	$K_{720 m\mu}$	K_{min}	B_1	K'_{av} $700-721_{m\mu}$
			Reflected Rays			
Tr. spelta	0.548	0.518	0.536	0.033	0.515	0.223
Tr. monococcum	392	392	270	020	372	124
Tr. milturum	282	130	282	048	234	195
Tr. melanopus	144	—	144	032	112	100
			Transmitted Rays			
Tr. spelta	0.518	0.420	0.518	0.023	0.495	0.221
Tr. monococcum	177	081	177	007	170	084
Tr. milturum	075	075	071	001	074	042
Tr. melanopus	0 9	053	059	001	058	031

53

Distinctive characteristics of the optical properties of wheat were defined mainly in the long-wave spectrum region, i.e., they are distinguished by the degree of absorption of the light energy of far red and near-infrared rays, which is associated with the nature of the plant, its heredity. For example, spelt is close in origin to common wheats. It has high brightness coefficients in the /47 long-wave spectrum, i.e., it appreciably reflects rays of the extreme-red region (Table 1).

Triticum monococcum - a wild mountain plant. Its ancestors grew in the cold mountain regions without irrigation, on the slopes and plateaus of Asia Minor, in the Balkans, in Syria, Armenia, the Carpathians, etc., utilizing short-day solar energy. The nature of this wheat plant developed under the
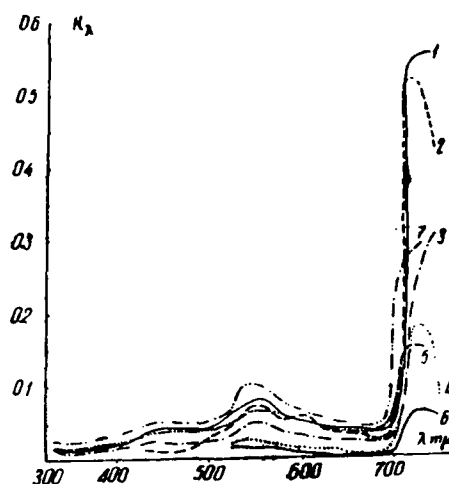
Fig.3 Curves of Spectral Brightness of Wheats in Reflected and Transmitted Light
Triticum spelta: 1 - In reflected light; 2 - In transmitted light. Tr. monococcum: 3 - In reflected light; 4 - In transmitted light. Tr. melanopus: 5 - In reflected light; 6 - In transmitted light

austere conditions of high mountainous regions, where the plants were forced to absorb a maximum of light energy. Evidently, its ancestors absorbed far-red rays, and photosynthesis proceeded in the long-wave spectrum region. This permits the assumption that Tr. monococcum is distinguished by a high conservation of hereditary traits and has retained the optical properties of its ancestors even to the present day.

Triticum melanopus - a durum wheat. This species belongs to the steppe-ecological group of wheats. It is distinguished by low brightness coefficients in the long-wave region of the visible spectrum in comparison with other wheats (Table 1). Evidently, the evolution of Tr. melanopus proceeded in the direction of utilizing far-red rays for photosynthesis, which explains its intense absorption of long-wave red and near-infrared radiation even on a sultry July day /48

54

during the noontime hours.

Triticum milturum – a common spring wheat. The optical properties of this species are characterized by higher coefficients of reflection of light energy in the visible spectrum.

The column headings in Table 1 have the following meaning: K_{max} denotes the coefficient of maximal brightness in far-red rays; K_{min} is the brightness coefficient of the lowest point of the spectral curve, in the region of the main absorption band of chlorophyll.

The quantity B_1 denotes a rise of the curve in the far-red rays. This rise is equal to the difference between the highest point of the peak K_{max} and K_{min} in the region of the chlorophyll absorption band, so that $B_1 = K_{max} - K_{min}$. The quantity K_{av} denotes the average brightness coefficients.

The spectral characteristics of the wheats in the long-wave spectrum region, given in the Table, show that different wheats, at the same developmental stage and growing under similar conditions, exhibit different optical properties. Consequently, they assimilate light energy differently. High brightness coefficients both in reflected and in transmitted light are observed for Tr. spelta, whereas both Tr. monococcus and melanopus reflect and transmit light energy to an appreciably lesser degree. Whereas the average brightness coefficient of spelt reached $K_{av} = 0.223$, it was $K_{av} = 0.124$ for Tr. monococcus and $K_{av} = 0.100$ for Tr. melanopus. The brightness coefficient at a wavelength of 722 for spelt was $K_{722} = 0.536$; for Tr. monococcus $K_{722} = 0.270$; for Tr. melanopus, $K_{722} = 0.144$.

Thus plants under identical environmental conditions assimilate light energy differently (Fig.3).

The data of the spectrophotometric observations confirm previous investigations (Bibl.1) concerning the fact that the optical properties are conservative despite their lability. They are formed during evolutionary and ecological development and are transmitted by heredity. When the metabolism of plants changes, their optical properties change.

BIBLIOGRAPHY

1. Semenenko, A.D.: Investigation of the Spectral Brightness of Vegetative Hybrids of the Family Solanaceae by the Method of Photographic Spectrophotometry (Issledovaniye spektral'noy yarkosti vegetativnykh gibridov semeystva Solanaceae metodom fotograficheskoy spektrofotometrii). Trudy Sekt. Astrobotan., Vol.VI, Alma-Ata, Izd. Akad. Nauk KazSSR, 1958.
2. Semenenko, A.D.: Spectral Brightness of Certain Vegetative Hybrids from the Solanaceae Family (Spektral'naya yarkost' nekotorykh vegetativnykh gibridov iz semeystva paslenovykh). Auth. Abstr. of Cand. Diss. Alma-Ata, 1959.
3. Tarakanov, K.N.: Historico-Ecological Principles of the Heredity of Certain Cereals (Istoriko-ekologicheskiye osnovy nasledstvennosti nekotorykh zlakov). Zh. Obshch. Biol., Vol.15, No.6, 1954.

SPECTRAL BRIGHTNESS OF THE WHEAT LEAF AND SPIKE

A.D.Semenenko

It is commonly considered that green leaves of plants mainly photosynthesize. It is assumed that reduced plant leaves, for example green awns and glumes, also somehow participate in photosynthesis. However, the literature contains no specific investigations on this subject.

To study the optical properties of spikes – to what extent and what rays of solar radiation they utilize – we investigated the spectral brightness of the spike and leaf of the Alban branched wheat (poulard).

The investigations were carried out in August 1957 by a method of relative spectrophotometry in the transpolar region, in the territory of the experimental section of the Polar-Alpine Botanical Gardens of the USSR Academy of Sciences, 3 km from the Apatity station of the Kirovsk railroad and 1 km from Lake Imandra.

In order to bring cereals into the transpolar region, a conventional procedure is to breed northern plant varieties with a short growing season which would be capable of maximum utilization of the high intensity of insolation there, namely, the continuous solar energy flux lasting the 45 days of the summer solstice when the sun rises to 45 – 46° and does not set below the horizon. The abundance of light during the polar day ensures a rapid development of vegetation in the transpolar region; however, sometimes the low temperatures cause changes in the pigment system of the plants. It is known that plants rapidly adapt to changes in climatic conditions, owing to their labile pigment system.

In the field, among cultivated herbaceous plants and wheats, it is often observed that, during the thaw, the more illuminated side of the leaves (upper or lower) acquires a violet color while the opposite side remains green for a long time. For example, upon a drop in air temperature and in the presence of intense diffuse insolation, the leaves of corn, whortleberries, the stems of potatoes, and the awns and glumes of wheat change to a violet color on the sunny side. It is important to define the role played by the violet color in plants and what rays it absorbs.

In this case, the massive coloring on the sun-exposed side of the spikes of poulard in violet light during the grain formation stage is evidently useful and indirectly promotes rapid maturation of the grains, creates certain radiation conditions, and enhances the metabolism of the plant.

At a young age, and especially at the flowering stage, cereals intensely absorb short-wave rays, which are needed for growth, respiration, and trans- location of various substances and particles; in particular, they direct phototaxis, promote the accumulation of protein, etc. (Bibl.2, 3). However, when the plants complete their growing season, i.e., at the grain-forming stage,

violet rays evidently have an adverse effect so that the plants reflect these rays.

Certain researchers consider that plants utilize ultraviolet rays as protective rays and acquire a violet color as a consequence of the accumulation of anthocyanins as complementary energy absorbers. It can be assumed that, in a young plant, extreme short-wave rays are beneficial for the organism, whereas during the aging stage of the leaf, when the chlorophyll is gradually released from the lipoprotein complex, they are harmful since they can accelerate this process of breakdown. For this reason, during the fall or spring, the plants, being protected from low temperatures and the destructive action of short-wave rays (in the presence of high insolation), acquire a violet color owing to the enhanced formation of anthocyanins.

To study the radiation conditions of poulard, we investigated the spectral brightness of the violet and green sides of the wheat spike in reflected light and also the upper leaf of this plant in reflected and transmitted light. This made it possible to define whether the spike, during the grain formation stage, is provided with the same plastic substances taken up from the leaves, and to what extent it additionally assimilates light energy.

It is known that each leaf level has its own biological significance and participates differently in the process of photosynthesis. At the grain-formation and ripening stage, the upper leaf plays the major role in photosynthesis. The photosynthetic products of the upper leaf enter into the spike. The purpose of our investigation was to study the spectral brightness of the wheat spike.

Spectrophotometric investigations were made with a standard field spectrograph. The plants were spectrographed in reflected and transmitted light at an angle of 20° from the normal, with respect to the axis of the collimator, and at an azimuth of 45°. For this purpose, we used attachments which permitted spectrographing unattached leaves at different light intensities.

The investigated leaf, or plaster-of-Paris screen, was placed in a frame mounted in a disk. The disk with the frame could be turned by means of a sunseeker through any angle to the incident light, along the horizontal axis. Furthermore, the frame itself also was rotatable about the vertical axis. The frame and disk are rotated with respect to a dial with divisions of $10 - 20^\circ$.

The light transmitted by the leaf was spectrographed with a different special attachment. The frame in which the leaf was placed was covered with a lightproof material which permitted turning it through any angle, up to 70°, relative to the incident light. A sunseeker was welded into the frame. The middle of both frames was centered with the slit of the spectrograph and was placed one object distance away, taking the solid angle into consideration.

The leaf and spike were not detached during spectrographing.

The spectrophotometric investigations showed that in every case at the stage of milk ripeness, the spike (its green side) absorbs light energy more intensely than the upper green leaf.

57

The Alban poulard (branched wheat) does not fully mature under transpolar conditions, since it does not have sufficient light energy. The Alban wheat
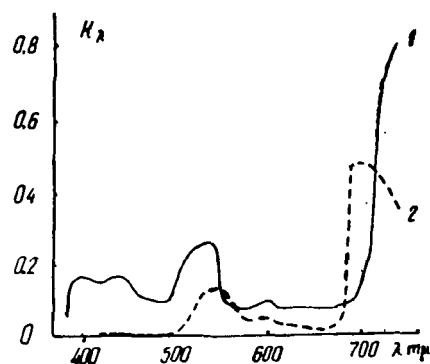

Fig.1 Spectral Brightness of the Upper Leaf of the Alban
       Poulard in Reflected and Transmitted Light
       1 – In reflected rays; 2 – In transmitted

never has become adapted to assimilate solar radiation at more accelerated rates or to use thermal and green rays like wild plants. As indicated by the curve /51

TABLE 1

SPECTRAL BRIGHTNESS COEFFICIENTS OF THE ALBAN POULARD

λ, m_μ	Leaf			Spike (Reflection)	
	Reflection	Transmission	Absorption	Green Side	Violet Side
388	0,053	—	0,947	0,188	0,819
395	160	—	840	088	366
420	150	0,006	8˙5	118	283
440	167	009	824	117	311
460	118	009	873	103	243
480	103	008	889	096	225
490	085	006	909	171	179
500	136	009	855	117	206
536	259	033	629	033	354
550	103	121	776	059	265
567	076	063	861	090	171
582	072	040	888	065	177
602	090	046	864	097	200
611	071	029	900	076	196
620	071	025	904	073	167
630	076	024	900	082	175
640	071	016	912	076	200
648	071	017	912	080	192
660	067	012	921	071	179
670	063	012	925	073	142
680	079	086	867	086	188
685	071	167	762	086	196
690	084	082	896	215	089
700	137	113	809	310	142
710	238	136	595	311	223
721	598	145	459	142	371
741	800	134	—	608	456
756	210	605	185	036	130

of spectral brightness (Fig.1), this wheat reflects thermal as well as green
rays uneconomically. The plant mainly utilizes yellow-orange and red rays.

The comparatively high reflection coefficients of the energy of short-wave
rays, shown in Table 1, indicate that the plant has not adapted to the radiation
conditions of transpolar regions. Short-wave rays are needed for grain forma-
tion and for protein accumulation, and if the plant does not completely assimi-
late the required energy, it will not have time to mature.

If the anatomicomorphological characteristics and the optical properties
of the leaf do not conform to the new environmental conditions and do not fully
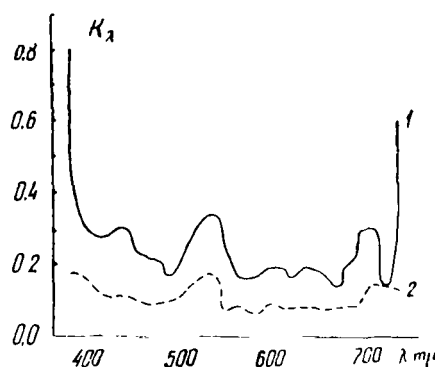adapt to them, the picture obtained for the spike will be different.

Fig.2 Spectral Brightness of the Green and Violet
Sides of the Spike of Alban Poulard
1 - Violet; 2 - Green

The violet side of the head reflects more light energy than the green   /52
side. This is because the green glumes and awns of the head absorb more light
energy than the violet ones.

However, this does not explain why the green side of a spike absorbs more
solar radiation than the green upper leaf.

The violet side of the spike, as shown by the spectral brightness curve,
completely reflects violet rays and far-red rays, and appreciably reflects blue-
green. The profile of the curve is torturous owing to the presence of absorp-
tion bands (the main absorption band is at $\lambda = 660 - 680$ mμ; second band is at
$\lambda = 616 - 630$ mμ; and the third at $\lambda = 570 - 580$ mμ). This indicates that, al-
though the glumes of the spike are violet, they contain also other pigments:
chlorophyll, carotenoids (the main absorption band of carotene is at $\lambda =$
$= 490$ mμ), etc.

The brightness coefficients obtained upon spectrographing the green side
of the spike (Table 1) have the opposite significance. The curve of the bright-
ness coefficients as a function of the wavelength is located lower, with respect
to axis of abscissas, than the spectral curve of the violet side of the spike

(Figs.1 - 3). Its profile is relatively smooth, without substantial maximal reflection peaks in the green and extreme-red regions of the spectrum. There are no distinct absorption bands; they blend into a general curve. The low brightness coefficients in the green and extreme-red regions (Table 1) indicate that the plant intensely assimilates these rays.
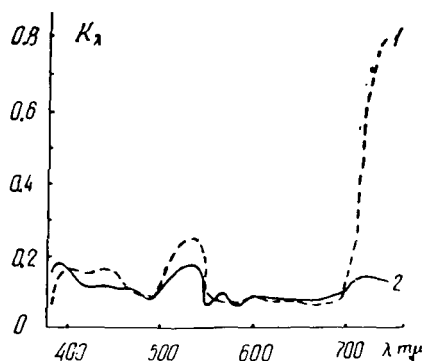

Fig.3 Spectral Brightness of the Upper Leaf and Green
Side of the Spike of Alban Poulard
1 - Leaf, 2 - Spike

How does one explain the fact that the green side of the spike absorbs light energy more intensely than the leaf? Could the anatomicomorphological properties change and become adapted to new environmental conditions more rapidly than those of leaves? Does the violet color promote an intense absorption of light energy?

It is possible that anthocyanins, themselves not directly participating in photosynthesis, as indicated by the brightness coefficient, indirectly promote assimilation of light energy. In some manner they act on the metabolism, increasing its rate. It is known that, in the presence of anthocyanins, the percent of soluble sugars and of polysaccharides, as well as the rate of redox processes, respiration, etc. increase, which leads to an increase in the in-   /53 tensity of assimilation.

Anthocyanins are formed at low temperatures and high insolation, in the presence of abundant ultraviolet rays (in mountains and in the transpolar region). Evidently, they promote higher metabolism and intense absorption of light energy by chlorophyll.

Plants that have acquired a violet color repulse the ultraviolet rays that are harmful at that time and utilize the extreme-red and infrared rays instead.

The exclusion of extreme short-wave rays at the critical time of plant life helps to increase the rate of absorption of thermal red and infrared rays by the leaf or spike. The brightness coefficients showed that the green side of the spike absorbs light radiation of the visible spectrum more intensely, and in particular thermal rays, than the green leaf of the same plant.

The results of the investigation permit the assumption that polar plants, similar to alpine plants, possess great plasticity and capacity for chromatic adaptation.

Conclusions

1. The Alban branched wheat intensely absorbs light energy in the red and orange-red region, but this intensity is not sufficient for complete maturation. Not having time to become adapted to the polar day, the plant repulses thermal rays although its nature, as the optical properties of the green side of the spike indicate, should be modified toward utilization of thermal rays (extreme red and infrared).

2. The results of the investigation showed that the spike, at the period of green maturation (more exactly, at the milky ripe stage), intensely absorbs the light energy of the entire spectral distribution in the visible region (from λ = 390 to 756 mμ). Intense assimilation of solar radiation indicates that the metabolism of the spike, at the grain maturation stage, is elevated and respiration is increased. It would be desirable to prevent mutual shading of the spikes so that the secondary growth could more freely and fully utilize light energy, since, apparently, the secondary growth cannot mature because of the lack of light.

BIBLIOGRAPHY

1. Voskresenskaya, N.P.: Effect of the Spectral Distribution of Light on the Rate of Photosynthesis (O vliyanii spektral'nogo sostava sveta na intensivnost' fotosinteza). Trudy Inst. Fiziol. Rast., Vol.X, Moscow, 1955.
2. Krasnovskiy, A.A. and Kosobutskaya, L.M.: Different States of Chlorophyll in Plant Leaves (Razlichnyye sostoyaniya khlorofilla v list'yakh rasteniy). Dokl. Akad. Nauk SSSR, Vol.XVI, nov. ser., No.2, Moscow, 1953.
3. Tabentskiy, A.A.: Structure of the Chlorophyll Granule as an Index of the Vital Activity of the Leaf (Struktura khlorofillovogo zerna kak pokazatel' zhiznedeyatel'nosti lista). Izv. Akad. Nauk SSSR, ser. biol., No.5, 1947.

OPTICAL PROPERTIES OF ETIOLATED OATS

A.D.Semenenko

Spectrophotographic investigations of oats (etiolated and green leaves) were carried out by a standard field spectrograph, using the method of relative spectrophotometry. The investigations were made in August 1957 at the Experimental Section of the Polar-Alpine Botanical Gardens, USSR Academy of Sciences, on Kola Peninsula, 3 km from the Apatity station.

The amount of pigment in the leaves of the experimental plants was determined simultaneously with the spectrum analysis (V.S.Shaydurov, Institute of Plant Physiology, USSR Academy of Sciences, Laboratory of Evolutionary Ecology and Physiology). The amount of pigment was determined by paper chromatography (accd. to Sapozhnikov) with the aid of an FEK-M photoelectric colorimeter.

The spectrograms of the plants were processed on the MF-2 microphotometer at the Astrobotany Sector of the Kazakh SSR Academy of Sciences.

The obtained results showed that the amount of pigment increases with exposure of the etiolated plants to light (Tables 1 - 3). This causes a corresponding broadening of the absorption bands of the pigments on the spectral curves.

The results of the spectrophotometric studies, yielding data on the process of adaptation of etiolated plants to illumination, agree with the literature data.

Hubbenet, who studied 9-day-old etiolated wheat seedlings, observed a gradual adaptation of the etiolated plants to an increase in light intensity.

N.V.Lyubimenko believed that the adaptability of etiolated plants to bright illumination is due to an increase in the number of enzymes and to the formation of a pigment complex in light; he also postulated that the rapid change of redox processes in the protoplasm, on transfer of the etiolated plants from the dark to light, induces various conversions of pigments in the plastids as well as migration and reorganization of molecules in the chromophore groups.

An increase in the amount of chlorophyll and carotene accumulation on exposure of etiolated leaves to light was observed by Lebedev. Western scientists Seybold and Egle, Beck and Nagel demonstrated that xanthophylls are formed most in etiolated plants in light. Blau-Jansen, Komen, and Thomas proved that the quantity of carotenes in 8-day-old oat seedlings increases in proportion to light intensity. This was also confirmed on wheat seedlings which were in- /55 vestigated by Barrenshin, Pani, et al. [cited by T.W.Goodwin, (Bibl.1)].

The pattern of changes in the spectral characteristics, obtained by us both in the region of the chlorophyll and carotene absorption bands and over the entire visible spectrum, showed that the etiolated plant adapts to conditions of

TABLE 1

OPTICAL PROPERTIES OF OATS

$\lambda_{m\mu}$	White	Yellow	Green	White	Yellow	Green	White	Yellow	Green
		Reflection			Transmission			Absorption	
395	0,145	0,111	0,104	0,027	0,048	—	0,798	0,811	0,856
420	212	138	105	051	062	—	707	770	866
440	196	119	096	049	056	—	725	795	874
480	228	129	094	058	065	0,008	684	777	868
490	232	126	087	072	079	010	665	765	872
500	267	134	083	005	005	012	698	831	875
536	212	182	119	112	178	055	645	610	796
550	212	179	113	123	200	061	635	591	796
567	241	196	090	101	131	051	628	643	829
582	235	182	089	091	124	037	644	664	843
602	246	183	081	076	089	037	648	698	853
611	286	200	077	076	096	032	608	675	860
630	237	186	070	050	054	024	679	825	850
640	246	179	071	050	054	019	774	738	880
648	258	161	066	048	054	017	664	756	887
660	230	145	059	042	046	011	698	779	900
670	210	110	053	039	042	011	722	818	906
680	252	155	056	043	043	015	675	772	899
685	209	145	055	036	083	027	725	742	888
690	224	192	074	038	178	022	708	600	873
700	251	219	131	039	178	032	680	573	807
710	276	243	176	051	045	042	649	675	753
721	521	289	258	091	107	078	358	574	635
741	575	298	324	116	168	141	279	494	504
756	138	369	293	090	224	138	741	377	539

illumination not just by an increase in the amount of pigment (Bibl.3).

The drooping brightness curves, for example, in the short-wave portion of the spectrum (Fig.1) indicate a utilization of blue and violet rays by the plant, which increases the intensity of the respiratory enzymes and in general the enzymatic activity of plastids, their shifting in the cell, movement of
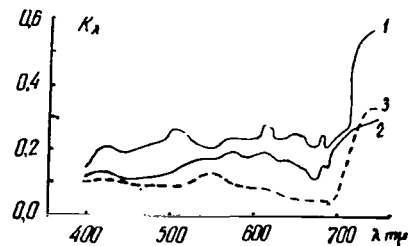

Fig.1 Curves of Spectral Brightness of Oats
in Reflected Light
1 – Etiolated white leaf; 2 – Etiolated yellow
leaf; 3 – Green control leaf

particles, and reorientation of molecules in the chromophore groups, in different relationships of the plastid pigments with protein, etc.

The enzymatic activity of plastids plays a major role in the adaptive reactions of etiolated plants to light conditions. The plastids are coacervates of vitally important substances: proteins, lipids, mineral elements, pigments, vitamins, and enzymes. They actively react to environmental changes.
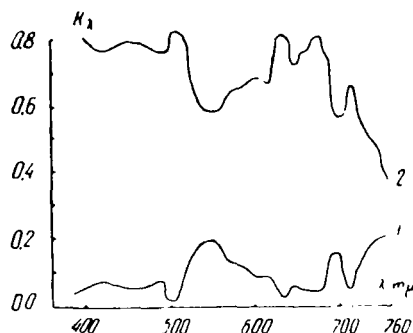
Fig.2 Spectral Brightness of Etiolated Yellow Oats
1 - In transmitted rays; 2 - In absorbed rays
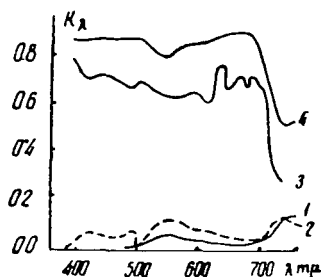
Fig.3 Curves of Spectral Brightness of Oats
in Transmitted Rays
1 - Of green oats; 2 - Of etiolated white oats.
Absorption curves of oats: 3 - Etiolated white
oats; 4 - Green oats

The curves of the spectral brightness show that the optical properties $\underline{/56}$ of etiolated oat plants, during the accumulation of pigments in light, are unstable (Figs.1 - 3). Probably, this can be explained by the fact that the heredity of oats had evidently been somewhat disturbed during acclimation to the transpolar region.

The etiolated plants with the disturbed pigment system and shattered heredity are good plastic material for the plant breeder. They can adapt easily and quickly to the light conditions of the transpolar region. Furthermore it was noted that, under the unique climatic conditions of the transpolar region with the high atmospheric humidity and high insolation in the region of the Apatity

station, etiolation of artificially shaded plants (oats, radishes) and the sub-
sequent restoration and new formation of their pigment system in direct light
under field conditions, take place rapidly. Thus, it seems that, to accelerate
acclimation of southern plants to transpolar conditions, the sprouts of plants
of the first and second year of sowing should be shaded for a short time.

TABLE 2

AMOUNT OF PIGMENT IN OAT LEAVES (in mg per 100 gm)
OF FRESH SUBSTANCE

Type of Pigment	Yellow Oats (not Completely Etiolated)	Green Oats	Ratio of Amount of Pigment (Green Oats to Etiolated Oats)
Chlorophyll a + b	3.54	150.0	42.4
Carotene	0.62	15.5	25.0
Lutein	1.51	12.5	8.3
Violaxanthin	0.37	5.2	11.2

TABLE 3

RATIO OF AMOUNT OF PIGMENT IN OAT LEAVES (in mg per 100 gm)
OF FRESH SUBSTANCE

Specimen	Carotene to Chlorophyll	Lutein to Chlorophyll	Violaxanthin to Chlorophyll	Lutein to Carotene	Lutein to Violaxanthin	Violaxanthin to Carotene	Violaxanthin to Lutein
Etiolated oats	0.20	0.42	0.10	2.13	4.08	0.59	0.24
Green oats	0.10	0.08	0.03	0.80	2.40	0.33	0.41

The slope of the spectral brightness curve of etiolated oats is streaked
by the narrow absorption bands of pigments, just as is the case for etiolated
hybrid tomato. The absorption curve of white etiolated oats is somewhat lower,
with respect to the abscissa, than the absorption curves of the yellow and green
leaves of oats. Three main but faint absorption bands of chlorophyll in the red
portion of the spectrum and the absorption band of carotene at a wavelength $\lambda =$
$= 500$ mμ were noted. There was also an appreciable reflection of the energy of
long-wave rays in comparison with a green plant.

After the etiolated plant had been placed in the light, its optical proper-
ties changed as a result of the formation of the pigment system. The quantity
of pigments increased and the leaves acquired a greenish-yellow color.

The absorption curve of the yellow oats shows distinctly expressed absorp-
tion bands of chlorophyll and carotenoid. The absorption coefficients in the

short-wave portion of the spectrum and in the region of red rays increase appreciably, which indicates an accumulation of pigments. The reflection curve of the yellow oat leaf is much lower, with respect to the abscissa, than the /57 curve of the white etiolated oats and occupies an intermediate position between the reflection curves of the white and green oat leaves. These have a smooth shape, which indicates uniform absorption of solar energy.

The results of the colorimetric determinations of the amount of pigment in etiolated and green (control) oat leaves confirmed the spectrophotometric data (Tables 2 and 3).

It should be mentioned that the amount of pigment could be determined colorimetrically only in the leaves of yellow oats (not completely etiolated) in comparison with the control oats (green), whereas very small amounts of pigments in white etiolated oat leaves were determined by spectrum analysis.

The results of the volumetric pigment analysis show that, for etiolated oats, lutein predominates among the carotenoids, whereas in green oats there is more carotene than lutein. For green oats, in relation to etiolated oats, the greatest difference is observed in the quantity of chlorophyll and carotene and the least difference in the quantity of lutein. In etiolated oats chlorophyll is decomposed to the greatest extent, followed by carotene, and finally by lutein.

Conclusions

On the basis of the above investigations, we can conclude that etiolated oat plants, during the period of their greening under transpolar conditions, gradually reorganize and adjust their assimilation apparatus to the light conditions. It can be assumed that a brief shading of plant sprouts, an alternation of dark and light, will stimulate the growth processes. The photosynthesiz- /58 ing apparatus of the plants is rapidly formed under illumination, due to the new formation of pigments.

BIBLIOGRAPHY

1. Gudvin (Goodwin), T.: Comparative Biochemistry of Carotenoids (Sravnitel'naya biokhimiya karotinoidov). Moscow, Izd-vo Inostr. Lit., 1954.
2. Kraskovskiy, A.A. and Kosobutskaya, L.M.: Spectral Investigation of the State of Chlorophyll during its Formation in Plants and in Colloidal Solutions of the Substance of Etiolated Leaves (Spektral'noye issledovaniye sostoyaniya khlorofilla pri yego obrazovanii v rastenii i v kolloidnykh rastvorakh veshchestva etiolirovannykh list'yev). Dokl. Akad. Nauk SSSR, Vol.85, No.1, Moscow, 1952.
3. Semenenko, A.D.: Dynamics in Spectral Brightness of Etiolated Plants (Dinamika spektral'noy yarkosti u etiolirovannykh rasteniy). Trudy Sekt. Astrobotan., Vol.5, Alma-Ata, Izd. Akad. Nauk KazSSR, 1957.

OPTICAL PROPERTIES OF CERTAIN PLANT SPECIES IN THE INFRARED REGION OF THE SPECTRUM IN TRANSMITTED LIGHT

M.P.Perevertun

Numerous attempts by various Soviet and other scientists to detect, in the visible portion of the spectrum, the chlorophyll absorption band and the Wood effect in a luminous flux reflected by the "seas" of Mars where vegetation is supposed to exist, led to negative results. Thus, for more than 100 years the absence of the chlorophyll absorption band and the Wood effect for the Martian "seas" was considered to be conclusive proof that there can be no vegetation on Mars. However, on the basis of a thorough analysis of the properties of true nature, such a conclusion is not tenable. In studying the optical properties of terrestrial plants under conditions of the dry and humid high mountains of Pamir, the cold desert of Central Tien Shan, Zailiyskiy Alatau, and the transpolar region, starting from the tundra, forest-tundra, taiga, and ending with the forest-steppe, as well as under conditions of the Kazakhstan steppes and deserts, scientists have demonstrated the presence of basic changes in the spectrophotometric properties of plants, both its higher and lower forms, depending on the environmental conditions.

As most subarctic plants move farther North, the chlorophyll absorption band becomes blurred and, in certain plants at Tiksi, completely disappears.

Extensive changes also occur in the phenomenon of the infrared effect of terrestrial plants. As the climatic conditions become more austere, the infrared effect of plants drops almost to zero.

Thus, on the basis of the optical properties of terrestrial plants, the absence from the Martian "seas" of the principal absorption band of chlorophyll and the infrared effect can be assumed as due to the severe temperature conditions for plant growth rather than to an absence of vegetation. Of course, this is not sufficient ground for far-reaching conclusions that would presuppose the existence on Mars of earthlike leafy vegetation such as chestnuts or branchy birches, pines, and spruces as they grow in the middle latitudes of our planet.

Taking into account the temperature conditions of Mars, the composition of its atmosphere and the quantitative water supply, it would be illogical to assume that a vigorous flora, resembling the flora of the Caucasus or the foothills of Zailiyskiy Alatau could exist there.

The method of analogy is widely used in astronomy and astrophysics and yields positive results when solid and experimentally verified bases exist. In solving the problem of the existence of extraterrestrial life, the method of /60 analogy must be used with great caution, although there is no doubt that, if plant life exists at all on Mars, it will exist there on the same biological base as on earth, since science does not know any other life on a nonprotein base; however, the forms of such life may differ greatly from those customarily encountered under earth conditions. Therefore, the idea of a direct proof of

the existence of organic life on Mars is quite tempting.

Spectral investigations of Mars in the visible spectrum region have yielded no positive results as to the presence of oxygen and water vapors in its atmosphere or as to the presence of molecules of an organic origin in the region of the Martian "seas". Apparently this spectrum region, reflected from the Martian surface, is strongly distorted on passing through the atmosphere of Mars and earth. The near-infrared rays are subjected to less changes, and the far-infrared rays reach us directly from the surface of Mars almost without distortion. Investigations in this region of the spectral properties of terrestrial plants and the "seas" of Mars open new possibilities for the direct study of the physical nature of individual formations of the Martian surface. Therefore, the purpose of our work was to establish the structural characteristics of the spectrum of plants in transmitted light in the range from 0.6 to 1.4 μ. Since the spectral curves of the transmission coefficients have a slope similar to that of the spectral curves of the brightness coefficients in reflected light, this indirectly permits a certain judgment as to the structure of the spectrum of plants in the long-wave portion of the spectrum and in reflected rays.

To study the optical properties of plants in the infrared region of the spectrum in transmitted rays, we used the SF-4 spectrophotometer.

Separate leaves of the investigated plants, fastened in a special stand rigidly connected with the movable carriage of the cuvette, were installed in the light of a certain wavelength, emerging from the spectrophotometer slit. The ratio of the light flux passing through the specimen to the light flux passing through air, whose transmission was taken as 100%, was determined from the transmission scale of the recording potentiometer. The scale readings yielded the transmission of plant leaves, directly in percent. The upper scale of the recording potentiometer gave the optical density of the leaf.

The stand, to which the leaf specimens were mounted, permitted a simultaneous study of three objects over all wavelengths. To retard drying and wilting of the detached leaves, the ends of their stems were provided with thin rubber tubes filled with water, or their stems were wound with water-soaked filter paper.

With the factory-assembled SF-4 and the attachment filters, reliable measurement of the intensity of the transmitted light was possible only up to 1.1 μ, since the scattered light within the instrument is comparable with the intensity of the flux being measured. To investigate the longer-wave portion of the spectrum of plants with the SF-4, we intensified the light flux entering the instrument and used an additional infrared filter which cut off all radiation below 1.1 μ. This permitted reliable measurements to 1.3 – 1.4 μ. The error of measurement did not exceed 3 – 8%.

We used the SF-4 spectrophotometer and the above attachments for investigating the optical properties of the young leaves of 20 plant species, in <u>/61</u> the range from 0.45 to 1.4 μ. As a result, we obtained 35 curves of the spectral transmission coefficients of solar radiation for leaves and flower petals of the studied plants.
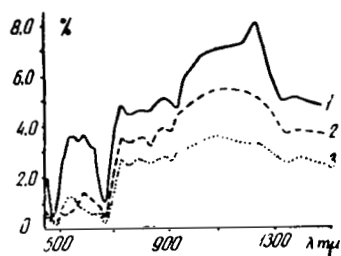
Fig.1

1 – Birch. Young leaf of brown color, abundant moisture (April 24); 2 – apple (Kul'zhinka). Young red-brown leaf (April 24); 3 – Mullen. Young leaf, center portion (April 24). Air temperature –2°
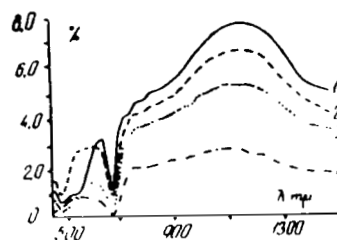
Fig.2

1 – Silver maple. Young red-brown leaf (May 25); 2 – Birch. Young leaf of red color under normal conditions (June 25); 3 – Spirea. Young dark-red leaf (April 25); 4 – Thistle. Old yellowish leaf (April 24)
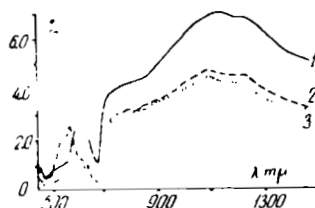
Fig.3

1 – Silver maple. Red-brown leaf (May 27); 2 – Mallow. Yellow leaf (April 27); 3 – Persian lilac. Red leaf (April 27)

Fig.4

1 – Green onion. Cut leaf (April 24); 2 – Maple. Young brown leaf (April 29); 3 – Horse radish. Young leaf (April 29); 4 – Horse sorrel. Young leaf (April 29)
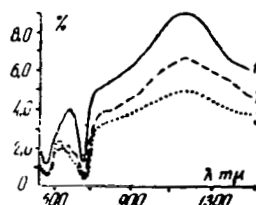
Fig.5

1 – Poplar. Young brown leaf (May 4); 2 – Maple. Young brown leaf (May 4); 3 – Maple. Young green leaf (May 4)
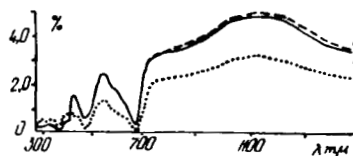
Fig.6

1 – Apricot. Young leaf (May 22); 2 – Plum. Young green leaf (May 22); 3 – Thistle. Young whitish leaf (May 22)

69
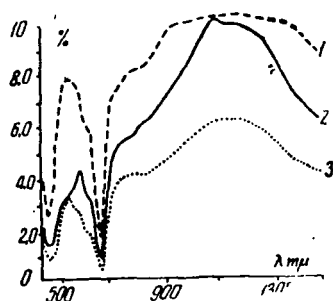
Fig.7

1 - Apricot. Young yellowish leaf
(May 8); 2 - Poplar. Young brown
leaf (May 8); 3 - Poplar. Young
green leaf (May 8)

Fig.8

1 - Plantain. Young leaf (May 17);
2 - Canadian spruce. Row of small
needles (May 17); 3 - Pine. Row of
small needles (May 17)
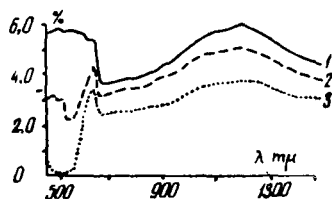
Fig.9

1 - White apple blossoms (May 9);
2 - Rasberry-red apple blossoms
(May 9); 3 - Red tulip blossoms
(May 9)
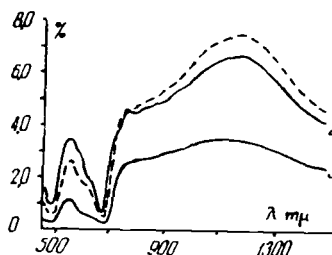
Fig.10

1 - Chestnut. Young green leaf
(May 10); 2 - Chestnut. Young yellow
leaf (May 10); 3 - Thistle. Normal
green leaf (May 10)

An analysis of the curves of the transmission coefficients led to the con-
clusion that carotenoids are present in young early-spring leaves regardless of
leaf color, since the absorption band of these pigments is distinctly present
on all curves. For most of the investigated plants, this band is located in
the range from 0.48 to 0.485 µ (Figs.1, 2, 3, 4, 5, 6, 8, 11). For mullen and
thistle (Figs.1 and 8), the absorption band of carotenoids is shifted to the /62
yellow spectrum region and is located at the wavelength of 0.5 - 0.505 µ. For
all green plants, the maximum both with respect to amplitude and effective wave-
length was distinctly expressed, being located in the wavelength range of 0.550
to 0.645 µ.

The slope of the curve in the region of the green maximum is intimately
connected with the ratio of additional pigments to chlorophyll occurring in that
particular plant. The amplitude of the green maximum depends on the concentra-
tion of all types of pigments, and its width on the total number of pigments
participating in the optical apparatus of the plant. Thus, the green maximum is
an individual characteristic of a given plant, which is readily expressed by the

70

value of the area bounded by the curve itself, i.e., the abscissa and ordinates of its boundaries. For the green maximum, it is easy to determine the effective wavelength which is also a specific individual characteristic of that plant. This peculiarity of the green maximum is a useful criterion in plant physiology and taxonomy.
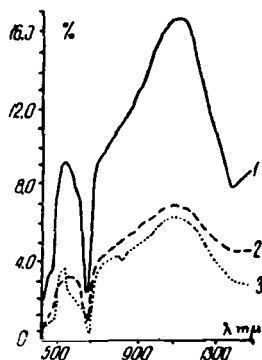
Fig.11

1 - Apricot. Young brown-green leaf. After frost -2°C; 2 - Silver maple. Young red-brown leaf. After frost -2°C; 3 - Ginkgo. Young yellowish leaf. After frost -2°C

It is particularly important to note that, for all investigated plant /63 species without exception, the principal absorption band of chlorophyll in the red portion of the spectrum is located exactly at a wavelength of 0.680 μ but the width and depth of the maximum of this band varies from plant to plant. The band is more distinct in transmitted rays than in reflected rays. This permits increasing the sensitivity of the spectrum analysis of plants, based on a determination of chlorophyll and other pigments found directly in the living cells of plants for which the "breakthrough" effect can be disregarded.

For this, it is necessary to determine the absorption and scattering coefficients in the living plant.

If the disperse-colloidal system of a leaf satisfies certain conditions, for example, random distribution of scattering centers with an equal probability of scattering in all directions, then the Dently or Wurmser nomogram can be used for determining absorption and the scattering coefficient. In the case of isotropic scattering, provided that the incident, transmitted, and reflected light is completely diffused, the abscissa in the Dently nomogram will simply represent the reflection coefficients and the ordinates will be the optical densities.

Knowing the reflection coefficients for a given wavelength λ and the optical density, the absorption and scattering coefficients can be determined from the nomogram. The results hold true if the incident light is parallel and the reflected and transmitted light is completely diffused.

Wurmser proposes a somewhat different method for determining the absorption

71

and scattering coefficients, using transmission with two layers of different optical density. Also this method can be used only if both layers scatter in such a manner that the transmitted light is completely diffused. The principle stipulating that the red band of chlorophyll and the absorption band of carotenoids are more distinct in transmitted light than in reflected light permits a more accurate determination of the transmission coefficient and thus also of the optical density of the pigment of interest. Having determined the scattering coefficient from the optical density, we can exclude the geometric effect of scattering and thus increase the selectivity of absorption; in turn, this will more accurately define the amount of pigments participating in the optical apparatus of the plant, the magnitude of their absorption coefficient, and thus their concentration.

A wide transmission band of infrared radiation is observed in transmitted rays in the investigated plants. The effective wavelength of this transmission maximum lies within 1.1 - 1.15 µ, slightly fluctuating in accordance with the plant species involved (Figs.1, 3, 4, 6). The height of the rise of the transmission maximum, i.e., its amplitude, varies from plant to plant and even within one plant species, depending on the color of the leaves and the environmental conditions. The spectral curve in this absorption region, for most plants, is almost smooth (Figs.2, 6, 8), which indicates the low selectivity of absorption and transmission in this portion of the spectrum.

The low selectivity of plant absorption in this spectrum region can be explained for the most part by the geometric optical effect, including here the effect of scattering and the "breakthrough" effect.

The "breakthrough" phenomenon results in an admixture of white light to the light which had been transmitted by the pigments of the cell sap, as a result of which the absorption of the leaf, at all wavelengths, decreases. This drop has a greater effect on the peaks than in the region of low absorption. /64 Flattening of the curve occurs and the degree of selectivity diminishes. The "breakthrough" effect is very small for compact leaves and appreciable for leaves with a granular chloroplast distribution system. The water and gas contents of the leaf also have a considerable effect on the selectivity of absorption (Fig.1, Curve 1; Fig.2, Curve 1).

The appreciable drop of absorption selectivity in the infrared spectrum region of the investigated plants might also be due to the fact that, when working with the SF-4 spectrophotometer, the transmission coefficient is calculated for all wavelengths with respect to the light flux having passed through air, which on passing through the leaf is partially reflected from the interior leaf walls. Therefore, for each wavelength, the transmission coefficient should be calculated with respect to the light that had passed through air, minus the reflected component. This correction is to be introduced in the final processing of the obtained data.

A preliminary analysis of the curves shows that this type of investigations should be continued, since they afford the opportunity to analyze the infrared effect in physical nature and shed light on the structure of the spectral curves of plant objects in the near-infrared region of the spectrum in transmitted rays and indirectly in reflected rays. The presence of a wide maximum of light trans-

72

mission by the plant in the region of 1.1 - 1.15 μ indicates to investigators of Mars that, if the region of the Martian "seas" should contain earthlike vegetation, then the brightness of the "seas" should be greatest at the wavelengths from 1.1 to 1.2 μ.

BIBLIOGRAPHY

1. Rabinovich, Ye.:   Photosynthesis (Fotosintez). Vol.II, Moscow, Izd. Inostr. Lit., 1953.
2. Perevertun, M.P.: Trudy Sekt. Astrobotan., Vol.III, Alma-Ata, Izd. Akad. Nauk KazSSR, 1955.
3. Perevertun, M.P.: Trudy Sekt. Astrobotan., Vol.V, Alma-Ata, Izd. Akad. Nauk KazSSR, 1957.
4. Tikhov, G.A.: Trudy Sekt. Astrobotan., Vol.V, Alma-Ata, Izd. Akad. Nauk KazSSR, 1955.

CHARACTERISTICS OF THE OPTICAL PROPERTIES OF ALPINE PLANTS OF EASTERN PAMIR

A.P.Kutyreva, B.B.Intykbayeva, and Zh.Kuatova

Introduction

The principle of uniformity of the basic laws of development of matter in the universe and of the difference of their manifestation, depending on the characteristics of the physical conditions and climate, is a pivotal point in the investigations by the Astrobotany Sector on the problem of predicting and determining the possibility of life on other planets.

Therefore, the scientific collective of the Sector considers it possible to use, as the foundation for predicting and determining the possibility of existence of organic forms under the conditions of other planets or other solar systems, not only the astrophysical investigations of the spectral and other physical characteristics of various surface areas of these planets, but also the study of the regularities of the changes in the spectral characteristics of the optical properties of terrestrial plants with any change in environmental conditions. The great Russian physiologist K.A.Timiryazev was the first to indicate the cosmic significance of plants and the importance of studying their optical properties to perceive the laws in the evolution of living matter (Bibl.82). The correctness of this trend is confirmed by the fact that already the first investigations by G.A.Tikhov on the spectral features of the "seas" and "canals" of Mars permitted establishing a number of peculiarities of the variation in the optical properties of plants with any variation in environmental conditions, heretofore unknown to science. Numerous subsequent spectral investigations of terrestrial plants, carried out by G.A.Tikhov and his pupils in various climatic zones of the Soviet Union, convincingly proved the correctness of the hypotheses put forward by him (Bibl.30, 31, 32, 85, 87, 89).

In the light of the above, it was of great interest to study the spectral characteristics of the optical properties of plants under conditions extreme for terrestrial plant life, in particular on the extremely dry alpine plateaus of Eastern Pamir and Tibet, which in a number of indices are close to the data obtained by astronomers for the Martian surface.

Results are given below of such investigations of a number of plant species at the great altitudes of the alpine semi-desert of Eastern Pamir. For one of the points (Zor-Chechekty), the data were obtained close to the upper limit of vegetation in Eastern Pamir (5000 m) and encompass vegetation of the lower part of the snow line.

The field spectral investigations of plants in the Pamirs were carried out in 1950 - 1951 by junior scientist, A.P.Kutyreva, and graduate student of the Astrobotany Sector, Sh.P.Darchiya. The senior laboratory technicians of the /66 Sector, B.B.Intykbayeva and Zh.Kuatova, participated in the photometric processing of the spectrographic materials. The laboratory technician, V.Golubchikov,

and the senior laboratory technician, L.G.Kuznetsova, participated in checking the results of processing some of the materials.

Sh.P.Darchiya's investigation of the Pamir plants comprised,in part, a study of the effect of environmental conditions and the spectral distribution of incident radiant energy on the fluorescence of these plants. Most of the results are contained in his monograph (Bibl.14) and in several articles on this problem (Bibl.13, 15).

The present paper discusses only some of his published results on individual plant species, together with results of the investigation of plants by K.I. Kozlova, senior scientist of the Sector, and by other coworkers and graduate students, which had the purpose of distinguishing the characteristics of the optical properties of Pamir plants from those of other zones.

General supervision and consultation was in hands of G.A.Tikhov, corresponding member of the USSR Academy of Sciences and active member of the Kazakh Academy of Sciences.

The large volume of field work and the satisfactory solution of the problems were made possible through the devoted work and assistance by the team at the Pamir base of the USSR Academy of Sciences, by the Presidium of the Tadzhik Academy of Sciences, Pamir Biological Station, and the Pamir Botanical Gardens.

The bulk of our investigations was carried out on experimental plots at the permanent alpine base of the Pamir Biological Station and on plantings of the Pamir Botanical Gardens, with its numerous species of local flora; introductory work was done on the testing of crop plants under Pamir conditions, including the world collection of barley of the All-Union Institute of Plant Production at the Lenin All-Union Academy of Agricultural Sciences.

The scientific team and management of these establishments assisted greatly in identifying the investigated plants, describing the characteristics of their biology and developmental physiology under Pamir conditions, and in arranging the organization and daily living, for which we express our profound appreciation.

Some of the plant species were identified at the Institute of Botany of the Kazakh Academy of Sciences (by Candidate of Biological Sciences, P.P.Polyakov, and Academician, N.V.Pavlov) and at the Komarov Botanical Institute, USSR Academy of Sciences, in the department for spore-bearing plants (by senior scientist, K.A.Rassadina), while the hot-spring algae were identified by Prof. M.M.Gollerbakh, senior scientist at the same Institute.

2. Area of Investigation

Pamir has long drawn the attention of investigators in all fields, particularly biologists. For more than 20 years, biologists of the Central Asia University, Union, and Tadzhik Academy of Sciences have been conducting expeditionary and laboratory ecological and physiological investigations of plants under these austere conditions. The main bases of the research works are the

experimental plots of the Pamir Biological Station of the Tadzhik Academy of
Sciences, situated in Eastern Pamir on an extensive, rather flat, high-mountain
plateau of the Chechekty natural landmark, intersected at right angles by the
valleys of the Ak-Baytak river and its tributary Chechektinka (average elevation
of this plateau is 3860 m above sea level) and also the permanent alpine base /67
of the Pamir Biological Station, opened in 1948, in an old glacial cirque at the
summit of Zor-Chechekty at an altitude of 4700 - 5000 m above sea level. The
permanent alpine base of the Pamir Biological Station encompasses the vegetation
of the upper part of the alpine zone and lower part of the snow line, growing on
an old moraine terrace and in the bed of a past glacier which descended from the
summit of Zor-Chechekty and extended to the upper limit of vegetation beyond
5000 m above sea level. At present, a small glacier which survives the entire
summer is descending from the Northwest, close to the steep rocky spurs of this
summit. Its influence is felt in an increase of humidity and moisture content
of the soil of adjacent areas and also in the frequency of clouds in nearby
regions.

TABLE 1

PHYSICOGEOGRAPHIC CHARACTERISTICS OF THE AREAS
OF INVESTIGATION

Point	Latitude	Longitude	Elevation above Sea Level, m	Natural Zones
Eastern Pamir:				
Chechekty	38°10'	73°58'	3860	Upper part of subalpine zone
Zor-Chechekty	38°07'	73°52'	4760 - 5000	Alpine zone and snow line
Lake Yashil'-Kul'	37°50'	73°	3660	Middle part of subalpine zone
Dzhilandy	37°10'	74°31'	3440	Lower part of subalpine zone
Western Pamir:				
Pamir Botanical Gardens, Khorog	37°29'	71°32'	2320	Mountain-tugai line (woodlands and shrubs)
Garm-Chashma	37°	71°40'	2325 - 2500	Tugai-shrub line
Stalinabad Botanical Gardens	38°35'	68°47'	824	Dry subtropics of foothills

The main base of the biological investigations in Western Pamir is at the
Pamir Botanical Gardens of the Tadzhik Academy of Sciences, situated in the
interfluve of the Gunt and Shakh-Dara rivers several kilometers from the city
of Khorog, at a height of 2320 m above sea level.

The first observations on the representatives of local flora and the harden-
ing of crops of cultivated plants at the main bases were carried out under the
supervision of P.A.Baranov and I.A.Raykova as long ago as in the 1930's; by the

76

time of the investigations by members of the Astrobotany Sector (1950 - 1951) on the plots of the Pamir Biological Station, there was a large collection of plants with different growth time periods under Pamir conditions. This made it possible to determine the variability of the optical properties of plants by years of reproduction, under growth conditions markedly differing from the initial conditions (see Table 8).

So as to facilitate the conversion of the spectral investigation data on terrestrial plants, grown at different height and in different climatic zones, to planetary conditions we made additional investigations in certain regions of the warm and hot springs of Eastern and Western Pamir. Table 1 gives the layout of the Pamir ranges with an indication of the areas of our studies.
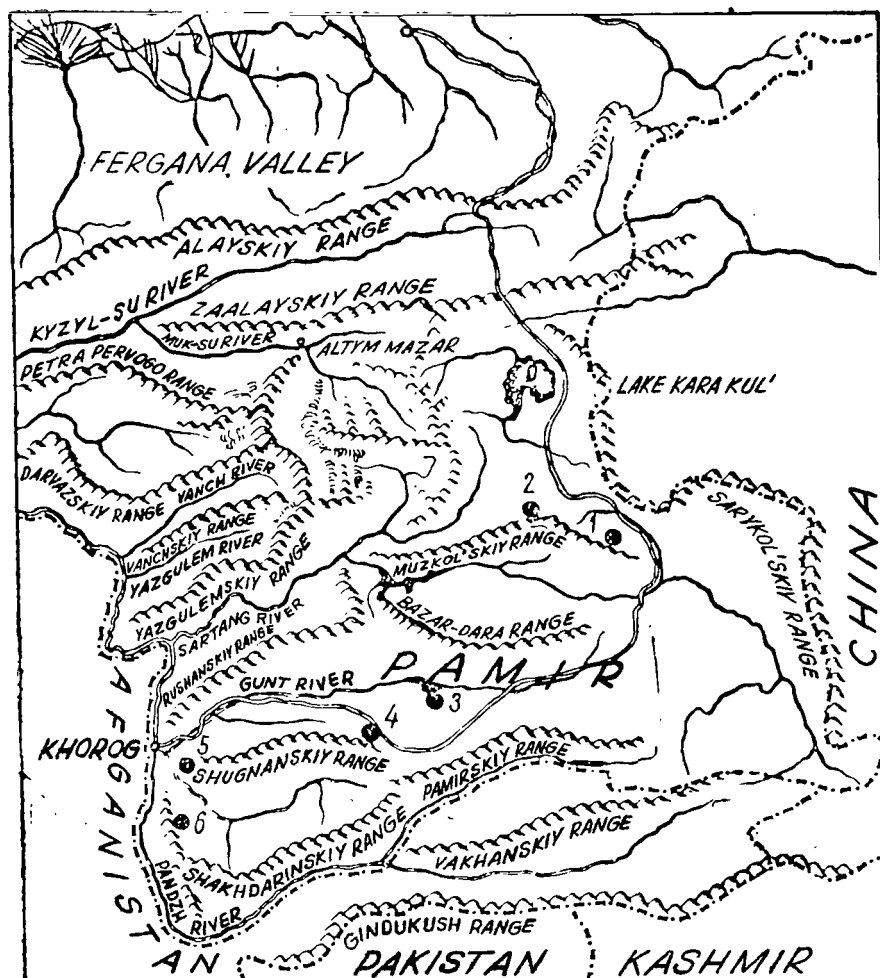
Fig.1 Map of the Pamir Ranges, with Indication of the
Areas of Spectral Investigations

During the long period of comprehensive biological investigations of Pamir plants, several detailed articles and monographs were published by scientists of the Central Asia University, Union Academy of Sciences, and scientists at the Pamir Biological Station and Botanical Gardens of the Tadzhik Academy of Sciences (Bibl.1, 2, 3, 5, 16, 17, 18, 19, 20, 21, 22, 23, 27, 28, 49, 50, 54, 55, 59, 60, 61, 65, 66, 68, 69, 70, 77-80), in which a detailed description was given of the climatic and ecological characteristics of Pamir and of many representatives of its flora, including those covered by our investigations. In our first articles (Bibl.35, 36), we gave an astrobotanical evaluation of the Pamir conditions and noted the problems of studying the optical properties of plants under these conditions. Therefore, in this article we will cite only individual numerical values emphasizing the climatic peculiarities of the compared zones and the immediate conditions of photographing (Tables 2, 3).

TABLE 2

RELATIONSHIP OF ANNUAL AND SEASONAL AVERAGE PRECIPITATION
(IN mm) FOR MANY YEARS IN THE DRY (PAMIR) AND HUMID ALPINE
REGIONS (NORTHERN TIEN SHAN, NORTHERN SLOPES OF THE
ZAILIYSKIY ALATAU MOUNTAINS)

Regions	Dry Highlands				Humid Highlands				Natural Zone
	Point	Total Precipitation, mm			Point	Total Precipitation, mm			
		During Year	During Warm Season	During Cold Season		During Year	During Warm Season	During Cold Season	
Eastern Pamir, subalpine zone (height (3600- 3800 m)	Markansu Valley, Kara-Kul' Lake, Murgab	42	32	10	Myn-Zhilki	734	609	125	Subalpine zone (height 2400- 3100 m)
		62	42	20	Verkhnii Gorel'nik	881	707	174	
		73	57	16	Ust'- Gorel'nik	816	662	154	Belt of spruce forest (height 2100- 1500 m)
Western Pamir, Tugai-shrub line (height 2000- 2500 m)	Ishkashim	98	75	23	Medeo	843	607	236	
	Khorog (AMSG)*	217	90	127	Kamenskoye Plateau	764	—	—	Mountain orchard belt (height 1350 m)
Foothills, dry subtropics (height 800- 850 m)	Stalinabad (Stalinabad Civil Def.),	611	236	255	Alma-Ata (Alma-Ata Civil Def.)	557	370	187	Foothills. Orchard-steppe belt (height 600- 850 m)
	Stalinabad (AMSG)	615	217	398	Alma-Ata (AMSG)	446	282	164	

* AMSG = Airborne Meteorological Station, Civil Air Fleet

According to the data of meteorological observations made at the Pamir Biological Station in Chechekty, as indicated by A.T.Steshenko in his mono-   graph (Bibl.80), the total precipitation during the 11-year period from 1941

TABLE 3

DATA ON ABSOLUTE AND RELATIVE HUMIDITY OF THE MURGAB METEORO-
LOGICAL STATION AT A HEIGHT OF 2 m ABOVE THE SURFACE DURING
AUGUST AND SEPTEMBER 1950 AND AUGUST 1951 IN DAYTIME (ELEVATION
OF THE LOCALE = 3640 m ABOVE SEA LEVEL)

Date	Hours	1950		
		Absolute Humidity, mb	Relative Humidity, %	Wind Direction and Velocity, m/sec
30 Aug.	7	1.0	12	WSW-4
	13	1.4	8	SSW-7
	19	1.6	8	SW-7
31 Aug.	7	1.5	23	SW-5
	13	2.5	4	S-9
	19	0.7	2	SSW-6
1 Sept.	7	2.0	25	0 (calm)
	13	0.7	4	SSW-4
	19	1.2	8	0 (calm)
17 Sept.	13	0.2	1	SE-4
	19	0.0	0	WNW-9
18 Sept.	13	1.7	14	E-2
	19	0.2	1	0 (calm)
19 Sept.	7	1.7	27	0 (calm)
	13	1.2	10	E-3
	19	1.0	9	0 (calm)

Date (August)	Absolute Humidity, mb		Relative Humidity, %		Wind Direction and Velocity, m/sec	
	13	19	13	19	13	19
1	2.7	1.7	11	7	0 (calm)	N-1
2	3.6	0.3	15	1	S-3	W-3
3	3.3	1.3	14	6	S-1	SW-2
4	2.8	2.2	13	10	S-2	SSW-2
5	2.3	2.6	10	12	0 (calm)	W-3
6	4.7	1.3	19	5	SSW-2	W-4
7	3.4	1.7	13	7	S-4	W-1
8	3.3	0.8	14	3	S-3	W-7
9	2.9	1.3	12	6	SSW-9	W-3
10	1.9	1.3	9	7	SSE-5	SW-9
11	2.8	2.1	12	11	N-3	WNW-1
12	2.7	2.8	13	15	W-4	NNW-4
13	1.9	0.8	9	4	E-2	SW-5
14	1.2	0.4	5	2	SW-1	0 (calm)
15	3.4	2.1	17	10	E-1	W-4
16	3.1	0.5	14	2	NW-3	E-3
17	1.8	3.8	8	19	ENE-1	W-7
18	4.1	5.9	28	38	SSW-3	0 (calm)
19	6.0	6.7	35	43	S-1	SW-3
20	3.9	5.0	19	23	0 (calm)	W-1
21	3.9	1.3	17	6	S-4	SW-5
24	1.2	1.2	6	6	S-3	SW-7
25	0.9	0.7	5	4	SSW-4	W-1
26	0.9	0.5	5	3	W-5	W-4
27	1.	1.2	6	7	SSW-3	SW-3
28	1.3	0.3	8	2	NE-1	NW-4
29	0.6	1.1	5	9	NE-1	NW-4
30	1.1	1.0	8	7	SSW-3	SW-3
31	0.7	0.3	4	2	W-1	SW-2

Notes:
1) July 18 and 19, 1951 brief downpours at times. Total precipitation 0.5 mm.
2) Average temperature for August 1951: mean monthly = +14.0°C; maximum =
= +24.1°C; minimum = –4.5°C in air at height 2 m above soil surface;
minimum at soil surface = –10.5°C.
3) The figures in the Table are actual data and are not reduced

to sea level.

4) Results of calculating the humidity were verified in the Analytical Department of the Tadzhik Administration, Hydrological and Meteorological Service.

5) The air temperature during the days of observation from August 30 to September 19, 1950 varied from $+10^{\circ}$ to $+19^{\circ}$C. Night frosts occurred on September 17 (-2.4°C) and on September 19 (-4.0°C).

6) On August 22 and 23 there were interruptions in the observations of the optical properties of plants owing to cloudy weather, for which reason the data on humidity, wind direction, and wind velocity are omitted.

7) N-E-S-W are the Latin designations of compass points for wind direction, used in meteorological practice and corresponding to North, East, South, and West; the different combinations of letters indicate intermediate points, for example: NW is northwesterly wind, SE is southwesterly, etc. (wind velocities are given in meters per second).

through 1951 in the region of the experimental plots of the Pamir Biological Station varied from 150 to 40 – 55 mm, at an average annual precipitation of 100 mm during this period. According to the neighboring meteorological station, Murgab, the mean annual precipitation during this period was 61 mm, the minimum during the year in this region dropped to 21 mm and the maximum reached 159 mm; the relative distribution of precipitation by seasons of the year (winter 24%; spring 32%; summer 44%; fall 0.0%) showed the constant predomination of spring-summer precipitation. Most of the atmospheric precipitation in the subalpine and alpine zones of Eastern Pamir fell in solid form, and toward the upper boundary of the alpine zone and at the snow line it amounted to 100%.

The observations by V.M.Sveshnikova showed that marked temperature fluctuations at the surface of the soil and plants (the diurnal amplitudes frequently reached $60 - 70^{\circ}$C and the annual amplitudes reached $102 - 109^{\circ}$C) promote condensation of moisture in the soil, which constitutes an important additional source of moisture for desert plants and permits them to remain alive even under the conditions of extremely dry air of Eastern Pamir, even at still scantier precipitation (Bibl.69). Our investigations showed that the plants are able to maintain moisture reserves in their tissue without extensive harm to vital activity.

Actually, the data of direct observations on the amplitude of fluctuations of the water content in the leaves of the investigated plants, in relative and absolute units, showed the following limits: from 83 to 92% (1.19 to 8.24 mg/cm^2 of leaf surface) in the humid high-mountains of the northern slopes of the Zailiyskiy Alatau mountains (altitude 848 – 3100 m) and from 36 to 72% (0.35 to 0.76 mg/cm^2 of leaf surface) in the dry high mountains of Eastern and Western Pamir (altitude 2320 – 5000 m). For some wild species of the local flora of Eastern Pamir the water-content indexes are even lower. It is entirely logical to expect that on Mars, with its even greater amplitudes of surface temperature and even scantier moisture reserves, the evolution of higher plants could proceed even farther in this direction.

The mean annual values of relative humidity, according to the Murgab Me-

teorological Station, fluctuate from 38 to 60% at a height of 2 m above the ground, varying from 10 to 100% on some days. Especially extensive are the humidity fluctuations during the middle of the growing season (August) when the mean daily variations range from 7 to 100%. Table 4 shows the daily readings of the absolute and relative humidity at a height of 2 m at the Murgab Meteorological Station during the days of our observations in the Chechekty region in August 1950 and 1951 and for certain days of September 1950, which show that on certain days in August and at the beginning of September the humidity during the second half of the day drops almost to zero, such catastrophic drops in humidity being accompanied by rather strong dry winds.

The strong winds blowing over the greater part of the year during the afternoon hours play a major role in the processes of cooling and drying of soils and plants in Eastern Pamir. They cause especially great damage during severe frosts, catastrophically drying out the soil which is not protected by a snow cover.

The water regime of the soils of Pamir depends on their texture and varies from 3.5 to 10.7% for the small-grained detrital varieties (characteristic /72 for certain experimental plots of the Pamir Biological Station). The lowest moisture content is observed for the gray-brown stony semi-desert soils of Eastern Pamir, since the weak water-retaining capacity of these types of soils causes their rapid drying. The herbarium specimens of Skornyakov's wormwood (Artemisia scorniakowii C.Winkl.), which we took from the soil, did not wilt for more than five years, despite the fact that, after keeping them for a long time in the herbarium screens between sheets of repeatedly changed blotters, we mounted them on cardboard with no moisture anywhere except that from the air. The specimens of these plants were long used as illustrative material in the lectures by G.A.Tikhov on astrobotany, not only as an example of the optical adaptation of plants to environmental conditions as shown by their grayish-blue color, but also as a striking example of the exceptional resistance of one of the members of the higher evolutional forms of the plant world to adverse conditions, mainly to a lack of moisture. The audience was able to see that here we did not have a dead dry herbaceous shrub similar to the specimens of other Pamir plants taken from somewhat "more humid" habitats, but delicate, silky, living leaves which had completely retained their elasticity, subtle perfume, and color characteristic only of a living plant, although in all other respects they did not differ from specimens of other plant species. They were stitched or glued to cardboard sheets, and for many years hung on the wall or were stored in herbarium cases. The specimens of older perennial representatives of this species, with a well-developed root system, exhibited the greatest vitality under these conditions whereas the younger plants changed more quickly to a semidry state. At the same time, other plant species of the semi-desert plateaus of Eastern Pamir, such as the oldworld winterfat (Eurotia ceratoides C.A.M.) or the sand and gravel feathergrasses which also grow under rather harsh conditions, did not show this property and, like other species, rather quickly dried out in the herbarium screens.

The temperature conditions are no less severe: Not only in the alpine, but also in the subalpine zone of Eastern Pamir the mean annual temperatures are negative (Murgab -0.9°C, Chechekty -1.9°C). During the summer, the average air temperature in the subalpine zone at a height of 2 m above ground, fluctuated

81

about +20°C, and in the near-earth layer (at a height of 25 cm), about +30°C, whereas at the surface of the soil and plants the temperature rises during the daytime hours almost to +60°C and higher. During the growing season, the maximum temperatures at the soil surface do not drop below +40.0°C.

Nevertheless, it is the minimum temperature that has the greatest effect on the physiology and vital activity of the Pamir plants.

According to meteorological observations of the Chechekty Biological Station, cited by A.P.Steshenko in his monograph (1956), during the period from 1949 through 1951 (Bibl.80) there was not a single month when the temperature of the near-ground layer of air at a height of 25 cm would not drop below zero. In the usual sense of the word there is no frost-free period here, and positive temperatures are retained at night only after the warmest days. The number of frost-free days vary, from year to year, from 20 to 50. The year 1951 was especially cold, with only 24 frost-free days.

At the surface of the soil and of the plants pressed close to the ground, the amplitudes of temperature fluctuation were even greater, reaching 60°C or even more, and the minima were lower. They frequently dropped to -10, -12°C during the growing season in the subalpine zone and to -15, -18° in the alpine zone. The temperature conditions at the greater altitudes of the alpine zone /73 and lower part of the snow line, where individual species of higher plants are still encountered, must be assumed to be even more austere, although this area has been studied comparatively little, since the meteorological network of the Pamirs encompasses mainly the "more inhabitable" regions of the subalpine zone, whereas at greater altitudes there are only glacier stations. The meteorological conditions recorded here are quite specific and differ widely from the weather characteristics of Alpine meadows. The meteorological observations in the region of the permanent Alpine Station of the Pamir Biological Station are being carried out quite unsystematically and only when scientists are working there.

According to the fragmentary data in the articles (1950) by T.N.Kishkovskiy (Bibl.27, 28), the maximal daytime temperatures of the surface lie in the range from +12° to +40°C in the region of this Station. The moisture content of the soil during the growing season varies within wide limits. For example, at the start of the growing season, the moisture reaches 30% at the soil surface and later drops below 3.6% at the surface and to 10 - 12% at a depth of 1 m. In August, the humidity during the daytime hours drops to 2.9 mm absolute and to 17% relative, and even to less on some days. However, such low humidity values as noted on the level plateaus of the subalpine zone are not encountered here, which again confirms the foehn-like dry wind nature of this phenomenon usually associated with strong winds caused by the breakthrough of considerable air masses from the highest mountain ranges surrounding the plateaus with the resultant intense adiabatic dehydration, followed by heating when the air masses descend to the lower lying (by 2000 - 2500 m) plains of the plateaus of Eastern Pamir. The Alpine meadows situated along the higher portion of the plateaus or along the slopes of the comparatively gentle intersecting plateaus of the ranges and individual summits, rising generally by no more than 1000 - 1500 m above the lowland as part of the plateaus, are less subject to the effect of the foehn-type winds. More precisely, the degree of adiabatic dehydration and warming of the subsiding air at these altitudes is appreciably less, although its effect is

not entirely absent. Actually, the appreciable increase in the intensity of
solar radiation, which we noted in several of our observations, in the presence
of a simultaneous decrease in the intensity of diffuse radiation and a no less
abrupt increase in the transparency of the atmosphere during the foehn winds
indicates the considerable thickness of the near-ground layer of air involved
in this phenomenon; as a rule, the greater the strength of the drying winds, the
more marked is the increase in the intensity of incident radiation on the plants
and the greater is the increase in the transparency of the atmosphere and, conse-
quently, the greater will be the thickness of the air layer subject to dehydra-
tion. Aero-synoptic analyses of the data of the Weather Bureau of the Admini-
stration, Hydrological and Meteorological Service of Tadzhik SSR, confirmed this
and showed that the generation of foehn-like winds is usually associated with
the passage of some portions of the periphery of intense anticyclones, leading
to the spilling of large air masses through the mountain ranges surrounding
Pamir. The usual afternoon rise in wind velocity is associated with an increase,
during the midday hours, of the temperature difference between the zone of
eternal snows and glaciers and the heated surface of the desert and semi-desert
of the lowland part of the plateau and cliffs in the subalpine zone of Eastern
Pamir. Taking into account the predominance of melanocratic components of the
main rocks, their decomposition products, and the prevailing soils of Eastern
Pamir, as well as the rather high intensity of solar radiation which is almost
twice the maximal indices for Tashkent, and the large number of clear sunny days
per year, we can easily imagine how great and stable these differences can be,
which is also true for the strength of the resultant winds and for the super- /74
position of adiabatic dehydration and heating processes in the subsiding air
masses.

The effect of the foehn phenomena and the persistent — for the most part
strong — winds during the afternoon hours makes the relative humidity, even in
the alpine zone of Eastern Pamir at altitudes of the order of 4200 – 5200 m
above sea level, approach the indices of the hottest desert regions of the USSR
where the latter drop below 30% only on a few isolated days.

On the average, only about 105 mm of precipitation falls during the growing
period in the alpine zone, and then only in solid form (snow, hail). Under
Pamir conditions, the boundary of all-year solid precipitation extends to a
height of 4000 – 4200 m above sea level or coincides approximately with the
lower boundary of the alpine zone.

The start of plant growth in this zone, according to the 1950 data by T.N.
Kishkovskiy (Bibl.28), occurs during the period between June 14 and 25 and pro-
ceeds rather rapidly. Already by the second or third day after thawing of the
snow cover, vigorous development of vegetation begins. The thawing periods of
the snow cover are intimately connected here with the character of the meso-
and microrelief and exposure of the slopes.

In the region of the permanent Alpine Station of the Pamir Biological Sta-
tion there are about 50 species of higher plants belonging to 16 families, of
which monocotyledons (Gramineae, Cyperaceae, Liliaceae, Juncaceae) comprise 25%
while dicotyledons [Leguminosae, Cruciferae (Brassicaceae), Compositae, Primu-
laceae, Ranunculaceae, Saxifraga, Gentianaceae, Labiatae, Polygonaceae, Caryo-
phyllaceae, Crassulaceae] comprise 75%. According to the types of viable forms

(Runkier) the helicryptophytes make up the overwhelming majority (up to 80%), followed by cryptophytes (12%), chamaephytes (6%), and therophytes (2%). There are no phanerophytes in this region.

Some plants (Primula nivalis Pall, oxygraphis glacialis (Fedtsch) Bge., Chorispora macropoda Trautv., etc.] begin to grow and even bloom here while still under the snow. Both during the first and last days of the growing season, the plants are subject for more than 12 hours to the effect of negative temperatures which, by morning, often reach -8°C at the soil surface and -12.5 to -15.0°C on the surface of the snow in the immediate vicinity of the plants. The total growing season lasts 85 – 95 days. Establishment of the vegetative and flower buds, even up to a differentiated flower, occurs while it is still summer. During the early spring, the plants rapidly react (within 1 – 2 days, according to data by T.N.Kishkovskiy) to an increase in daytime temperature and frequently, even under a heavy snow cover, start growing; in a number of cases, blossoming occurs before complete melting of the snow.

The start of the blossoming and fruit-bearing stages of other plant species of the alpine zone of Eastern Pamir is shifted to the end of July and beginning of August (first half).

The vegetative stage in all plant species ends by September 20. Despite the predominance of negative soil temperatures during 9 – 10 months of the year, the root systems of a number of plants [for example, Oxytropis immersa (Baker) Bge., Parrya excapa C.A.Mey, etc.] reach a depth of 35 – 40 cm and, more rarely, even 70 cm. T.N.Kishkovskiy explains this by the rapid heating of the soil at great altitudes owing to the intense insolation (Bibl.28).

TABLE 4

TEMPERATURE FLUCTUATIONS AT THE SOIL SURFACE, VICINITY
OF THE PERMANENT ALPINE STATION OF THE PAMIR BIOLOGICAL
STATION (ELEVATION, 4800 m ABOVE SEA LEVEL) FROM
AUGUST 25 TO SEPTEMBER 2, 1951 (IN $^{\circ}$C)

Temperature	August						September	
	26	27	28	29	30	31	1	2
Maximum	$+30^{\circ},0$	$+25^{\circ},8$	$+25^{\circ},6$	$+25^{\circ},0$	$+26^{\circ},7$	$+25^{\circ},1$	$+26^{\circ},6$	—
Minimum	$-10^{\circ},8$	$-9^{\circ},8$	$-9^{\circ},1$	$-8^{\circ},5$	$-7^{\circ},3$	$-6^{\circ},9$	$-7^{\circ},1$	$-7^{\circ},0$

With respect to the characteristics of temperature conditions in the regions of the permanent Alpine Station of the Pamir Biological Station encountered /75 during our spectral survey of the plants, we are giving (Table 4) the absolute deviations of surface temperature based on the observational data by Sh.P. Darchiya (August 25–27) and A.P.Kutyreva (August 28 to September 2). In addition, the temperature of the plants, at the moment of photographing, is indicated on all spectral brightness curves of the plants.

TABLE 5

MEAN ATMOSPHERIC PRESSURE IN (mm)[*] DURING OBSERVATIONAL
PERIOD OF THE OPTICAL PROPERTIES OF PLANTS AT VARIOUS
ALTITUDE ZONES OF PAMIR AND AT ALMA–ATA, AND HIGHEST
STAND OF THE SUN ON THE DAY OF THE SUMMER SOLSTICE
AT THESE POINTS

| Observation Point | Natural Zone | Geographic Coordinates | | | Highest Stand of Sun during Day of Summer Solstice (June 22) | Mean Atmospheric Pressure, mm |
		Latitude	Longitude	Height above Sea Level, m		
		Eastern Pamir				
Zor-Chechekty	Snow line	38°07′	73°52′,4	5200	75°29′	395
Chechekty	Alpine zone	.	.	4760	.	428
	Subalpine zone	38°11′	74°11′	3860	75°17′	475
Southeastern shore of Lake Yashil'-Kul' (Sasyk-Bulak Gorge)	.	37°50′	73°00′	3660	75°37′	485
Dzhelandy	.	37°40′	74°31′	3440	75°47′	495
		Western Pamir				
Garm-Chashma	Tugai-shrub belt	37°	71°	2500	76°10′	560
Khorog, Botanical Garden	.	37°29′	71°32′	2320	75°58′	580
Stalinabad, Botanical Garden	Foothill zone of dry subtropics of Central Asia	38°35′	68°17′	824.03	74°52′	698
		Foothills of Zailiyskiy Alatau (Northern Tien Shan)				
Alma-Ata, Astrobotanical Garden	Foothill orchard-steppe zone	43°15′	76°56′	847.8	70°12′	695 mm

Note: [*] At all high–mountain points, the atmospheric pressure
was read from an aneroid barometer, subsequently corrected
for the scale and temperature.

In concluding our discussion of the physical characteristics of the spectral
investigation region in Pamir and of the main experimental base of the Astro- /76
botany Sector in Alma–Ata taken for comparison, we are giving (Table 5) the mean
atmospheric pressure observed during the observational period, for the elevation
of these sites and the highest stand of the sun on the day of summer solstice,
which are needed for extrapolating the results of spectral investigations of
terrestrial plants to planetary data.

3. Instruments, Method of Observation, and Work-Up of Data of the Field Spectral Recording of Plants

So as to most fully cover all aspects of the radiation regime and radiation properties of plants, with a possibility for their subsequent classification by standard characteristics and also to account for their variability during days of atmospheric optical periods, the observations were carried out with a large assembly of actinometric and optical instruments.

To calculate the energy balance of the incident radiant energy and its utilization by the plants, with summation of the radiant energy for the three portions of the spectrum most important to the vital activity of plants (360 - 570; 570 - 680; and 680 - 3000 mμ), we used Yu.D.Yanishevskiy's pyranometer system with a set of Schott color filters and filters made by the Izyumskiy plant. For the detailed methodological investigations at the main base of the Sector at Alma-Ata, we used a large set of narrower light filters, including ultraviolet and ebonite-infrared; the latter separated the portions of the spectrum from 900 to 1700 mμ.

For a finer calculation of the changes in optical properties of the atmosphere, we used a sapphire cyanometer of G.A.Tikhov's system with a set of colored glass Schott filters, by means of which we recorded the brightness distribution and the color of the celestial vault at the solar vertical (every 15° on both sides of the sun) and observed the magnitude and brightness of the solar corona. The preliminary results of these investigations were published in Vol.III of the Transactions of the Astrobotany Sector (Bibl.37, 1955).

For a more differentiated (by wavelengths) calculation of the spectral distribution of direct, diffuse, and total radiation incident on the plants and for a calculation of the variation in energy distribution over the spectrum at the investigated altitude zones, by seasons of the year and by days of atmospheric optical periods, and in some cases the abrupt changes in optical properties of the atmosphere, for example, in the presence of foehn-like winds in Eastern Pamir, etc., we used a quartz spectrograph. Since these investigations were carried out in parallel and simultaneously with the field spectral investigations of plants which were also in direct sunlight and in diffuse light, the results can be published only after complete work-up of all data of the spectral photographing by A.P.Kutyreva pertaining to this subject (1950 - 1955), both of the high-mountain and seasonal and methodological investigations at the main base of the Sector.

The publication of the material of the pyranometric investigations will be held up, since the mentioned data of the spectral investigations are needed in correcting the results of the pyranometric observations for the fluctuations in sensitivity of these instruments, which take place on variations in the spectral energy distribution of the radiation recorded by the instrument. A calculation of such corrections is especially important when analyzing the materials of the Alpine investigations.

The general results will be given in a summary monograph; in this article, we will mainly discuss the results obtained from the spectral photographs of /77 the plants of the two upper regions.

dd NNcP
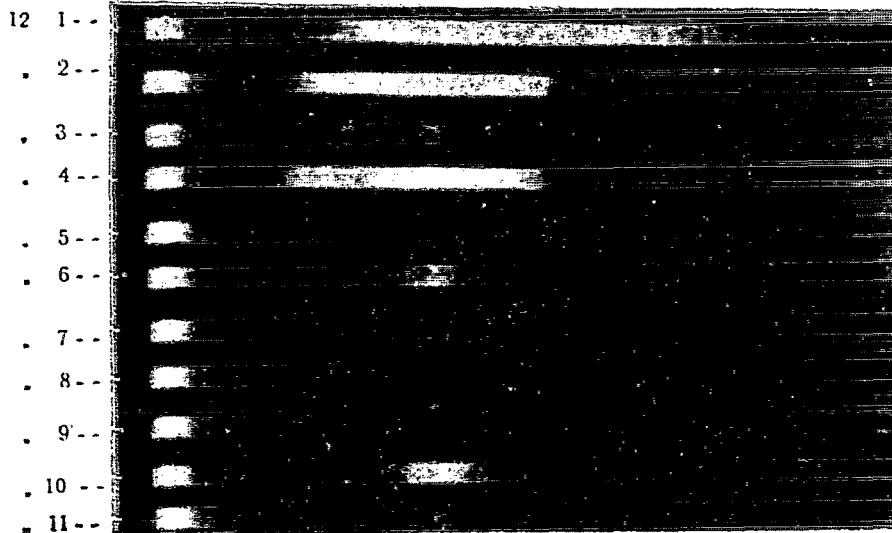
Fig.2
Neg.1C8
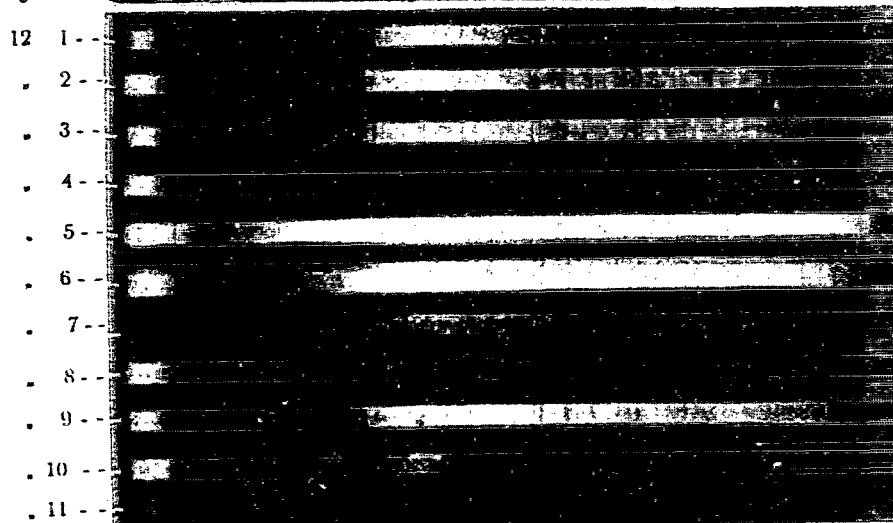
Fig.3
Neg.107
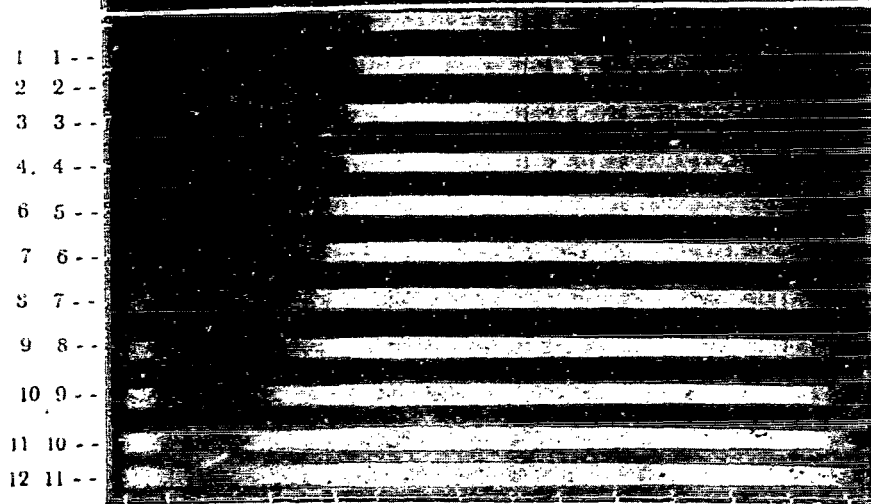
Fig.4
Neg.106

Lines		A	C	D	E	G	H K	M	N	O	Q	R	S	T
λ mμ	860	759,4	658	589	527	430	396,9	376	357	344	329	317,9	310	300

(For explanation see following page)

First, Initial Stage in the Field Determinations of the Spectrum of Plants and Subsequent Calculation of their Radiation Balance.

Spectral characteristics of individual elements of the optical properties of plants (reflection, transmission) plus self-emission which combines fluorescence and chemiluminescence and enters as an inevitable component into the spectrum of both the former and the latter element of the optical properties of plants under field conditions.

Fig.2 1 – Spectrum of light reflected by a lettuce leaf along the normal in direction of the incident rays.
2 – Spectrum of light transmitted through the lettuce leaf along the normal in direction of the incident rays, along the solar ray, in broad daylight.
3 – Same, through a plantain leaf (Plantago lanceolata L.).
4 – Same, through a yellow cabbage leaf (variety Slava).
5 – Same, through a dark-lilac collard leaf.
6 – Same, through a dark-green wild chickory leaf (Cichorium intubus L.)
7 – Same, through a dark-claret leaf of the red beet.
8 – Same, through a dark-green leaf of the red beet.
9 – Same, through a light leaf of the yellow-green beet.
10 – Same, through a pale, dull-green sunflower leaf (Helianthus onnuus).
11 – Same, through cucumber leaf.

Fig.3 1 – Spectrum of light reflected by dark-cerise of the seed cluster of the red amaranth plant (Amaranthus caudatus var. rubra).
2 – Same, by lilac leaves with bluish dull blush, of kohlrabi.
3 – Same, by young leaves of another plant of this cabbage species of an even darker lilac color.
4 – Spectrum of solar rays transmitted through the leaf of this cabbage species.
5 – Same, for rays reflected by plaster of Paris, through leaf.
6 – Spectrum of light reflected by a cabbage leaf, variety Amager (late-ripening) with distinct bluish sheen.
7 – Same, by leaf of early cabbage No.1 (with more pronounced greenish hue).
8 – Spectrum of total sunlight transmitted through leaf of late-ripening cabbage Amager.
9 – Same, transmitted by leaf of early cabbage No.1 from upper side.
10 – Same, from underside of same leaf.
11 – Spectrum of light reflected by plaster-of-Paris screen, through same leaf (cabbage No.1).

Fig.4 1 – 11 – Spectra of photometric scale obtained from standard plaster-of-Paris screen, with a large set of diaphragms (characteristics shown in Table 7).

The photographs were taken by A.P.Kutyreva of the Astrobotany Sector, using a quartz spectrograph with infrared plates made by AGFA (German Democratic Republic) in the region of the Pamir Botanical Garden, Academy of Sciences Tadzhik SSR (in the vicinity of Khorog, Western Pamir, elevation 2320 m above sea level).

The plant spectra were obtained with a field quartz spectrograph of the British Hilger system, modified for field work by G.A.Tikhov, using the method of field investigations based on the principle of relative spectrophotometry which is standard procedure in the Astrobotany Sector.

The instrument itself and the basic principles and techniques of field investigations were described in detail in several monographs and articles of scientific coworkers and postgraduates of the Astrobotany Sector (Bibl.14, 30, 32, 87, 89); therefore, we will omit their description and cite only the characteristics of certain of the most important general and specific aspects of the field work in the Pamirs.

Photographing of the plants and the comparison standard (a plaster-of-Paris screen) with the spectrograph was carried out along a sun ray in a direction normal to the surface of the investigated plant. In the determinations of the spectrum of light reflected by the plant we permitted only small deviations from the normal, within ±5°, whereas the determination of the spectrum of light transmitted by the plant was done strictly along the normal, i.e., with direct sighting at the sun. We rigorously maintained the same distance to the photographed objects and plaster-of-Paris screen. To take into account the effect, on the optical properties of plants, of the intensity and spectral distribution of the flux of radiant energy, the transmission spectrum of the leaf was determined both from the sun and from the plaster-of-Paris screen, i.e., after photographing the transmission spectrum of the leaf with direct sighting at the sun, the spectrograph was turned through 180°, after which we photographed the spectrum of the rays reflected by the plaster-of-Paris screen and transmitted through the leaf in broad daylight and from the plaster of Paris, protected by a special shading screen.

The spectrum of rays reflected by the plant was also photographed in full daylight and in diffuse light; in the latter case, the direct solar rays were obstructed by a special shading shield. The photometric scale for the plaster of Paris was obtained under the same conditions. To take into account the superposition of the effect of illumination and temperature conditions before photographing, individual plant species were photographed both on clear and on uniformly overcast days. Spectral photographing of the plants was carried out for the most part in double and triple replications, and in individual portions of the spectrum, in six- and eightfold replications (photographing of the same plants on three types of photographic plates with a set of diaphragms).

In each case, when photographing the plants, we determined the temperature by a thermometer placed among the plants close to the investigated portion of their surface.

Furthermore, three times a day we determined the surface temperature and

humidity close to the plants by means of a portable Assmann psychrometer; the limiting and prevalent temperatures at the surface of the soil and of the plant as well as the wind velocity were measured by a mercury anemometer and the atmospheric pressure, by an aneroid barometer.

Visual observations of the cloud cover and state of the atmosphere were carried out during the entire photographic period; the visibility was determined in various directions to the horizon, etc., with the data being recorded in a log.

To photograph the spectra of plants, we used Soviet photographic plates produced by the All-Union Research Motion Picture Photographic Institute, "Paninfrachrome" with a sensitivity of H & D of 400 and "Infrachrome" with a speed rating of H & D of 25 and 260, as well as imported German plates of AGFA "Astroplaten" panchromatic and AGFA "Infrarot Platen" 850 Rapid. This set of plates enabled us, together with the quartz spectrograph, to obtain the char- /78 acteristics of plants over a rather large portion of the spectrum, from 300 to 900 mμ. The German infrared plates permitted a relatively far penetration into the infrared spectrum region (up to 900 mμ and more), and the high sensitivity of these plates in the visible spectrum region was highly useful in determining the negligibly small coefficients of spectral brightness of the Pamir alpine plants in this region, especially in overcast weather, as well as in determining the spectrum of rays transmitted by the leaf. Plates with a counter-corona layer (AGFA-Astroplaten, panchromatic) were used to refine the characteristics in the region of the yellow-green maximum of reflection and transmission of light by the plants and for photographing colors, since the Soviet plates Paninfrachrome and Infrachrome had a large dead spot precisely in this region. Figures 2, 3, and 4 show the spectra of plants and the photometric scale with respect to plaster of Paris on infrared photoplates made by Agfa (German Democratic Republic). To develop the plates we used metol-hydroquinone developer. Development of each individual plate took 4 min at a developer temperature of +18° C. Fixing of the developed negatives was done in an acid fixing bath and took 15 - 20 min. In all cases of development and fixing, only fresh solutions were used. The negatives were washed with distilled water for 2 hrs. Paired negatives ("booklets") were developed and fixed simultaneously.

Photometering of some of the negatives was done on a nonrecording photoelectric microphotometer MF-2 and some on a recording microphotometer MF-4, which are available at the Astrobotany Sector. A check showed satisfactory agreement of the photometric results (the relative error did not exceed ±2%). The check was carried out for plant spectra photographed in three and more replications.

It was necessary to eliminate the random errors in the calculations produced by reducing the brightness coefficients recorded from the characteristic curves to the first diaphragm and baryta (the brightness coefficient of baryta at all wavelengths of the investigated portion of the spectrum was taken as unity). For this purpose, after checking on the constancy of the ratios of spectral brightness coefficient of the plaster-of-Paris screen used in our work to baryta in the 310 - 750 mμ spectral region (average $K_\lambda = 0.82 \pm 0.019$) and thus on the direct relationship between the initial and unknown values, we plotted the curve for extrapolation from the values of K_λ taken from the characteristic curve to

TABLE 6

CHARACTERISTICS OF THE DIAPHRAGM SET OF THE QUARTZ SPECTROGRAPH USED IN THE WORK

Characteristic	Number of Diaphragm				
	1	2	3	4	5
Diameter	0.526	0.642	0.835	1.049	1.309
Brightness in relative units	1.0000	1.4804	2.520	3.9774	6.1945
Logarithm of brightness	0.0000	0.1730	0.4064	0.5993	0.7920

6	7	8	9	10	11	12
1.646	2.056	2.470	3.162	4.005	5.076	6.357
9.7904	15.283	22.050	35.550	58.050	93.110	146.083
0.9908	1.1842	1.3434	1.5580	1.7638	1.9690	2.1616

the unknown corrected value of the brightness coefficient referred to baryta (Fig.5).

This dependence is extremely simple in a logarithmic expression, namely:

$$\log I_1 = \log I_0 - \log I_d - \log \Lambda,$$

where /79

$\log I_0$ = value of K_λ recorded from the characteristic curve;

$\log I_d$ = logarithm of the brightness of the diaphragm through which a particular object was photographed;

$\log \Lambda$ = logarithm of the difference of the brightness coefficients of baryta and plaster of Paris at a given wavelength;

$\log I_1$ = unknown value of K_λ expressed in logarithms.

Table 6 shows the characteristics of the set of diaphragms of our spectrograph, used for obtaining the photometric scale and a portion of the Table /80 of extrapolation from the values of the spectral brightness taken from the characteristic curve to the final data reduced to the first diaphragm and baryta for the 12th diaphragm. For each other diaphragm, the dependences change according to the change of the value of log d.

To allow for the superposition of the moisture saturation of the investigated plant tissue in the humid and dry alpine regions on the spectral characteristics of the optical properties of the plants, we determined the moisture content both in relative (in % of dry weight) and in absolute units (mg/cm^2),

91

i.e., per unit of leaf surface; only those leaves whose spectrum was photographed were investigated. The conventional analytical method was used. Results are indicated at the beginning of the article.
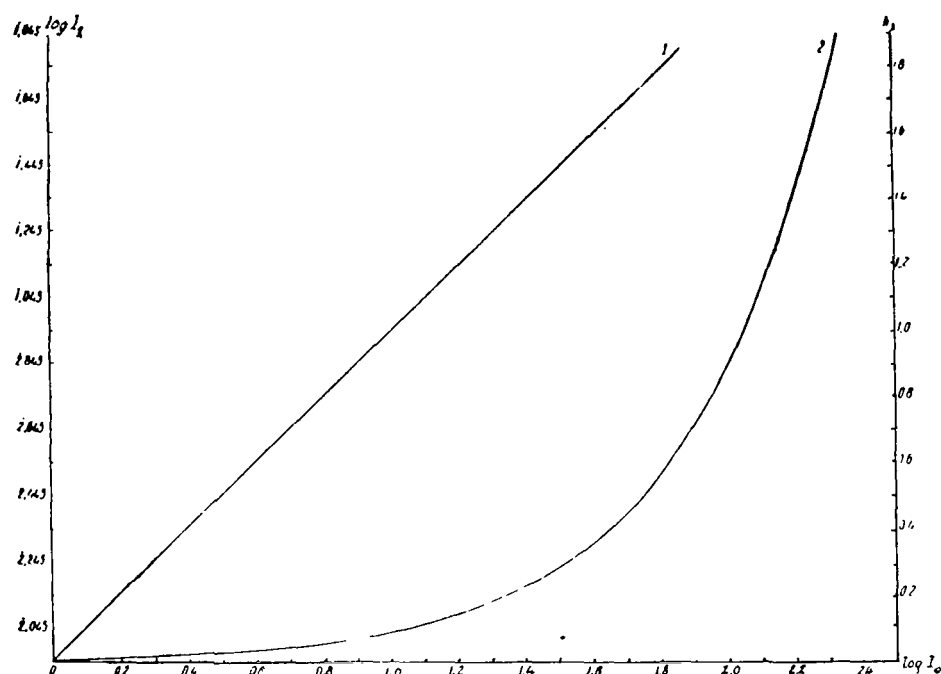
Fig.5 Curve for Extrapolation from the Spectral Brightness (log I_0) Taken from the Characteristic Curves to the Final Results Reduced to the First Diaphragm and Baryta (Reflection of the Baryta Screen in the Investigated Portion of the Spectrum 320 - 760 mμ Arbitrarily Taken as Unity)

1 - log I_1 is the logarithmic expression of the unknown relative values of the spectral brightness of plants photographed through the 12th diaphragm for a stable average difference between the logarithms of the spectral brightness of the baryta and plaster-of-Paris screens at each given wavelength (average, log = 0.0861 in the spectral portion from 320 to 750 mμ). The numerical values of log I_1 are laid off on the ordinate to the left. 2 - K_λ are the numerical values of the coefficient of spectral brightness of the plant reduced to the first diaphragm and baryta (for the case of photographing plants through the 12th diaphragms). The numerical expressions of K_λ are laid off on the ordinate to the right.

Prior to publication, we repeatedly checked the calculations for all spectra and photometering was repeated for the most prominent peaks, which confirmed the correctness of the characteristics of the optical properties of Pamir plants recorded on spectra and of their individual pathological deviations upon abrupt changes in environmental conditions.

To conclude the description of the method of astrobotanical investigations

92

TABLE 7

EXAMPLE OF EXTRAPOLATION FROM INITIAL VALUES OF THE SPECTRAL
BRIGHTNESS ($\log I_0 \lambda$) TAKEN FROM THE CHARACTERISTIC CURVE
TO THE FINAL RESULT ($\log I_1 \lambda$) REDUCED TO THE FIRST
DIAPHRAGM AND BARYTA (12th DIAPHRAGM)[*]

log I_0	log I_1	log I_0	log I_1	log I_0	log I_1	log I_0	log I_1
1,000	$\bar{2}$,7505	1,250	$\bar{1}$,00	1,500	$\bar{1}$,2505	1,750	$\bar{1}$,5005
01	7605	26	01	51	26	76	51
02	77	27	02	52	27	77	52
03	78	28	03	53	28	78	53
04	79	29	04	54	29	79	54
1,050	$\bar{2}$,8005	1,300	$\bar{1}$,0505	1,550	$\bar{1}$,3005	1,800	$\bar{1}$,5505
06	81	31	06	56	31	81	56
07	82	32	07	57	32	82	57
08	83	33	18	58	33	83	58
09	84	34	09	59	34	84	59
1,100	$\bar{2}$,8505	1,350	$\bar{1}$,1005	1,600	$\bar{1}$,3505	1,850	$\bar{1}$,6005
11	86	36	11	61	36	86	61
12	87	37	12	62	37	87	62
13	88	38	13	63	38	88	63
14	89	39	14	64	39	89	64
1,150	$\bar{2}$,9005	1,400	$\bar{1}$,1505	1,650	$\bar{1}$,4005	1,900	$\bar{1}$,6505
16	91	41	16	66	41	91	66
17	92	42	17	67	42	92	67
18	93	43	18	68	43	93	68
19	94	44	19	69	44	94	69
1,200	$\bar{2}$,9505	1,450	$\bar{1}$,2005	1,700	$\bar{1}$,4505	1,950	$\bar{1}$,7005
21	96	46	21	71	46	96	71
22	97	47	22	72	47	97	72
23	98	48	23	73	48	98	73
24	99	49	24	74	49	99	74

[*] A standard matte plaster-of-Paris plate manufactured from chemically pure gypsum with 10% magnesium was used as the control screen.

carried out in the Pamirs, we should note the excessive difficulties and the
present impossibility of taking into account, in the field, the widely fluctuating conditions of photography and illumination intensity which greatly handicaps the processing of the data. An example is the unexpectedly high increase in intensity of the radiation striking the plants during the foehn, even at low position of the sun. A sudden sandstorm, that blew up while photographing during a gusty foehn-like wind, upset the spectrograph and the minute dust particles which penetrated the film holder caused small white spots to appear on the spectra. Consequently, the spectra could be processed only on a highly sensitive microphotometer with photoelectron amplifiers, since a measurement of the density of the negative with respect to the spectrum in this case is possible only with a very narrow and low slit. (There is presently one such microphotometer at the Shternberg State Astronomical Institute.) Or another example: Taking into account the appreciable environmental temperature rise in the hot-spring region of the Pamirs, we reduced the exposure by a factor of 3 in photographing the plant spectra; nevertheless, some of the spectra proved to be overexposed, with a high density, which could not be measured on low-sensitive

microphotometers.

4. Results of Investigations

Before analyzing the results of the investigation, we will give a brief historical review over the development and formation of the vegetation of Eastern Pamir encountered by us.

Despite the excessively austere climate and severe growing conditions, the flora of Pamir includes about 600 species of higher plants of considerable diversity as to origin (of these, about 50 species have penetrated to the boundaries of the snow line at 5000 m above sea level).

Of the flora of Eastern Pamir, about 62% of the species are the same as those of Pamir-Alay, 38% as those of anterior Asia; 32% are identical to species of the lowlands of Central Asia and 25% to those of Tibet. Endemic plants, i.e., plants encountered exclusively in a given region, account for only 7%, which indicates that Pamir must be classified as a floristically young mountain region (Vasilevskaya, 1940).

The vegetation of Pamir underwent considerable alterations during the Quaternary, under the effect of the extensive glaciation that occurred here. However, the glaciers mainly encompassed the extreme North and South of Pamir and free areas were left in its central parts on which vegetation similar to contemporary vegetation existed (Tolmachev, 1944), which serves as an indirect indication of the great antiquity of a portion of the present-day flora of Pamir and permits us to consider it as a relict, at least, of the glacial epoch.

The retreat of the glacial masses was accompanied by an increase in dryness and by general cooling during the continued uplifting of the mountains, which promoted the formation of deserts. Such changes, accompanied by spreading of deserts as the result of contraction of the meadows and steppes, is even now continuing.

The central regions of Eastern Pamir, comprising the subalpine zone, are characterized by wide river valleys and lake basins situated on the average at an altitude of about 3500 – 4000 m above sea level. The individual systems /82 of river valleys are separated by mountain ranges rising 1100 – 1500 m above the valley floor.

The extreme dryness of the climate of this region is responsible for the prevalence of desert and semi-desert plant formations, with predominance of xerophytic subshrubs, tomentose winterfat (Eurotia lanata) and Skornyakov's mugwort (Artemisia skorniakowii); the steppe type of vegetation occupies the piedmont benchlands or gentle slopes with fine-grained soils. The cushion plants usually prefer stony soils. The meadows are situated along river beds, lake shores, and where ground waters outcrop. The most characteristic feature of the vegetation cover of the central regions of Eastern Pamir in the subalpine zone is its extensive discontinuity on the surface and almost complete interlocking of root systems in the soil.

The upper boundary of the vegetation areas of the subalpine and alpine zones and the snow line is located here appreciably higher than in other mountain systems, including the Tibetian Highland.
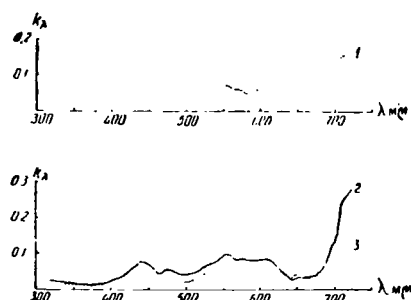
Fig.6 First Group: Spectra of the Main (Predominating)
Plant Species of the Cold High-Mountain Semi-Desert of
the Subalpine Zone of Eastern Pamir
(The spectra were obtained by A.P.Kutyreva at an altitude
of 3860 m above sea level in the region of the Chechekty
landmark at the beginning of August 1951.) 1 – Winterfat
(Eurotia ceratoides C.A.Mey). Average of four replica-
tions. 2 – Skornyakov's mugwort (Artemisia Skorniakowii
C. Winkl). Average of three replications. 3 – Summer
sagebrush (Artemisia macrocephala Jacq.). Average of three
replications

The increasing inclemency of the climatic conditions, as the glaciers melted, led to appreciable changes of the viable forms. The local species of vegetation of the subalpine zone are now represented primarily by low subshrubs, soil-hugging plant cushions, and clumps of perennial grasses. They comprise 75% of the entire plant composition of the Pamirs. Aside from the xerophylic subshrubs, herbaceous perennials are most numerous. The latter are divided into two groups: helicryptophytes and cryptophytes. The first group includes feathergrasses, sedges, cobresia cinquefoil (Potentila multifida, P. pamiro-alaica, etc.) and the second group (cryptophytes) includes irises, onions, meadow grass, some species of cinquefoil, for example, Potentila moor-koftii Will., milk vetch (Astragalus chajanensis Franch.), and others. Annuals such as the annual brome grasses Bromus Dantonial Frin., Bromus tectorum L., etc. are least widespread. They, like the horse sorrel, entered the flora of Pamir from without. Each of the named desert forms has its own biological and morpho-logical characteristics which permit them to be distinguished not only by their outward shape, but also by their development.

The great diversity of the origin of various representatives of the flora of Eastern Pamir also leaves its impression on the spectral characteristics of the optical properties of these plants. These differences are especially great near the yellow-green maximum and the near-infrared region (see Figs.6, 7, 8).

An even greater effect is exerted by the duration of the sprouting of vari-

ous species under given conditions and thus by the extent of genetic assimilation of the properties acquired under the extremely harsh environmental conditions.
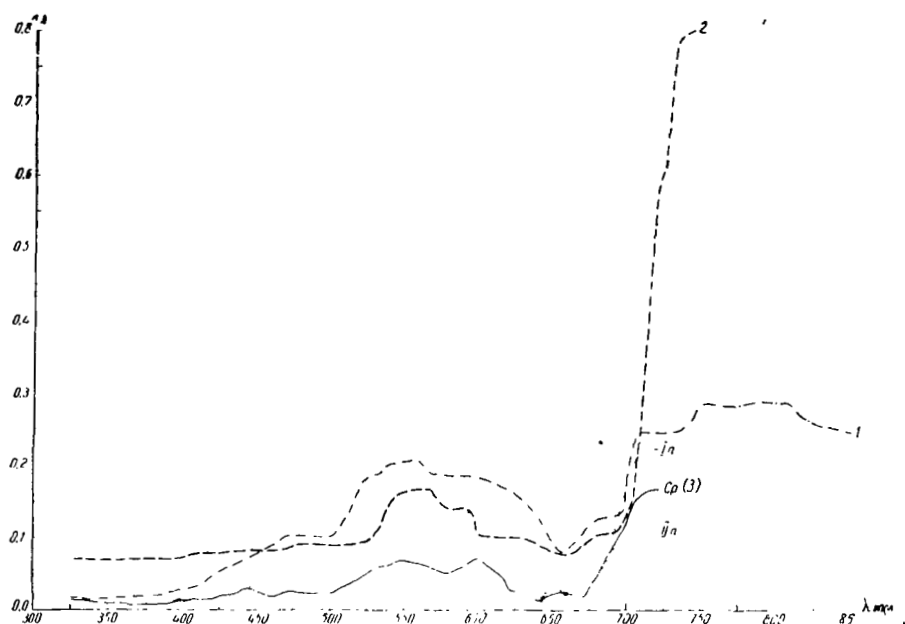
Fig.7   Change in the Optical Properties of Eurotia
Ceratoides Relative to its Habitat and
Weather Conditions

1 – Semi–desert steppe foothills of Zailiyskiy Alatau in the
vicinity of Chemolgan, altitude 840 m above sea level, June 2,
1948 (based on K.I.Kozlova's data); 2 – Central Asia desert
(vicinity of Kokanda, altitude 300 m above sea level, October 19,
1950, data by K.I.Kozlova); 3 – Alpine desert of Eastern Pamir
(vicinity of the Pamir Biological Station at the Chechekty land-
mark, stony saline soils). The first replication (I n) was
photographed at 15:00 local time, temperature among the plants
$+24^{\circ}$ C, calm; second replication (II n) photographed 40 minutes
later during gusts of fresh wind up to 2 – 3 m/sec and temperature
drop to 22.4° C, average of four replications (data by A.P.Kutyreva)

In Table 8 we attempted to show these differences, based on the character-
istics of five markedly differing plant species of the subalpine zone of Eastern
Pamir, for which we had more or less definite information as to the time of   /83
their existence (whereas the differences of specific plants are given in Figs.6,
7, 8, and 10).

As indicated in Table 8, the position of the yellow-green maximum for the
species under consideration shifts within 50 mμ (fluctuations of the position
of $K_{\lambda_{max}}$ from 525 to 575 mμ), whereas its height or level of radiation changes
almost by a factor of 10 (from 32 to 3.2%); for the most part, the maximum occu-
pied the lower position for plants with a longer period of habitation under

96

given conditions. The maximum disappears almost completely under the conditions of the alpine zone and snow line, as is apparent from Figs.12 and 13.

TABLE 8

SPECTRAL CHARACTERISTICS OF THE OPTICAL PROPERTIES OF VARIOUS PLANT SPECIES OF THE SUBALPINE ZONE OF EASTERN PAMIR (CHECHEKTY, ALTITUDE 3860 m ABOVE SEA LEVEL)

Plant Species	Yellow-Green Reflection Maximum	
	$\lambda_{max,}$ $m\mu$	$K_{\lambda max,}$ %
Horse sorrel (Rumex confertus Willd.)	525	31.6%
Couch grass (Agropyrum terenum)	554	17.6%
Solenanthus stylosus Lipsky (Solenanthus)	570	12.2
Milk vetch (Astragalus Chajanensis)	574	8.9
Yellow sweet clover (Melilotus officinalis Desz.)	570	3.2

Infrared Effect				Length of Period of Habitation in the Given Belt of Eastern Pamir
Start		Maximum		
λ of Start, $m\mu$	K_{λ} of Start, %	λ of Greatest Maximum, $m\mu$	K_{λ} of Greatest Maximum, %	
660	35.5%	740	80.0	First year
714	20.8	780	73.2	Third year
703	9.8	755 – 772	79.0	More than 10 years
714	10.2	805	66.7	Many centuries
714	3.02	770 – 780	30.2 – 28.8	More than 15 years

Note: The start of the infrared effect at sea level (Batumi) for the horse sorrel is at 660.0 mμ, whereas in the humid alpine regions of Tien Shan it shifts to 690 mμ and stays at this value almost up to the snow line (altitude 3100 m above sea level) at a general drop in intensity by 7 – 8% in reflected light and 15 – 20% in light transmitted through the leaf [data from printed publications of the Sector (Bibl.75)].

The start of increase in the reflection of long-wave red rays shifts from 660 mμ to 714 mμ for some plant species, and the greatest rise (maximum) of reflection shifts from 740 to 805 mμ. The infrared maximum varies from 80 to 20%, occupying the lowest position for the most ancient representatives of the flora (see Fig.6 and Table 8); the radiation maximum for these species shifts to the longer-wave region of the spectrum (beyond 800 mμ).

With mountain elevation or, more exactly, with an increase of the height of habitation above sea level of all the investigated plant species, there is a general tendency toward an increase of the absorption of radiant energy and   /84

its greater utilization by the plant owing to a decrease of the wasteful losses to reflection, transmission, and radiation. According to the data by O.V.Zelenskiy (Bibl.17, 18, 21), the efficiency of photosynthesis of alpine Pamir plants is many times greater than that of valley plants.
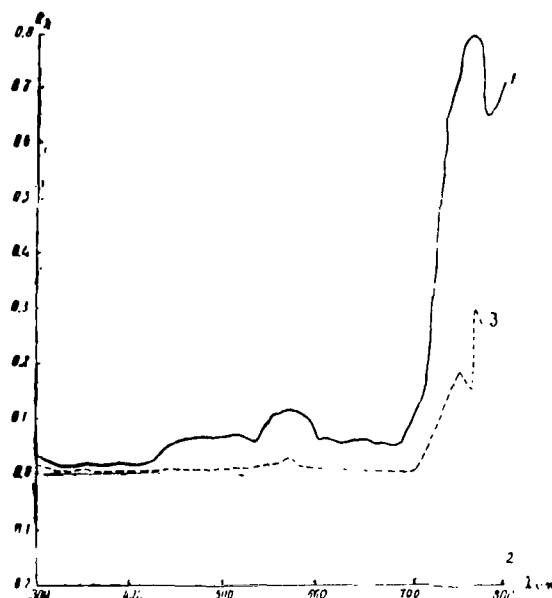
Fig.8 Optical Properties of Plants of the Subalpine Zone
of Eastern Pamir (according to Data by A.P.Kutyreva)
1 - Spectrum of light, reflection loss of solenanthus plant
(Solenanthus stylosus Lipsky). Color of leaves pale, dull,
bluish-green. 2 - Spectrum of sunlight, previously transparent
leaf of solenanthus. 3 - Spectrum of light, reflection of dark
purplish-green leaves of yellow sweet clover (Melilotus
officinalis Desz)

The greatest changes were noted in the region of the yellow-green maximum of the main absorption band of chlorophyll; these were especially abrupt near the infrared maximum of the reflection and transmission of light by the leaf in the corresponding portion of the spectrum.

Similar changes in the spectral characteristics of the optical properties of plants were noted by coworkers and postgraduates of the Sector, in investigating the change in the optical properties of common species of plants as they advanced from South to North (meridional profiles for the eastern, central, and western zones of the USSR from the coastline of the Arctic Ocean to the most southern points in the territory of the USSR (Bibl.30, 52, 89).

As one of the most striking examples of this type of change, Table 9 and Figs.9 and 10 give the data by Sh.P.Darchiya based on the results of investigating the spectral brightness of one of the species of horse sorrel (Rumex confertus Willd.) at diametrically opposed climatic zones, namely, on the shores

of the Black Sea in the humid subtropics of the Caucasian littoral, and under
conditions of the extremely dry mountain desert of the subalpine zone of Eastern
Pamir (true, the results are somewhat modified by the regular waterings of the
experimental plots at the Pamir Biological Station). When analyzing the data of
Table 9 one must allow for the fact that, in the region of Chechekty, horse
sorrel plants were investigated that had been brought in with the seeds of crop

TABLE 9

RELATIONSHIP OF THE COEFFICIENTS OF SPECTRAL BRIGHTNESS
OF THE HORSE SORREL LEAF GROWING IN DIAMETRICALLY OPPO-
SITE CLIMATIC REGIONS, BASED ON DATA BY SH.P.DARCHIYA
(BIBL.14)
(Expressed in Relative Units or Percent of Incident
Flux at Each Wavelength.)

Wavelength, $\Delta\lambda m_\mu$	Coefficients of Spectral Brightness,%		Differences in Changes Upward
	Humid Subtropics of Batumi, Elevation = 0.0 m	Extremely Dry High-Mountain Desert of Eastern Pamir, Chechekty, Altitude = 3860 m	
300—390	0,5	13,2	+ 12,7
391—400	5,0	8,2	+ 3,2
401—422	10,3	11,4	+ 1,1
423—455	13,1	12,42	— 0,68
456—490	14,1	12,45	— 1,65
495 515	17,0	27,0	+ 10,0
516—595	Dead Spot of Photographic Plate		
596—655	12,9	17,4	+ 4,5
656—670	20,2	35,5	+ 15,3
671—675	76,4	53,5	— 22,0
676—690	81,5	51,6	— 30,0
691—706	141,0	37,2	—103,86
707—716	153,8	57,8	— 96,0
717—732	162,0	69,0	— 93,0
733—773	187,2	74,3	—112,9
775—785	164,0	73,75	— 90,25
790—805	118,8%	74,1%	— 44,7

plants and had been growing in this area for not more than 1 – 2 years, so that
they still retained most properties inherent to this species under valley
conditions. The numerical data in the Table are broken down by portions of the
spectrum which showed the common features of the reaction of the optical plant
properties to changes in environment. These data clearly show that, with an
increase in altitude of habitat (almost by 4000 m) and at the marked decrease
in humidity and temperature of the environment, the plant exhibits the greatest
reduction in losses in the long-wave red (beyond 670 mµ) and near-infrared
region, whereas near the radiation maximum and near the steepest transitions,
the decrease in radiation and the increase in absorption of radiant energy may
reach 60 – 70% and more.

Considerable interest is offered by comparison of the variation in the
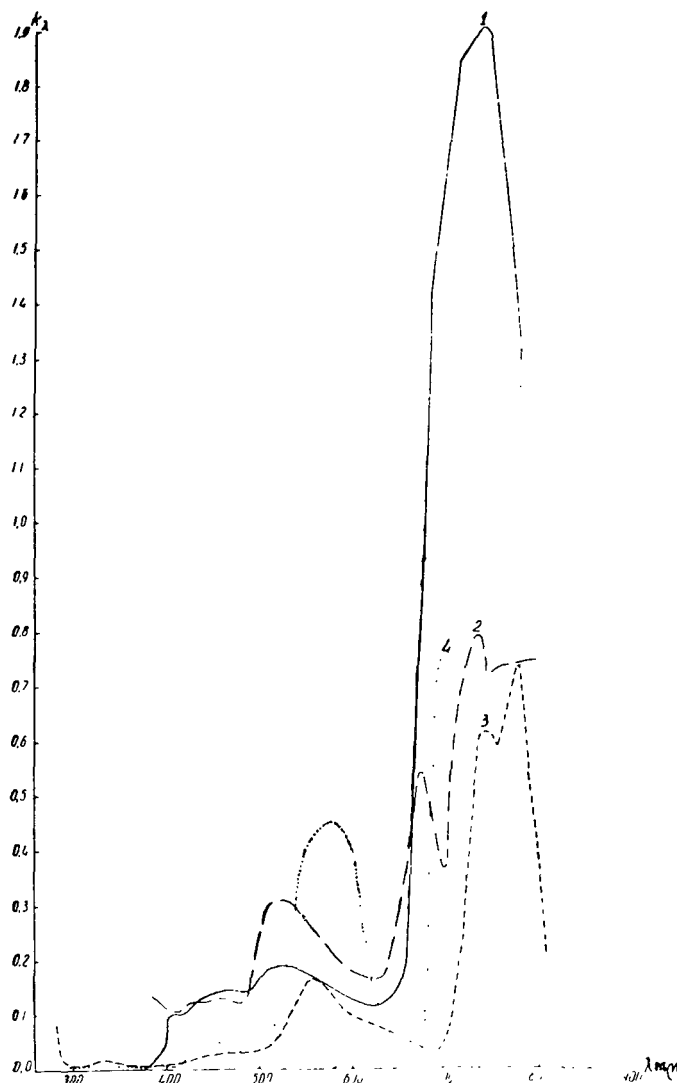
Fig.9 Optical Properties of the Second Group of Plants of
the Subalpine Zone of Eastern Pamir: Cultivated (Fodder
Grasses) and Semi-Cultivated (Weed Plants Imported into
the Pamirs Accidentally with Seeds of Cultivated Plants)
during the First Years of Reproduction in Eastern Pamir
1 - Horsè sorrel (Rumex confertus Willd.) at Batumi, elevation 0.0 m
above sea level (data by Sh.P.Darchiya). 2 - Same, in the area of
the Chechekty landmark: Eastern Pamir, elevation 3860 m above sea
level at the experimental plots of the Pamir Biological Station,
Academy of Sciences Tadzhik SSR (data by Sh.P.Darchiya). 3 - Couch
grass (Agropyrum tenerum Varey), third year of development there (data
by A.P.Kutyreva). 4 - Awnless brome grass (Bromus inermis Leyss),
second year of development there (data by A.P.Kutyreva)

100

optical plant properties with altitude, under conditions of both dry and humid high-mountain regions. The data published in the article by V.P.Bedenko, S.A. Stanko, and M.S.Nebogatikova (Bibl.75), together with the results of our own investigations, indicate that, at uniformity of the general trend toward an increase in light absorption with altitude under the humid high-mountain conditions
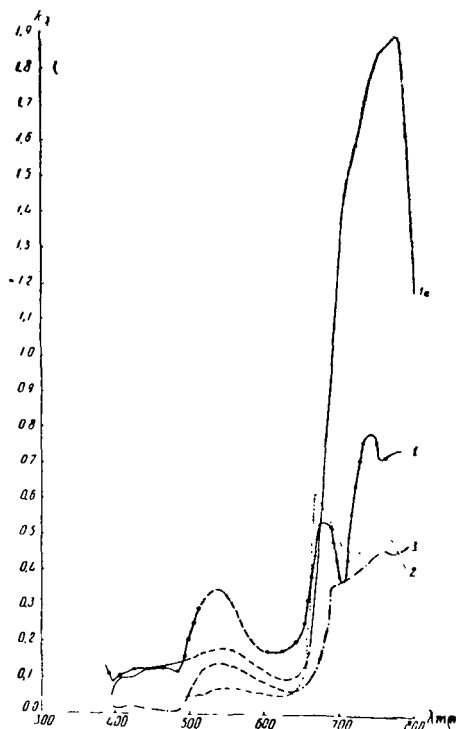
Fig.10 Plants of the Second Group, but after a Long
Period of Habitation in the Lower Part of the
Subalpine Zone of Eastern Pamir
Photographed at the collective farm field in the lower reaches
of the Sasyk-Bulak gorge, irrigated by hot-spring waters; altitude 3660 m above sea level, southeastern shore of Lake Yashil'-Kul'.
[The data by Sh.P.Darchiya (Bibl.14) were obtained with the same
comparison standard on Soviet photographic plates sensitive to
infrared rays.] 1 and 1a - Horse sorrel (Rumex confertus Willd.)
in areas with diametrically opposite climate (Chechekty-Batumi)
at an altitude difference of about 4000 m. 2 - Western Pamir common
naked barley at the grain-ripening stage (elevation 3660 m above
sea level. Collective farm crops on the southeastern shore of
Lake Yashil'-Kul', Eastern Pamir). 3 - Red goosefoot (Chenopodium
latifolium rubra), same place.

of Northern Tien Shan, the reflected flux decreases more abruptly and the amount of radiation transmitted by the leaf more slowly. Under the extremely dry high-mountain conditions of Pamir, where the boundaries of the vegetation

zones extend much farther upward and where a much sharper difference exists in the climatic conditions as well as in the spectral energy distribution, the optical properties of the plants change such that the transmission by the leaf is much less at lower amounts of reflected light flux. This agrees well with the modification of the anatomic structure of Pamir plants with altitude, consisting of a reduction of intercellular interstices and greater parvicellulosity of the tissues (V.K.Vasilevskaya, 1940). The data by V.K.Vasilevskaya were confirmed in our tests on the anatomic structure in the investigated plants, which were analyzed for the Sector by Candidate of Biological Sciences L.I. Lipayeva, senior scientist at the Institute of Desert Assimilation of the Academy of Sciences, Kazakh SSR, on whose demand samples of plants of the alpine and subalpine zones of Eastern Pamir were collected and processed for an an- /88 atomic analysis. Numerous biological analyses of the vegetation of the humid alpine zones of Northern Tien Shan show that, although under these conditions there is a certain intensification of the xeromorphic character of plants with altitude, quite a few mesophytes are found and appreciably larger cells are observed in the plant tissues in comparison with the Pamir plants; similarly, their less compact "packing" with practically unchanged intercellular spaces is retained.

TABLE 10

DIFFERENCE OF ABSORPTION OF RADIANT ENERGY BY HORSE SORREL
LEAVES (RUMEX CONFERTUS WILLD.) AND SOLENANTHUS
(SOLENANTHUS STYLOSUS LIPSKY) IN THE SUBALPINE
ZONE OF DRY AND HUMID ALPINE REGIONS

Wavelength, $\Delta\lambda$ mμ	Absorption of Radiant Energy, %		Difference in Absorption in Dry Highlands
	Humid Highlands, Altitude 3100 m	Dry Highlands, Altitude 3860 m	
300—416	99,3	99,0	— 0,3
420—450	97 0	96,0	— 1,0
455—550	94,3	92,1	— 2,2
555—595	87,9	87,6	— 0,3
596—614	88,4	91,6	+ 3,2
615—680	92,5	93,5	+ 1,0
680—692	89,5	94,0	+ 4,5
693—703	53,0	91,0	+ 38,0
703—714	42,0	85,5	+43,5
715—725	36,0	76,6	+40,6
726—738	40,0	50,9	+10,9
738—751	40,5	24,8	—16,7
752	41,0	15,0	—26,0
755—765	41,0	7,4	—33,6
765 - 772	—	8,4	
773—780	—	19,3	
780—788	—	28,4	
788—805	—	25,2	
805—815	—	16,6	

As a typical example, Table 10 shows the spectral characteristics of light absorption by broad-leafed representatives of the weed vegetation of the subalpine zone of the humid and dry highlands: horse sorrel (Rumex confertus

Willd.) and solenanthus (Solenanthus stylosus Lipsky). The data in the Table are divided by spectrum regions, in whose portions the average indices show a more or less good constancy. The differences in the fourth column of the Table show a slight increase in reflection in the ultraviolet spectrum region and the short-wave portion of the visible region, owing to a significant increase in the intensity of the radiant flux incident on the plants in this region and also as the result of the expansion of the ultraviolet end of the spectrum, owing to the shorter-wave rays with high energy. On a reduction in size of the transparent sky over the subalpine zone of the humid highlands, this part of the spectrum is either cut off entirely or, in the rare cases of an amelioration in the transparent sky cover, is appreciably weakened.

The fourth column of Table 10 distinctly shows that the broadening of the main absorption band for plants of the subalpine zone of Eastern Pamir is less distinct toward the yellow portion (up to 595 mµ) and more distinct toward the long-wave red portion, with an average absorption increase up to 38 - 44% in the spectrum region from 690 to 725 mµ and with a corresponding shift of the incipient rise and maximum of infrared effect toward the longer-wave region. /89
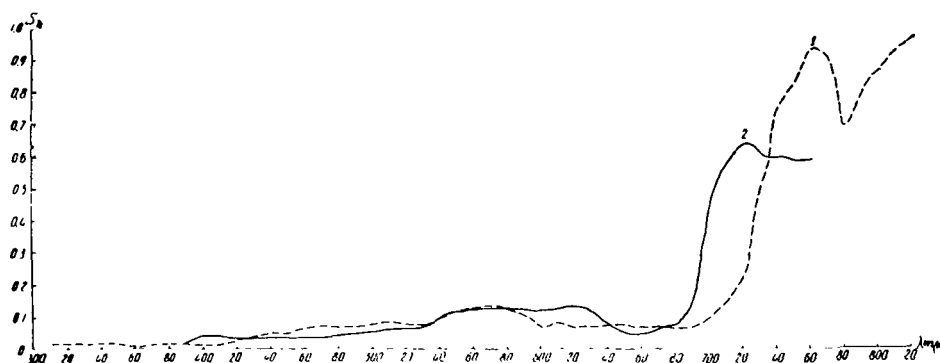
Fig.11 Total Losses of Radiant Energy by Plants of the
Subalpine Zone of the Dry (Eastern Pamir) and Humid
Highlands (Northern Slopes of the Zailiyskiy Alatau
Mountains, Northern Tien Shan)
1 - Solenanthus (Solenanthus stylosus Lipsky), data by A.P.
Kutyreva obtained on August 24, 1951 in Eastern Pamir in the
area of the Chechekty landmark, altitude 3860 m above sea level.
2 - Horse sorrel (Rumex confertus Willd.) data for the subalpine
zone of the humid highlands (northern slope of Zailiyskiy Alatau
mountains, in the vicinity of Alma-Ata, Chimbulak landmark,
height 2980 m above sea level) taken from the article by S.A.Stanko,
V.P.Bedenko, and M.S.Nebogatikova (Bibl.75)

Here, the decrease of losses in the 690 - 725 mµ portion is compensated by the increase in the longer-wave region of 740 - 820 mµ. The total value of the radiation balance for the entire solar-energy spectrum (300 - 900 mµ) for each plant species, by altitude belt or by individual natural zones, is quite close or almost the same for the humid and for the dry alpine regions. Here, depend-

ing on the environmental conditions and the characteristics of the spectral energy distribution in the flux of radiant energy incident on the plants, which in turn is associated with the characteristics of the optical properties of the atmosphere in a given natural zone, the region of the solar spectrum actively utilized by plants somewhat constricts or expands, under strict obeyance of the general physical law of the conservation of energy. This is especially pronounced on the curve of total losses for the spectrum region from 300 to 820 mμ, compiled on suggestion by G.A.Tikhov [see his article in this volume (Bibl.86)] for these very same plants in the subalpine zone of the dry and humid highlands (see Fig.11). The diagram gives one curve for the radiant energy loss by a plant to reflection, transmission, and radiation; this smoothes out the appreciable differences in the change of the magnitude of the optical properties of plants (i.e., of reflection, transmission, and radiation separately) in the humid and dry alpine regions, which hamper a general analysis; in addition, the basic laws of the significant broadening of the main absorption band of chlorophyll and the shift of the infrared maximum of self-radiation of plants toward the longer-wave region of the spectrum are much better defined. This is especially pronounced at the great altitudes of the subalpine zone in the dry highlands of Eastern Pamir (3860 m instead of 2980 m above sea level). These regularities were already pointed out by A.N.Danilov (Bibl.11, 12) who made laboratory experiments on the effect of combinations of rays of different spectrum portions on the photosynthesis of algae. As early as in the Thirties, he stated, based on his experiments, that a combination of the radiant energy flux incident on plants with the somewhat shorter-wave ultraviolet rays (carrying quanta of higher energy than under the usual conditions of the temperate zone) will   /90 result in a shift of the photosynthetic activity of algae toward the longer-wave red and near-infrared regions. Unfortunately, the statements of this author were rejected by most of the conservative biologists.

Even now, scientists in some of the scientific institutes of the Union and Kazakh Academy and even in various departments of the Institute of Plant Physiology, believe in the presence of a fixed physiological spectrum region bounded by the visible rays, with complete indifference for the vital processes of plants in regions lying outside these boundaries. The prevalence of such views severely inhibited, and continues to inhibit, any study of the main regularities of light utilization by plants and their relation with environmental conditions. This does great harm in the investigation of the development of life on other planets, where the spectral characteristics of the surface and their variability with changes in the environmental conditions and optical properties of the planetary atmosphere are the only means of studying vital laws.

Calculations of the total absorption of light by the same two plants of the subalpine zone of the dry and humid highlands, for the spectral region from 390 to 760 mμ and from 300 to 820 mμ and for a narrower region, clearly show how much this can distort the concept of the basic regularities of the mutual relation between the changes of optical properties of plants and a change of the environmental conditions when studying these properties by the so-called discontinuous spectrum (see Fig.11 and Table 11)[*].

---

[*] Tables of the coefficients of spectral brightness of these plants every 10 mμ are given in the article by G.A.Tikhov at the beginning of this volume (Bibl.86); therefore, we will not repeat them here.

TABLE 11

ABSORPTION OF RADIANT ENERGY BY LEAF OF SOLENANTHUS STYLOSUS LIPSKY IN THE REGION OF CHECHEKTY (EASTERN PAMIR, ALTITUDE 3860 m ABOVE SEA LEVEL) IN VARIOUS PORTIONS OF THE SPECTRUM, AUGUST 24, 1951

$\Delta\lambda$, mμ	Absorption in Relative Units (%)	Comments
300–420	98.5–99	
420–550	95–90	
555–595	89–87	Green reflection maximum
596–703	91–94	
704–726	Drops from 87 to 74	Start of sharp drop in absorption and increase in self-emission
727–752	Drops from 51 to 15	
753–771	7–9	First greatest maximum of self-emission and absolute minimum of absorption
772–780	Slight increase from 10 to 30	
780–815	Drops from 30 to 15	Second–smaller maximum of self-emission
300–820	Total absorption 79.2	Total losses in this portion 20.8%

Actually, if we are guided by the recent strict rule that a comparison of the optical properties of plant species or of the main species by different natural zones is possible only in rigorously defined identical portions of the spectrum or at the same wavelength, we will inevitably become quite confused (as they say, "among three pine trees") and will be quite far from recognizing the true natural regularities.

Let us analyze a numerical example which graphically confirms this, based /91 on Fig.11 and the data of Tables 8 and 9 (from the article of G.A.Tikhov at the beginning of the volume) (Bibl.86). The total sum of losses for solenanthus (Eastern Pamir) in the 390 – 760 mμ region is $\sum_{1}^{n-1} = 5.2367$; in relative units (%) with respect to the entire flux of radiant energy striking the plant at a given portion of the spectrum (which is taken as 100%), this is expressed as 14% (1/38 S = 0.1404); consequently, the plant absorbs 86% (A = 0.8596).

For the horse sorrel, in the same portion of the spectrum, the total losses of radiant energy in the subalpine zone of the humid highlands are $\sum_{1}^{n-1} = 6.278$; in percent of the total flux of radiant energy incident on the plant in this

portion of the spectrum, this amounts to 16.5% (1/38 S = 0.165); the absorption will be 83.5%. On the basis of these calculations, one could assume that, under the conditions of the subalpine zone of Eastern Pamir, the absorption of radiant energy increases within the limits of about 2.5% which can be ascribed to the characteristics of the natural conditions. However, this is far from being the case. If the boundaries of the investigated spectrum region are slightly expanded, then the total value of the radiation balance for the entire spectrum of the portion of the solar energy actively used by plant species of the subalpine zone, both of the dry and of the humid highlands, completely coincides; the curve shows clearly that, under the effect of the different environmental conditions, only the spectral energy distribution (radiation reflected and transmitted by the leaf) will undergo a change while the extent of the losses will vary only in conjunction with the shift of the radiation maxima and minima from some wavelengths to others. These may be adjacent or more or less remote from the original position, depending on the degree of abruptness of the change in environment and on the energy distribution of the spectrum of the radiant energy flux striking the plant. It is true that, in some portions of the spectrum under the dry highlands conditions, the magnitude of the losses may increase more than on an adjacent portion of the spectrum in the lower lying natural zone of this belt of the humid highlands. However, such an increase will be compensated by the greater increase in absorption at another portion of the spectrum; thus, the law of the conservation of energy within separate natural zones and high-mountain belts will remain valid in all cases of variation in optical properties under the effect of environmental conditions. An analysis of the data shows that a definite level of vital energy, associated with no less definite quantitative indices of utilization of the incoming solar energy in the vital processes of plants, corresponds to a definite natural zone. The high vegetation belts belong to such zones. A shift of the boundaries in height, in connection with the greater or lesser difference of climatic conditions in various mountain systems, leads only to a change in the form of adaptation of plants to these conditions. This is expressed in the more or less marked fluctuations of the value and in the shift of the position of the radiation maxima and minima in the spectrum of individual elements of the radiation balance (reflection, transmission, self-emission) while keeping fixed the total value for the biologically active part of the spectrum. The boundaries of the spectrum region actively used by plants, in turn, may vary with any variation in the environmental conditions over a wide range, encompassing the short-wave ultraviolet and the near-infrared region. Knowledge of these laws considerably facilitates an investigation of other planets, since the universal law of the conservation of energy and the investigated regularities of the change in energy distribu- /92 tion of the light flux, rejected by the plant cover in relation to the physical conditions occurring in various natural zones of this or another planet, as well as the change in optical properties of its atmosphere, can be used for predicting the spectral-optical characteristics of the plant cover of such a planet. /93 On this basis, no scientist would deny the presence of vegetation on the "seas" of Mars, merely from the absence in their spectra of the main absorption band of chlorophyll and the infrared effect in the accessible region of the spectrum, at the present state of the art in science and measuring technique. This might at least reduce the number of scientists who attempt to apply the laws of vegetation of the temperate zone of the earth to conditions on other planets, while disregarding the peculiarities of the physical conditions in the natural zones of such planets.
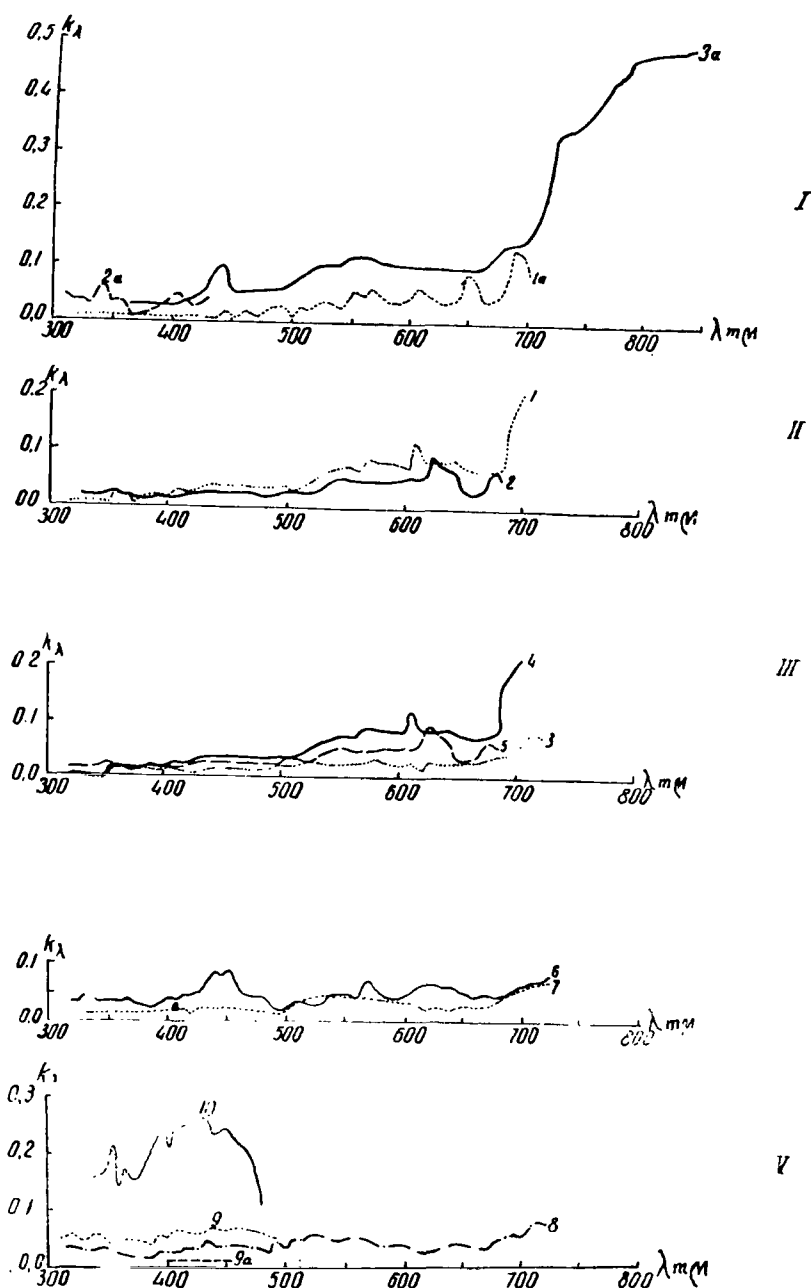
Fig.12   Spectral Brightness of the Basic Plant Species of
the Upper Part of the Alpine Zone and Lower Part of
the Snow Line of Eastern Pamir, and Character of
its Change under Different Illumination
Data of photographing plants with a quartz spectrograph in the
area of the permanent Alpine Station of the Pamir Biological
Station (altitude 4760 - 5000 m above sea level) during the
period from August 28 to September 2, 1951, calculated by A.P.
Kutyreva.   For comparison, Section I gives the data by   (cont'd)

107

K.I.Kozlova (Bibl.30) for the spectral brightness of a large
brownish-green cushion of sibbaldia (Sibbaldia tetrandra Bge.)
in the alpine zone of Central Tien Shan, altitude 3820 m above sea
level (3 a) photographed on August 24, 1949 at $h_\odot 51^\circ$.

Section I: (1, a) and (2, a) Same, in the region of Eastern
Pamir at an altitude of 4760 m above sea level (temperature 10.5°C
and 6.4°C) with and without sunlight. Time of photographing 16:00,
August 31 and September 1, 1951. The color of the sibbaldia cushion
was bright reddish-orange owing to the numerous bright color
bracts (data by A.P.Kutyreva).

Section II: 1 - Spectral brightness of Neogaya simplex (L)
Meisn with dark-green leaves having a purplish margin and large air
vesicles in the seed pods with dark brownish-lilac stripes. Photo-
graphed in full daylight in the area of Zor-Chechekty, altitude
4800 m above sea level, August 30, 1951. Temperature among the
plants was 11°C (data by A.P.Kutyreva); 2 - Same, but at uniform
overcast.

Section III: 3 - Alpine poa (Poa litwinowiana Ovcz.) with
brownish-lilac spikelets (photographed at the same place at uniform
overcast, August 30, 1951, 16:15; temperature 12.4°C), data by
A.P.Kutyreva. 4 and 5 - Second replication of Neogaya simplex (L)
Meisn, photographed September 1, 1951 in full daylight (4) and
uniform cloud cover at the boundary of the snow line (5000 m above
sea level) in the area of Zor-Chechekty (5).

Section IV: 6 - Spectral brightness of bluish green pea [Oxy-
tropis immersa (Baker) Bge.] in full daylight. 7 - Same, but at
uniform overcast; elevation 4800 - 5000 m above sea level, in the
area of Zor-Chechekty, August 30, 1951. Temperature 11.8°C.

Section V: Spectral brightness of the bluish verdure of two
species of alpine tansy under different lighting conditions and
different age in the area of the Alpine Station of the Pamir Bio-
logical Station at the summit of Zor-Chechekty, altitude 4760 - 5000 m
above sea level. 8 - A large old cushion of tansy (Tanacetum chylor-
rhihsum H. Krahs), photographed at uniform overcast on August 30,
1951, time of photographing 16:00; temperature in cushion 13.4°C.
9 - Bluish verdure of Tanacetum gracila Hook et th.; in full day-
light; photographed on August 30, 1951 in the same area at a
cushion temperature of 13.8°C; 9a - Same, at uniform overcast and
at the same cushion temperature. 10 - Small young bluish silver
cushion of the same species of tansy photographed under the same
weather conditions and cushion temperature of 9.8°C.

An analysis of the spectral data on the vegetation of the alpine zone and
snow line of Eastern Pamir shows that, under these conditions, as the height
above sea level increases, there is a further decrease in the spectral bright-
ness coefficients in all the investigated spectrum regions and at all wave-

lengths, as evidenced by the rate of smoothing of the profile and the droop of the spectral curves. The yellow-green maximum disappears almost completely, and the main chlorophyll absorption band broadens so much that it extends over almost the entire visible spectrum (see Fig.12, III, 5 and Fig.13, B, 6). The start of the infrared effect for a number of plants shifts to 720 - 760 mμ, /94 with its greatest rise probably located beyond the limits of the accessible photographic recording of the wavelengths (with the photographic materials
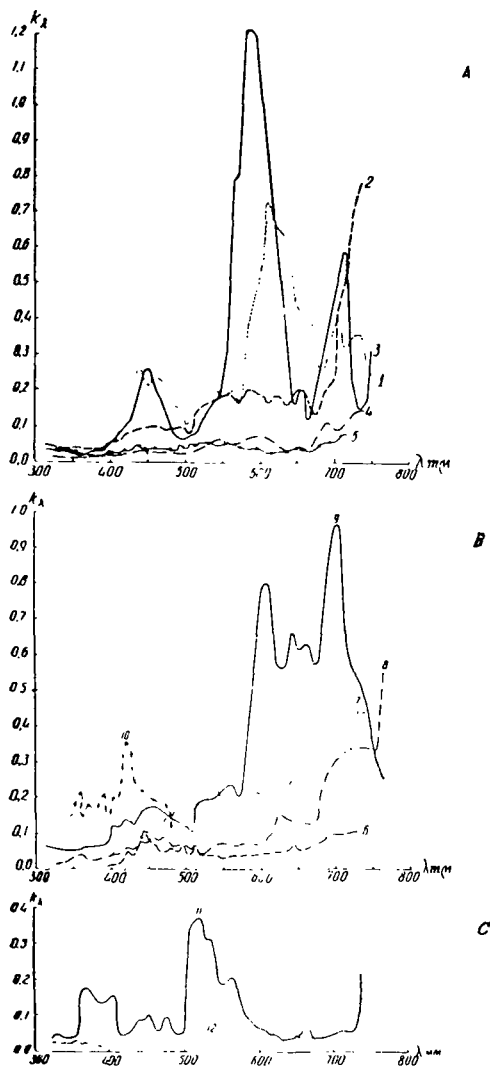
Fig.13 Spectral Brightness of the Flowers of the Subalpine and Alpine Zones and Snow Line of Eastern Pamir

Section A. Yellow flowers of the subalpine and alpine zones of Eastern Pamir. 1 - Large yellowish-orange flower cushions of Tanacetum gracila Hook et th., photographed in the alpine zone of Eastern Pamir

(cont'd)

109

at an altitude of 4800 m above sea level at uniform overcast at 15:00 on August 30, 1951, at a temperature among the plants of 15.4°C. 2 - Bright-yellow flowers of a large cushion of polypetalous cinquefoil (Potentilla multifida L.), photographed against the background of its dark-green feathery leaflets on August 30, 1951 at 13:40 at uniform cirrostratus cloud cover (Cist); temperature among the plants, 15.2°C. 3 - Large bright orange-reddish flower cushion of biennial wormwood (Artemisia macrocephala Jacq.) in the subalpine zone, photographed in full daylight on August 5 - 9, 1951 (average of three replications) in the area of the Chechekty landmark, altitude 3860 m above sea level, at a temperature among the plants of 18.4 - 19°C. 4 - Its bluish verdure, photographed under the same conditions (average of four replications). 5 - Bluish, severely dissected and drooped leaflets of tansy (Tanacetum gracila Hook et th.), photographed under the same conditions as the flowers of this plant.

Section B. Pinkish-lilac flowers of the alpine zone of Eastern Pamir, photographed by the author in the area of the Alpine Station of the Pamir Biological Station on the past glacier moraine at Zor-Chechekty (altitude 4760 - 4800 m above sea level) during the period from August 29 to September 2, 1951. 6 - Dark-green leaflets with lilac margin of Waldcheimia tridactylites Kar. et Kir.; temperature +12.1°C. 7 - Its pinkish-lilac flowers (average of three replications); the temperature among the plants varied within 10 - 14.5°C. 8 - Bright pinkish-lilac feathery flowers of Saussurea pamirica C. Winkl., resembling very large flowers of agrimony (average of two replications), photographed by the author on August 31 and September 1, 1951 at 16:30 and 17:00 ZT at a temperature among the plants of 5.6°C and 11.5°C. 9 - Continuous cover of pale pink small flowers with a dark-lilac core of primula (Androsace lanatiflora Ovez) (average of three replications); temperature, 18.3 - 21.8°C. 10 - Bluish-silver feathery flowers of edelweiss (Leontopodium ochroleucum Bod.), photographed by the author on August 29 and 30, 1951 at a temperature of 7.6° and 8.7°C among the plants.

Section C. 11 - Bright lilac-violet flowers of peas (Oxytropis immersa (Baker) Bge.], photographed by A.P.Kutyreva in the lower portion of the snow line of Eastern Pamir at 5000 m above sea level on August 29 and September 2, 1951 in full daylight at a temperature of 12.8° and 9.4°C among the plants (average of two replications). 12 - Spectral brightness of bluish verdure of pea, photographed under the same conditions at a temperature from 7.1° to 14.8°C among the plants (average of four replications). Photographed on August 29, 30, and 31 and September 1, 1951.

available to the expedition). Within the investigated spectrum region, the infrared maximum rose more than 20% only for flowers; for most of the green (or, more exactly, the bluish-gray or brownish-lilac) plants it was in the range of 7 - 8% and lower (see Figs.12 and 13). /95

During the entire investigations in the areas of the alpine zone and snow

line, we had cold weather with cloud formation during the second half of the day; on some days, there was unbroken cloud cover, which made it possible to determine the type of change in the optical properties of alpine plants during the transition from full daylight to uniform overcast. At altitudes of the order of 5000 m above sea level, at an exceptionally transparent sky and negligible diffuse radiation, this resulted in wide fluctuations in intensity of the total radiant energy flux striking the plant surface. However, as shown in Fig.12 and Table 4, the fluctuations in spectral brightness of the alpine plants /96 were comparatively slight. Under the low temperature conditions of this period,
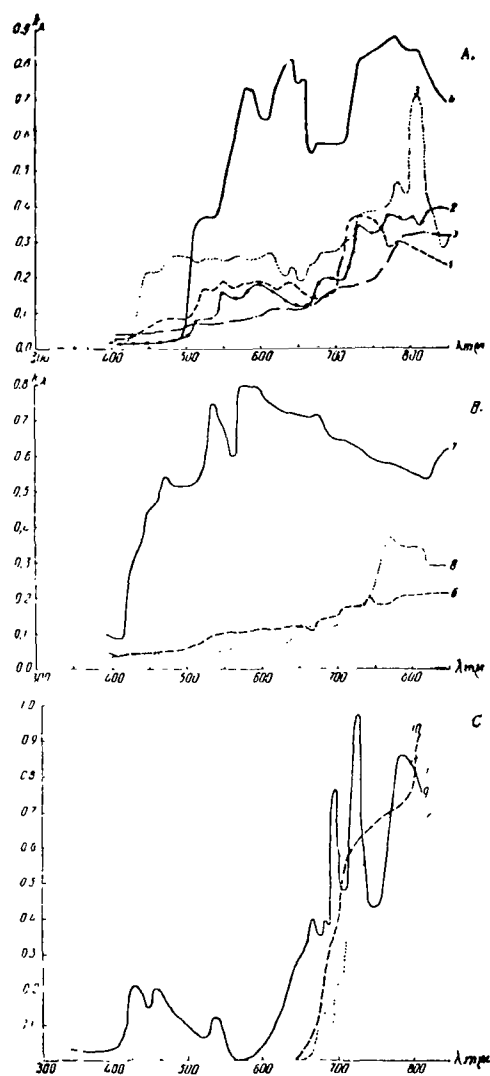
Fig.14 Spectral Brightness of Flowers of the Same Colors
and their Verdure of the Alpine Zone of Tien Shan and the
Subarctic. Based on Data by A.G.Tikhov (Bibl.84)
and K.I.Kozlova (Bibl.30)

(cont'd)

111

Section A_1. Yellow flowers of central Tien Shan: 1 - Yellow flowers (Chorispora macropoda Trautv.) in the valley of Lake Chatyr-Kul' (cold desert of central Tien Shan, 3619 m above sea level, June 17, 1950, $h_\odot 56^\circ$; data by K.I.Kozlova). 2 - Same, August 23, 1949 in the vicinity of the Alpine Geophysical Observatory (central Tien Shan, 3820 m above sea level, $h_\odot 56^\circ$; data by K.I.Kozlova). 3 - Yellow flowers of Smelovskya calycina, photographed by K.I. Kozlova on the same day and under the same conditions as for curve 1, but at $h_\odot 73^\circ$, i.e., around noon. 4 - Yellow flowers of Oxygraphis glacialis (Fedtsch.) Bge., photographed by K.I.Kozlova in the vicinity of the Alpine Geophysical Observatory; altitude 3820 m above sea level on August 29, 1949 at $h_\odot 40^\circ$. 5 - Its green growth photographed simultaneously under the same conditions.

Section B_1. Pink flowers from the forest-tundra of the sub-arctic (vicinity of Salekhard) and alpine zone of Tien Shan. 6-7 - Green growth and pink flowers of rosemary (Ledum palustra). Forest-tundra in the vicinity of Salekhard, altitude 35 m above sea level; photographed on July 9, 1948 at $h_\odot 46^\circ$ (data by K.I. Kozlova). 8 - Lilac-pink flowers of alpine betony (Pedicularis rhinanthoides), photographed by K.I.Kozlova on August 23, 1949 in the vicinity of the Tien Shan Alpine Geophysical Observatory at $h_\odot 56^\circ$ (central Tien Shan, 3820 m above sea level).

Section C_1. Violet and blue flowers in the alpine and sub-alpine zones and in the foothills of northern Tien Shan (based on data by G.A.Tikhov; Bibl.84, 85). 9 - Cortusa altaica, bluish-lilac flowers, photographed on July 26, 1946 (3000 m above sea level). 10 - Dark-violet velvet-like fringe of iris, May 19, 1946; Alma-Ata, Astrobotanical Gardens, 850 m above sea level. 11 - Viola altaica; dry range (3000 m), July 26, 1946; large bluish-lilac velvety flowers.

the temperature maximum even at the soil surface reached $+30^\circ$ C only occasionally (August 26) although it did not drop below this $(+25^\circ$ C), while the minimum stayed within -7° to -11.2° C. In the first Section (I) of Fig.12 (curve 3 a) we show for comparison, based on the data by K.I.Kozlova (Bibl.30), the spectral brightness of a large cushion of Sibbaldia tetrandra Bge. in the cold desert of Central Tien Shan (in the vicinity of the Alpine Geophysical Observatory, altitude 3820 m above sea level), which demonstrates the appreciably greater reflection for all wavelengths, and particularly in the infrared region, in comparison with the alpine belt of Eastern Pamir. Curve (10) in Section V of Fig.12 shows that young plants, under the conditions of the great heights of the alpine zone of Eastern Pamir, retain their properties of greater spectral brightness only if the maximum is shifted to the shorter-wave region of the visible spectrum and to the ultraviolet.

A comparison of the curves in Figs.12 and 13 (for green growth) with the changes in the optical properties of Eurotia ceratoides in the subalpine zone of Eastern Pamir, under the effect of the considerably smaller variations in environmental conditions (Fig.7), shows the significantly greater range of vari-

ability, especially in the infrared region of the spectrum, for plants of the subalpine zone. This again confirms that, with increasing elevation of the locality above sea level and an increase in radiant energy absorption, the constancy of the optical properties increases or the amplitude of fluctuations decreases under the effect of various environmental factors.

Of great interest is a comparison of the spectral brightness of the flowers of the subalpine and alpine zones of Eastern Pamir with the flowers of other climatic regions. A comparison of the spectral brightness of flowers of different color shows that, in the subalpine and alpine zones of Eastern Pamir (Figs.13 and 14, Sections A-A$_1$, B-B$_1$, and C-C$_1$), the brightness and brilliant colors of the flowers (to attract insects for pollination) is achieved at a greater economy of energy than in other climatic regions, including the humid highlands and subarctic regions. Nevertheless, in some, although narrower portions of the spectrum, radiation for some plants of the subalpine zone (Artemisia macrocephala Jacq.) can reach large values exceeding unity (see Curve 3 of Section A, Fig.13, λ 580 - 590 mµ and Curve 9, and for the alpine plants Tanacetum gracila Hook et th. and Androsace lanatiflora Ovez, Sections A and B of the same diagram). The spectral brightness curves of one or two plants (Curves 4 - 5 of Section A and 5 of Section A$_1$, 6 of Section B and B$_1$ and 12 of Section C) clearly show the enormous differences in the values of the brightness between the flowers and green growth. This shows the abundant expenditure of energy by the plants during the period of vigorous blossoming, even under the most austere environmental conditions.

The bluish-silvery downy flowers of edelweiss (Curve 10, Section B, Fig.13) and the pale lilac and violet flowers of the many legumes of Eastern Pamir differ greatly in their spectral characteristics. As a typical example, Section B of Fig.13 gives the spectral characteristic of the pale violet flowers of peas (Oxytropis immersa (Baker) Bge.) which penetrate almost to the upper boundary of vegetation at the snow line of Eastern Pamir (beyond 5000 m above sea level). It is impossible to give an analogy with the flowers of other climatic zones of similar colors for this Section (C) on the basis of the material at our disposal, which is quite clear from the spectral brightness   /97 curves of the lilac and violet flowers of other zones (Fig.14, Section C$_1$).

In concluding the analysis of the material of the spectral investigations of plants in the subalpine and alpine zones and the snow line of Eastern Pamir, we will specifically discuss the encountered pathological changes in the optical properties of plants. Such phenomena are due primarily to the marked changes in the force and intensity of illumination of plants that had required a long time in adapting themselves to the conditions of extremely weak illumination by diffuse light. Under the conditions of the excessive air and soil dryness in Eastern Pamir, one rarely encounters representatives of bryophytes; therefore, we were interested in determining the spectral characteristics of the bright-green stonecrop we found in a chink of rock at the boundary of the snow line (the widest part of the chink faced North, and the moss received only faint illumination by diffuse light during the day and entire year). It was impossible to photograph the moss and the comparison scale (plaster of Paris) in the chink; therefore the moss, together with a rock fragment, was extracted from the chink and photographed in full daylight, using all rules of field photography of plants. The results obtained from this photograph were similar to the results

recently published by A.F.Kleshnin and I.A.Shul'gin (Bibl.29) on the spectral photography of plants at artificial lighting at the instant of turning on the light; only, the magnitude of emission or repulsion by the plant of the instantaneous bright light flux was as many times greater as the intensity of sunlight is greater in August, at an altitude of 5000 m above sea level at latitude 30^0 during the midday hours, than the artificial light source. Since we could not photograph this plant in its normal environment of illumination by weak diffuse light and since the variable cloud cover that formed during the second half of the day did not permit us to verify whether the plant could adapt its optical apparatus to strong sunlight, we will not now publish its spectral curves.

A second case of disruption of the normal activity of the optical apparatus of plants was encountered in the vicinity of Chechekty, during a rather strong foehn with wind velocities up to 14 - 15 m/sec and a drop in absolute and relative humidity to almost zero, at a completely cloudless dark-blue, almost violet, sky and exceptionally high transparency of the air. Since, during such phenomena, we had detected more or less significant changes in the spectral
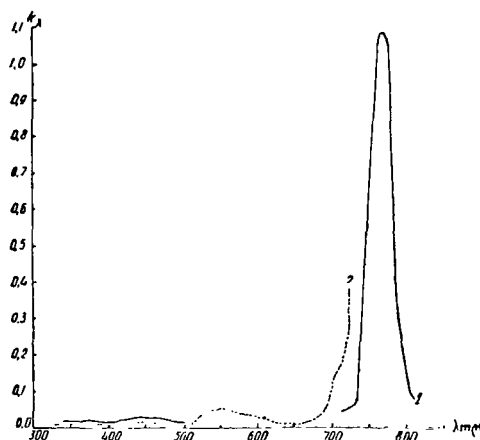
Fig.15 Example of Change in Optical Properties of
Subalpine Plants of Eastern Pamir at the Start of a
Foehn (Data by A.P.Kutyreva)
1 - Hirsute pea (Oxytropis hirsutiusculla Freyn) photographed
August 9, 1951 in the area of the Chechekty landmark (3860 m
above sea level) on the bank of a permanent irrigation ditch at
the start of the foehn. Temperature among the plants, 17.6^0C,
full daylight, strong westerly gusts up to 9 - 10 m/sec. 2 - Oxy-
tropis chiliophylla Royle, photographed at the same place under
normal weather conditions August 5, 1951 at a temperature among the
plants of 24.2^0C. Completely cloudless weather, light southeasterly
breeze up to 1 - 2 m/sec.

characteristics of the incident radiant energy, evidenced in a greater or lesser shift of the energy maximum in the spectrum, we were interested in how plants

in different habitats would react to these phenomena (at the highest and lowest uptake of moisture at the start, middle, close to the end of the foehn, i.e., during the greatest intensity and severity of the foehn conditions created for the plants). As mentioned in part in the Chapter on the methodological portion of the investigations, we made such observations on August 9, 1951 in the vicinity of Chechekty (subalpine zone of Eastern Pamir, altitude 3860 m above sea level).

Figure 15 shows the results of the spectral photography of one type of /98 Oxytropis (Oxytropis hirsutiusculla Freyn) which had been growing on the bank of a permanent irrigation ditch at the start of the foehn-like wind. The spectrum of another species (Oxytropis chiliophylla Royle), which is close in optical properties, obtained under normal conditions is given for comparison. As indicated by Curve 1 of this diagram, already at the start of the foehn and despite the good supply of moisture, the plant showed a noticeable reaction to the new adverse condition. This was expressed by an abrupt increase in emission (up to values greater than unity) in a comparatively narrow portion of the near infrared (750 – 770 mu), possibly a defense mechanism of the plant to prevent overheating of its tissues and interference with transpiration during the abruptly increasing aridity of the air.

Photographing in dry semi-desert areas of the local aborigines which had become most adapted over many centuries to the severe climatic and ecological conditions of this region showed that, even in the middle of the foehn when the development of the all adverse phenomena approaches a maximum, the reaction of their optical properties is less obvious or entirely unnoticeable, which can be explained only by the hardening of the plants to the constant exceptionally great dryness of the air and the high temperatures of the surface during the midday hours.

The most striking response was that of the fodder grasses at the nursery of the Pamir Biological Station in the area of the drainage ditches from the experimental plots of the Station.

The investigation here was carried out before the end of the foehn, at the period of greatest intensity of the unfavorable factors. As shown by a preliminary investigation and check test, bands of intense emission appear for a number of plants, not only in the near infrared but also in the visible spectrum region. The data of the spectral investigations of plants during the foehn at the most arid semi-desert portion of the plateau and at the nursery for fodder grasses, as indicated above, will require additional processing and verification.

5. Conclusions; Method of Analysis   /99

Using the direct correlation between the initial values of the spectral brightness of the plants, taken from the characteristics, and the final result reduced to the first diaphragm and referred to the brightness of baryta at the same wavelengths, the computational part of the photometric analysis of the spectrograms can be reduced by precalculating Tables for extrapolating the initial data to the final result, for those portions of the spectrum where the

mean difference between the brightness of baryta and the plaster-of-Paris plate used for obtaining the photometric scale has a stable character.

This correlation varies when photographing plant spectra through different diaphragms, for which reason the Tables are compiled for several diaphragms, most frequently used in photography. As an example, Table 7 gives a part of this conversion Table for the diaphragm No.12 used in the work with the quartz spectrograph.

Use of the conversion Table accelerates the analysis process and precludes random calculation errors and thus increases the accuracy of the obtained results.

6. Conclusions: Results of the Field Spectral Photography of Plants under Alpine Conditions

1. A comparison of the results of the field spectral investigations of the plants of Pamir with the published data for other climatic zones and the humid highlands of Tien Shan yielded the following basic functionalities and correlations of the change in optical properties of plants: a) species modifications, b) temporal changes, i.e., with respect to the time of habitation under Pamir conditions (see Table 8 and Figs.8, 9, and 10), and c) change in altitude above sea level (see Tables 9 and 10 and Figs.7, 9, 10, 11, 12, 13, and 14).

2. The greatest changes in magnitude and qualitative indices (i.e., the shift in the rise or decline of radiation and the position of the extreme points in the spectrum and the width of the encompassed region of the spectrum) are noted near the infrared and yellow-green maxima of the reflection and transmission of light through the leaf, as well as in the width and depth of the main absorption band of chlorophyll. Among the investigated plant species, the changes were as high as $50 - 60 \mu$ in the spectrum position and up to tenfold in magnitude (see Tables 8, 9, 10 and Figs.9, 10, 12).

3. With an increase in altitude of habitat above sea level, both in the humid and dry highlands, there is a general tendency toward an increase in the absorption of light by plants, owing to the more or less appreciable broadening of the main absorption band of chlorophyll, and a general decrease in losses of energy taken up by the plant due to reflection, transmission through the leaf, and self-emission*.

4. The character of modification of individual optical properties of plants with altitude differs in the humid and in the dry highlands (under the con- /100 ditions of the humid highlands, the reflection indices undergo extensive changes, whereas under conditions of the dry highlands, it is the transmission indices

---

* By self-emission we mean all types of emission occurring in plants, such as fluorescence, chemiluminescence and, possibly, other little investigated types of radiation associated with various vital processes and types of metabolism. The expenditure of absorbed energy for transpiration, photosynthesis, and other physiological processes was not taken into account here.

that undergo changes).

The altitude shift of the vegetation zones, the appreciable increase of atmospheric transmittance and, associated with this, the shift in energy distribution of the spectrum of radiant energy incident on the plants toward shorter wavelengths, with the addition of the shorter ultraviolet rays to the spectrum (in comparison with the valleys), as well as the significant increase in intensity of the infrared rays, lead not only to an increase in the absorption of light but also to a broadening of the biologically active spectrum region (primarily owing to the shift in the spectrum of the start and greatest rise of the infrared reflection maximum). This was found long ago by A.N.Danilov, although he arrived at this conclusion in a completely different manner (Bibl.11, 12).

5. Plotting the total losses of radiant energy of the plant in the spectrum (Fig.11) will appreciably smoothen the peaks in the spectral characteristics of individual optical properties, produced by the great differences in the natural conditions of the individual zones; such plotting also gives a better view over the basic laws of utilization of radiant energy by plants in the main zones. Thus, with an increase in austerity of the environmental conditions (altitude, northward migration), the absorption of radiant energy by the plants also increases. In this case, the limits of the biologically active spectrum region widen, and the losses of radiant energy at the yellow-green and infrared maxima decrease sharply. The infrared maximum shifts to the longer-wave region of the spectrum, with a more or less considerable broadening of the main absorption band of chlorophyll in the mountains.

6. These changes in the optical properties of plants, in connection with changes in environment, lead to a modification of the spectral distribution of the radiant energy reflected from and transmitted through the leaf. On the basis of this regularity and the law of the conservation of energy, we can predict the spectral characteristics of the optical properties of the plant cover on other planets. Toward this end, a detailed analysis will be required of the superposition of the characteristics of the physical conditions and of the optical properties of the atmosphere of such planets.

7. In addition to the above general regularities in the change of the optical plant properties with any radical change in environmental conditions, there are also more or less marked changes in their individual elements during transitory comparatively brief changes in environment. Figure 7 shows the distribution of such changes in various portions of the spectrum. As with changes of a more profound nature, the region of the infrared effect is the most sensitive and, to a lesser degree, the yellow-green maximum and the main absorption band of chlorophyll.

An analysis of these changes at various altitude zones shows that, with an increase of radiant energy absorption with height, as the austerity of environmental conditions increases, the magnitude and amplitude of the appearance of these changes diminish noticeably (see Fig.12).

8. The optical properties of flowers have different regularities, namely: Their economy of energy with an increase in severity of environmental conditions is either weakly manifest or, as is apparent from Fig.13, there is a narrow high

117

radiation maximum in some portions of the spectrum.

9. In addition to the above changes in the optical properties of plants, there are so-called pathological phenomena probably associated with a disturbance of the normal functions or regulatory activity of the optical apparatus /101 of plants under the most adverse conditions. These phenomena include the effect of foehns and the abrupt change from protracted exposure to weak illumination by diffuse light to full daylight. In the latter case, we have an analogy with the phenomenon, noted by A.F.Kleshnin and I.A.Shul'gin, of the brief increase in emission by plants cultivated under artificial light at the instant of turning on the light.

BIBLIOGRAPHY

1. Baranov, P.A. and Raykova, I.A.: Byull. Sredneaz. Univ., No.20, 1935.
2. Baranov, P.A.: Trudy Sredneaz. Univ., Seriya VIII, No.30, Tashkent, 1936.
3. Baranov, P.A.: Plants and Environments (Rasteniye i sreda). Moscow-Leningrad, Izd. Akad. Nauk SSSR, 1940.
4. Berg, L.S.: Climate of the USSR (Klimat SSSR). Vol.I, Moscow, 1938.
5. Vasilevskaya, V.K.: Uch. Zap. Leningr. Gos. Univ., Ser. Biol. Nauk, No.6, 1940.
6. Voskresenskaya, N.P.: Tr. Inst. Fiziol. Rast. im. K.A.Timiryazeva, Vol.8, No.1, Moscow, Izd. Akad. Nauk SSSR, 1953.
7. Grigor'yev, Yu.S.: Soobshchen. Tadzhiksk. Filiala, Akad. Nauk SSSR, No.III, Stalinabad, 1948.
8. Dadykin, V.P.: Peculiarities of Plant Behavior in Cold Soils (Osobennosti povedeniya rasteniy na kholodnykh pochvakh). Moscow, Izd. Akad. Nauk SSSR, 1952.
9. Dadykin, V.P. and Stanko, S.A.: Izv. Vost. Filialov Akad. Nauk SSSR, No.1, 1957.
10. Dadykin, V.P., Stanko, S.A., Gorbunova, G.S., and Igumnova, Z.S.: Dokl. Akad. Nauk SSSR, Vol.115, No.1, Moscow, 1957.
11. Danilov, A.N.: Sovetskaya botanika, No.4, 1935.
12. Danilov, A.N.: Arkh. Biolog. Nauk, Vol.43, No.2-3, 1936.
13. Darchiya, Sh.P.: Trudy Sekt. Astrobotan., Vol.III, Alma-Ata, Izd. Akad. Nauk KazSSR, 1955.
14. Darchiya, Sh.P.: Fluorescence of Plants when Exposed to Light of Various Wavelengths (Fluorestsentsiya rasteniy pri obluchenii svetom raznoy dliny volny). Alma-Ata, Izd. Akad. Nauk KazSSR, 1956.
15. Darchiya, Sh.P.: Trudy Sekt. Astrobotan., Vol.V, Alma-Ata, Izd. Akad. Nauk KazSSR, 1957.
16. Zaytseva, M.G.: Izv. Otd. Yestestv. Nauk, Akad. Nauk Tadzh. SSR, No.3, pp.109-122, Stalinabad, 1953.
17. Zalenskiy, O.V.: Dokl. Akad. Nauk SSSR, Vol.XXXI, No.1, 1941.
18. Zalenskiy, O.V.: Izv. Tadzh. Filiala, Akad. Nauk SSSR, No.8, 1944.
19. Zalenskiy, O.V.: Botan. Zh., Vol.33, No.6, 1948.
20. Zalenskiy, O.V.: Botan. Zh., Vol.34, No.4, 1949.
21. Zalenskiy, O.V.: Soobshchen. Tadzhiksk. Filiala, Akad. Nauk SSSR, No.17, Stalinabad, 1949.
22. Zalenskiy, O.V.: Deserts of the USSR and their Utilization (Pustyni SSSR

i ikh osvoyeniye). Moscow-Leningrad, Izd. Akad. Nauk SSSR, 1950.

23. Zalenskiy, O.V.: Botan. Zh., No.5, 1952.

24. Il'ina, A.A.: Zh. Fiz. Khim., Vol.XXI, No.2, 1947.

25. Keller, B.A.: Vegetation of the USSR (Rastitel'nost' SSSR). Vol.1,
Moscow, Izd. Akad. Nauk SSSR, 1938.

26. Keller, B.A.: Principles of Plant Evolution (Osnovy evolyutsii rasteniy).
Moscow-Leningrad, Izd. Akad. Nauk SSSR, 1948.

27. Kishkovskiy, T.N. and Artyushenko, Z.T.: Botan. Zh., No.5, 1950.

28. Kishkovskiy, T.N.: Soobshchen. Tadzhiksk. Filiala, Akad. Nauk SSSR,
No.XXIX, Stalinabad, 1950.

29. Kleshnin, A.F. and Shul'gin, I.A.: Vestn. Mosk. Univ., Ser. Biol., Pochvoved.,
Geol. i Geogr., No.1, 1959.

30. Kozlova, K.I.: Spectrophotometry of Plants of Various Climatic Zones in
Reflected Rays (Spektrofotometriya rasteniy raznykh klimaticheskikh zon
v otrazhennykh luchakh). Alma-Ata, Izd. Akad. Nauk KazSSR, 1955.

31. Krinov, Ye.L.: Astron. Zh., Vol.XII, No.6, 1935.

32. Krinov, Ye.L.: Spectral Reflectance of Natural Formations (Spektral'naya
otrazhatel'naya sposobnost' prirodnykh obrazovaniy). Moscow-Leningrad,
Izd. Akad. Nauk SSSR, 1947.

33. Kul'tiasov, M.V.: Probl. Botan., No.1, Moscow-Leningrad, Izd. Akad. Nauk
SSSR, 1950.

34. Kul'tiasov, M.V.: Characteristics of the Ecology of Alpine Plants of
Western Tien Shan (Osobennosti ekologii al'piyskikh rasteniy zapadnogo
Tyan'-Shanya). Author's Abstract Cand. Diss. (Avtoreferat kandidatskoy
dissertatsii). Moscow, 1951.

35. Kutyreva, A.P.: Vestn. Akad. Nauk KazSSR, No.6, 1951.

36. Kutyreva, A.P.: Trudy Sekt. Astrobotan., Vol.II, Alma-Ata, Izd. Akad.   /102
Nauk KazSSR, 1953.

37. Kutyreva, A.P.: Trudy Sekt. Astrobotan., Vol.III, Alma-Ata, Izd. Akad.
Nauk KazSSR, 1955.

38. Makarevskiy, N.I.: Tr. Lab. Svetofiziol. Fiz.-Agron. Inst., No.1, Moscow-
Leningrad, Sel'khozgiz, 1938.

39. Mal'chevskiy, F.P.: Tr. Lab. Svetofiziol. Fiz.-Agron. Inst., No.1, Moscow-
Leningrad, Sel'khozgiz, 1938.

40. Michurin, I.V.: Collection of Works (Sobraniye sochineniy). Vol.III,
Moscow-Leningrad, Sel'khozgiz, 1948.

41. Moshkov, B.S.: Tr. Lab. Svetofiziol. Fiz.-Agron. Inst., No.1, Moscow-
Leningrad, Sel'khozgiz, 1938.

42. Moshkov, B.S.: Vestn. Akad. Nauk SSSR, No.8, 1949.

43. Moshkov, B.S.: Dokl. Akad. Nauk SSSR, Vol.71, No.2, 1950.

44. Moshkov, B.S.: Tr. Inst. Fiziol. Rast. im. K.A.Timiryazeva, Vol.8, No.1,
Sel'khozgiz, 1953.

45. Moshkov, B.S.: Cultivation of Plants in Artificial Light (Vyrashchivaniye
rasteniy pri iskusstvennom osveshchenii). Moscow-Leningrad, Sel'khozgiz,
1953.

46. Myuller, F. and Gekkel', E.: The Basic Law of Biogenetics (Osnovnoy bio-
geneticheskiy zakon). Moscow-Leningrad, Izd. Akad. Nauk SSSR, 1940.

47. Nebol'sin, S.I.: Meteorol. vestn., No.5, 1925.

48. Nichiporovich, A.A.: Vestn. Akad. Nauk SSSR, No.4, 1953.

49. Ovchinnikov, P.N.: Summaries of the Conference on the Agricultural Utiliza-
tion of the Pamirs (Tezisy konferentsiy po sel'skokhozyaystvennomu
osvoyeniyu Pamira). Tashkent, Uzbeksk. Geol. Zh., 1936.

50. Ovchinnikov, P.N.: Izv. Geogr. Obshchestva, No.8, 1939.
51. Ovchinnikov, P.N.: Sov. Botan., No.1-2, 1941.
52. Parshina, Z.S., Bedenko, V.P., and Gorbunova, G.S.: Trudy Sekt. Astrobotan., Vol.VIII, Alma-Ata, Izd. Akad. Nauk KazSSR, 1960.
53. Poplavskaya: Tr. Leningr. Yestestv. Ispyt., Vol.68, No.3, 1940.
54. Popova, I.A.: Botan. Zh., Vol.48, No.11, 1958.
55. Pryakhin, M.I.: Izv. Vses. Geogr. Obshchestva, Vol.22, No.6, 1940.
56. Rabinovich, Ye.: Photosynthesis (Fotosintez). Moscow, Izd. Inostr. Lit., Vol.I and II, 1951, 1953.
57. Radlova, A.N.: Zh. Tekhn. Fiz., Vol.XIII, No.4-5, 1943.
58. Razumov, V.I.: Prikl. Botan., Vol.I, Moscow-Leningrad, Izd. Akad. Nauk SSSR, 1950.
59. Raykova, I.A.: Trudy Sredneaz. Univ., Ser. VIII, No.12, Tashkent, Izd. Sredneaz. Univ., 1930.
60. Raykova, I.A.: Papers of the Conference on Agricultural Appropriation (Tezisy konferentsii po sel'skokhozyaystvennomu osvoyeniyu). Pamira, 1936.
61. Raykova, I.A.: Trudy Sredneaz. Univ., novaya seriya, Vol.1, Tashkent, 1945.
62. Raykova, I.A.: Soobshchen. Tadzhiksk. Filiala Akad. Nauk SSSR, No.XXIV, Stalinabad, 1950.
63. Raykova, I.A.: Soobshchen. Tadzhiksk. Filiala Akad. Nauk SSSR, No.XXV, Stalinabad, 1950.
64. Raykova, I.A.: Izv. Otd. Yestestv. Nauk Akad. Nauk Tadzh. SSR, Stalinabad, No.2, 1953.
65. Raykova, I.A.: Trudy Sredneaz. Univ., No.XLI, book 14, Tashkent, 1953.
66. Reynus, R.M.: Izv. Otd. Yestestv. Nauk Akad. Nauk Tadzh. SSR, No.3, 1953.
67. Rubin, B.A. and Chernavina, I.A.: Vestn. Mosk. Univ., No.8, 1955.
68. Sveshnikova, V.M.: Soobshchen. Tadzhiksk. Filiala Akad. Nauk SSSR, No.XVII, Stalinabad, 1949.
69. Sveshnikova, V.M.: Tr. Inst. Botan. Akad. Nauk Tadzh. SSR, Vol.IV, Stalinabad, 1952.
70. Semikhatova, O.A.: Botan. Zh., No.5, 1950.
71. Semikhatova, O.A.: Eksperim. Botan., Vol.IX, 1951.
72. Sidorin, M.I.: Botan. Zh., Vol.30, No.6, 1945.
73. Sidorin, M.I.: Botan. Zh., Vol.35, No.1, 1950.
74. Sidorin, M.I.: Botan. Zh., Vol.37, No.6, 1952.
75. Stanko, S.A., Bedenko, V.P., and Nebogatikova, M.S.: Trudy Sekt. Astrobotan., Vol.VI, Alma-Ata, Izd. Akad. Nauk KazSSR, 1958.
76. Stanyukovich, K.V.: The Plant Cover of Eastern Pamir (Rastitel'nyy pokrov vostochnogo Pamira). Moscow, Geografgiz, 1949.
77. Stanyukovich, K.V.: Zap. Vses. Geogr. o-va, Vol.10, 1949.
78. Steshenko, A.P.: Soobshchen. Tadzhiksk. Filiala Akad. Nauk SSSR, No.XVII, Stalinabad, 1949. /103
79. Steshenko, A.P.: Izv. Otd. Yestestv. Nauk Akad. Nauk Tadzh. SSR, No.1, 1952.
80. Steshenko, A.P.: Formation of the Structure of Subshrubs in the High-Mountain Regions of Pamir (Formirovaniye struktury polukustarnikov v usloviyakh vysokogoriy Pamira). Tr. Inst. Botan. Akad. Nauk Tadzh. SSR, Vol.L, Stalinabad, Edited by P.N.Ovchinnikov, 1956.
81. Terenin, A.N.: Photochemistry of Chlorophyll and Photosynthesis (Fotokhimiya khlorofilla i fotosintez). Moscow, Izd. Akad. Nauk SSSR, 1951.
82. Timiryazev, K.A.: Izbr. soch., Vol.1, Moscow, Sel'khozgiz, 1948.
83. Tikhov, G.A.: Dokl. Akad. Nauk SSSR, Vol.LVII, No.7, Moscow, 1947.

84. Tikhov, G.A.: Priroda, No.6, pp.3-7, 1949.
85. Tikhov, G.A.: Principal Works (Osnovnyye trudy). Vol.I, II, III, IV, V, Alma-Ata, Izd. Akad. Nauk KazSSR, 1960.
86. Tikhov, G.A.: Trudy Sekt. Astrobotan., Vol.VIII, Alma-Ata, Izd. Akad. Nauk KazSSR, 1960.
87. Tikhomirov, V.S.: Seasonal Changes of Certain Reflection Properties of Plants and the Question of Vegetation on Mars (Sezonnyye izmeneniya nekotorykh otrazhatel'nykh svoystv rasteniy i vopros o rastitel'nosti na Marse). Alma-Ata, Izd. Akad. Nauk KazSSR, 1951.
88. Tolmachev, A.I.: Izv. Tadzhiksk. Filiala Akad. Nauk SSSR, No.7, 1944.
89. - Trudy Sekt. Astrobotan. Akad. Nauk KazSSR, Vols.I, II, III, IV, V, VI, VII, VIII, Alma-Ata, Izd. Akad. Nauk KazSSR, 1953-1960.
90. Tumanov, I.I.: Physiological Basis of the Winter Hardiness of Cultivated Plants (Fiziologicheskiye osnovy zimostoykosti kul'turnykh rasteniy). Moscow-Leningrad, Sel'khozgiz, 1950.
91. Shpol'skiy, E.V.: Usp. Fiz. Nauk, Vol.XXIX, No.3-4, Leningrad, Izd. Akad. Nauk SSSR, 1946.
92. Sharonov, V.V.: Collection of Articles on Aerophotometry (Sbornik statey po aerofotometrii). No.2, Moscow-Leningrad, Izd. Akad. Nauk SSSR, 1934.
93. Yakovlev, F.S.: Botan. Zh., No.6, 1950.
94. Duggar, B.M.: Biological Effects of Radiation, Vols.I-II, New York-London, 1936, 1938.
95. Götz, P. and Schönmann, E.: Helvetica Physica Acta, Vol.21, No.22, 1948.
96. Hess, P.: Gerlands Beitr. Geophys., Vol.55, pp.204-220, 1939.

CARTOGRAPHY OF THE SEAS OF MARS BASED ON THE NEGATIVES
OBTAINED BY G.A.TIKHOV IN 1909

A.K.Suslov

1. Purpose and Problems of the Work

The first drawings of Mars were made as long ago as 1636 by Fontana. His
work was continued by Huygens in 1656. Huygen's drawing of October 28, 1659
already shows the region of Syrtis Major. On Cassini's chart of 1666 even
greater details are noted. Maraldi made further drawings in 1704. By this time
the first maps of Mars with a network of meridians and parallels appeared. In
1719, Biancini prepared charts, followed by Herschel in 1777, whose observations
were used for compiling a rather good map of half of the surface of Mars. In
1877, Schiaparelli, who detected the canals, began his investigations (Bibl.1).

Detailed and systematic investigations of the Martian surface have been
going on since this time. On the map by Burton and Dreyer of 1879, the canals
show distinctly. Great changes in outlines in the region of Solis Lacus were
noted upon comparing the observations of 1830 - 1862 - 1877.

The most outstanding observers of Mars, after Schiaparelli, were Lowell and
Antoniada. In Russia, maps were compiled from visual observations by D.Ya.
Martynov, L.V.Sorokin, N.P.Barabashov, and others (Bibl.8).

However, visual observations are fraught with numerous subjective evalua-
tions, which hampers a comparison of the maps of different observers. For ex-
ample, Antoniada's charts barely show the canals, while they are abundant on
Lowell's maps.

A comparison of the charts of Mars, based on accurate observations, is
quite important to permit conclusions as to the changes on the planet's surface,
by comparing maps compiled at different times. Changes in the outlines of the
continents and seas indicate processes occurring in the crust or on the surface
of Mars. The question of the evolution of the Martian surface is also quite
important from the astrobiological viewpoint and is of great biological and
philosophical value. If living organisms exist on Mars, they must be able to
modify the appearance of its surface, an effect that would be noticeable for
decades.

G.A.Tikhov raised the question as to the existence of intelligent beings
on Mars, whose presence could be proved from rapid (on the order of several
days) alternations in the color and outlines of dark and light regions during a
given season of the year, as a consequence, for example, of agricultural work
done simultaneously over large areas.

Any attempt at a planned modification of nature, as it is characteristic
of all societies of intelligent beings in the universe at a certain stage of
their social development, could also be detected. For such purposes, accurate

charts of Mars are needed.

In addition to numerous visual observations, astrophotography was enlisted in making maps of Mars.

In 1909, G.A.Tikhov at Pulkovo photographed Mars (Bibl.4). In 1924, Trumpler at the Lick Observatory in the US resumed this work and compiled a detailed chart of the equatorial region and of the entire southern hemisphere of Mars (Bibl.7). At present, work is being done on processing Tikhov's negatives in order to compile the first Soviet photographic map of Mars of the 1909 epoch and, after comparing it with Trumpler's later map, to check from convergence with the latter, whether photographic observations have an advantage over visual observations. If the intrinsic convergence of the points along their coordinates, within the limits of our map, proves to be sufficiently high, one could define the actual changes on the Martian surface. In comparison with the results of visual observations, which yield greater details, the photographic map has greater objectivity.

The purpose of this work is to compile a map of Mars on the basis of Tikhov's negatives.

2. Description of Negatives

In the "Report for 1909 - 1910 Presented to the Committee of the Niko-layevskaya Main Astronomical Observatory by its Director", in the Chapter "Astrospectroscopy", we read: "The instrument (30-inch refractor) was presented to Mr. Tikhov for experiments of photographing celestial bodies (mainly Mars) through color filters".

TABLE 1

No. of Filter	Sensitivity of Emulsion	$\Delta\lambda$, $m\mu$	λ_9, $m\mu$	Reading of Focus on Refractor Scale, mm	No. of Negative
59	Pinacyanol	690—655	670	6.7	45.49.56
57	Pinacyanol	680—600	640	4.9	24.35.44.50.54. 58.60.65
34	Orthochrome or	615—545	580	0.0	23
43	pinaverdol	615—495	555	1.0	Not measured
32		550—495	520	1.6	46.55.66

Thus, photography through color filters was used for the first time in planetary astronomy. As a result of these experiments, G.A.Tikhov obtained several dozen negatives with pictures of Mars. Subsequently, 16 of the best negatives were selected, each of which contained about 30 pictures of Mars with various exposures. The systems of relative spectral sensitivity of the photographic plates in combination with the filters used are given in Table 1.

See Table 2 for details on the negatives.

Each negative shows a series of photographs with various exposures. The negative No.10 of August 4 contains a track of Mars obtained when the clockwork of the refractor was stopped. All negatives are well preserved. A network of dark lines, with lengths reaching 0.1 mm, is noticeable on the disk of Mars. The network intersects both the dark and light details and is clearly noticeable at tenfold magnification. A similar network, although weakly defined, is   /106 noted also on the fog of the negative. Evidently, this is some kind of structure that formed on the emulsion during the long period of storage of the negatives and has no relation to the photographed object.

TABLE 2

No. of Negative	Date of Photographing (Aug. 1909)	Time of Photographing	Exposure, sec	B	P	L
23	14	22 hr. 06 min. 49.0 sec.	4.0	$-19^\circ.7$	$331^\circ.6$	$258^\circ9$
24	14	22 . 41 . 46.0	10.0	-19.7	331.6	267.0
35	1S	23 . 54 . 36.0	5.0	-19.6	331.5	214.4
44	22	23 . 41 . 47.5	5.0	-19.5	331.5	200.8
45	22	23 . 04 . 51.5	30.0	-19.5	331.5	182.6
46	22	23 . 30 . 29.5	5.0	-19.5	331.5	199.1
49	23	23 . 24 . 25.5	30.0	-19.5	331.5	181.1
50	23	23 . 30 . 07.0	6.0	-19.5	331.5	185.6
54	25	22 . 50 . 00.0	3.0	-19.4	331.5	158.3
55	25	23 . 08 . 46.0	5.0	-19.4	331.5	162.8
56	25	23 . 53 . 16.0	70.0	-19.4	331.5	175.4
58	27	23 . 59 . 58.5	7.0	-19.4	331.0	135.2
60	27	00 . 35 . 29.0	5.0	-19.4	331.5	163.9
61	29	23 . 45 . 47.5	7.0	-19.4	331.6	131.8
65	30	23 . 38 . 06.0	5.0	-19.4	331.7	120.0
66	30	23 . 26 . 04.5	5.0	-19.4	331 7	117.1

Note: B = latitude of the center of the Martian disk; P = position angle of axis of rotation; L = longitude of central meridian. Time of photographing is given in local sidereal time.

3. Measuring Technique

We measured the negatives in June 1952 at Alma-Ata. On each negative, we selected a frame showing the greatest clarity of detail at a given magnifica-

tion. A Hartmann No.70026 microphotometer was used for measuring the rectangular Cartesian coordinates of the details. The stage of the microphotometer
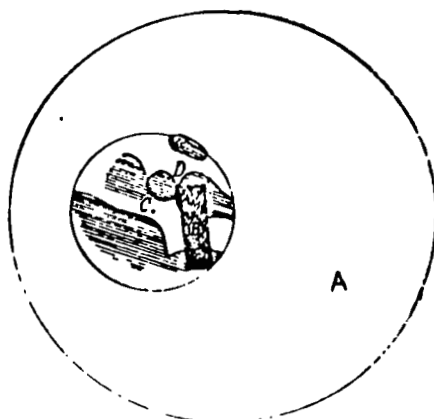
Fig.1   Image of Mars on a Negative, Examined in the Field
of View of a Hartmann Microphotometer with a Rectangular
Diaphragm of the Comparison Field

could be moved in two mutually perpendicular directions by means of two racks. Both scales were equipped with verniers which permitted readings with an accuracy of ±0.05 mm. The induced development of the print of Mars on the negative C
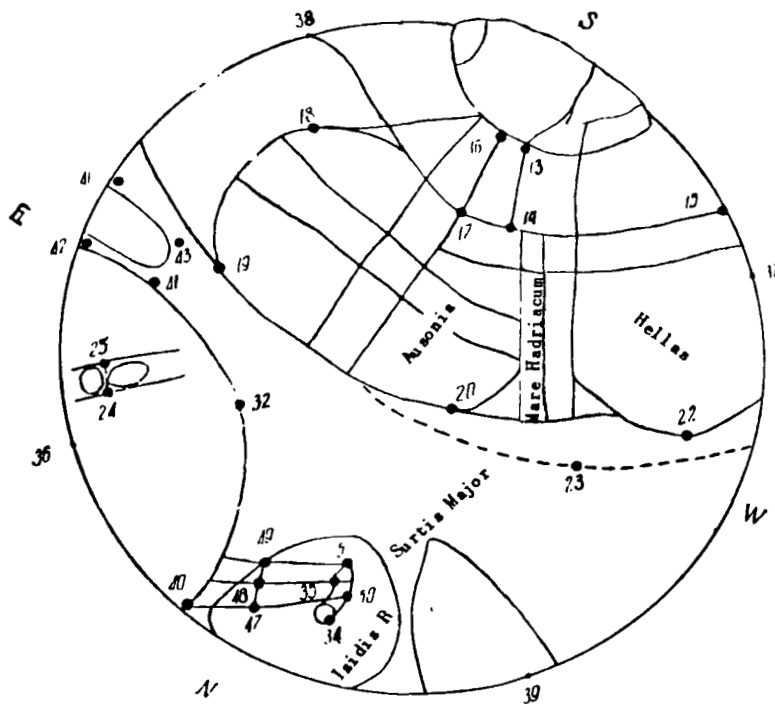
Fig.2   Diagram of Details Noted on the Negative of Mars

125
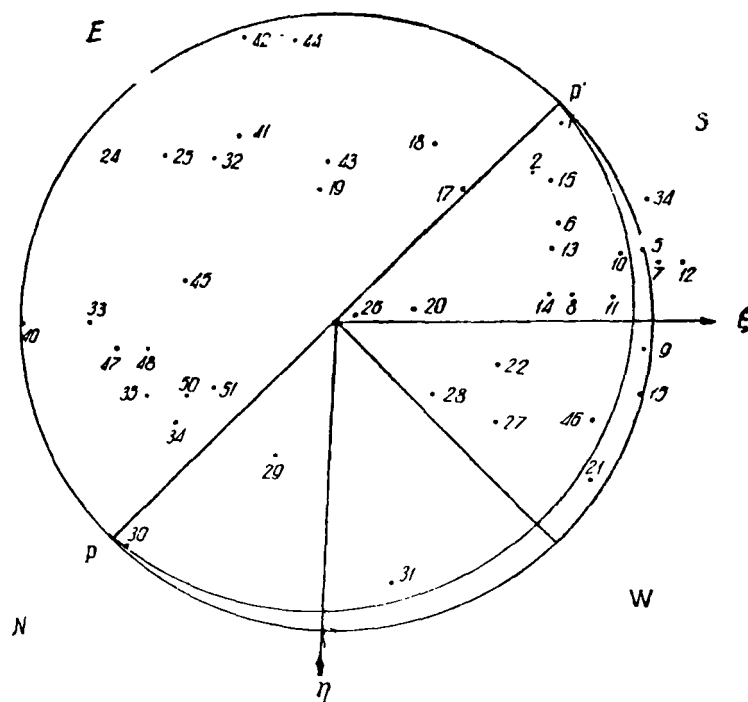
Fig.3 Image of Mars, Magnification × 100, on Negative
Plotted by Measuring the Rectangular Coordinates
of Individual Points
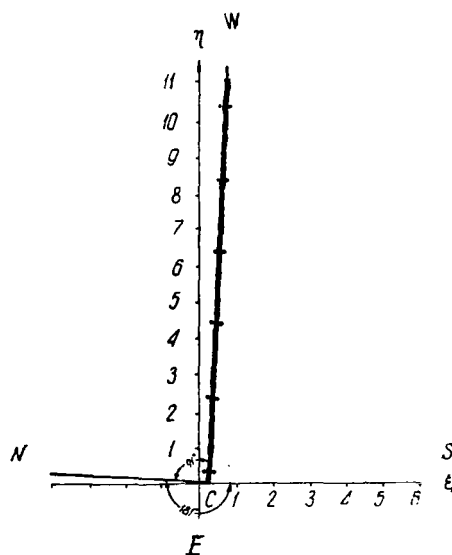
Fig.4 Projection of the Track of Mars on a Negative, Taken
at Stopped Clockwork of the Telescope and Plotted at
Full Scale, Based on Measurements of the Rectangular
Coordinates of Several Points

126

was done in the left upper corner D of the rectangular image, visible in the field of view of the ocular A, of the photometer diaphragm B (Fig.1).

One development was made on each detail. This was completely sufficient with this method of measuring, since observations have shown that, on several developments, always the same reading is obtained, and even when developing on two very close but separated (by a scarcely noticeable interval) details, the same result is almost always obtained. Different readings were obtained when /107 developing details relatively far apart. Thus, the accuracy of one measurement was not so much determined by the personal error in taking the measurement but by the instrument error, which amounted to 3% at a disk radius of about 0.7 mm. It was quite difficult to correlate the details on the disk with the chart of Mars, because of the distortions due to the projection. Therefore, for each photograph we compiled a diagram of the measured details on which the test points were applied and numbered (Fig.2).

As a rule, we measured the projection of the south polar cap - point No.4; several points near the boundary of the polar cap, and the places of its inter- section with the limb, for example, Nos.1, 2, 3, 10 on Fig.3; the projections and depressions of the seas - Nos.33, 29 and of the continents - Nos.26, 27, 45; the points of intersection of the boundaries of the continents with the limb - Nos.42, 44, 46; the start and end of the canals - Nos.29, 30, 41, 42. The /109 canals showed in the form of very faint wide belts intersecting the continents, almost at the threshold of contrast sensitivity of the eye. Developments were also made on the right, left, upper, and lower limbs, with three developments on each limb, in view of the fuzziness of the latter (see Fig.2 - points Nos.36, 37, 38, 39). The measurements of the track from the diurnal movement of Mars across the sky were made every 20 mm on both sides of the track. The track was measured twice during the work (Fig.4).

4. Processing of the Test Data

The coordinates of about 50 points were obtained from each photograph. To explain the measuring methods, we will give an example of calculating the coordi- nates of the northern extremity of Syrtis Major which was point No.33, as shown in the identification of the details at the end of the work. In measuring the negative No.24 for processing the point No.33, the coordinates x = 93.55 and y = = 41.35 were obtained.

To determine the x and y coordinates of the center of the disk, the points Nos.36, 37, 38, 39 were measured:

№ 36	№ 37	№ 38	№ 39
x	x	y	y
93.40	94.75	40.70	41.95
93.40	91.75	40.70	41.95
93.40	94.70	40.70	41.95
93.40	94.73	40.70	41.95

$$93.40 \qquad 40.70$$

$$x_0 = \frac{94.73}{94.06} \qquad y_0 = \frac{41.95}{41.32}$$

127

The corrections for the phase angle of the planet can be introduced into these values (Fig.5).

From the Nautical Almanac (Bibl.6), we will interpolate the value of q which is the greatest distance between the terminator and the limb and the value of Q which is the position angle of the line of the horns. Thus, q = 1".5 at a
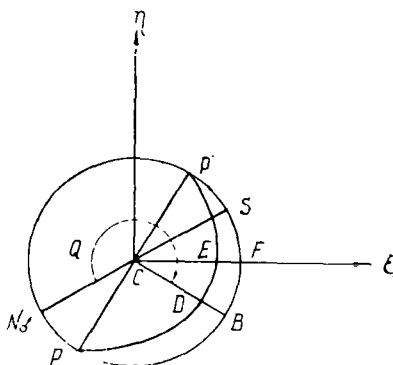
Fig.5 Projection of the Apparent Disk of Mars onto the
Celestial Sphere, Demonstrating the Phase Phenomenon

Martian apparent diameter of D = 20"; Q = 252°. In order to find the angle BCξ, we will use the quantity P = $\angle$NCNσ , which will be discussed later in the text; P = $331^o 6'$. As we see from Figs.5 and 6, $\angle$BCξ = P - U_o - $(360^o - Q)$ = = $42^o 6'$.

As a consequence of the phase phenomenon, the coordinates of the point No.37 represent point E in place of point F. This has an effect on the magnitude of the disk radius and on the position of its center. To correct the latter, we introduced the correction

$$\Delta x_0 = \frac{\overline{EF}}{2} = 0.02; \ \Delta y_0 = 0.02; \ x_0 = x_0'' + \Delta x_0 = 94.08; \ y_0 = 41.34.$$

We see that the correction for the position of the center is so small that it can be disregarded. It has a much greater effect on the disk radius, where it should be used.   /110

Let us reduce the coordinates to the center of the disk and express everything in planetocentric rectangular coordinates ξ, η:

$$\xi = x - x_0, \ \eta = y - y_0; \ \xi = -0.53, \ \eta = +0.01,$$

and then, on millimeter graph paper, trace accurate maps of each photograph at magnification × 100 (see Fig.2). From these maps, let us record the polar coordinates of each point: The distance from the center of the disk ρ is recorded by a scale and the position angle U_0 by a protractor.

128

To convert to the conventional coordinate system, we will change the sign of the quantity η

$$CM = \rho = \sqrt{\xi^2 + \eta^2} = 0.53;$$
$$\angle CM = \tan^{-1} \frac{\eta}{\xi} = 181°.3.$$

Let us find the position angle of the axis ξ. For this purpose, we will use the drawing on which the points, taken along both sides of the track from the disk
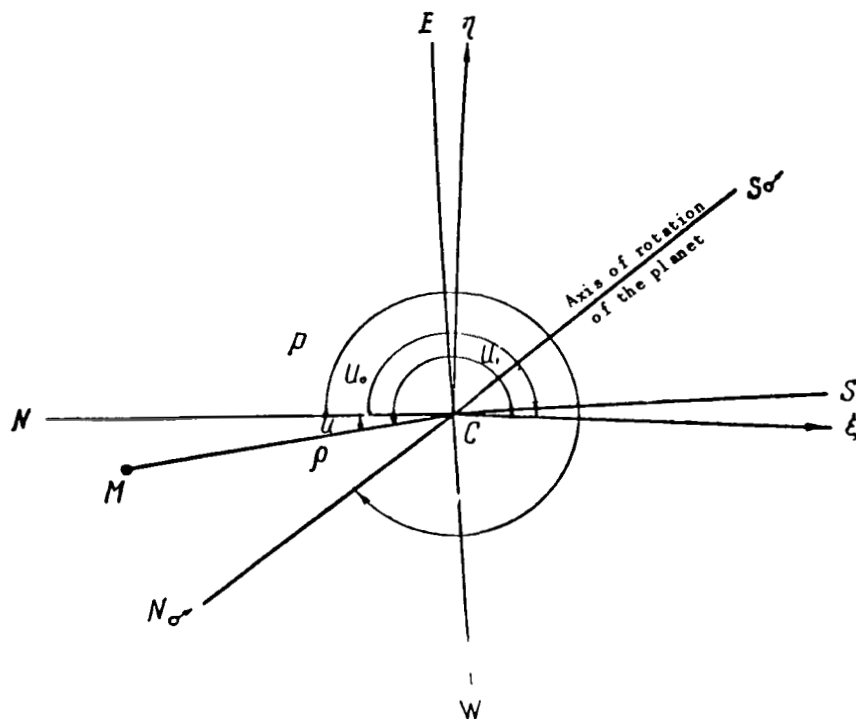
Fig.6 Diagram Elucidating the Determination of the
Polar Coordinates of the Martian Details

of Mars, are plotted (Fig.4). The track of Mars represents a projection of the celestial parallel onto the plane of the negative, represented by the line EW in Fig.4. From the measurements, we find $\angle EC\xi = 91°$. The position angle U_0 is read from the north end of the meridian N and will be 90° greater; $\angle NC\xi =$ $= U_0 = 181°$ All this permits expressing the angles in the conventional system. The position angle of our point M is found from the formula $\angle NCM = U = U' - - U_0 = 0.3°$, but for convenience of calculation it is usually read off in a direction opposite to the usual direction for leading position angles. From the ephemerides (Bibl.6) for 1909 in the "Appendix" we took the physical coordinates of Mars: P = position angle of the axis of rotation; B = latitude of the center of the disk; L_0 = longitude of the central meridian.

As the radius of the disk, we took the average of two values obtained by

measuring in two mutually perpendicular directions; a correction for phase was introduced by the graphic method described above:

$$r_x = \frac{94.73 - 93.40}{2} = 0.66; \quad r_y = 0.62;$$

$$\Delta r = \frac{0.04}{0.70}; \quad \Delta r = \frac{0.04}{0.66},$$

with the average being r = 0.68.

It should be noted that, as a consequence of photographic irradiation, the polar caps and the adjacent bright regions protrude beyond the limb and thus introduce an error in the radius (see Fig.3, points Nos.3, 4, 5, 7, 9, 12, etc.).

Fig.7 Sketch Showing the Use of Wulff's Net for Converting
Planetocentric Spherical Coordinates to
Aerographic Coordinates

The next step in the work was to convert from the system of spherical coordinates P + U, γ to the system β, λ – L of aerographic coordinates. Here, γ is the angular distance of the detail from the center of the disk, sin γ =

$= \frac{\rho}{r} = 0.779$, γ = 51.0°. The second coordinate will be P + u = 331° 9'. This

is done by means of a Wulff net or a Kavrayskiy planisphere. In this case, the center of the disk (C) is placed at the pole P, and P + U is read off from the meridian lying in the plane of the paper (Fig.7). This is one of the methods /112 of solving the problem in spherical astronomy, namely, that of converting from one system of spherical coordinates to another (Fig.8). In this manner, the points were plotted. Then the drawing, outlined on tracing paper, was turned about its own center so that the pole of the planet, which had previously been plotted with respect to the value B = $-19°7'$, became the pole. The aerographic latitude was read off from the equator, and the values λ − L were read off from the meridian, but in a direction opposite to the conventional, used for readings of P + U; B = $+24°$, λ − L = $340°$. This ended the graphic portion of the processing.
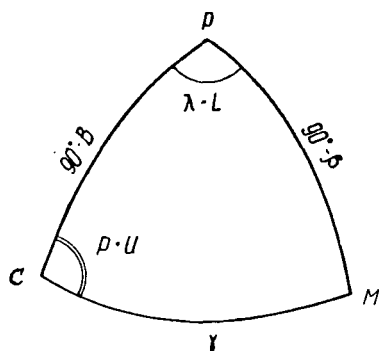
Fig.8 Spherical Triangle Formed by the Pole of Mars P,
the Center of its Disk C, and the Investigated Point M

Photographing of Mars was carried out, with time recording by a Dent chronometer with an accuracy to 0.5 sec. The chronometer was periodically compared with Kassel's sidereal clocks, to which the Pulkovo Time Service furnished the corrections. Thus, the instant of exposure was known with sufficient accuracy. Such an accuracy is needed for interpolating the value of L, which changes in proportion to time. The sidereal time of observation was converted to universal time, after which the time interval which elapsed from Greenwich mean noon, expressed in degrees, was added to L_0 and a correction introduced for the difference in the periods of rotation of the earth and Mars about their own axes. Thus, the longitude of the central meridian at the instant of observation was calculated. This made it possible to obtain the aerographic longitude of the given detail λ = $247°$.

5. Drawing the Maps

All of the above processing yielded Tables of the points for each negative. From these data we had to draw the maps.

For this, it is preferable to use a Mercator projection provided the latitude does not exceed $60°$, and a polar stereographic projection when the latitude lies within the limits from 30 to $90°$ (Bibl.2, 3, 5).
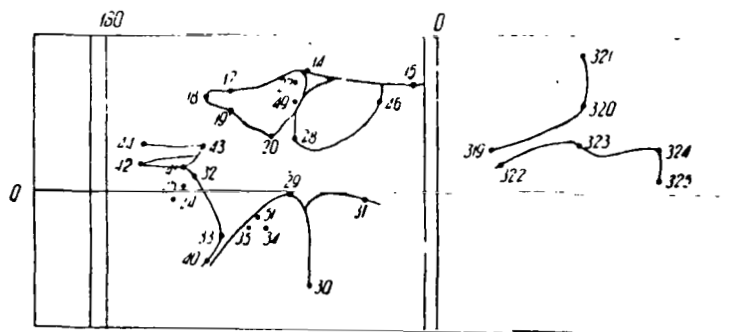
F: .9 Map of the Martian Surface in a Mercator Projection,
Obtained from One of the Negatives

On tracing paper, we drew the network of meridians and parallels in a
Mercator projection identical in scale with Trumpler's map (Bibl.7) and plotted
our points on the tracing paper, separately for each negative (Figs.9, 10).
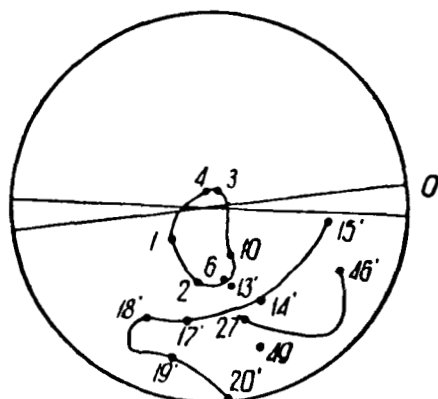
Fig.10 Map of the Polar Region of Mars in Polar
Stereographic Projection, Obtained from One
of the Negatives

We connected the plotted points by lines according to the diagrams drawn /113
from measuring the negatives. Then, the obtained map was superposed on Trum-
pler's map and identified by the configuration of these details. In this manner,
all objects given below were identified. The canals in the equatorial region
could not be identified, because of the extensive scattering (of the order of
$10°$) of their positions on our maps. A comparison of the maps obtained for dif-
ferent wavelengths showed that the differences between them lie within the
limits of the random error of a given map. Therefore, we added them to our
main system $\gamma = 640$ mu, at which the majority of negatives had been photographed.
To average out the configurations on all negatives, we drew each object, conti-
nent, or outline of a given sea on an individual map on which we plotted the
corresponding points, as they had been obtained on all negatives where this ob-

132

ject was encountered (Fig.11). The average contour of the detail was drawn along these points. Then, the transparent maps were superposed, and a general map of Mars was drawn in Mercator projection (Fig.12). The same was done for
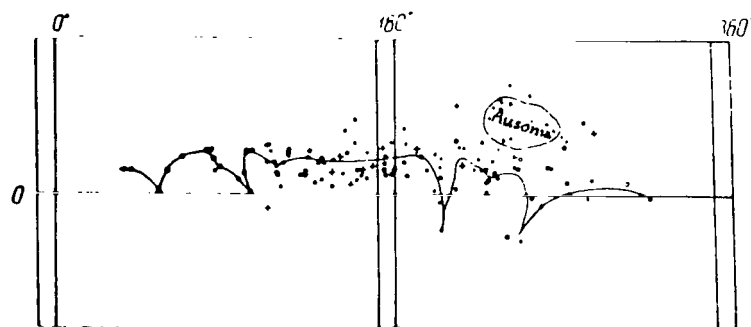
Fig.11 Map of the Northern Shore of the Southern
Seas and the Continent Ausonia
The symbols correspond to different λ_e (see Table 1)

the polar region (Figs.13 and 14). The convergence was satisfactory. The root-mean-square error was calculated for the northern boundary of the seas by the formula

$$\varepsilon = \sqrt{\frac{\Sigma \Delta^2}{n\,(n-1)}}$$

and proved to be $\pm 1°0'$. Trumpler's (Bibl.7) error was of the order of $\pm 0°1'$ and that of Camichel $\pm 0°01'$ (Bibl.9).

6. Comparison of the Obtained Map with Maps of Other Authors

A deviation from Trumpler's map, obtained in 1924, is observed at three main points. The near-polar continent Thyle I was shifted $40°$ in longitude. /114 At the place of the continent Thaumasia we have a mare, whereas south of this location there is an unidentified continent. On Trumpler's map, there is a light area in this region. Finally, our Syrtis Major is appreciably smaller because of an enlargement of Isidis Regio, just as it occurs on the visual chart prepared by Burton and Dreyer in 1879, with which our map fully coincides in this region. The outlines of the southern continents are similar to those on the visual map of Ye.Ya.Perepelkin of 1924, but are shifted equatorward with respect to the visual map of D.Martynov, which was compiled in the same year (Bibl.8). Calculation of the coordinates of Syrtis Major by the method of Ye.Ya.Perepelkin (Bibl.2) showed complete agreement with our method of processing.

7. Catalogue of the Point Coordinates of the Martian Surface

The catalogue is a list of coordinates of points corresponding to the maps

133

Fig.12 Map of the Surface of Mars in Mercator Projection
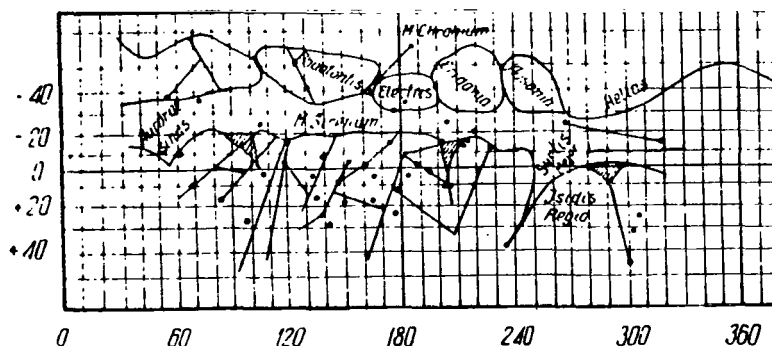
(Figs.12 and 14) where the final averaged contours from all measurements of all negatives are entered. These are mainly the coordinates of arbitrary points taken at the boundary between sea and continent. The physical meaning of this

Fig.13 Map of the Southern Shore of the Continents of Mars and the Polar Cap
Symbols correspond to different values of λ_e (see Table 1)

Fig.14 Map of the Southern Polar Region of Mars
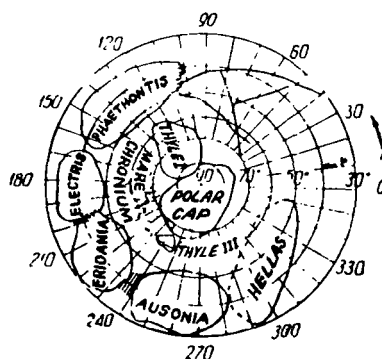
boundary, according to the basic concept of the method of investigation, is that it represents the line of the greatest gradient of photographic density on   /116 the image of Mars. We took points every $10°$ in longitude and recorded from the map the values of latitude, which then were entered into the catalogue. Where the latitude changed slowly, the points were taken less frequently, for example, Thyle I and the southern polar cap. Where there were evident projections or depressions on the edge of a given detail, these places were also fixed, for example, Ausonia $\beta = -40°$, $\lambda = 266°$; northern shore of the seas: Aurorae Sinus $\beta = 0°$, $\lambda = 55°$, Laestrygonum Sinus, and others.

Thus, we have the outlines of six continents: Ausonia, Eridania, Electris,

TABLE 3

/115

Column group 1

β	λ
Northern margin of Helles	
−30°	270°
−27	280
−27	290
−30	300
−33	310
−39	320
−44	330
−47	340
−49	350
Ausonia	
−33	240
−30	250
−31	260
−40	266
−48	260
−52	250
−52	240
Thyle III	
−60	230
−58	240
−58	248
−68	243
−66	240
Southern polar cap	
−69	240
−67	260
−69	280
−73	300
−76	320
−76	20
−77	30
−79	50
−81	80
−82	100
−81	160
−79	170
−73	190
−70	210
Canale	
+20	130
−19	146
+8	149
−20	180
−7	182
−17	210

Column group 2

β	λ
Eridania	
−31°	210°
−30	220
−30	230
−51	230
−56	220
−54	210
−50	200
Scamander	
−35	202
−46	197
Electris	
233	170
−31	180
−31	190
−33	200
−46	190
−46	180
Unknown Continent	
−35	30
−36	40
−38	70
−39	80
−41	90
−43	100
−53	100
−55	90
−58	80
−59	70
−57	60
−53	50
−58	30
Canale	
+17	83
−20	115
+50	93
−18	120
−7	120
+14	131
+13	145
+21	172
−7	182
+8	209
+37	237
+20	248

Column group 3

β	λ
Phaethontis	
−47°	110°
−42	120
−37	130
−35	140
−36	150
−40	160
−49	170
−52	160
−53	150
−54	140
−56	130
−56	120
−55	110
−53	104
Xanthus	
−38	236
−47	235
Northern shore	
−15	40
−10	50
0	55*
−10	60
−20	70
−23	80
−17	90
−10	100
−22	110
−18	120
−20	130
−20	190
−18	200
+17	205**
−18	210
−19	220
−13	230
−11	233***
−13	240
−10	250
+7	260
0	270
0	280
+5	290
−2	300
0	310
+3	320

Column group 4

β	λ
Thyle I	
−60°	130°
−61	120
−63	110
−69	100
−75	90
−80	80
−82	120
−78	170
−72	160
−68	150
−62	140
Simois	
−39	162
−55	182
Canale	
−36	52
−53	73
−40	83
−58	67
−36	135
−56	122
−24	268
−17	320
+15	60
−23	103
−2	80
+1	96
+43	108
−18	122
+32	126
−7	155
+45	161
−7	182
+11	177
+32	209
+44	300
+7	290
+32	209
−14	225

* Sinus Aurorae
** Sinus Laestrygonum
*** Sinus Cimmerium

135

Phaethontis, Thyle I, Thyle III; the outlines of the southern polar cap, incomplete outlines of Hellas, and an unidentified continent and the northern shore of the seas over its entire extent; three gulfs: Xanthus, Scamander, Simois, for which the coordinates of the beginning and end are given; three bays: Aurorae, Laestrygonum, and Cimmerium, and 21 canals (Table 3).

BIBLIOGRAPHY

1. Flammarion, C.: The Planet Mars (La planète Mars). Paris, pp.6, 16, 58, 293, 1892.
2. Perepelkin, Ye.Ya.: Geometric Method of Processing Drawings of Planets and Compilation of Surface Charts (Geometricheskiy sposob obrabotki risunkov planet i sostavleniye kart poverkhnosti). Russkiy astron. kalendar', Vol.29, p.168, 1926.
3. Tikhov, G.A.: Cartographic Grids for Analyzing Observations of Mars (Kartograficheskiye setki dlya obrabotki nablyudeniy Marsa). Mirovedeniye, Vol.47, No.2, pp.165-174, 1924.
4. Tikhov, G.A.: Photographing of the Planet Mars in 1909 with the 30-Inch Pulkovo Refractor (Fotografirovaniye planety Mars v 1909 g. 30" pulkovskim refraktorom). Izv. Rossiyskoy adademii nauk, pp.881-890, 1910.
5. Suslov, A.K.: Cartography of the Martian Maria from Negatives Obtained by G.A.Tikhov in 1909 (Kartografiya morey Marsa po negativam, poluchennym G.A.Tikhovym v 1909 g.). Uch. Zap. Leningr. Gos. Univ., Ser. Mat. Nauk, No.29; Tr. Astron. Observ., No.190, Leningrad, Izd. Len. Gos. Univ., 1957.
6. - The Nautical Almanac, Vol.86, Appendix, pp.32-39, 48, 1909.
7. Trumpler, R.: Lick Obs. Bull., Vol.13, No.387, pp.19-45.
8. Martynov, D.Ya.: Map of the Martian Surface Based on Observations during the 1924 Opposition (Karta poverkhnosti Marsa po nablyudeniyam v oppozitsii 1924 g.). Russkiy astron. kalendar', Vol.29, p.29, 1926.
9. Camichel, H.: Ann. Univ. Paris, Vol.23, No.2, pp.317-319, 1953.

M.P.Perevertun

The numerous attempts by many scientists to detect, by spectrophotometric means, the presence of absorption bands of chlorophyll in the visible spectrum region and the Wood effect in a light flux reflected by the "seas" of Mars where vegetation is presumed to exist, all were unsuccessful. Therefore, the only direct proof of the existence of plant life on Mars so far is constituted by the seasonal changes in the color of the "maria", oases, and canals, as they have been noted by many investigators of this mysterious planet on visual observation. However, visual observations are prone to subjective errors which at times (when the observer is inexperienced or has preconceived ideas, etc.) make the results worthless even if the observer himself is qualified. Nevertheless, it is an unfortunate fact that the solution of all problems by objective methods of investigation, such as polarimetry, photography in various spectrum regions, electrophotometry, and spectrophotometry is quite impossible; therefore, direct observations of Mars will retain their importance even in the future. The distinct advantage of visual observations, especially for studying minute details, still is and will remain obvious until photographing with very short exposure times, permitting full use of the resolving power of existing instruments, becomes possible over a broad area. Even then, visual observations and drawings will be of great interest from the viewpoint of establishing the interrelations of reproducible details in photography.

However, one should not overestimate the accuracy of photographic, electrophotographic, and spectrophotometric recordings since the photosensitive layer, just as the human eye, is subject to complex systematic errors which play a decisive role when dealing with minute details of the image. The main drawback of electrophotometric observations lies in the low threshold of contrast sensitivity in the presence of a bright background as it is always involved in observations of planets, and in particular of Mars, since the radiation pickup generates a current proportional to the incident light flux regardless of the source of such radiation (scattering of the radiation flux in the instrument or of the background of the photometering surface). It is also impossible to assert that only the descriptive or qualitative part of the investigations will pertain to the visual observations. Allowing for the objective and subjective errors of visual observations, the latter may contribute greatly in solving various problems /118 of aerophysics. The human eye is an extremely sensitive physical instrument provided one knows how to use it. For example, the human eye is able to perceive a brightness difference of individual details at a contrast of 0.02, whereas such contrast lies at the limit of sensitivity in the electrometric method. Therefore, the visual method of observation of planets must not be rejected simply because it has recently become popular to resort to "impersonal" apparatus; rather, there is need for its further development. During its entire history, visual observation of planets has never been improved, which greatly inhibited further development of this method. The use of modern physical instruments and methods of visual photometry for visual observations of planets may

substantially modify the accuracy of visual observations and the field of application of the human eye as a physical instrument. The development of the visual photometer, making use of modern methods of colorimetry, holds great promise in this respect.

Visual observations of Mars were carried out at the Astrobotany Sector from October 1, 1958 to December 5, 1959, using an AZT-7 reflector at a magnification of 270 and 400. In all, a total of 110 drawings of Mars with red, yellow, green, azure, blue, and color-contrast filters, as well as without filters, were prepared. Simultaneously with the drawings of all visible details of the Martian disk, all noted atmospheric and light phenomena were recorded in detail. A visual estimate of the brightness T of individual details, as they moved across the disk of the planet, was made on a 10-point scale during days of persistent images and good visibility of the Martian formations. These data will later make it possible to determine the brightness values β of individual areas of Mars, depending on their distance δ from the center of the disk. The values of β and δ are interrelated by the following rather simple formula:

$$\beta = \beta_0 + \beta_1 \sec \delta,\tag{1}$$

where β_0 is the intrinsic brightness of the surface area of Mars and β_1 is the brightness of the Martian atmosphere.

On the other hand, the following relation exists between β and T:

$$\beta = 10^{-0.125\,(T-2)},\tag{2}$$

or T = 2 − 8 log β. Using eqs.(1) and (2) the value of β_1 is easily determined from the values of T, from which, in turn, the atmospheric pressure and its density and atmospheric thickness can be determined.

During the period of this opposition of Mars, an attempt was also made at an objective estimate of the possible existence of green and azure colors of the individual "seas" of Mars and its polar caps. For this purpose, a simple design of a visual photometer was worked out. Its basic part is a Lummer-Brodhun cube; into the central part of its field, the image of the Martian disk is reflected by an additional optical system, while the peripheral part of the field of the photometer is illuminated by a bulb through a set of suitable filters. The filters are changed by rotating the disk with an automatic catch. The bulb is powered by a battery and monitored by a wattmeter. The brightness of the peripheral field of view of the photometer is varied by moving the light source either closer or farther away from the Lummer-Brodhun cube. A thin sheet of opal glass or groundglass is placed in front of the bulb to eliminate fulguration. Scattering inside the tubes of the photometer is eliminated by installing diaphragms in conical arrangement, with the apex facing the cube. /119

A prototype instrument was tested and showed good results. We used it successfully to estimate the color of Solis Lacus, Mare Sirenum, and Mare Cimmerium. We found that Solis Lacus has a dark-yellow color, Mare Sirenum a violet color, and Mare Cimmerium a yellow color.

Polar Caps

The polar caps were recorded very poorly during this opposition. The south polar cap in October and in the first few days of November was seldom recorded as a point. Its brightness was greatest through green and yellow filters, whereas through a red filter it was completely lost and could not be detected. The north polar cap, during the first days of October, was clearly seen as a narrow segment extending along the terminator. Its color, without filter, was light azure. On October 6, the north polar cap was poorly recorded, and after October 7 it disappeared entirely and was not observed thereafter. The greatest brightness of the north polar cap, when it was recorded, was also located in the green, yellow, and sometimes, in the azure region. After November 12, a thick haze appeared on Mars in the region of the south and north polar caps which covered both near-polar regions, and after November 16 not a single detail could be seen in the polar regions through any filter; even the polar regions themselves were not detectable without filters. This phenomenon indicates the extremely great variability of the Martian atmosphere and its turbidity produced by aerosols. This state of the Martian atmosphere in the near-polar regions persisted until the end of November.

Dark Regions

The following dark regions of Mars were clearly seen in October and the first part of November: Mare Sirenum, Mare Cimmerium, Solis Lacus, Sinus Aurorae, Sinus Sabaeus, Syrtis Major, Sinus Aonius, Mare Chronium, Mare Erythraeum.

The contrast of the dark regions with the continents in the visible, especially in the green, spectrum region was always considerably lower than in the red region; as the details moved toward the limb, the contrast in the red spectrum decreased appreciably more slowly than in the green. In this case, the "seas" so to speak contracted through a red filter and their contrast with the continents increased. Furthermore, in green rays the central part of the "seas" was darker than the periphery, whereas in yellow rays, the central part was appreciably lighter than their edges. It was also noted that the dark regions, for example, Syrtis Major, Solis Lacus, and others, are not continuous formations but have a mosaic structure consisting of individual small spots.

In the second half of November, visibility deteriorated also in the equatorial region. The dark regions were recorded faintly through all filters. After November 26, the transparency of the Martian atmosphere again improved, although the near-polar regions remained as usual in a haze.

The color of the "seas" in October was mainly greenish azure, whereas in November it began to pale and change to dark-gray with a light-yellow hue.

Light Regions   /120

Of the light regions we could clearly see Ausonia, Deucalionis Regio, Pyrchae Regio, Hellas, and others. On the night of November 8 – 9, a light spot was noted in the region of the north pole of Mars which exceeded in brightness

the brightness of the region of the polar cap itself.

BIBLIOGRAPHY

1. Tikhov, G.A.: Trudy Sekt. Astrobotan., Vol.V, Alma-Ata, Izd. Akad. Nauk KazSSR, 1955.
2. Kozlova, K.I.: Trudy Sekt. Astrobotan., Vol.V, Alma-Ata, Izd. Akad Nauk KazSSR, 1955.
3. Tikhov, G.A.: Trudy Sekt. Astrobotan., Vol.VI, Alma-Ata, Izd. Akad. Nauk KazSSR, 1958.

CHANGES IN THE COLOR OF MARS BASED ON PHOTOELECTRIC OBSERVATIONS OF 1958

K.I.Kozlova and Yu.V.Glagolevskiy

Determination of the color of planet surfaces is an important problem in astronomy, since the color of various formations on the surface of a given planet is one of the characteristics determining the nature and properties of the rocks comprising it. A single color characteristic, of course, is insufficient to solve such an important problem; therefore, it is necessary, besides determining the color of the planet (determination of the color excess, color indices, and color temperature), to investigate also the law of light reflection, albedo of the surface, energy distribution in the spectrum, polarization, change in temperature, etc.

TABLE 1

CALENDAR OF MARTIAN OBSERVATIONS

Date (October) 1958	Sidereal Time		Date (November) 1958	Sidereal Time	
14/15	23^{hr}	42^{min}	4/5	0^{hr}	54^{min}
	0	19		1	54
16/17	23	51	20/21	1	00
.	0	22		1	35
.	0	49	27/28	0	21
	1	29	.	0	46
23 24	22	59	.	1	12
.	23	24			
.	0	01			
.	0	46			

During the 1958 opposition, Mars was observed through the AZT-7 telescope by means of the AFM-3 electrophotometer at an equivalent focus of 10 m (Table 1). The electrophotometer was described by us earlier (Bibl.3). The maximal linear dimension of Mars on the AZT-7 telescope was only 0.925 mm; therefore, the entire disk of the planet was photometered as a whole through two optical filters, blue and yellow. The slit of the electrophotometer was established on the planet disk as shown in Fig.1. The system of telescope, filters, and photomultiplier yielded λ_{eff} = 420 and 535 mμ, respectively. Judging by the effective wavelengths, our color system somewhat differed from the International System (λ_{eff} = 440 and 553 mμ), but this difference is negligible. The comparison star was α Aurigae (Go), which was photometered through the same color filters. /122 Mars was photometered with a slit of 0.25 mm, according to the scheme: star – Mars – star – Mars – star. The comparison star and Mars were measured 10 times through each filter, after which the average value was taken. During the night, several series of observations of Mars and α Aurigae were made, over a total

time of about two hours. During the observations, Mars and the comparison star were at near zenith distances; the difference in z was $0.5 - 2°$ and only on November 27 - 28 was it $7°$. When processing the observations, both Mars and the comparison star were reduced to 1 zenith distance.
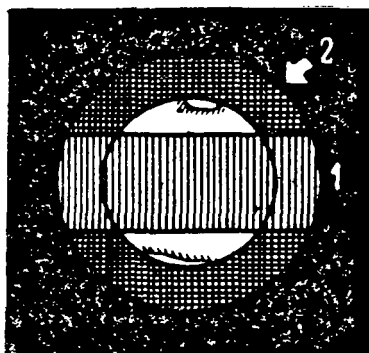
Fig.1   Diagram of the Position of the Electrophotometer
Slit on the Disk of the Planet Mars
1 - Slit of electrophotometer; 2 - Diaphragm of electro-
photometer

The color excess (CE) of Mars in comparison with α Aurigae was determined for each instant of observation by the conventional formula

$$CE = -2.5 \left(\log \frac{I_{M420}}{I_{M535}} - \log \frac{I_{\alpha420}}{I_{\alpha535}} \right),$$
(1)

where I_M and I_α are the brightnesses of Mars and α Aurigae, respectively. The average value was taken from all the color excesses calculated for each night.

TABLE 2

PHOTOELECTRIC COLOR EXCESSES OF MARS WITH RESPECT TO
α AURIGAE, DURING THE 1958 OPPOSITION

Date (October)	CE	Error	Date (November)	CE	Error
14/15	$+0^m.66$	$\pm0^m.02$	4/5	$+0^m.56$	$\pm0^m.10$
16/17	$+0^m.61$	$\pm0^m.01$	20/21	$+0^m.46$	$\pm0^m.02$
23/24	$+0^m.538$	$\pm0^m.007$	27/28	$+0^m.49$	$\pm0^m.02$

The data in Table 2 and Fig.2,A show that, during the period of our observations, the CE of Mars changed; they decreased as Mars approached the date of opposition

(November 16) and increased again after the opposition.

The color index of Mars (CI_M) was determined as

$$CI_M = CI_a + CE_M,$$ (2)

where CI_a is the color index of α Aurigae according to the data in the literature, equal to +0.82.

Let us compare the change in the found color indices of Mars relative to the phase angle (i), based on the results of our observations of 1956 (Bibl.3)
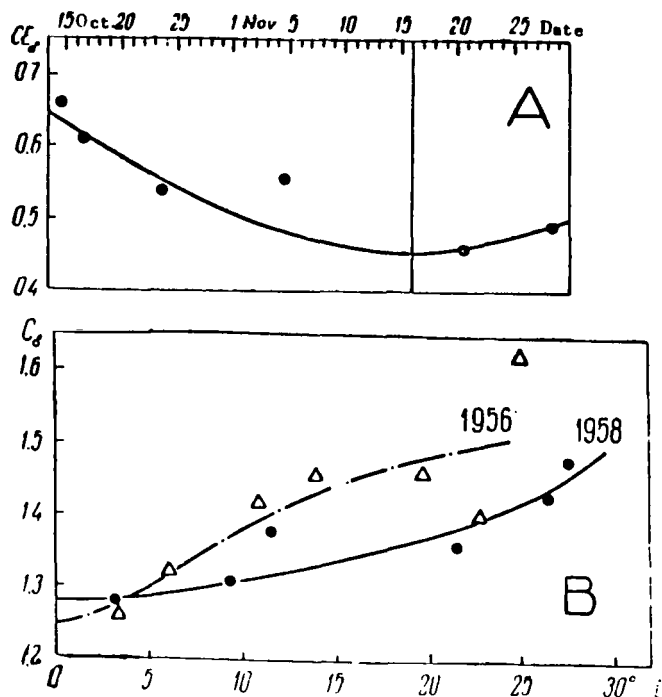
Fig.2 A – Change in Color Excess (CE) of Mars during
the Observation Period from October 14 to November 27,
1958. B – Comparison of the Change of the Color Indices
of Mars (C) as a Function of the Phase Angle (i) of
the Planet, Based on Observations of 1956 and 1958

and 1958. According to Fig.2,B, a certain dependence of the color of Mars on /123
its phase is noted: the color index increases with an increase in phase angle.
The curves for the variation in the color indices of Mars with the phase differ
markedly. The curve of 1956 is more convex and lies higher. This is due to
the fact that, at the opposition of 1956, the atmosphere of the planet was extremely opaque, with rapid fluctuations in this turbidity. As Mars moved from
the opposition toward i = 30° (Fig.2), its color index increased by 0.27 in 1956
(Bibl.1, 3) and by 0.10 in 1958. Vaucouleurs (Bibl.2) g : a change in the

143

color index of Mars from the opposition to the quadrature equal to $0.^m20$ (i =
= $47°$):

Position of Mars in orbit	Opposition	Quadrature
At aphelion	$+1.^m30$	$+1.^m50$
At perihelion	$+1.^m45$	$+1.^m65$

According to the data by Vaucouleurs (Bibl.2), the difference in the color indices of Mars when the planet is at aphelion and at perihelion is $0.^m15$, both at opposition and at quadrature. Apparently, this is due to the different seasons on Mars. The change in the color of Mars from opposition to quadrature by $0.^m20$ is probably caused by the characteristics of the Martian atmosphere.

According to our data and those by Vaucouleurs, the color index of Mars changes with time, and Mars appears "redder" when it is far from opposition. The data of other observers (Bibl.6, 7) do not confirm this.

Another characteristic of the planet is the color temperature T_c which is purely a color characteristic of the light flux and is in no way associated /124 with the actual temperature of the reflecting surface of the planet. To calculate the color temperature on the basis of the color index (C_M) we used the conventional formula

$$T_c = \frac{7200}{C_M + 0.64} .$$

(3)

The T_c of Mars was calculated for each day of observation and had the following values: October 14 – 15, $3396°$; 16 – 17, $3478°$; 23 – 24, $3622°$; November 4 – 5, $3564°$; 20 – 21, $3750°$; and 27 – 28, $3692°$.

In our case, the difference between λ_2 and λ_1 (535 and 420 mμ) did not exceed the limits of the visible spectrum region; as is known (Bibl.8, 9), the spectral curve of Mars in this range of wavelengths changes monotonically, so that our colorimetric characteristics CE, C_M, and T_c reliably express the spectral reflectance of Mars at $\lambda = 420 - 535$ mμ.

We are convinced that the appreciable changes of C_M and CE are real and ascribe them to changes in the atmosphere and on the surface of the planet, as well as to the fact that, in observing Mars, owing to its rotation, various details of its surface entered the slit of the electrophotometer.

BIBLIOGRAPHY

1. Barabashov, N.P.: Basic Results of Observations of Mars during the Great Opposition of 1956 (Osnovnyye rezul'taty nablyudeniy Marsa vo vremya Velikogo protivostoyaniya 1956 g.). Astron. Zh., Vol.35, No.6, 1958.
2. Vokuler, Zh. (Vaucouleurs, G.): Physics of the Planet Mars (Fizika planety Mars). Moscow, Izd. Inostr. Lit., 1956.

3. Glagolevskiy, Yu.V. and Kozlova, K.I.: Photometry of Areas of the Martian Surface in 1956, with the AFM-3 Electrophotometer (Fotometriya uchastkov poverkhnosti Marsa v 1956 g. na elektrofotometre AFM-3). Trudy Sekt. Astrobotan., Vol.VI, Alma-Ata, Izd. Akad. Nauk KazSSR, 1958.

4. Sharonov, V.V.: The Problem of the Role of the True Absorption in the Atmosphere of Mars (K voprosu o roli istinnogo pogloshcheniya v atmosfere Marsa). Astron. Zh., Vol.34, No.4, 1957.

5. Moroz, V.I. and Kharitonov, A.V.: Photoelectric Photometry of Areas of the Martian Surface (Fotoelektricheskaya fotometriya uchastkov poverkhnosti Marsa). Astron. Zh., Vol.34, No.6, 1957.

6. Gurtovenko, E.A. and Gordeladze, Sh.G.: Three-Color Colorimetry of the Integrated Brightness of Mars Based on the Observations of 1956 (Trekhtsvetnaya kolorimetriya integral'noy yarkosti Marsa po nablyudeniyam 1956 g.). Astron. Zh., Vol.34, No.6, 1957.

7. Radlova, L.N.: Visual Photometry and Colorimetry of Mars during the 1939 Opposition (Vizual'naya fotometriya i kolorimetriya Marsa vo vremya oppozitsii 1939 g.). Astron. Zh., Vol.17, No.4, 1940.

8. Barabashov, N.P.: Comments on the Determination of Color of Light-Reflecting Surfaces (Zamechaniye ob opredelenii tsveta otrazhayushchikh svet poverkhnostey). Tsirk. Astron. Observatorii, Khar'kov, No.15, 1956.

9. Barabashov, N.P.: Investigation of the Physical Conditions on the Moon and Planets (Issledovaniye fizicheskikh usloviy na Lune i planetakh). Khar'kov, Izd. Khar'kov. Univ., 1952.

COLOR EXCESSES AND COLOR INDICES OF SEVERAL CRATERS ON THE MOON, BASED ON PHOTOELECTRIC PHOTOMETRY

K.I.Kozlova and Yu.V.Glagolevskiy

Photoelectric observations of lunar craters were carried out at Alma-Ata, using an AFM-3 electrophotometer mounted on the AZT-7 telescope. The electrophotometer is described elsewhere (Bibl.2).

The observations were made only at full moon, so as to minimize the influence of the polarization effect (Bibl.3). The material discussed in this article was accumulated over a period of twelve nights (Table 1); during the other months it was impossible to observe the full moon owing to overcast. The bottom of 15 lunar craters were photometered, and the bottom of the crater Manilius was used as the reference region.

TABLE 1

CALENDAR OF OBSERVATIONS

Date of Observation	Evaluation of the Observation night
1958	
May 1/2	Satisfactory
August 31	Good
September 26/27	Satisfactory
" 28/29	"
October 26/27	Good
November 27/28	Satisfactory
December 25/26	"
1959	
February 24/25	"
" 25/26	"
March 25/26	"
September 15/16	"
November 16/17	"

Photometry was carried out in yellow and blue light. The system telescope – filters – spectral sensitivity of the photomultiplier yielded 420 and 535 mμ. The optical filters were checked for transmission by means of the SF-4 spectrophotometer. In order to define the transmissivity of the entire system, it was necessary to investigate all surfaces in the light path: meniscus, mirror, small reflector with an aperture defining the photometered portions, and a Fabry

lens. The Fabry lens and the optical filters were checked on the spectrophoto-
meter; as expected, their absorptivity was too small and remained practically
without influence on λ_{eff}.
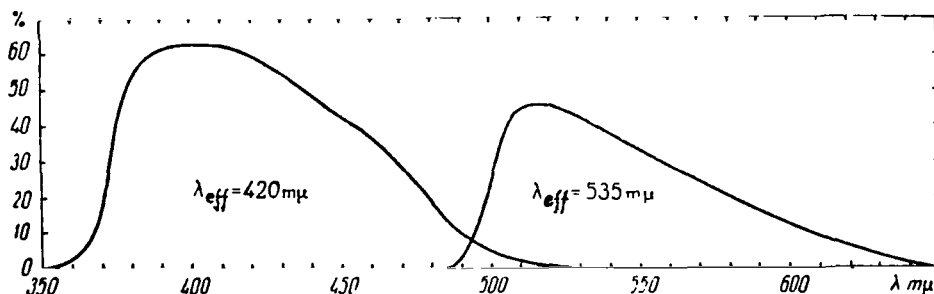
Fig.1 Spectral Sensitivity Curves for the Photometric
System of the Electrophotometer

When investigating the transmission of the telescope (meniscus + mirror)
the latter was directed at the zenith and the spectrum of the sky was photo-
graphed when the sky was cloudless. Then, the spectrum of the sky was photo-
graphed at the zenith through different diaphragms, using the same spectrograph
without a telescope. After the usual processing, we obtained the transmission
coefficients. The spectral sensitivity curves for our entire system are shown
in Fig.1. The quantity λ_{eff} was defined as the center of gravity of the areas
under these curves. Figure 2 shows the diagrams of all the investigated craters
and the main surrounding details. The measured craters are outlined by a heavy
line, and the number in the upper right-hand corner indicates the commonly /126
accepted number of the crater. The hatched circle represents the sector defined
by the hole in the mirror during photometering. The diameter of the hole, de-
fining the photometered areas, was equal to approximately 3/4 of the diameter
of Manilius.

All the craters in the reference region were photometered 10 times through
each filter. After each investigated crater we immediately photometered the
reference region. During the night, each crater and the reference region were
measured several times. Photometering was carried out according to the follow-
ing time scheme: reference – first crater – reference – second crater – ... –
last crater – reference. To obtain one "complete observation" according to the
scheme, took on the average about 6 min. If now the curve for the time rate of
change in brightness of the reference crater (Manilius) is plotted, readings can
be taken for the instants at which the studied crater was photometered. This
method eliminates many errors produced by variations in the sensitivity of /127
the photometer, by changes in the transparency of the atmosphere, etc.

Before the observations, the amplifier and the photomultiplier were placed
for several hours in a dry warm room for drying, the desiccant was changed each
time in the photomultiplier unit, and the electrophotometer was switched on
1.5 – 2 hrs before work. These measures substantially increased the operational
reliability of the photometer. Furthermore, the high voltage across the photo-
multiplier was reduced to the minimum at which the sensitivity was still suffi-
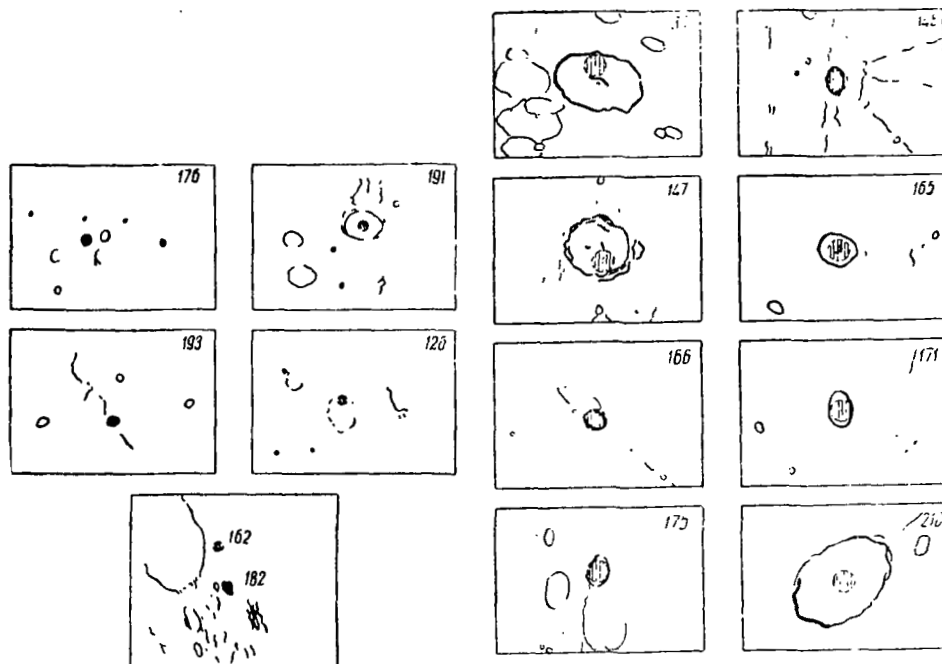
Fig.2   Diagrams of the Position of the Mirror Diaphragm
of the Electrophotometer (Hatched Area) at the
Bottom of the Photometered Craters

cient. To obtain an even greater operational reliability of the photometer, beginning in 1959 the photomultipliers were powered by 65–ANMTs–1.3 II plate-filament batteries connected in series and producing a voltage up to 1100 volts. The high-voltage regulator inside the electrophotometer was disconnected to prevent a direct-current voltage during voltage fluctuations of the circuit.

We photometered 15 lunar craters; the observation of a large number of lunar objects was limited by the method of observation, which precluded the possibility of simultaneous observation of more than one detail. This is a major shortcoming of the photoelectric method in the sense of the excessive time required for obtaining mass observational material.

For each photometered crater, we determined the color excess (CE) with respect to the reference crater Manilius. The CE was determined by the known formula

$$CE = -2.5\left(\log\frac{I_{420}}{I_{535}} - \log\frac{I^o_{420}}{I^o_{535}}\right).$$ (1)

where I_{420}, I_{535}, I^o_{420}, I^o_{535} are the brightnesses of the investigated and reference craters, respectively. The color excesses were determined as the arithmetic means of all measurements (n); see Table 2.

To obtain the color indices (CI) of the investigated craters we must know CI_o of the reference crater Manilius. To determine CI_o of Manilius, we tied in

148

the reference crater to the star α Aurigae with a known color index ($CI_3B =$ <u>/128</u>
= +0.82). First, we determined the color excess (CE) of Manilius with respect

TABLE 2

PHOTOELECTRIC COLOR EXCESS (CE) AT THE BOTTOM OF
LUNAR CRATERS IN RELATION TO MANILIUS,
DURING THE FULL MOON

Crater	No. in Catalogue	CE	r_λ	n
Copernicus	147	−0.013	±0.002	40
Plato	210	+0.037	±0.007	40
Plinius	165	−0.040	±0.009	30
Kepler	146	+0.023	±0.008	30
Tycho	30	+0.002	±0.006	20
Menelaus	166	−0.042	±0.020	20
Aristarchu	176	−0.044	±0.005	40
Archimedes	191	0.000		10
Herodotus	175	−0.024	±0.010	30
Lambert	193	−0.133	±0.035	30
Marius	171	+0.0 9	±0.002	30
Macrobius	182	+0.018	±0.032	10
Proclus	162	+0.040	±0.022	10
Flamsteed	126	−0.089	±0.020	30

TABLE 3

PHOTOELECTRIC COLOR INDICES (CI) AT THE
BOTTOM OF LUNAR CRATERS

Crater	CI
Copernicus	+0.837
Plato	+0.887
Plinius	+0.810
Kepler	+0.873
Tycho	+0.852
Menelaus	+0.808
Aristarchus	+0.806
Archimedes	+0.850
Herodotus	+0.826
Lambert	+0.717
Marius	+0.841
Macrobius	+0.868
Proclus	+0.890
Flamsteed	+0.761
Average CI	+0.830

to α Aurigae, taking into account the selectivity of the mirror diaphragm of the
electrophotometer. This proved to be equal to $CE_0 = +0.026 \pm 0.008$. Then we
determined the color index of Manilius as

$$CI_0 = CI_{3B} + CE_0 . \tag{2}$$

CI_0 proved to be equal to $0.^{\bullet}846$. The color indices of the investigated lunar craters were obtained as the sum of the color index of the reference region and the color excess (CE) of the lunar objects:

$$CI = CI_0 + CE . \tag{3}$$

During photometering we endeavored to obtain results with the maximal accuracy which our electrophotometer could give. The intrinsic accuracy of the observations can be judged by the root-mean square error of the arithmetic mean or the standard deviation (σ) which was calculated for each series of observations through each optical filter for all observed craters of the lunar surface. The standard deviation was determined by the formula

$$\sigma = \pm \sqrt{\frac{\Sigma \varepsilon^2}{n(n-1)}} , \tag{4}$$

where ε is the deviation from the arithmetic mean and n is the number of measurements.

The color excess was obtained as the arithmetic mean from the results of a series of measurements whose number (n) is shown in Table 2. For each color excess of the crater with respect to Manilius, we calculated the probable error of the arithmetic mean (r_A) (Bibl.5) which was defined as

$$r_A = 0.675 \cdot \sigma, \tag{5}$$

where σ is the standard deviation.

We see from the data of Table 2 that the probable error of the results does not exceed $\pm 0.^{\bullet}020$. The signs of CE were certain even for the craters Tycho and Macrobius for which the probable error was greater than the value itself.

We can see from the data of Tables 2 and 3 that there is no great difference in the color of the investigated craters. The results of the investigation can be reduced to the following: First, there are small differences in the color of the investigated craters; second, the normal photoelectric color indices of the craters vary within the limits of $+0.^{\bullet}717$ to $+0.^{\bullet}890$, i.e., the amplitude amounts to only $+0.^{\bullet}173$; third, the average color index for the 14 craters with respect to Manilius is $+0.^{\bullet}830$, which agrees well with the data by other authors (Bibl.3 and 4).

BIBLIOGRAPHY

1. Kozlova, K.I. and Glagolevskiy, Yu.V.: Color Excesses of Six Craters of the Moon, Based on Electrophotometric Measurements (Izbytki tsveta 6 kraterov Luny po elektrofotometricheskim izmereniyam). Astron. Zh., No.198, 1958.

2. Glagolevskiy, Yu.V. and Kozlova, K.I.: Photometry of Areas of the Martian Surface in 1956 with the AFM-3 Electrophotometer (Fotometriya uchastkov poverkhnosti Marsa v 1956 g. na elektrofotometre AFM-3). Trudy Sekt. Astrobotan., Vol.VI, Alma-Ata, Izd. Akad. Nauk KazSSR, 1958.

3. Dzhapiashvili, V.P.: Investigation of the Polarization Properties of   /129
   Lunar Surface Formations, Based on Electrophotometric Measurements (Issle-
   dovaniye polyarizatsionnykh svoystv obrazovaniy lunnoy poverkhnosti po
   elektrofotometricheskim izmereniyam). Byull. Abast. Observatorii, No.21,
   1957.

4. Teyfel', V.G.: Normal Color Indices and the Color-Brightness Dependence of
   Lunar Surface Areas (O normal'nykh pokazatelyakh tsveta i zavisimosti
   tsvet-yarkost' uchastkov lunnoy poverkhnosti). Astron. Zh., Vol.36, No.1,
   1959.

5. Yakovlev, K.P.: Mathematical Analysis of the Results of Observations
   (Matematicheskaya obrabotka rezul'tatov nablyudeniy). Moscow-Leningrad,
   Gostekhizdat, 1950.

PART II: CATALOGUE OF THE COLOR INDICES OF LUNAR OBJECTS

V.G.Teyfel'

By using the data on the lunar surface regions, obtained with a high slit of the spectrogram, for spectrophotometering individual areas of the moon, it is possible to obtain estimates of the color of numerous small details for which it is difficult to plot the spectral curves. In this paper, the technique and results of determining the color indices of 262 small areas of the lunar surface are given.

Observation Technique and Analysis

The minimal dimensions of an area of the lunar surface for which we can obtain a brightness distribution curve over the entire spectrum are determined by the scale of the lunar image produced on the photographic plate by the optical system of the instrument. When photographing spectra with a high slit (for brevity, we will call these "broad spectra") with the AZT-7 reflecting telescope, the image of the moon at the principal focus of the instrument projected onto the slit of the spectrograph has a diameter of the order of 18 - 19 mm. Correspondingly, the width of the spectrum obtained with a high slit is 4 mm. The smallest linear dimensions of an object whose spectrum can be measured along the dispersion on a microphotometer are about 40 - 50 km. However, at this image scale it is best to avoid measurements of objects of even such dimensions. To measure the spectrum of a small object along the dispersion on a microphotometer it is necessary to use a very low height of the receiving slit of the photocell, which inevitably leads to loss of a portion of the light striking the photocell and also intensifies the effect of the graininess of the photographic image on the accuracy of tracing a continuous spectrum. Furthermore, small objects frequently have an uneven image density, decreasing toward the edges of the object. In bright objects, this effect might distort the values on the traces of the galvanometer deflections in various spectrum portions. Therefore, to measure spectra along the dispersion it is necessary to select only sufficiently large (at a given image scale) areas of the investigated lunar region.

At the same time, it is of considerable interest to obtain the color characteristics of small details, which are especially numerous in the zone of the lunar maria. Visually and photographically, it is easy to see that the lunar maria, which have a general dark hue in comparison with the continents, are /131 mottled by a vast number of irregular light patches, bands, and spots, to say nothing of the radiant aureole of the craters situated in the zone of the maria.

No doubt, the small details that are distinguished by brightness may have other dissimilar optical characteristics, such as color and polarization. Actually, on the basis of color photographs of the moon, N.P.Barabashov noted that most maria have a mosaic structure: reddish and greenish spots are scattered at

random over the entire surface of the maria (Bibl.2).

The color of small areas of the lunar surface can be obtained by measuring the lunar spectrogram (a certain region of it) across the dispersion on the microphotometer trace at certain wavelengths of the spectrogram. The broad spectra of 11 lunar regions obtained at the Astrobotany Sector were measured on the MF-4 microphotometer across the dispersion at areas corresponding to wavelengths of 550 and 443 mu. The selection of precisely these wavelengths was determined as follows: First of all, by calculating the brightness ratios of the details at λ = 550 and 440 mu, we obtain the normal color indices of the details since the selected wavelengths almost exactly coincide with the effective wavelengths used in the international system of standard color indices. Although the color index does not change the spectral curve since [as shown by N.P.Barabashov (Bibl.1)] several different spectral curves may correspond to one and the same color index in the case of reflecting surfaces, it is the only numerical characteristic that can be used for comparison with other optical characteristics of lunar objects. In any case, the color index as applied to the moon is more convenient than such characteristics as the color temperature or spectral class.

These wavelengths were also selected because the spectral sensitivity of the photographic emulsion shows the least change close to these wavelengths, as is apparent from the microphotograms of the spectra taken on Agfa Spektral Rot Rapid plates, which were used in the lunar studies (Fig.1). In other spectrum regions, especially in the red region, the sensitivity changes more rapidly, and even a small inaccuracy of setting the slit in the direction of the dispersion could cause noticeable errors in the blackening of the negative.

In the yellow region (λ = 550 mu), the position of the microphotometer slit was fixed by a millimeter scale placed in front of the screen of the MF-4, relative to the line Na 5852 Å. In the blue region (443 mu) the measurement was carried out between the lines Fe 4409 Å and 4455 Å, where there were no intense lines whose effect on the blackening accuracy would differ, depending on the blackening density. So that the graininess of the negative would not produce small variations on the microphotogram, the image was slightly defocused on the screen. Such defocusing did not affect the actual degree of blackening, since the details of the lunar surface many times exceed the size of the grains on the negative.

Thus, photometric profiles of investigated regions were obtained on the microphotometer (Fig.2). It was assumed that, because of the negligible color contrast, the errors of measurement inherent to photographic methods would be rather large. Therefore, for each region of the moon, 11 - 14 spectrograms obtained on various dates were rated.

The negatives were calibrated by means of a platinum echelon (on glass). /132 The parameters of the risers of this step wedge were determined both in integrated light (on the MF-2 microphotometer) and for each wavelength (every 10 mu) in the range of λ = 390 - 620 mu in relative units (on the SF-4 spectroelectrophotometer).

An important problem was the proper selection of the light source for calibrating the negatives. The gradation of the steps of the wedge was compara-

tively small and encompassed only 1.110 of the range of the intensity logarithms. Therefore, so that the spectra of the investigated object in all portions of the spectrum would enter one normal exposure scale, the spectral brightness distribution of the light source had to be close to that of the investigated object.
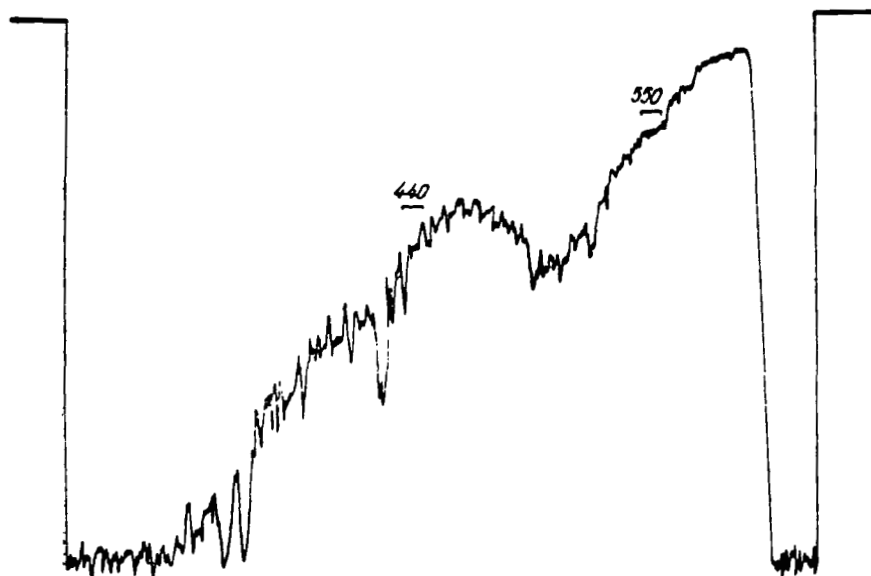
Fig.1
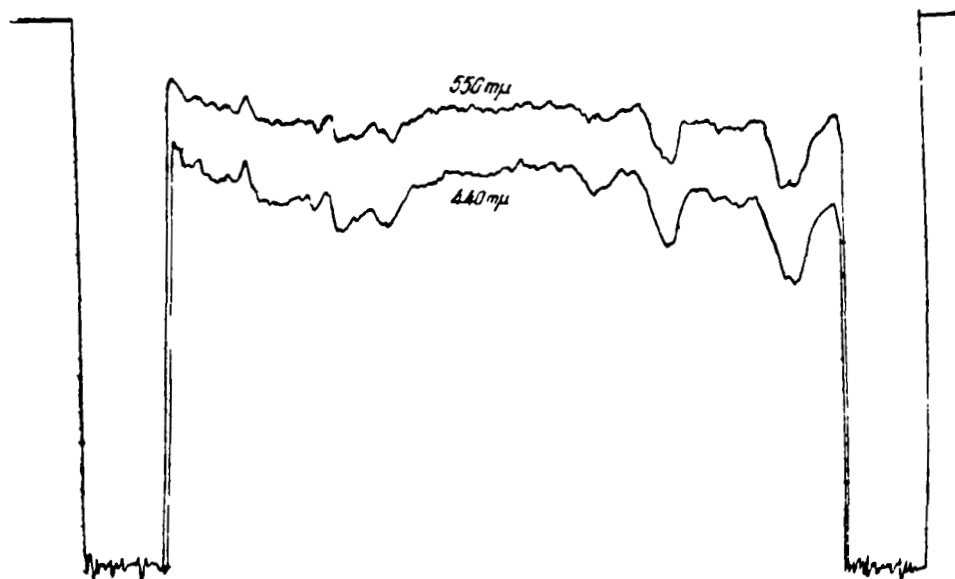
Fig.2

Consequently, the use of bright stars of the early class for calibrating the /133 lunar spectra was impossible. Calibration with respect to α Aurigae was possible, but not at all seasons of the year. Furthermore, vibration of the stellar

images frequently creates longitudinal bands on the spectra, which makes the spectrogram of the scale unsuitable for analysis. It would also be difficult to use sunlight for calibration, since such light would have to be greatly attenuated, not to speak of the unstable weather encountered. The sky frequently cleared only after sunset or, conversely, the next day was cloudy.

Therefore, calibration of the negatives relative to the moon itself proved most convenient. For this, the slit of the spectrograph was oriented along the daily parallel of the moon, so that the moon, at stopped clock mechanism of the telescope, passed through the entire field of view. Thus, the brightness inhomogeneities of individual lunar regions were averaged similarly at all risers of the echelon. Because of the relatively minor differences in brightness on the lunar surface, such a method of calibrating the illumination of the scale steps by a variable light source presumably will not noticeably distort the characteristic curves.

A second important problem in lunar spectrophotometry is the standardization of the spectrograms obtained, i.e., reference of the characteristics of the lunar objects to a certain colorimetric system. The characteristics of light-reflecting lens systems are usually referred to the light characteristics

Fig.3

of the source illuminating the object. However, in the investigation of planets, the star α Aurigae whose spectral class is close to that of the sun is frequently used for correlating the spectrograms, in place of the light source (the sun). Since, in our case, we are dealing not with spectral curves but with light indices, reference to this star is completely permissible. This greatly facilitates the standardization. However, it is impossible to refer the spectra of the moon to the star every single night. This would greatly complicate the observations and their work-up. Therefore, just as was done by N.P.Barabashov and A.T.Chekirda (Bibl.3), as the correlation object in the observations we selected a certain area of the lunar surface, whose spectrum was recorded on each plate almost simultaneously with the broad spectra of the investigated regions. The time required for photographing five broad spectra on one plate was no more than 5 - 6 min; during this time, the zenith distance of the moon

could not change noticeably, and both the investigated and reference regions were photographed at identical values of air masses and spectral transparency of the atmosphere. The reference area (Fig.3) was a small region in the Sea of Vapors (Mare Vaporum) whose spectrum was measured on the microphotometer along the dispersion in view of the sufficient extent of the uniformly bright area of the sea. Measurement along the dispersion, as shown by a comparison with transverse profiles of the reference region, will not introduce errors into the brightness ratio at the selected wavelengths. Since measurement of the reference region along the dispersion is also required for the spectrophotometric investigations, this reduces the amount of subsequent work.

When photographing the spectra of lunar regions, a polaroid was always placed in the same position in front of the slit of the spectrograph so that the plane of polarization of the light entering the slit would always be orientated identically with respect to the slit. In this manner, according to Yu.N.Lipskiy (Bibl.6), the effect of different polarization of lunar objects on the spectral curve can be partly eliminated. Since the spectra were photographed mainly close to noon, when the degree of polarization of the lunar surface is at a minimum, polarization could not have a noticeable effect on the observational data.

The photometric profiles on the traces were analyzed in the conventional manner. On all profiles of a given region, we selected 24 details for which we recorded the blackenings, which were then converted to intensity logarithms, by corresponding monochromatic characteristics. We calculated the differences of the logarithms in blue and yellow light, which pertained to the same differences for the reference region. As a result the color excess of the investigated object with respect to the reference object was determined as

$$CE = -2,5\left(\log\frac{I_{440}}{I_{550}} - \log\frac{I^0_{440}}{I^0_{550}}\right),$$

where I is the brightness of the investigated region and I_0 is the brightness of the reference region.

To obtain the color indices of the investigated details, the color index of the reference region had to be known. For this, the spectra of the reference region and the star α Aurigae were photographed simultaneously at their different zenith distances. Such observations were carried out on November 9 - 10, 1957 and February 6 - 7, 1958. From the values of the differences in the intensity logarithms at the selected wavelengths (440 and 550 mu), we plotted the curves of the dependence of these values on the air masses (M), both for the reference region of the moon and for α Aurigae. From these curves, we recorded the value log C = log I_{440} - log I_{550} for M = 0. The color excess of the reference region with respect to α Aurigae CE_0 = -2.5 log $\dfrac{C_0}{C_\alpha}$ was equal on the average to $-0^m.05 \pm 0^m.03$. The comparatively large error in determining the color excess was due to the fact that the moon and α Aurigae were recorded only at values of M ≤ 2.5 (we had reason to suspect a change in the coefficient of atmospheric transparency with time and therefore reduced the observation period). Thus, the drawing of a straight line on the graphs became somewhat uncertain.

However, since the color index of α Aurigae itself is not known with great accuracy, this error cannot fundamentally change the results of the observations, the more so since, in estimates of the color index of the sun with which the color indices of lunar details are compared, divergences up to 0.20 and more are found in the literature. The color index of α Aurigae was taken as equal to +0.82 according to the most current data (Bibl.5). The color index of the reference region was then found to be equal to +0.77.

On the basis of observations and measurements carried out by the described method, we compiled a catalogue of normal color indices for 262 areas of the lunar surface. The selenographic coordinates of these areas were determined on a lunar map, which was a reduced copy of the chart by Karl Andel published in 1926. Figure 3 shows the position of the spectrograph slit against the background of the lunar surface and the designations of the investigated regions. In the diagram and in the catalogue, the regions are designated by the letters A, B, C, etc. and the areas by ordinal numbers in each region. The omission of the regions I, M, N, P in the catalogue is due to the insufficient number of /135 spectrograms obtained for these regions, because of unfavorable weather conditions. The color indices of the areas of these regions will be published some time in the future.

Photographing of broad spectra of the moon permits comparing the color of lunar details with their brightness. Within a given region, such a comparison is made by simply comparing the color excesses of the details with their relative brightness. The latter is determined from the spectra recorded near noon when, according to the investigations by N.P.Barabashov, A.V.Markov (Bibl.7), V.A.Fedorets (Bibl.13), and V.V.Sharonov (Bibl.16), all areas of the lunar surface regardless of their position on the lunar disk, reach a maximal brightness corresponding to their albedo.

TABLE 1

Date	α	No. of Negative
1957		
11—12 Sept.	+27°	58—63
5—6 Nov.	—23°	85—90
9—10 Nov.	+25°	91—96
1958		
3—4 Jan.	—28°	105—114
4—5 Jan.	—15°	115—120
4—5 Mar.	—15°	123—126

Comparisons by relative brightness of different regions are impossible, owing to differences in spectral density produced by slight deviations in exposure time and also by the fact that a diaphragm was used on the telescope objective for photographing bright mountainous regions. Therefore, we used the observations by L.N.Radlova (Bibl.8) who determined the brightness coefficients

157

Region A

No.	Object	φ	λ	CE	σ_A	$\log I_{550}$	CI	ρ_{550}	n
A 1	Continent	−12°.0	+44°.0	0^m.18	0^m.03	0.296	0^m.95	0.174	6
2	Magelhaens wall W	−11.5	+44.5	0.12	0.02	0.222	0.89	0.147	7
3	Between Magelhaens and Goclenius	−11.0	+45.0	0.08	0.02	0.022	0.85	0.092	14
4	Goclenius, S-wall	−10.0	+45.0	0.17	0.02	0.192	0.94	0.137	10
5	Goclenius, center	−9.0	+45.5	0.01	0.02	0.022	0.78	0.092	10
6	Goclenius, N-wall	−8.5	+46.0	0.17	0.02	0.189	0.94	0.135	14
7	Mare Foecunditatis	−8.0	+46.0	0.06	0.02	0.003	0.83	0.089	14
8	Mare Foecunditatis	−7.0	+46.5	0.09	0.02	0.036	0.86	0.096	14
9	Mare Foecunditatis	−6.0	+46.5	0.06	0.02	9.953	0.83	0.079	14
10	Messier-Pickering	−1.0	+47.0	0.06	0.02	0.026	0.83	0.093	14
11	Light band	0.0	+48.0	0.13	0.03	0.029	0.90	0.094	14
12	Mare Foecunditatis	+1.0	+50.0	0.07	0.02	9.960	0.84	0.080	14
13	Taruntius ray	+2.5	+50.5	0.10	0.01	0.033	0.87	0.095	14
14	Mare Foecunditatis	+3.0	+50.5	0.04	0.02	9.971	0.81	0.082	14
15	Taruntius ray	+7.0	+51.0	0.09	0.02	0.115	0.86	0.114	14
16	Taruntius ray	+7.5	+51.0	0.10	0.02	0.0'5	0.87	0.1'0	14
17	Continent	+7.5	+52.0	0.14	0.02	0.262	0.91	0.161	12
18	Continent	+11.5	+55.0	0.12	0.02	0.214	0.89	0.154	12
19	Mare Crisium SW	+13.0	+55.0	0.06	0.02	0.004	0.83	0.089	13
20	Mare Crisium, near Picard	+15.0	+56.0	0.10	0.02	0.049	0.87	0.099	13
21	Mare Crisium, near center	+16.0	+58.0	0.07	0.02	0.000	0.84	0.088	14
22	Mare Crisium	+20.0	+60.0	0.10	0.02	0.093	0.87	0.109	14
23	Mare Crisium	+22.0	+61.0	0.08	0.01	0.006	0.85	0.089	14
24	Mare Crisium N	+23.0	+61.5	0.18	0.03	0.230	0.95	0.149	13

Region B

No.	Object	φ	λ	CE	σ_A	$\log I_{550}$	CI	ρ_{550}	n
1	2	3	4	5	6	7	8	9	10
B1	Censorinus	0°.0	+32°.0	0^m.20	0^m.02	0.532	0^m.97	0.255	10
2	Mare Tranquillitatis	+1.0	+31.0	0.05	0.01	0.036	0.82	0.082	13
3	Near Maskelyne	+2.5	+31.0	0.09	0.02	0.108	0.86	0.096	13
4	Mare Tranquillitatis	+3.0	+30.5	0.04	0.01	0.018	0.81	0.078	13
5	Mare Tranquillitatis	+3.5	+30.0	0.04	0.01	0.054	0.81	0.085	11
6	Mare Tranquillitatis	+5.0	+28.0	0.03	0.01	0.002	0.80	0.075	13
7	Light band	+8.0	+27.5	0.02	0.01	0.049	0.79	0.084	13
8	Mare Tranquillitatis	+9.0	+27.0	0.02	0.01	0.000	0.79	0.075	12
9	Nimbus near Janssen B	+11.0	+25.0	0.04	0.02	0.108	0.81	0.096	13
10	Mare Tranquillitatis	+12.0	+25.0	0.01	0.01	0.018	0.78	0.078	13
11	Mare Tranquillitatis	+13.0	+24.5	0.01	0.01	0.044	0.78	0.083	13
12	Near Plinius	+14.0	+24.0	−0.01	0.01	9.998	0.76	0.075	13
13	Plinius, center	+15.5	+23.0	0.14	0.02	0.267	0.90	0.139	12
14	Dark margin of Mare Serenitatis	+16.5	+22.5	−0.01	0.01	9.972	0.76	0.071	13
15	Mare Serenitatis	+19.0	+21.0	0.07	0.01	0.066	0.84	0.088	13

1	2	3	4	5	6	7	8	9	10
16	Mare Serenitatis	+21.0	+20.5	0.07	0.01	0.057	0.84	0.086	13
17	Mare Serenitatis	+23.0	+20.0	0.07	0.01	0.086	0.84	0.092	13
18	Light rays of Bessel	+25.0	+19.0	0.10	0.02	0.119	0.87	0.099	13
19	Mare Serenitatis, near center	+25.5	+17.5	0.08	0.02	0.048	0.85	0.084	12
20	Mare Serenitatis	+26.5	+16.0	0.10	0.01	0.097	0.87	0.094	13
21	Mare Serenitatis	+28.5	+14.5	0.08	0.02	0.018	0.85	0.084	13
22	Mare Serenitatis	+30.5	+12.5	0.11	0.02	0.145	0.88	0.105	13

Region **C**

No.	Object	φ	λ	CE	σ_A	$\log I_{550}$	CI	ρ_{550}	n
C 1	Between the Apennines and Carpathians	+14°.5	−15°.0	$0^m.08$	$0^m.03$	0.124	$0^m.85$	0.106	11
2	Near Eratosthenes	+14.5	−13.5	0.06	0.02	0.058	0.83	0.091	12
3	Eratosthenes, E-wall	+14.5	−13.0	0.06	0.01	0.120	0.83	0.106	12
4	Eratosthenes, center	+14.5	−12.0	0.04	0.02	0.062	0.81	0.092	13
5	Eratosthenes, W-slope	+14.5	−10.5	0.12	0.02	0.153	0.89	0.114	13
6	Sinus Caloris	+14.5	− 9.5	0.00	0.02	0.012	0.77	0.082	13
7	Sinus Caloris	+14.5	− 8.0	0.06	0.02	0.031	0.83	0.086	13
8	Sinus Caloris	+14.5	− 7.5	0.05	0.02	0.039	0.82	0.087	13
9	Sinus Caloris	+14.5	− 5.5	0.03	0.02	9.992	0.80	0.078	13
10	Apennines S	+14.5	− 5.0	0.10	0.02	0.120	0.87	0.106	13
11	Apennines S	+14.5	− 4.5	0.06	0.02	0.032	0.83	0.086	13
12	Apennines S	•14.5	− 3.5	0.06	0.02	0.084	0.83	0.097	13
13	Apennines S	+14.5	− 2.5	0.05	0.02	0.099	0.82	0.101	12
14	Apennines S	+14.5	− 2.0	0.05	0.02	0.117	0.82	0.105	12
15	Mare Vaporum E	+14.5	− 0.5	0.03	0.02	0.044	0.80	0.089	12
16	Mare Vaporum	+14.5	+ 1.5	0.05	0.02	0.051	0.82	0.090	12
17	Mare Vaporum	+14.5	+ 4.0	0.04	0.02	0.000	0.81	0.080	13
18	Mare Vaporum W	+14.5	+ 7.0	0.04	0.02	0.002	0.81	0.080	13
19	Manilius, E-wall	+14.5	+ 8.0	0.12	0.02	0.257	0.89	0.145	12
20	Manilius, W-slope	+14.5	+ 9.5	0.06	0.02	0.218	0.83	0.132	13
21	Dark region	+14.5	+11.5	0.02	9.946	9.946	0.79	0.070	12
22	Continent	+14.5	+13.0	0.08	0.02	0.100	0.85	0.101	13
23	Dark patch	+14.5	+14.0	0.05	0.02	0.041	0.82	0.088	13
24	Promontorium Acherusia E	+14.5	+15.5	0.08	0.02	0.138	0.85	0.110	13

Region **D**

No.	Object	φ	λ	CE	σ_A	$\log I_{550}$	CI	ρ_{550}	n
1	2	3	4	5	6	7	8	9	10
D 1	Hercules, wall	+46°.0	+40°.0	$0^m.19$	$0^m.01$	0.143	$0^m.96$	0.179	10
2	Lacus Mortis	+44.0	+39.5	0.12	0.02	9.984	0.89	0.124	11
3	Continent	+41.0	+39.0	0.15	0.02	0.029	0.92	0.138	11
4	Continent	+40.5	+39.0	0.11	0.02	9.964	0.88	0.119	11
5	Continent	+40.0	+39.0	0.18	0.02	0.042	0.95	0.142	11
6	Lacus Somniorum	+39.0	+39.0	0.10	0.02	9.910	0.87	0.105	11
7	Continent	+37.0	+38.5	0.17	0.02	9.988	0.94	0.125	10
8	Lacus Somniorum	+35.0	+38.5	0.08	0.02	9.905	0.85	0.103	11
9	Continent	+33.0	+39.0	0.12	0.02	0.018	0.89	0.134	11

1	2	3	4	5	6	7	8	9	10
10	Continent	+32.0	+32.0	0.15	0.02	0.087	0.92	0.157	11
11	"	+30.5	+30.5	0.13	0.02	0.057	0.90	0.147	11
12	"	+30.0	+30.5	0.15	0.03	0.106	0.92	0.165	11
13	"	+28.5	+44.0	0.14	0.02	0.063	0.91	0.150	10
14	"	+28.0	+40 0	0.17	0.02	0.105	0.94	0.164	11
15	"	+27.0	+40.0	0.14	0.01	0.059	0.91	0.148	11
16	"	+25.0	+40.5	0.16	0.01	0.086	0.93	0.157	11
17	"	+23.0	+41.0	0.13	0.01	0.009	0.90	0.132	11
18	"	+20.0	+41.0	0.16	0.01	0.119	0.93	0.169	8
19	Mare Tranquillitatis W	+18.5	+41.0	0.06	0.02	9.856	0.83	0.093	11
20	Palus Somnii	+18.0	+42.0	0.15	0.03	0.010	0.92	0.131	11
21	"	+17.0	+42.0	0.12	0.02	0.000	0.89	0.129	11
22	"	+16.5	+43.0	0.13	0.01	9.958	0.90	0.117	11
23	"	+13.5	+43.5	0.14	0.02	0.014	0.91	0.134	11
24	Mare Tranquillitatis W	+11.5	+44.0	0.03	0.03	9.768	0.80	0.076	9

Region E

No.	Object	φ	λ	CE	σ_A	$\log I_{550}$	CI	ρ_{550}	n
E 1	S- shore of Mare Nectaris	+20.0	+37.0	$0^m.17$	$0^m.03$	0.245	$0^m.91$	0.173	11
2	Mare Nectaris	−19.0	+36.0	0.05	0.03	9.927	0.82	0.082	11
3	"	−17.0	+35.0	0.10	0.03	0.000	0.87	0.098	11
4	"	−14.0	+34.0	0.06	0.02	9.962	0.83	0.090	11
5	"	−13.5	+33.5	0.09	0.02	0.009	0.86	0.100	11
6	"	−12.0	+32.5	0.05	0.03	9.954	0.82	0.098	11
7	Light projection from Mädler	−11.0	+32.0	0.10	0.02	0.137	0.87	0.134	10
8	Gulf between Mare Nectaris and Tranquillitatis	−10.0	+31.5	0.06	0.02	9.993	0.83	0.096	11
9	Continent near Isydorus	−9.0	+31.0	0.09	0.02	0.070	0.86	0.116	11
10	Continent	−7.5	+30.5	0.07	0.02	0.091	0.84	0.121	11
11	Mare Tranquillitatis S	−6.0	+30.0	0.07	0.02	0.003	0.84	0.099	11
12	Torricelli A	−4.0	+29.0	0.07	0.02	0.045	0.84	0.109	11
13	Mare Tranquillitatis	−2.5	+28.5	0.00	0.02	9.929	0.77	0.083	11
14	"	−0.0	+27.5	0.04	0.02	9.967	0.81	0.091	10
15	"	+2.0	+27.0	0.02	0.02	9.993	0.79	0.084	10
16	"	+2.5	+26.5	0.02	0.02	9.912	0.79	0.080	11
17	"	+5.0	+26.0	0.04	0.02	9.915	0.81	0.080	11
18	"	+5.5	+25.5	0.02	0.02	9.860	0.79	0.075	11
19	Light patch in Mare Tranquillitatis	+7.0	+25.0	0.05	0.02	9.964	0.82	0.090	11
20	Mare Tranquillitatis	+7.5	+25.0	0.00	0.02	9.860	0.77	0.070	11
21	"	+11.5	+24.5	0.01	0.02	9.896	0.78	0.078	11
22	"	+13.0	+24.0	0.03	0.02	9.861	0.80	0.070	10
23	"	+14.0	+24.0	0.02	0.02	9.886	0.79	0.076	11
24	Plinius	+15.5	+23.0	0.18	0.02	0.210	0.95	0.159	10

Region F

No.	Object	φ	λ	CF	σ_A	$\log I_{550}$	CI	ρ_{550}	n
				+	±		+		
F 1	Tycho ray near Polubius	−22º,5	+27º,0	$0^m,12$	$0^m,03$	0,040	$0^m,89$	0,193	8
2	Continent	−23,0	+26,5	0,03	0,03	—	0,80	—	6
3	•	−23,5	+26,0	0,12	0,02	9,977	0,89	0,171	7
4	•	−24,0	+24,0	0,07	0,01	9,907	0,84	0,146	10
5	•	−25,0	+23,5	0,08	0,02	0,000	0,85	0,180	10
6	••	−25,0	+23,0	0,08	0,01	9,978	0,85	0,171	10
7	•	−26,0	+21,5	0,07	0,02	0,016	0,84	0,187	10
8	•	−27,5	+19,0	0,05	0,02	9,960	0,82	0,164	10
9	•	−28,0	+18,0	0.06	0,02	0,013	0,83	0,185	10
10	Near Pontanus crater	−29,0	+15,0	0,05	0,02	9,918	0,82	0,149	10
11	Continent	−30,5	+13,5	0,08	0,02	0,004	0,85	0,182	10
12	•	−31,0	+11,5	0,05	0,02	9,923	0,82	0,151	10
13	•	−32,0	+10,5	0,07	0,02	9,999	0,84	0,180	10
14	•	−33,0	+7,5	0,05	0,02	9,916	0,82	0,147	10
15	•	−34,5	+6,0	0,06	0,02	9,971	0,83	0,169	10
16	•	−35,0	+5,0	0,05	0,02	9,906	0,82	0,144	9
17	•	−35,5	+4,0	0,04	0,02	9,933	0,81	0,155	10
18	•	−37,0	+1,5	0,06	0,02	9,960	0,83	0,164	10
19	•	−37,5	0,0	0,05	0,02	9,890	0,82	0,140	10
20	•	−38,0	−1,5	0,07	0,02	0,003	0,84	0,182	10
21	Orontius crater	−40,0	−4,0	0,07	0,02	9,907	0,84	0,146	10
22	Continent	−41,5	−6,0	0,08	0,01	0,029	0,85	0,192	10
23	Ring around Tycho	−42,0	−7,0	0,07	0,02	9,994	0,84	0,178	10
24	Tycho	−43,0	−10,5	0,14	0,02	0,179	0,91	0,272	6

Region G

No.	Object	φ	λ	CE	σ_A	$\log I_{550}$	CI	ρ_{550}	n
1	2	3	4	5	6	7	8	9	10
				+	±		+		
G 1	Apennines, N-slope	+20º,0	−3º,0	$0^m,19$	$0^m,03$	0,334	$0^m,96$	0,162	10
2	Mare Imbrium SW	+21,0	−3,0	0,06	0,02	0,155	0,83	0,107	10
3	Palus Putredinis E	+21,5	−3,5	0,14	0,02	0,266	0,91	0,138	12
4	Palus Putredinis	+22,0	−3,5	0,04	0,02	0,159	0,81	0,108	12
5	Elevation south of Archimedes	+23,0	−4,0	0,14	0,03	0,281	0,91	0,143	13
6	•	+25,0	−4,0	0,07	0,02	0,128	0,84	0,101	13
7	•	+27,0	−4,5	0,14	0,02	0,300	0,91	0,149	13
8	•	+27,5	−4,5	0,05	0,02	0,191	0,82	0,116	12
9	•	+28,0	−4,5	0,01	0,02	0,116	0,78	0,098	13
10	Archimedes, floor	+30,0	−5,0	0,01	0,03	0,095	0,78	0,094	13
11	Archimedes, N-wall	+31,0	−5,0	0,11	0,03	0,194	0,88	0,117	13
12	Mare Imbrium	+32,0	−5,0	−0,01	0,02	0,021	0,76	0,079	13
13	Spitzbergen	+34,5	−5,5	0,12	0,03	0,267	0,89	0,138	13
14	Mare Imbrium	+36,5	−5,5	0,04	0,02	0,120	0,81	0,099	13
15	Mare Imbrium near Kirch	+38,5	−6,0	0,05	0,02	0,175	0,82	0,112	13
16	Mare Imbrium near Pico	+45,0	−7,0	0,07	0,03	0,144	0,84	0,104	13
17	Mare Imbrium	+48,0	−8,0	0,00	0,02	0,076	0,77	0,089	13
18	Plato, S-wall	+50,0	−9,0	0,15	0,03	0,203	0,92	0,119	13
19	Plato, floor	+52,0	−10,0	−0,01	0,02	0,000	0,76	0,075	13

1	2	3	4	5	6	7	8	9	10
20	Plato, N-wall	+53,5	—10,0	0,20	0,03	0,334	0,97	0,162	12
21	Mare Frigoris	+56,5	—11.0	0,03	0,02	0,095	0,80	0.094	13
22	"	+58,0	—12,0	0,09	0,02	0,151	0,86	0,107	12
23	"	+60,0	..12,5	0,05	0,03	0,109	0,82	0,097	13
24	Continent	+63,0	-15,0	0,14	0,04	0,338	0,91	0,163	10

Region H

No.	Object	φ	λ	CE	σ_λ	$\log I_{550}$	CI	ρ_{560}	n
H 1	Mare Trigoris	+52°,5	—40°,0	$+0^m,06$	$+0^m,05$	0,000	$+0^m,83$	0,078	7
2	Continent	+51,5	—39,0	0,09	0,02	0,134	0 86	0,106	7
3	"	+48,0	—37,0	0,17	0,02	0,249	0,94	0,138	11
4	Bianchini	+47,5	—36,5	0,14	0,02	0,198	0,91	0,123	11
5	Continent	+47,0	—34,0	0,16	0,02	0,256	0,93	0,140	11
6	Sinus Iridum	+47,0	—32,5	0,09	0,03	0,000	0,86	0,078	10
7	"	+45,0	—30,0	0,10	0,03	0,044	0,87	0,087	8
8	Mare Imbrium	+42,0	—26,5	0,01	0,02	9,905	0,78	0,062	11
9	"	+40,0	—25,5	0,03	0,02	9,965	0,80	0,072	11
10	"	+37,5	—24,0	0,01	0,02	9,938	0,78	0,068	11
11	"	+34,5	—23,0	0,04	0,02	9,963	0,81	0,072	10
12	"	+32,5	—21,5	0,01	0,02	9,965	0,78	0,072	11
13	"	+32,0	—21,0	0,01	0,02	9,930	0,78	0,066	11
14	"	+30,0	—19,5	0,03	0,02	9,986	0,80	0,076	11
15	"	+27,5	—18,5	0,00	0,02	9,926	0,77	0,066	11
16	Copernicus ray	+26,5	—17,0	0,07	0,01	0,067	0,84	0,091	11
17	Mare Imbrium	+23,0	—15,0	0,02	0,02	9,971	0,79	0,073	11
18	"	+21,0	—14,0	0,06	0,01	0,021	0,83	0,082	11
19	"	+18,0	—13,5	0,06	0,02	0,028	0,83	0,083	11
20	"	+17,5	—13.0	0,06	0,02	0,035	0,83	0,084	11
21	Copernicus ray	+17,0	—13,0	0,05	0,02	0,112	0,83	0,100	11
22	Mare Imbrium	+16,5	—12,5	0,04	0,02	0,064	0,81	0,090	11
23	Eratosthenes, N-wall	+15,5	—12,0	0,12	0,02	0,149	0,89	0,110	11
24	Eratosthenes, floor	+15,0	-12,0	0,12	0,03	0,125	0,89	0,104	7

Region K

No.	Object	φ	λ	CE	σ_A	$\log I_{550}$	CI	ρ_{560}	n
1	2	3	4	5	6	7	8	9	10
K 1	Mare Humorum	—21°,5	—42°,0	$+0^m,03$	$±0^m,02$	9,927	$+0^m,80$	0,060	12
2	Gassendi, SW-wall	—18,0	—38,5	0,16	0,02	0,222	0,94	0,094	11
3	Gulf between Mare Humorum and Oceanus Procellarum	—16,5	—37,0	0,05	0,02	9,968	0,82	0,066	12
4	Light patch	—15,0	—35,5	0,14	0,02	0,208	0,91	0,115	12
5	Oceanus Procellarum	—14,0	—34,5	0,05	0,02	9,948	0,82	0,063	12
6	Crater Herigonius	—13,0	—34,0	0,09	0,01	0,083	0,86	0,086	12
7	Oceanus Procellarum	—12,0	—33,0	0,03	0,01	0,000	0,80	0,071	12
8	Riphaen Mountains	—8,0	—31,0	0,14	0,01	0,166	0,91	0,104	12
9	"	—7,5	—30,5	0,08	0,01	0,122	0,85	0,094	12

1	2	3	4	5	6	7	8	9	10
10	Riphaen Mountains	− 6,5	−29,0	0,18	0,02	0,262	0,95	0,130	12
11	"	− 6,0	−29,0	0,05?	0,01	0,093	0,82	0,088	11
12	"	− 5,5	−28,5	0,16	0,02	0,186	0,93	0,109	10
13	Oceanus Procellarum	− 4,5	−28,0	0,06	0,01	0,000	0,83	0,071	12
14	"	− 3,0	−27,0	0,12	0,02	0,136	0,89	0,097	12
15	"	− 2,0	−26,5	0,05	0,01	0 056	0,82	0,081	12
16	"	− 1,5	−26,0	0,10	0,02	0,132	0,87	0,096	12
17	"	− 0,5	−25,5	0,09	0,01	0,082	0,86	0,086	12
18	"	+ 0,5	−25,0	0,12	0,02	0,150	0,89	0,100	12
19	Radiant aureole of Copernicus	+ 1,0	−25,0	0,10	0,01	0,112	0,87	0,092	11
20	"	+ 2,0	−24,5	0,05	0,01	0,098	0,82	0,089	12
21	Crater Reinhold	+ 3,5	−23,5	0,12	0,02	0,228	0,89	0,120	11
22	Radiant aureole of Copernicus	+ 5,5	−22,5	0,08	0,01	0,158	0,85	0,102	11
23	Near Copernicus	+ 7,0	−22,0	0,08	0,01	0,122	0,85	0,094	11
24	Copernicus, floor	+ 9,0	−21,0	0,17	0,02	0,280	0,94	0,135	10

Region L

No.	Object	φ	λ	CE	σ_A	$\log I_{550}$	CI	ρ_{550}	n
1	2	3	4	5	6	7	8	9	10
L 1	Continent	−27º,0	−50º,0	$0^m,20$	$0^m,03$	0,410	$0^m,97$	0,159	10
2	Mare Humorum	−26 0	−48,5	0,04	0,02	0,048	0,81	0,070	12
3	Mare Humorum, light patch	−26,0	−45,5	0,10	0,03	0,187	0,87	0,095	12
4	Mare Humorum	−25,5	−44,0	0,02	0,02	0,046	0,89	0,069	12
5	"	−25,0	−40,0	0,05	0,02	0,086	0,82	0,076	12
6	"	−24,0	−36,0	0,03	0,02	0,072	0,80	0,073	12
7	"	−23,0	−35,0	0,00	0,02	0,000	0,77	0,062	12
8	Peninsula between Mare Humorum and Mare Nubium	−23,0	−33,5	0,10	0,03	0,228	0,87	0,105	11
9	"	−23,0	−30,5	0,09	0,02	0,210	0,86	0,100	12
10	"	−22,5	−29,0	0,02	0,02	0,103	0,79	0,079	12
11	"	−22,0	−28,0	0,09	0,02	0,209	0,86	0,100	12
12	Mare Nubium	−21,5	−25,5	0,04	0,02	0,141	0,81	0,086	11
13	Tycho ray in Mare Nubium	−21,5	−25,0	0,06	0,02	0,231	0,83	0,105	11
14	Mare Nubium	−21,0	−24,5	0,00	0,01	0,121	0,77	0,082	11
15	Bullialdus ·	−21,0	−22,5	0,18	0,03	0,381	0,95	0,149	12
16	Mare Nubium	−20,0	−18,5	0,02	0,02	0,107	0,79	0,079	12
17	"	−19,5	−18,5	0,07	0,02	0,167	0,84	0,091	12
18	"	−18,5	−18,0	0,06	0,02	0,179	0,83	0,093	12
19	"	−18,0	−15,0	0,03	0,02	0,099	0,80	0,078	12
20	"	−18,0	−14,0	0,05	0,02	0,126	0,82	0,083	12
21	"	−17,5	−12,5	−0,01	0,02	0,029	0,76	0,066	12
22	"	−17,5	−11,0	0,08	0,02	0,177	0,85	0,093	12
23	"	−16 5	− 7,5	0,00	0,01	0,061	0,77	0,071	12
24	Crater Alpetragius	−16.0	− 5,0	0,09	0,02	0,292	0,86	0,121	12

No.	Object	φ	λ	CE	σ_A	$\log I_{550}$	CI	ρ_550	n
O 1	Oceanus Procellarum	+28°,5	−67°,0	$0^m,10$	$0^m\,03$	0,048	$0^m,87$	0,088	6
2	•	+28,0	−66,0	0,05	0,03	9,994	0,82	0,078	6
3	Ray Seleucus	+27,5	−62,0	0,04	0,03	0,048	0,81	0,088	9
4	Near Aristarchus	+26,0	−55,0	0,14	0,02	0,076	0,91	0,094	11
5	•	+25,0	−52,5	9,08	0,03	0,052	0,85	0,089	12
6	Aristarchus	+23,5	−47,0	0,13	0,05	0,428	0,90	0,212	11
7	Near Aristarchus	+23,5	−46,0	0,04	0,02	0,076	0,81	0,094	13
8	Ray system of Aristarchus	+22,5	−45,5	0,08	0,02	0,124	0,85	0,105	13
9	Oceanus Procellarum	+21,0	−42,5	0,04	0,02	0,066	0,81	0,092	13
10	•	+21,5	−42,0	0,05	0,02	0,080	0,82	0 095	13
11	•	+20,0	−40,0	0,04	0,02	9,994	0,81	0 078	13
12	•	+18,5	36,0	0,06	0,02	0,052	0,83	0,089	13
13	•	+18,0	35,5	0,02	0,02	0,000	0,79	0,079	13
14	•	+17,0	−33,5	0,04	0,02	0,036	0,81	0,086	13
15	Ch. Mayer Crater	+15,5	−29,0	0,07	0,02	0,080	0,84	0,095	13
16	Carpathians	+14,5	−28,0	0,09	0,02	0,098	0,86	0,099	13
17	•	+14,0	−26,5	0,15	0,02	0,162	0,92	0,115	13
18	Ray system of Copernicus	+13,5	−26,0	0,07	0,03	—	0,84	—	12
19	•	+12,5	−25,0	0,13	0,03	—	0,90	—	12
20	•	+12,0	−24,0	0,12	0,03	—	0,89	—	11
21	•	+11,5	−23,0	0,09	0,02	0,124	0,86	0,105	13
22	Copernicus, NE-wall	+11,0	22,0	0,18	0,03	0,223	0,95	0,132	12
23	Copernicus, center	+10,0	−20,5	0,18	0,04	0,232	0,95	0,135	12
24	Ray system SW from Copernicus	+8,0	−18,0	0,10	0,02	—	0,87	—	8

in different spectrum regions for numerous lunar objects. In each of the regions investigated by us, we found details coinciding with those in the L.N. Radlova's catalogue. L.N.Radlova determined the brightness coefficients in green rays with an optical filter having an effective transmission wavelength of 560 mµ (ρ_{560}). We can consider that the brightness coefficients at λ = = 550 mµ will not substantially differ from those determined by L.N.Radlova. Knowing ρ_{550} for the selected details, we can easily determine the brightness coefficients of all other details of a given region. The Tables in our catalogue give the logarithms of relative brightnesses ($\log I_{550}$) and the values of ρ_{550} obtained by the indicated method. Of course, the values of ρ in the Tables can in no way claim particular accuracy since, first, the details coinciding with Radlova's catalogue cannot always be absolutely identical and second, the spectra from which we determined ρ_{550} were not obtained at the phase angle $\alpha = 12°$ as by Radlova, but at other values of α. Owing to the cloudy weather during our observations, it was impossible to photograph the moon at the smallest phase angles. Therefore, to calculate ρ_{560} we had to use spectra for which the phase angles were included within the limits of $-28° < \alpha \le +27°$. The dates of these observations are shown in Table 1.

For the regions close to the limb in the western hemisphere of the moon, we measured the spectra that were photographed only at negative values of α and, for the regions in the eastern hemisphere, those that were recorded only at positive values of α.

The color excess CE in the Tables of the catalogue are given as the mean arithmetic from the results of measuring several spectrograms, whose number n is indicated in the last column of the Tables. The great number of measurements permits determining the standard deviation of the measurement and of the results. The standard deviation σ of the measurements of the color is on the average $\pm0\overset{m}{.}06 - 0\overset{m}{.}05$. The Tables give the values of the standard deviation of the result σ_Λ which are usually rounded off to the highest absolute value. As we see from the Tables, these rarely exceed $0\overset{m}{.}03$ and for most objects are /142 equal to $\pm0\overset{m}{.}02$. Of course, these values are only a formal characteristic of the accuracy of observations with respect to random errors of measurement. This accuracy is not below the accuracy usually obtained in photographic photometry and spectrophotometry.

It should be mentioned that the compilation of a catalogue of color indices for a large number of lunar details is necessary for subsequent spectrophotometric measurements, since this permits selecting objects (already less numerous) from the number of most similar or most different (in color and brightness) objects of the catalogue or whole areas. This, in turn, permits comparisons between the color index and spectral curve and thus to define the degree of conformity of these values when applying them to the lunar surface.

Discussion of Catalogue Data

On the basis of the obtained values of the color excess or color indices of the lunar details, we can first establish the value and limits of color contrast on the lunar surface, for selected portions of the spectrum (in which the
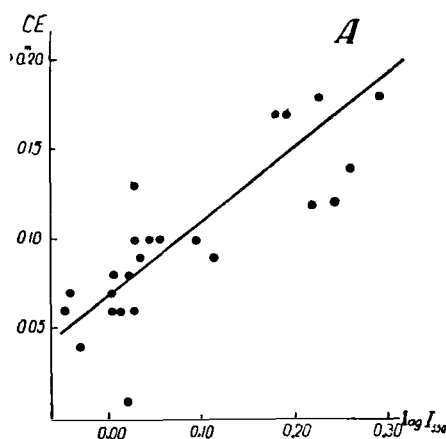

Fig.4

color indices were calculated). As indicated in the Tables of the catalogue, the color excess CE of lunar details with respect to the reference region in the Mare Vaporum are in the majority of cases positive and range from $-0\overset{m}{.}01$ to $+0\overset{m}{.}20$, i.e., the amplitude of the standard color indices amounts to $0\overset{m}{.}21$. The color indices themselves of the lunar areas vary from $+0\overset{m}{.}76$ to $+0\overset{m}{.}97$. If we

165

take the arithmetic mean of all the color indices, then the color index is
equal to +0.85. This value can be considered close to the general color index
of the moon, but is not equal to it in accuracy. Actually, most of the investi-
gated regions of the lunar surface lie in the zone of maria. At the same time
the continental regions differing in color from the sea regions should suffi-
ciently affect the general color index to cause it to increase, since most
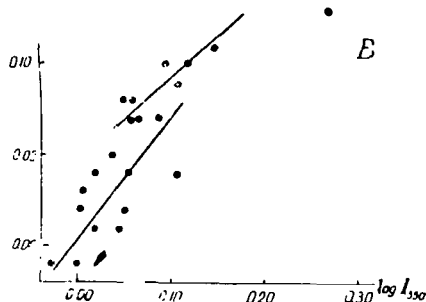continental areas have a more reddish hue than the maria.
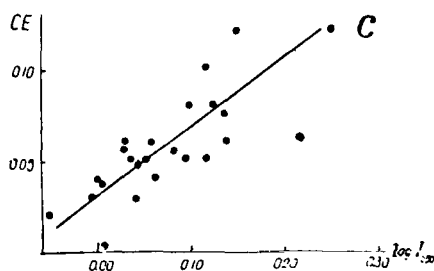

Fig.5

Fig.6

Since, in determining the color indices, we used the value of the color
index for α Aurigae which considerably differs from that used by L.N.Radlova,
the data by King would indicate that the mean color index from our measurements
is correspondingly lower than that obtained by L.N.Radlova. If we take the
color index of the sun as equal to +0.57 (Bibl.5), then the color excess of the
general color index of the moon is +0.28, which is close to the results obtained
by V.V.Sharonov who determined the color excess for the entire moon, based on
many years of observing the integrated light of the moon, and found it to be
equal to +0.33.

As is known, almost all authors who have investigated the color properties
of the lunar surface note that, in general, the lighter regions on the moon have
the most pronounced reddish hue in comparison with the dark region.

On comparing the values of CE of our catalogue with the corresponding
values log I_{550} or the values of CI with the brightness coefficients ρ_{550}, a
distinct dependence of the color on the brightness of lunar objects is observed
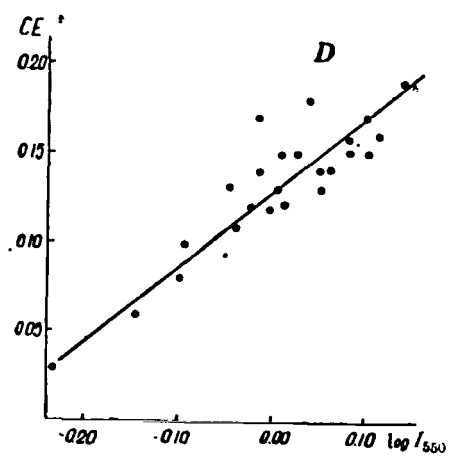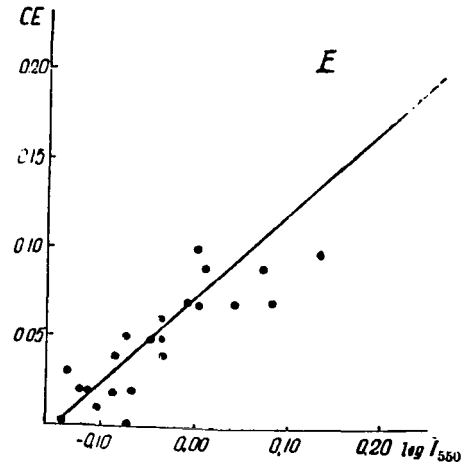for most of the investigated regions. Figures 4 - 14 show the correlations
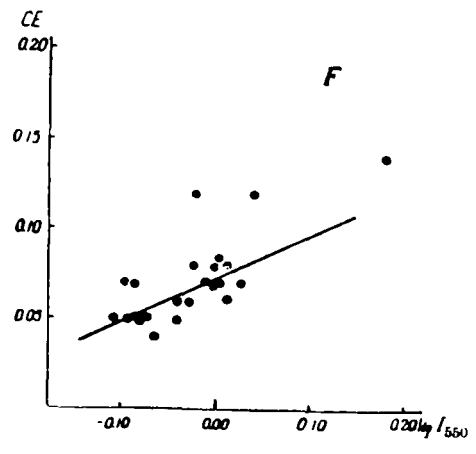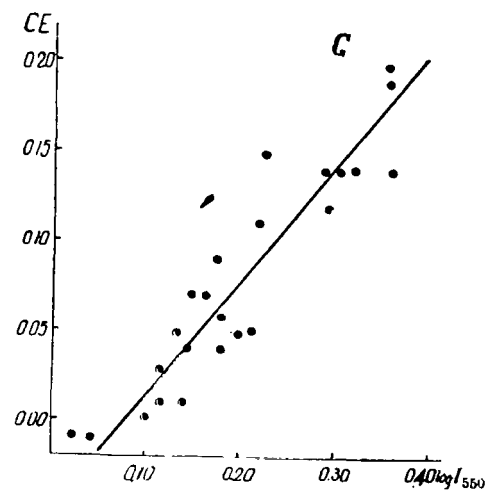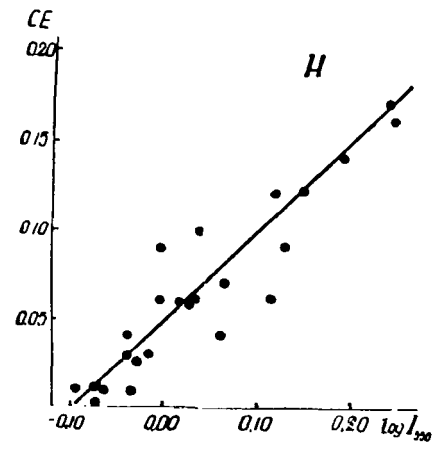
166

Fig.7

Fig.8

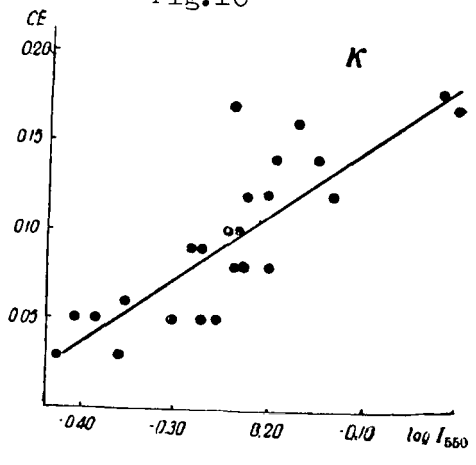

Fig.9

Fig.10

Fig.11

Fig.12

between color excess and relative brightness logarithms for all areas located in the given region. Each point on these curves corresponds to a specific area, whose color and brightness characteristics were taken from the catalogue.

All of the curves show a direct relation between color and brightness of the areas of the lunar surface. Disregarding a certain scattering of the points on the curve, it is quite obvious that most points of a given region lie approximately on a straight line. A curious feature is that the slope of this
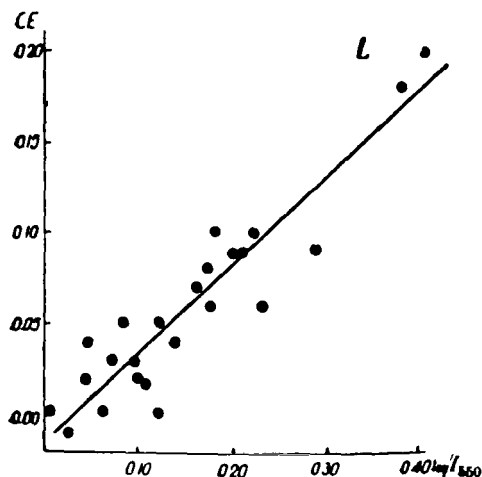
Fig.13
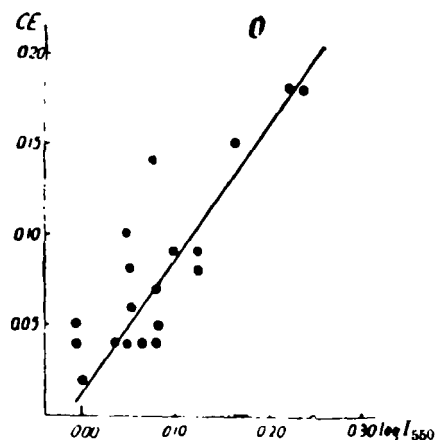
Fig.14

straight line in the graphs, corresponding to different lunar regions, is dissimilar. In order to make a quantitative estimate of the difference in the slope of the straight lines, we will introduce a conditional value for the gradient of the light versus brightness curve of a given region of the moon:

$$G = \frac{\Delta \cdot CE}{\Delta \log I_{550}} \ .$$

A graphic determination of the value of this gradient will yield the values of G in Table 2, for the investigated regions. Although a graphic determination

TABLE 2

Region	G	Region	G
A	0.42	G	0.65
B	0.67 and 0.47	H	0.48
C	0.36	K	0.37
D	0.41	L	0.47
E	0.50	O	0.72
F	0.24		

of G is somewhat arbitrary, since the scattering of the points on the graphs is sufficiently great and permits drawing a straight line at various angles, the differences in the obtained gradients appreciably exceed the possible errors in drawing the straight line.

A comparison of the gradients with a morphological affiliation of the regions yields no explicit relation, although the continental regions of C, D, and F have smaller gradients than most regions of the maria. In the region B, a certain difference of the gradient (although relatively minor) is observed for the Mare Serenitatis (0.47) and the Mare Tranquillitatis (0.67).
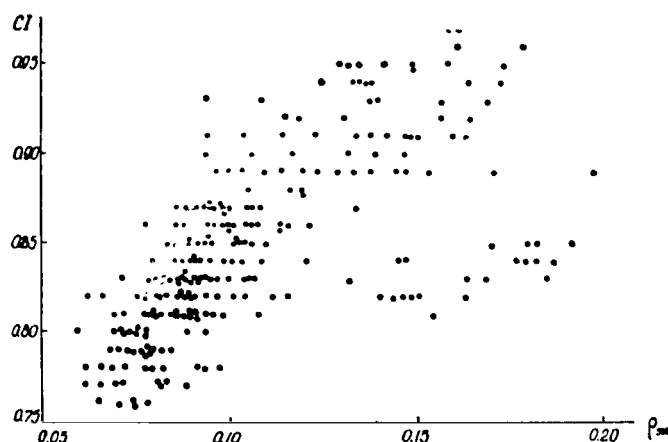
Fig.15

If all points of the catalogue are plotted in one diagram, relative to the values of CI and ρ_{550}, a distinct relation between color and reflectance (Fig.15) will be obtained. For comparison, Fig.16 shows a similar graph, plotted on the basis of the same values for the catalogue of L.N.Radlova (Bibl.8). The general slope of the light versus brightness curve on both graphs is approximately the same, although the scattering of the points for the amplitude of the light indices in L.N.Radlova's catalogue is appreciably greater. The amplitude of CI, according to the observations by L.N.Radlova, is equal to $0^m.46$ ($0^m.88 - 1^m.34$) if we disregard one abnormally red point, with CI = $+1^m.55$.

In calculating the corresponding average values of CI for a group of /146 objects characterizing a certain average brightness, L.N.Radlova obtained the following values (Table 3).

Table 3 gives the values of the logarithm $\overline{\rho'_{560}} = \dfrac{\overline{\rho_{560}}}{0.077}$ for convenient comparison with the color indices. In Fig.17, the relation of CI and log $\overline{\rho'_{560}}$ is shown graphically, analogous to Figs.4 - 14. The gradient for the straight line in Fig.17 is equal to 0.60. This value is very close to those given in Table 2.

Let us return to Fig.15. Most of the points lie within 0.060 to 0.110 for

$\bar{\rho}_{550}$ and from $0^m.77$ to $0^m.87$, for the color indices. The points corresponding to the brightest objects are located primarily in the zone with the largest values
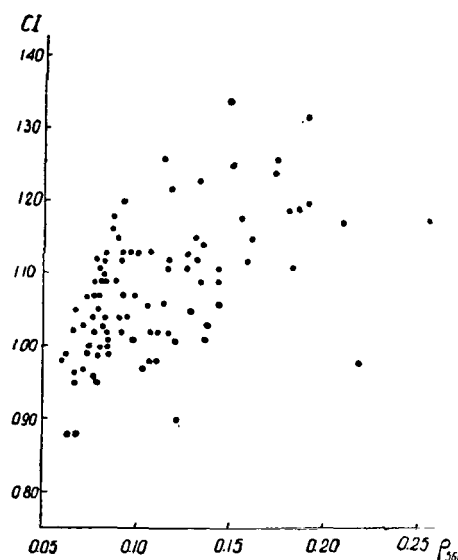
Fig.16

of CI. At the same time, different CI can correspond to the same value of ρ_{550}; objects with $\rho_{550} > 0.100$ are characterized by the greatest amplitude of the color indices.

TABLE 3

$\bar{\rho}_{550}$	$\log \bar{\rho}'_{550}$	$\overline{CI}$
		m
0,077	0,000	1,03
0,103	0,127	1,08
0,137	0,250	1,11
0,188	0,386	1,25

The existence of a correlation between color and brightness of lunar objects is of special significance for the problem as to the origin, structure, /147 and composition of the crust of the lunar surface. Therefore, it is necessary to define whether this relation is truly valid in our observations. The negligible differences in the color indices of lunar areas causes the errors of observations to have a greatly distorting effect on the real color of the lunar objects. V.V.Sharonov believed (Bibl.14) that all random observation errors in photographic photometry and spectrophotometry will cause an increase in the obtained color dispersion. As shown in the Table of the catalogue, the errors in

our observations, in most cases, are smaller than the values of the color excesses CE obtained as an average of 10 – 14 observations. However, as stated above, the values of σ characterize only random errors of measurement. In most cases, these errors are caused by the inevitable error of determining the difference of $\log I_{440} - \log I_{550}$ for the reference region on a given negative since, in analyzing the signs and magnitudes of the deviations from the mean, it is frequently found that, for all areas of the lunar region on one and the same negative, the sign of the deviation is the same and the magnitudes differ negligibly.
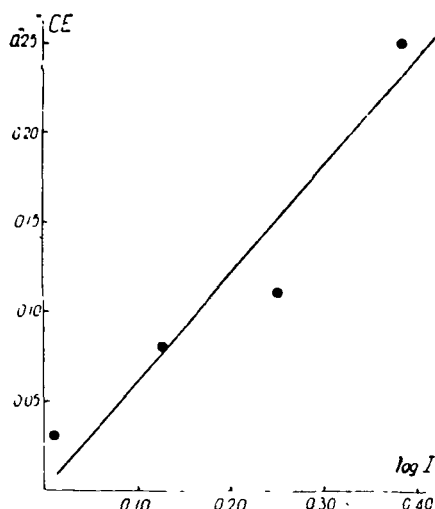

Fig.17

The presence of systematic errors will affect the results in a certain prescribed direction, unlike random errors which simply cause a scattering of the points corresponding to individual measurements. In our case, the increase in CI with brightness of the object can be caused by systematic differences of the values of gamma (γ) at wavelengths of 440 and 550 mμ. If this difference exceeds the true (always existing) variation in γ with wavelength, then an increase in the general brightness of the objects will cause their brightness in two different portions of the spectrum to increase differently, resulting in a variation of the color excess of the object with respect to the reference region.

To establish the presence and magnitude of this type of systematic error, we selected from the catalogue details with the same average color indices. One group of details was selected with $\overline{CE} = 0.^{m}06 - 0.^{m}07$, and another group with $\overline{CE} = 0.^{m}16 - 0.^{m}17$. For each individual observation of each detail, we calculated the difference $\Delta = \log I_{550} - \log I_{550}^{0}$, where I_{550} is the intensity of a given detail and I_{550}^{0} is the intensity of the reference region on the same negative. If an increase in the color excess CE is associated only with an increase in the brightness of the detail relative to the reference region, i.e., with an increase Δ (because of photographing the details at somewhat different exposures and with diaphragms on different negatives, the values of Δ are dissimilar),

171

then we should obtain for the same detail, or group of details with the same average color, the same dependence of CE on Λ as it is obtained for different details of one region differing in brightness and in color. In other words, in such an investigation we should obtain a gradient value coinciding with the gradient of the light versus brightness curve for lunar regions. Figure 18 shows the results of obtaining the dependence of CE on Λ for the above-mentioned two groups of details. Each point on the graph corresponds to an average /148 value of CE from a whole series (up to 30) of individual observations, for which the values of Λ were included in a 0.04 range. The open circles pertain to data

Fig.18
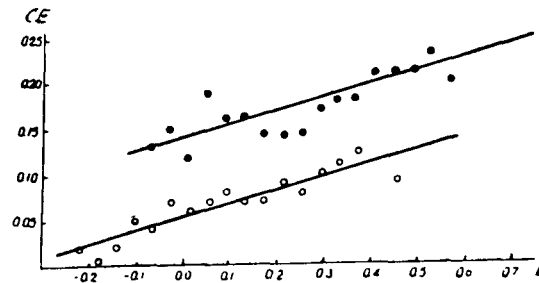
for Group 1 (CE = 0^m.06 - 0^m.07) and the solid circles, for Group 2 ($\overline{CE}$ = = 0^m.16 - 0^m.17). Obviously, the slope of the dependence of CE on Λ is not very uniform, and shows a certain increase of CE toward large values of Λ for both groups. The gradient of this increase is appreciably less than that obtained when investigating different details in one region. Here, G = 0.14. Furthermore, at the same values of Λ the points of Group 1 always lie below the points of Group 2. The difference of CE between both groups on the average is 0^m.08 (instead of the original 0^m.10). Thus, although a systematic error exists and causes the values of CE to increase with brightness, it does not wholly explain the dependence of color on brightness for lunar objects, as obtained from the observations. Only the gradients of the regions should be slightly reduced.

Control photographs of the spectra of the same lunar object, with identical exposure but different diaphragm (the size of the aperture of the sector diaphragm was changed) led to the same result.

It is difficult to formulate the explanation for the existence of such a systematic error. The inaccuracy in determining the selectivity of the echelon, as shown by a comparison of the characteristic curves plotted with and without consideration of selectivity, introduces a negligible error. The different exposures when photographing the calibration scale (2^m) and lunar objects (6^s) might possibly be the basic cause of our errors of measurement. However, as was shown in the work by E.V.Kononovich (Bibl.4), although such a difference in exposure for Agfa Spektral Rot Rapid plates cause an error in brightness determination of up to 18%, the magnitude of the error itself is completely independent of the wavelength, i.e., the slope of all the characteristics varies identically and does not affect the relative spectral brightness distribution.

172

How real is the difference in the gradients for different regions? Here, the characteristic curves may also have an effect, since these characteristics were plotted for a series of negatives of a given observation night, for a region whose spectra were recorded partially on different nights and were analyzed with respect to different characteristics. For example, the spectra of the regions L and O, which were analyzed only with respect to characteristic curves common to both regions, nevertheless yield gradients of 0.47 and 0.72 respectively, so that the difference in the gradients apparently is caused not only by errors of measurement but also by the actual difference in color properties of different regions of the moon.
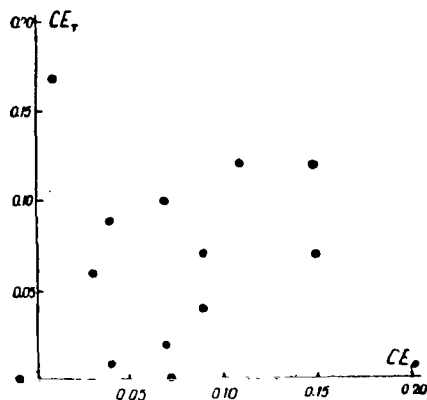
Fig.19

Thus, the correlation between the color and brightness of details of the lunar surface may be considered as real. This is substantiated by the fact that the dependence of color on brightness was detected in investigations of the moon by different methods, by which it is difficult to assume the presence of systematic errors acting in a completely identical manner. An increase in the color index with brightness of the lunar objects is also obtained in visual spectrophotometry (Bibl.15) and in photographic photometry with filters and /149 in photographic spectrophotometry.

It is known that it is almost impossible to detect any differences in color of surface details when examining the lunar surface visually through a telescope. The existence of a dependence between color and brightness of lunar objects, for which a minor increase in the color index corresponds to an increase of brightness by a factor of 2 - 3, suggests the possibility that the apparent monochromaticity of the moon can be explained by an incorrect perception of such a relation between color and brightness, due to the physiological characteristics of human vision. To define this point, a laboratory experiment is needed in which the eye will have to estimate the color of a surface, at slight reddening with an appreciable increase in brightness.

Let us now check the agreement of our data on the color of lunar objects with the results obtained by other authors.

173

For this, let us first compare the results of measuring the color of details
identical or similar, with respect to coordinates and morphological properties,
in the catalogues of two investigators, just as had been done by L.N.Radlova
(Bibl.10). Laying off the data of one catalogue on the abscissa and the data of
another catalogue on the ordinate, for the same objects, the degree of similari-
ty of the obtained results can be estimated from the presence or absence of a
correlation between them on the graph. Figure 19 shows such a comparison of the
color indices from L.N.Radlova's catalogue and our own catalogue. The number
of common details is very small, and the scattering of test points on the graph
results in an almost complete absence of coincidence of the data, although
certain features of a positive correlation can still be discerned.
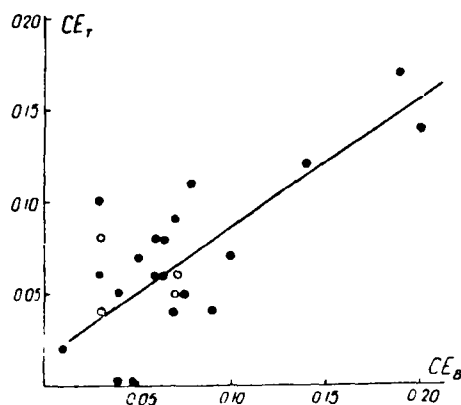
Fig.20

A similar comparison was made with the data by N.P.Barabashov and A.T.
Chekirda (Bibl.3). Since they gave no color indices, we used, for comparison,
their ratios of the brightness of lunar details for green and blue color filters
(their effective wavelengths were, respectively, 502 and 415 mu), expressed in
stellar magnitudes. Since the brightness of lunar objects increases with an in-
crease in wavelength and since the difference in effective wavelengths differs
only slightly from the wavelengths at which our measurements were carried out
(87 mu and 107 mu), we can expect that the difference between the standard and
special color indices (Bibl.3) will either be negligible or, at least, will
always have the same sign. Figure 20 shows that the correlation between the
data by the above authors (Bibl.3) and our own data is quite definite. In this
diagram, the solid circles mark the details coinciding in both catalogues /150
and the open circles, those closely adjacent and similar in morphological char-
acteristics. As we see, the scattering of the test points, on the whole, does
not exceed the errors of measurement. If we simply compare lunar areas, ap-
preciably differing in coordinates but similar in morphological characteristics
(for example, mountainous regions), we will obtain satisfactory agreement be-
tween the data by N.P.Barabashov and A.T.Chekirda and the color indices of our
own catalogue. The maximal difference of the special color indices for λ =
= 502 and 415 mu (Bibl.3) is 0$^{\text{m}}$34, whereas most of the investigated regions in
this work, with the exception of two, yield a difference of 0$^{\text{m}}$24, which almost
coincides with the difference of the color indices of our catalogue.

174

The values of the color excess (color indices) of individual lunar areas, or whole groups of details, do not show a noticeable dependence on the phase angle (α) within the limits of the angles at which the observations were made, i.e., from -56° to $+50^\circ$. Of course, since the comparison of CE with α must be carried out with respect to individual observations and not on the basis of average results, we can state that such a dependence vanishes only beyond the limits of random errors.

Conclusions

1. Small details of the lunar surface, investigated by photometric profiles of spectrograms, showed no color differences greater than those observed for sufficiently extended lunar objects.

2. The color contrasts on the lunar surface are small and, for normal color indices, yield differences not exceeding $0^m.21$, which confirms the results of our preliminary investigations (Bibl.11, 12).

3. The standard color indices of lunar objects are comprised in the intervals $+0^m.76$ to $0^m.97$ (at a color index of the reference star α Aurigae of $+0^m.22$).

4. The dependence of color on brightness of details of the lunar surface, noted by many investigators, is confirmed. All regions investigated by us reveal a direct dependence between CE and $\log I_{550}$, although the relationship of these values, expressed conditionally by a gradient G, proves to be dissimilar for different regions.

BIBLIOGRAPHY

1. Barabashov, N.P.: Comments on the Determination of the Color of Light-Reflecting Surfaces (Zamechaniye ob opredelenii tsveta otrazhayushchikh svet poverkhnostey). Tsirk. Astron. Observatorii Khar'kov. Univ., No.15, 1956.
2. Barabashov, N.P.: Investigation of the Physical Conditions on the Moon and Planets (Issledovaniye fizicheskikh usloviy na Lune i planetakh). Khar'kov, Izd. Khar'kov. Univ., 1952.
3. Barabashov, N.P. and Chekirda, A.T.: Color Contrasts of the Lunar Surface (O tsvetnykh kontrastakh lunnoy poverkhnosti). Tr. Astron. Observatorii Khar'kov. Univ., Vol.3(11), Khar'kov, Izd. Khar'kovsk. Gos. Univ., 1954.
4. Kononovich, E.V.: Effect of Different Time Exposures of Main and Calibrated Photographs on the Accuracy of Spectrophotometric Studies (Vliyaniye razlichiya vremen ekspozitsii osnovnykh i kalibrovochnykh snimkov na tochnost' spektrofotometricheskikh rabot). Soobshch. Gos. Astron. Inst., No.96, 1954.
5. Kulikovskiy, P.G.: Manual for the Amateur Astronomer (Spravochnik astronoma-lyubitelya). Moscow, Gostekhizdat, 1953.
6. Lipskiy, Yu.N.: Polarization-Spectrophotometric Method of Investigating Light Scattered by Dull Surfaces (Polyarizatsionno-spektrofotometricheskiy

metod issledovaniya sveta, rasseyannogo matovymi poverkhnostyami).
Vestnik Mosk. Univ., No.9, 1954.

7. Markov, A.V. and Barabashov, N.P.: Reflection of Light from the Lunar
   Surface (Ob otrazhenii sveta ot lunnoy poverkhnosti). Russkiy astronomi-
   cheskiy zhurnal, Vol.3, No.1, 1926.

8. Radlova, L.N.: Photographic Colorimetry of the Moon (Fotograficheskaya /151
   kolorimetriya Luny). Astron. Zh., Vol.20, No.5-6, 1943.

9. Radlova, L.N.: Visual Colorimetry of the Moon (Vizual'naya kolorimetriya
   Luny). Uch. Zap. Leningr. Gos. Univ., No.82, Issue 11, 1941.

10. Radlova, L.N.: Magnitude of Color Contrasts on the Lunar Surface (O veli-
    chine tsvetovykh kontrastov na lunnoy poverkhnosti). Astron. Zh., No.179,
    1957.

11. Teyfel', V.G.: Color Contrasts on the Lunar Surface in the Visible Spectrum
    Region (O tsvetovykh kontrastakh na lunnoy poverkhnosti v vidimoy oblasti
    spektra). Astron. Tsirk., No.179, 1957.

12. Teyfel', V.G.: Spectrophotometry of the Lunar Surface (Part I) [Spektro-
    fotometriya poverkhnosti Luny (soobshcheniye I)]. Trudy Sekt. Astrobotan.,
    Vol.VII, Alma-Ata, Izd. Akad. Nauk KazSSR, 1959.

13. Fedorets, V.A.: Photographic Photometry of the Lunar Surface (Fotografi-
    cheskaya fotometriya lunnoy poverkhnosti). Tr. Astron. Observatorii
    Khar'kov. Univ., Vol.2(10), Khar'kov, Izd. Khar'kovsk. Gos. Univ., 1952.

14. Sharonov, V.V.: On the Problem of Color Differences on the Lunar Surface
    (K voprosu o tsvetovykh razlichiyakh na lunnoy poverkhnosti). Astron.
    Tsirk., No.166, 1956.

15. Sharonov, V.V.: Colorimetric Investigation of the Moon. Part I: New
    Analysis of the Potsdam Spectrophotometry (Issledovaniya po kolorimetrii
    Luny. 1. Novaya obrabotka Potsdamskoy spektrofotometrii). Vestn. Leningr.
    Gos. Univ., Issue 1, 1956.

16. Sharonov, V.V.: Experience in Measuring Absolute Values of the Brightness
    Coefficients of the Lunar Surface (Opyt izmereniya absolyutnykh znacheniy
    koeffitsiyenta yarkosti lunnoy poverkhnosti). Uch. Zap. Leningr. Gos.
    Univ., No.31, 1939.

PART III. DIFFERENCES IN SPECTRAL PROPERTIES
OF LUNAR FORMATIONS

V.G.Teyfel'

1. The most important color characteristic of a celestial body is its re-
flectance distribution curve over the spectrum. Therefore, for a final explana-
tion of the problem concerning the magnitude of color contrast on the lunar
surface we must, in addition to determining the color indices of numerous areas
and details of the moon, plot the spectral curves of different lunar formations.
For this, in each of 15 investigated regions of the moon whose spectra were
photographed with a high slit (Bibl.7), we selected six areas in each, which
were readily identifiable on different negatives of the given region. The
spectrograms were measured along the dispersion on an MF-4 recording microphoto-
meter. Analysis of the microphotograms, with the subsequent conversion of
blackenings to intensities, ultimately yielded the difference of the logarithms
of the monochromatic intensities of the investigated area (I_λ) and of the refer-
ence region (I_λ^0):

$$\log I_\lambda' = \log I_\lambda'' - \log I_\lambda^0.$$

For a sufficiently reliable plotting of the spectral curve of the investi-
gated object it is necessary to calculate the mean from the results of measuring
several spectrograms. Because of the low accuracy of photographic photometry
and spectrophotometry, single measurements may lead to completely incorrect con-
clusions as to the spectral properties of lunar details. Here, we must take
into account that the main errors do not arise in rating the negatives but in
the photographic processing, where inefficient developing, calibrating, etc. may
introduce substantial distortions. Processing on a microphotometer, as shown
in control measurements, gives practically the same results for repeated measure-
ments of the same negative. Therefore, one cannot judge the accuracy of observa-
tions exclusively from the results of repeated photometric analyses of the same
negative, as was done for example by Yezerskiy (Bibl.3).

It is not suggested to calculate the average values for plotting the spec-
tral curves on the basis of the values of log I_λ', since these may differ from
negative to negative because of the phase effect, wrong exposure, and using
stops when photographing the brightest areas of the moon. In spectrophotometry
of planets, it is common to plot the spectral intensity distribution curve (if
the absolute study program does not call for absolute photometry of the object)
in relative units, with the intensity of all objects at a certain defined   /153
wavelength taken as unity. For the visible spectrum region it is conventional
to assume that I_λ = 1 for λ = 500 mμ.

The spectral curve is plotted on the basis of the values of log I_λ or
simply I_λ, where

177

$$I_\lambda = \frac{I'_\lambda}{I'_{500}} = \frac{I''_\lambda}{I^0_\lambda} : \frac{I''_{500}}{I^0_{500}}.$$

These relative quantities permit calculating their average values on the basis of numerous observations.

Based on the observational data from spectrophotometry of the moon, obtained at the Observatory of the Astrobotany Sector in 1957 - 1958, we processed 610 spectrograms of 90 areas of the lunar surface. The spectral curve of each area was plotted as the average of the measurements of 6 - 8 spectrograms, with respect to the reference region in the Mare Vaporum ($\varphi = +13^\circ.0$; $\lambda = +5^\circ.0$).

Figures 1 - 5 show the spectral curves of all investigated areas of the moon, plotted from the average values of $\overline{I_\lambda}$. Each division on the ordinate of these graphs corresponds to 0.2 relative intensity. For compactness, the curves are arbitrarily shifted along this axis. A horizontal axis $I_\lambda = 1$ is drawn for every third spectral curve.

The position of the investigated areas on the lunar surface, their indices, and selenographic coordinates φ and λ are given in Table 1. The selenographic coordinates are given within an accuracy of 1°, since areas longer than 60 km were measured. The index of the area consists of a letter designation of the region and the number of the area in this region. The location of the regions on the lunar disk is given elsewhere (Bibl.7), so that we need not discuss it here.
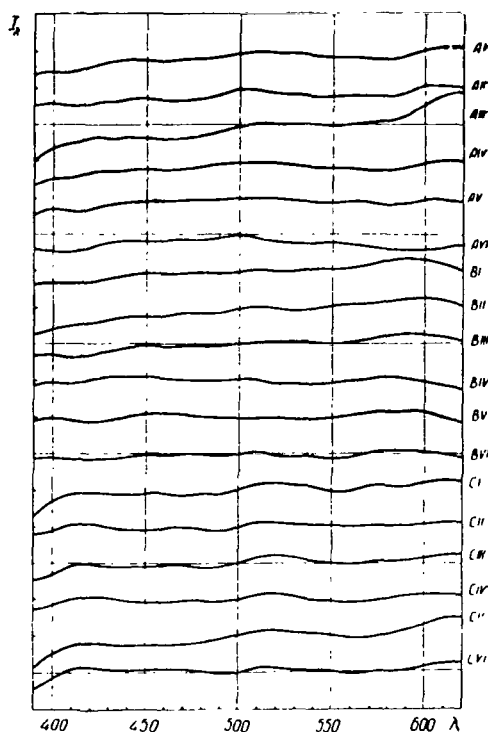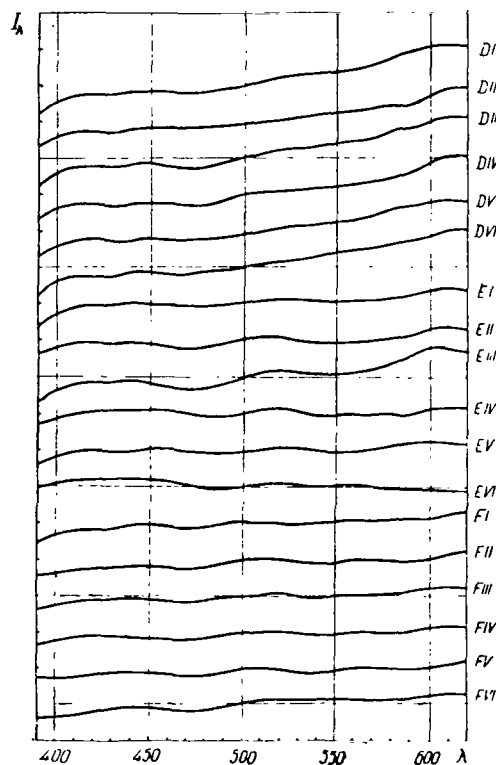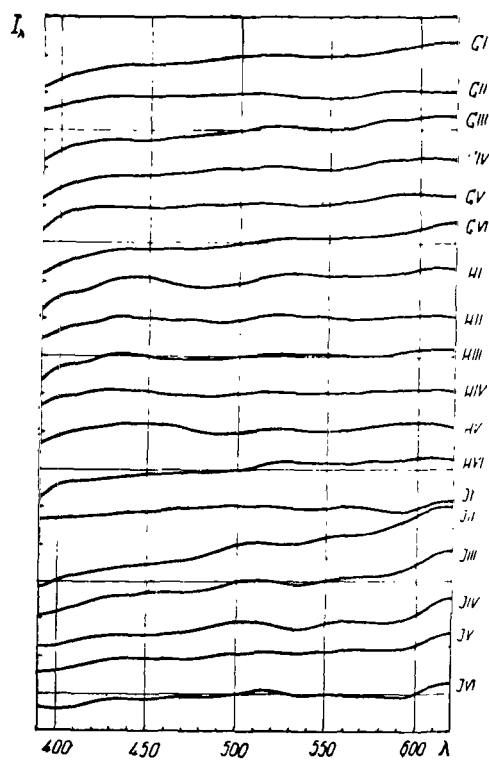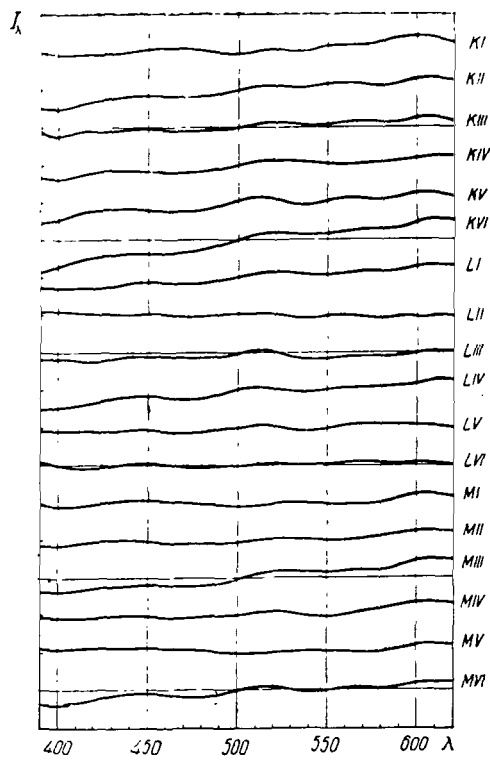

Fig.1

Fig.2

178

Fig.3

Fig.4
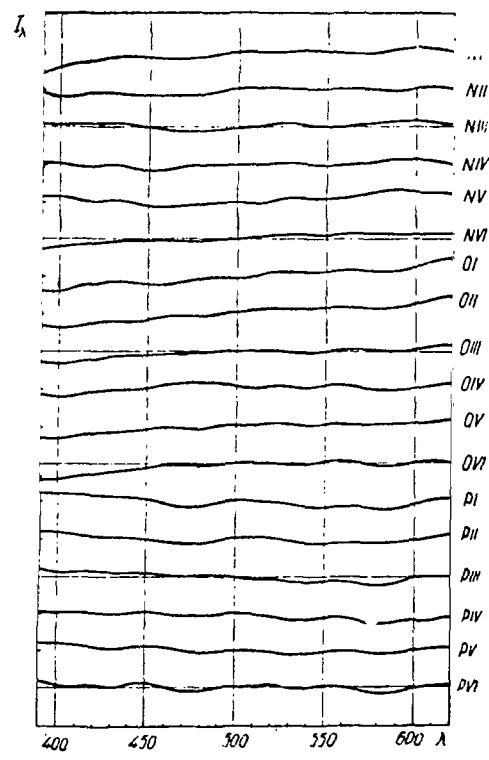
Fig.5

TABLE 1

/155

No.	Index	Name of Object	φ	λ
1	A I	Mare Crisium (north of center)	+19°	+59°
2	A II	Mare Crisium (southern part)	+ 3	+56
3	A III	Continent between Mare Crisium and Mare Foecunditatis	+ 8	+54
4	A IV	Mare Foecunditatis	+ 1	+49
5	A V	"	— 4	+48
6	A VI	"	— 6	+46
7	B I	Mare Serenitatis	+28	+14
8	B II	"	+23	+20
9	BIII	"	+20	+21
10	BIV	Mare Tranquillitatis (middle)	+ 9	+27
11	BV	Mare Tranquillitatis	+ 6	+28
12	BVI	Mare Tranquillitatis (north of Censorinus)	+ 1	+30
13	CI	Eratosthenes	+14	—13
14	CII	Sinus Aestuum	+14	— 8
15	CIII	Southern spurs of Apennines	+14	— 4
16	CIV	Mare Vaporum near Manilius	+11	+ 5
17	CV	Manilius	+14	+ 9
18	CVI	Promentorium Acherusia	+14	+15
19	DI	Continent	+41	+39
20	DII	Lacus Somniorum	+36	+38
21	DIII	Continent	+32	+39
22	DIV	"	+30	+40
23	DV	Palus Somnii	+18	+42
24	DVI	"	+14	+43
25	EI	Mare Nectaris (middle)	—17	+35
26	EII	Mare Nectaris (northern part)	—12	+33
27	EIII	Continent	— 8	+31
28	EIV	Mare Tranquillitatis (southern part)	— 2	+28
29	EV	Mare Tranquillitatis	+ 8	+25
30	EVI	Mare Tranquillitatis (northeast)	+12	+24
31	FI	Dark rim of Tycho	—42	— 8
32	FII	Light nimbus around Tycho	—38	— 2
33	FIII	Continent	—35	— 4
34	FIV	"	—33	+ 8
35	FV	Continent	—28	+18
36	FVI	Tycho ray near Mare Nectaris	—23	+27
37	GI	Mare Frigoris	+58	—12
38	GII	Plato (floor)	+52	—10
39	GIII	Mare Imbrium (northern part)	+46	— 8
40	GIV	Mare Imbrium	+37	— 6
41	GV	Dark spot north of Archimedes	+32	— 5
42	GVI	Elevation south of Archimedes	+26	— 4
43	HI	Mare Imbrium, near Erathosthenes	+16	—25
44	HII	Mare Imbrium	+22	—15
45	HIII	Copernican ray in Mare Imbrium	+26	—17
46	HIV	Mare Imbrium	+27	—18
47	HV	"	+39	—26
48	HVI	Sinus Iridum	+44	—30
49	I I	Oceanus Procellarum, between Aristarchus and Reiner	+17	—28
50	I II	Aristarchus	+23	—29
51	I III	Northern part of ray system of Aristarchus	+24	—29
52	I IV	Northwestern part of "Wood's spot"	+27	—29
53	I V	Oceanus Procellarum, north of Aristarchus	+32	—50
54	I VI	Sinus Roris	+43	—54
55	K I	Mare Humorum	—21	—42
56	KII	Gassendi, SW-wall	—18	—38
57	KIII	Oceanus Procellarum	—12	—33

TABLE 1 (cont'd) /156

No.	Index	Name of Object	φ	λ
58	KIV	Oceanus Procellarum	— 1°	—26°
59	KV	Reinhold crater	+ 4	—21
60	KVI	Copernicus	+ 6	—22
61	LI	Alpetragius	—16	— 5
62	LII	Mare Nubium	—17	— 9
63	LIII	"	—19	—18
64	LIV	Bullialdus	—21	—22
65	LV	Elevated area in Mare Nubium	—22	—28
66	LVI	Mare Humorum	—24	—37
67	MI	Sinus Caloris	+12	—10
68.	MII	Ray nimbus of Copernicus	+11	—17
69	MIII	Copernicus	+10	—22
70	MIV	Ray nimbus of Copernicus	+ 9	—25
71	MV	Oceanus Procellarum	+ 9	—32
72	MVI	Kepler	+ 8	—38
73	NI	Tycho	+43	—12
74	NII	Continent	—32	— 5
75	NIII	"	—28	— 4
76	NIV	"	—15	— 2
77	NV	Albategnius	—11	+ 4
78	NVI	Halley	— 8	+ 6
79	OI	Ray nimbus of Copernicus	+12	—23
80	OII	Carpathians (southern spurs)	+14	—26
81	OIII	Oceanus Procellarum	+16	—32
82	OIV	"	+20	—40
83	OV	Ray nimbus of Aristarchus	+23	—46
84	OVI	"	+24	—52
85	PI	Continent	— 4	+33
86	PII	"	— 6	+36
87	PIII	"	— 10	+38
88	PIV	Continent-Pyrenees	—16	+41
89	PV	Continent	— 20	+45
90	PVI	"	— 24	+48

From even a simple examination of the spectral curves we see that the differences of the spectral properties of the lunar objects are very small. In most the spectral curves are rather smooth. The small curvatures on them can be explained by random errors of the measurements. Although the shapes of the curves are different, all differences in the distribution of the intensity over the spectrum lie in very narrow intervals, sometimes not exceeding ±0.20 and for most objects ±0.10. No particular anomalies are noted in the spectra of the lunar details. Only the Sea of Rains and certain other areas of the moon, as the spectral curves show, have a noticeably lower brightness in ultraviolet rays. This drop of intensity encompasses the portion of the spectrum from 390 to 430 – 440 mu, so that it can hardly be explained just by observation errors.

3. We will not dwell on a description of the qualitative differences of the spectral curves. A verbal estimate cannot be used when comparing with other optical properties of lunar details. It is necessary to introduce quantitative, numerical characteristics of the spectral curves.

In stellar spectrophotometry, we have a completely defined and physi-cally well-substantiated characteristic of the energy distribution in the spec-trum of a radiating object, namely, the relative spectrophotometric gradient

$$G = - \frac{d \ln \frac{I_1(\lambda)}{I_0(\lambda)}}{d(1/\lambda)} = - 2.30 \frac{d \lg \frac{I_1(\lambda)}{I_0(\lambda)}}{d(1/\lambda)},$$

where $I_0(\lambda)$ is the energy distribution in the spectrum of the comparison star; $I_1(\lambda)$ is the same for the investigated star.

Reddish objects (having a temperature less than the comparison object) are characterized by a positive gradient, while bluish objects (with a higher tem-perature) are characterized by a negative gradient. Thus, the value of the gradient can serve as a quantitative expression for the color of the object.

The situation is somewhat different for reflecting surfaces. Whereas the energy distribution in the spectrum of a radiating body (we have in mind the temperature radiation) can be represented exactly or approximately by Planck's formula, for most reflecting surfaces the spectral energy distribution of the light reflected by these surfaces cannot be presented in any analytical form.

However, as shown in Figs.1 - 5, the relative spectral curves of the areas of the lunar surface are characterized by a smooth, almost monotonic intensity change with wavelength. The small curvatures, as stated above, are most probably due to inaccuracies of measurement. However, even if they are real, they have no substantial effect on the general character of the slope of the spectral curve. Therefore, we can consider that the spectral differences between areas of the lunar surface, in first approximation, are similar to the differences of energy distribution in the spectra of temperature radiations, meaning that, within a certain range of wavelengths, the slope of the spectral curve can be represented by the relative spectrophotometric gradient.

For the investigated areas of the moon, we calculated the relative spectro-photometric gradients both in the entire spectral interval of 390 - 620 mμ (G) and in the half-intervals of 390 - 500 mμ (G_1) and 510 - 620 mμ (G_2). These values are given in Table 2. Here are also shown the values of log I'_{500} which is the logarithm of the relative brightness of the object with respect to the reference region, at λ = 500 mμ. From these values, we can make a comparison of the color and brightness of the details inside a given region, just as was done elsewhere (Bibl.7). Table 2 also contains the color excess of the details, relative to the reference region (CE), and the differences of the partial grad-ients ($G_2 - G_1$).

Since the spectral curve, plotted as a function of log I (λ^{-1}), is not a straight line in the entire range of wavelengths, a reliable application of the general gradient G to some particular spectral curve is not always possible. To estimate the degree of applicability of the value of G to a given spectral curve, let us introduce the quantity a which represents the deviation of the point of intersection of the fictitious straight line whose angular coefficient deter-mines the value of G with the abscissa, for log I = 0, from the point of inter-section of the real (observed) spectral curve with the same axis. The latter,

182

TABLE 2 /158

№	Index	G	$\log I'_{500}$	CE	G_1	G_2	G_2-G_1	$a \cdot 10^{-4}$
1	2	3	4	5	6	7	8	9
1	AI	+0.114	0.147	+0.^{m}030	+0.240	−0.029	−0.269	−0.014
2	AII	+0 087	0.156	+0. 025	+0.252	−0.103	−0.355	−0.019
3	AIII	+0.268	0.340	+0. 085	+0.343	+0.195	−0.148	−0.007
4	AIV	+0.066	0.155	+0. 015	+0.206	−0.094	−0.300	−0.016
5	AV	+0.050	0.106	+0. 022	+0.155	−0.070	−0.255	−0.012
6	AVI	+0.010	0.100	0. 000	+0.192	−0.195	−0.387	−0.020
7	BI	+0.128	0.042	+0. 050	+0.154	+0.101	−0.053	−0.003
8	BII	+0.158	0.083	+0. 057	+0.262	+0.034	−0.296	−0.012
9	BIII	+0.116	0.052	+0. 032	+0.147	+0.080	−0.067	−0.004
10	BIV	−0.022	9.997	−0. 032	−0 004	−0.042	−0.038	−0.002
11	BV	+0.018	9.995	−0. 010	+0.018	+0.018	0.000	0.000
12	BVI	+0.020	0.038	+0. 010	+0.052	−0.017	−0.069	−0.005
13	CI	∓0.102	0.120	+0. 025	+0.102	+0.102	0.0:0	0.000
14	CII	+0.039	0.040	+0. 012	+0.040	+0.038	−0.002	0.000
15	CIII	+0.109	0.087	+0. 038	+0.117	+0.099	−0.018	−0.001
16	CIV	+0.053	0.042	+0. 005	+0.052	+0.053	+0.001	0.000
17	CV	+0.184	0.243	+0. 060	+0.240	+0.119	0.121	−0.006
18	CVI	+0.047	0.072	−0. 008	+0.008	+0.091	+0.083	+0.004
19	DI	+0.338	9.942	+0. 128	+0.176	+0.521	+0.345	+0.018
20	DII	+0 263	9.892	+0. 110	+0.171	+0.366	+0.195	+0.010
21	DIII	+0.346	9.999	+0. 127	+0.195	+0.518	+0.323	+0.017
22	DIV	+0.304	0.050	+0. 115	+0.235	+0.379	+0.144	+0.008
23	DV	+0.308	9.947	+0. 113	+0.196	+0.434	+0.238	+0.012
24	DVI	+0.306	9.935	+0. 123	+0.183	+0.445	+0.262	+0.014
25	EI	+0.096	0.115	+0. 005	+0.087	+0.131	+0.044	+0.001
26	EII	+0.100	0.137	+0. 015	+0.120	+0.078	−0.042	−0.002
27	EIII	+0. 36	0.216	+0. 048	+0.172	+0.300	+0.128	+0.005
28	EIV	+0.029	0.075	−0. 025	+0.0 5	+0.045	+0 030	+0.001
29	EV	+0.065	0.047	0. 000	+0.047	+0.086	+0.039	+0.002
30	EVI	−0.035	9.997	−0. 030	−0.056	0.011	+0.045	+0.002
31	FI	+0.105	0.070	+0. 032	+0.121	+0.086	−0.035	−0.002
32	FII	+0.112	0.133	+0. 04	+0.169	+0.046	−0.123	−0.006
33	FIII	+0.124	0.053	+0. 027	+0.083	+0.169	+0.086	+0 004
34	FIV	+0.094	0.047	+0. 038	+0.120	+0.063	−0.057	−0.003
35	FV	+0.079	9.968	+0. 022	+0.111	+0.042	0.069	−0.003
36	FVI	+0.129	0.010	+0. 013	+0.118	+0.141	+0.023	+0.001
37	GI	+0.194	0.112	+0. 06	+0.222	+0.160	−0.062	−0.003
38	GII	+0.053	0.030	+0. 002	+0.096	+0.005	−0.091	0.005
39	GIII	+0.212	0.063	+0. 078	+0.202	+0.222	+0.020	+0.001
40	GIV	+0.161	0.108	+0. 046	+0.191	+0.126	−0.065	−0.003
41	GV	+0.105	0.055	+0. 081	+0 081	+0.124	+0.043	+0 002
42	GVI	+0.216	0.180	+0. 070	+0.209	+0 223	+0.014	+0.001
43	HI	+0.163	0.130	+0. 018	+0.106	+0.229	+0 123	+0.006
44	HII	+0.069	0.032	+0. 002	+0.061	+0.079	+0.018	+0.001
45	HIII	+0.113	0.068	+0. 018	+0.088	+0.141	+0.0 3	+0.003
46	HIV	+0.045	9.995	−0. 015	+0.005	+0.095	+0.090	+0 004
47	HV	+0.042	9.960	−0. 022	−0.031	+0.126	+0.157	+0.008
48	HVI	+0.168	0.040	+0. 060	+0.152	+0.185	+0.033	+0.002
49	I I	+0.057	0.116	+0. 038	+0.086	+0.024	−0.062	−0.003
50	I II	+0.410	0.594	+0. 160	+0.494	+0.312	−0.182	−0.010
51	I III	+0.242	0.358	+0. 088	+0.316	+0.156	−0.160	−0.008
52	I IV	+0.177	0.224	+0. 078	+0.308	+0.0 6	−0.282	−0.015
53	I V	+0.129	0.146	+0. 032	+0.115	+0.144	+0.029	+0.001
54	I VI	+0.073	0.132	+0. 027	+0.110	+0.032	0.078	−0.004
55	KI	+0.081	0.080	+0. 025	−0.005	+0.179	+0.184	+0.020
56	KII	+0.180	0.266	+0. 082	+0.184	+0.176	−0 008	0.000
57	KIII	+0.086	0.125	+0. 027	+0.052	+0.123	+0.071	+0.004
58	KIV	+0.137	0 197	+0. 052	+0.145	+0.128	−0.017	−0.001
59	KV	+0.146	0.274	+0. 057	+0.175	+0.114	−0.061	−0.003
60	KVI	+0.280	0.432	+0. 123	+0.340	+0.210	−0.130	−0.007
61	LI	+0.156	0.178	+0. 060	+0.161	+0.150	−0.011	−0.001
62	LII	−0.013	0.015	0. 000	−0.020	−0.004	+0.016	+0.001

183

TABLE 2 (cont'd)   /159

1	2	3	4	5	6	7	8	9
63	LIII	+0,037	0,063	+0,^{m}002	+0,089	—0,021	—0,110	—0,006
64	LIV	+0,153	0,195	+0, 045	+0,199	+0,100	—0,099	—0,005
65	LV	+0,042	0,060	+0, 038	+0,038	+0,046	+0,008	0,000
66	LVI	+0,012	9,952	—0, 005	0,000	+0,026	+0,026	+0,001
67	MI	+0,033	0,035	—0, 015	—0,024	+0,097	+0,121	+0,006
68	MII	+0,070	0,110	+0, 005	+0,032	+0,112	+0,080	+0,004
69	MIII	+0,200	0,275	+0, 078	+0,157	+0,248	+0,091	+0,005
70	MIV	+0,068	0,125	+0, 007	+0,035	+0,120	+0,085	+0,005
71	MV	+0,006	9,985	—0, 018	—0,077	—0,090	+0,167	+0,008
72	MVI	+0,122	0,125	+0, 028	+0,133	—0,106	—0,027	—0,001
73	NI	+0,102	0,133	+0, 032	+0,153	—0,044	—0,109	—0,006
74	NII	+0,061	0,097	+0, 042	+0,071	—0,049	—0,022	—0,001
75	NIII	+0,045	9,925	+0, 002	+0,011	—0,083	—0,072	+0,004
76	NIV	+0,030	9,913	+0, 017	+0,025	—0,036	—0,011	+0,001
77	NV	+0,085	9,888	+0, 032	+0,013	+0,166	—0,153	+0,008
78	NVI	+0,091	0,005	+0, 035	—0,070	—0,115	—0,045	+0,002
79	OI	+0,164	0,140	+0, 068	+0,104	—0,232	—0,128	—0,007
80	OII	+0,175	0,150	+0, 084	+0,127	—0,229	—0,102	—0,005
81	OIII	+0,077	9,985	+0, 035	+0,0·3	—0,070	—0,013	—0,001
82	OIV	+0,024	9,960	+0, 022	0,000	—0,054	—0,054	+0,003
83	OV	+0,089	9,990	+0, 012	+0,092	+0,085	—0,007	0,000
84	OVI	+0,104	9,945	+0, 060	+0,130	—0,073	0,057	—0,003
85	PI	—0,061	0,097	0, 040	—0,048	—0,076	—0,028	0,001
86	PII	0,005	0,014	—0, 010	—0,025	—0,019	—0,034	—0,002
87	PIII	—0,045	9,936	—0, 027	—0,073	—0,013	—0,060	—0,003
88	PIV	—0,034	9,961	—0, 012	—0,013	—0,057	0,044	—0,002
89	PV	0,043	9,880	—0, 027	—0,050	—0,037	—0,013	—0,001
90	PVI	—0,004	0,005	—0, 010	—0,021	+0,017	+0,038	+0,002

based on the conditions of calculating the relative intensities, corresponds to
λ_0 = 500 mu. Thus,

$$a = \lambda_o^{-1} - \lambda_f^{-1}. \qquad\qquad a = \lambda_{\text{н}}^{-1} - \lambda_{\text{ф}}^{-1}.$$

The values of $a \cdot 10^{-4}$ cm^{-1} are given in the last column of Table 2. On comparing the values of "a" with the differences of $G_2 - G_1$ we see that, at equality or very slight difference of G_1 and G_2, the values of $a \cdot 10^{-4}$ are equal to zero or very small. For $|a \cdot 10^{-4}| \leq 0.003$ the partial gradients differ from the total by no more than ±0.03, i.e., the total and partial gradients practically coincide.

On the basis of the data of Table 2 we can already draw quantitative conclusions as to the magnitude of the spectral and color differences on the lunar surface.

The relative spectrophotometric gradients of lunar objects lie within the limits: G from −0.06 to +0.41; G_1 from −0.8 to +0.49; G_2 from −0.20 to +0.52.

If we express the maximum limits of the variations in the spectrophotometric gradients in a scale of spectral classes, based on suitable Tables [for example, those by Aller (Bibl.1)], it will be found that the greatest differences of the spectral properties of lunar details are no more than 0.6 of the

spectral class dG.

The color excess CE, calculated from the spectral curves, lies within the limits from $-0^m.04$ to $+0^m.16$. Thus, the variations in the color indices on the lunar surface, according to the spectrophotometric observations, are $0^m.20$. This value actually coincides with that obtained by photometric cross sections of our earlier spectrograms (Bibl.7). However, the color excess is systematically reduced by about $0^m.04$ in comparison with the previous data (Bibl.7), apparently due to the method of determining the color excess. In our other report, the

intensity ratio $\dfrac{I_{440}}{I_{550}}$, for the investigated object, was determined from the

photometric profile of the spectrogram and, for the reference region, from a microphotogram of its spectrum along the dispersion. In spectrophotometering lunar details, the intensity ratios both in the investigated and in the reference regions were determined from microphotograms. The small systematic difference of CE obtained in either case is not of fundamental importance.

4. Let us now examine how the spectrophotometric gradients are distributed over the main morphological groups of lunar objects. Table 3 contains the average values of the gradients calculated for n details of a given group, and the limits of changes of the gradients.

TABLE 3

Morphological Group	G	G_1	G_2	n
Maria	$+0.09$ $-0.02 - +0.22$	$+0.10$ $-0.08 - +0.31$	$+0.08$ $-0.20 - +0.23$	42
Continents and mountainous regions	$+0.10$ $-0.06 - +0.35$	$+0.08$ $-0.07 - +0.34$	$+0.13$ $-0.06 - +0.52$	22
Craters (light)	$+0.17$ $+0.08 - +0.41$	$+0.18$ $+0.01 - +0.49$	$+0.15$ $+0.04 - +0.31$	13
Rays and haloes of craters	$+0.10$ $+0.07 - +0.16$	$+0.10$ $+0.03 - +0.17$	$+0.12$ $+0.05 - +0.23$	8

As we see from the data of Table 3, the maria of the moon are characterized by the smallest average value of the gradient and the light lunar craters by the highest. The continents differ from the seas by a substantially greater gradient in the yellow spectrum region at an almost coinciding gradient in the blue region. At the same time, $G_1 > G_2$ for seas; $G_1 < G_2$ for continents; and $G_1 > G_2$ for craters. The ray systems and haloes of the craters differ less from the continents. For them, $G_1 < G_2$, and the limits of G_1 and G_2 are appreciably narrower than for craters and continents. The data in Table 3 are in good agreement with our earlier Table (Bibl.8), listing the average values and limits of the change in color indices for different morphological groups of lunar objects.

5. It is of interest to define the degree of conformity of the spectral and color (colorimetric) characteristics of lunar objects. Spectrophotometry of numerous lunar surface details is very laborious; at the rather negligible

differences in the spectral properties of these details, it hardly justifies the time spent for processing several spectrograms of each detail. On the other hand, it is necessary to continue investigations of the color properties of small lunar areas, so as to obtain conclusive data on the distribution of color hues over the entire visible lunar surface. This raises the moot question of the possibility and admissibility of substituting detailed spectral characteristics by colorimetric characteristic, namely, the normal or special color index.

Figure 6 shows the dependence of the total gradient G on the color excess CE. This dependence is rectilinear; there is a one-to-one correspondence between G and CE. With rare exceptions, the deviations of individual points from a straight line on the graph do not exceed $\pm 0\overset{m}{.}02$ and $\pm 0\overset{m}{.}03$, i.e., they are within the errors of determining CE and G. Taking into account that, for all objects (as shown in Table 2)

$$G \approx \frac{G_1 + G_2}{2},$$

and that the spectral curves of the lunar details show no intensity fluctuations greater than those due to possible errors of measurement, then the admissibility of substituting the colorimetric characteristics for spectral characteristics seems justified.
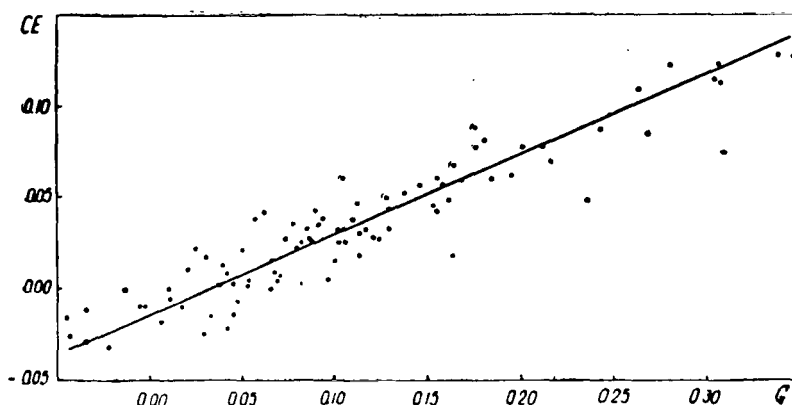

Fig.6

N.P.Barabashov (Bibl.2) showed that, in the case of reflecting objects on the earth, the one-to-one correspondence of the spectral curve with the color index is not always observed. One and the same value of the color index may correspond to substantially different curves. This phenomenon does not occur for the lunar surface, which greatly simplifies the problem of colorimetric investigation of numerous lunar objects. Of course, individual small nuances of the spectral curves when using the color indices will not be revealed and thus not be allowed for; however, at the existing accuracy of photographic spectrophotometry it is doubtful that such fine differences exist at all. They also could not be taken into account in statistical investigations.

6. Let us briefly discuss the difference in the relative spectrophotometric

gradients, calculated in half-ranges of the investigated spectrum region. Generally speaking, the difference in the gradients G_1 and G_2, for one and the same spectral curve, is not surprising since even in a case of radiating objects the gradients in adjacent ranges of the order of 1000 Å need not coincide. A similar phenomenon is also completely possible for a reflecting surface. If the spectral properties of reflecting lunar objects were to differ appreciably in spectrum energy distribution from the properties of radiating objects of a corresponding temperature, we could expect that the values of G_1 and G_2 would be identical only in rare cases. In other words, the probability of $G_2 \approx G_1$ could not appreciably exceed the probability of other ratios of G_1 to G_2 since, for equality of G_1 and G_2, a very specific intensity distribution in the spectrum would be required. However, as shown in Fig.7a, which depicts the distribution of objects with respect to values of a (see above), the probability of coincidence of partial gradients by far exceeds the probability of other combinations of G_1 and G_2, and the distribution curve differs very little from the normal /162
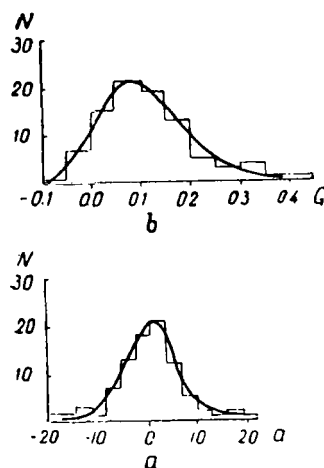
Fig.7

Gaussian law of distribution. The latter, however, is still unable to indicate a random character of the deviations of the values of a from zero, since the values of G are also characterized by approximately the same distribution curve (Fig.7b). If a definite relationship were to exist between G and a, then the distribution of the objects with respect to the quantity G would be reflected in the distribution with respect to the values of a. As is apparent from Fig.8, no correlation between a and G is observed. The objects are concentrated in the region $|a| \leq 3$ regardless of the corresponding values of G. The deviations of a to either side have an explicitly random character with respect to G. In the region $|a| \leq 3$, about 50% of the object are located, i.e., for half the investigated lunar details the partial gradients practically coincide with the total gradient and with each other.

It is difficult to define at present whether the random deviations of a toward greater absolute values are due to real characteristics of the lunar surface or to some observation errors. However, the fact that most of the investigated objects — regardless of their color (values of G or CE) — reveal only

a small difference of the partial gradients, speaks in favor of the opinion that colorimetric measurements can be used for obtaining the color characteristics of areas and details of the moon.

7. Spectrophotometry of lunar details confirms the existence of a correlation between color and reflectivity of lunar areas. A comparison of the quantity G with the quantity log I'_{500} (logarithm of the relative intensity of the lunar detail) shows that the total gradient of the spectral curves increases with an increase in brightness of the objects.
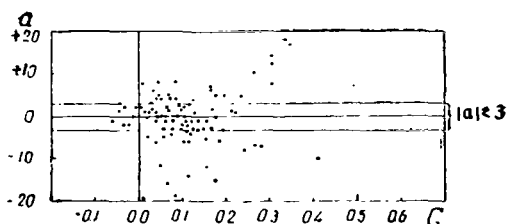

Fig.8

8. As is known, Yu.N.Lipskiy in several reports (Bibl.4, 5, 6) showed that the polarization of light in a given instrument may have a noticeable effect on the results of spectrophotometric investigations. In order to define the degree of polarization in our instrumentation (AZT-7 telescope with ASP-9 spectrograph) we carried out the following small investigation. According to Yu.N. Lipskiy, the characteristic of the polarization properties of a spectrograph

is the quantity $\beta_\lambda = \dfrac{I_{\lambda \parallel}}{I_{\lambda \perp}}$, which represents the ratio of the intensities of

the linearly polarized light which passed through the spectrograph when the polarization plane was oriented parallel ($I_{\lambda \parallel}$) and perpendicular ($I_{\lambda \perp}$) to the slit of the spectrograph. The quantity β_λ may appreciably change along the spectrum. The degree of change of this quantity with wavelength characterizes the distortions introduced by the spectrograph into the spectral curves of /163 the investigated objects.

In the simplest case, we can obtain the spectral–polarization characteristic of the instrument by using a natural light source and a polaroid placed in front of the slit. As a natural light source, we used the star α Lyrae whose spectra were photographed when the star was almost at zenith in order to avoid the effect of image vibration. Since the position of the polarization plane of the polaroid was not known, the spectra of the star were photographed at angles of rotation of the polaroid ω, read from an arbitrary zero-point every $30°$. Having taken the intensity ratio measured on the negative for the mutually perpendicular positions of the polaroid, we obtained a series of values β'_λ: $\beta'_\lambda =$

$= \dfrac{I_{\lambda \omega}}{I_{\lambda \omega + 90}}$, one of which will most closely correspond to the required values

of β_λ. The difference in orientation of the polarization plane of the polaroid from the position parallel and perpendicular to the slit cannot exceed $15°$ in

188

this case. Table 4 shows the monochromatic values of β'_λ for four combinations of mutually perpendicular positions of the polaroid, whose angles ω are designated as indexes of I. The last column of the Table gives the value of the intensity ratios of spectra, photographed at identical positions of the polaroid.

TABLE 4

λ	$I_{90}:I_0$	$I_{120}:I_{30}$	$I_{150}:I_{60}$	$I_{180}:I_{90}$	$I_0':I_0''$
390$m\mu$	0.93	0.97	1.00	1.10	1.05
400	0.93	0.98	0.99	1.08	1.04
410	0.93	0.98	0.99	1.07	0.99
420	0.95	0.99	0.98	1.07	1.00
430	0.94	0.99	0.99	1.06	0.98
440	0.95	0.95	1.00	1.07	0.99
450	0.94	1.00	0.99	1.05	1.00
460	0.97	1.03	1.01	1.01	0.98
470	0.98	1.08	0.99	1.04	1.00
480	0.95	1.08	1.00	1.06	1.04
490	0.97	1.02	1.02	1.04	0.97
500	1.00	1.00	1.00	1.00	1.00
510	1.00	0.99	1.00	0.99	1.01
520	0.97	1.01	1.00	1.00	1.00
530	0.98	1.01	0.97	1.00	1.01
540	0.97	1.02	1.00	1.00	0.99
550	0.97	1.02	1.00	1.00	0.98
560	0.94	1.01	0.98	1.02	0.95
570	0.95	1.01	0.97	1.01	0.98
580	0.95	0.99	0.98	1.01	0.98
590	0.98	1.00	0.98	1.00	0.99
600	0.99	1.01	1.00	1.00	0.99
610	0.94	1.01	0.99	1.04	0.94
620	0.94	1.02	0.98	0.99	0.91

The intensity ratios at λ = 500 mu in all columns are taken as equal to 1.00. As shown in the Table, the value of β'_λ undergoes only minor variations with the wavelength, usually not exceeding 10% and more likely associated with errors of measurement than with the effect of polarization/ of the spectrograph.

Actually, the values of $\dfrac{I_0'}{I_0''}$ from the last column suffered the same changes as the values of β'_λ in other columns. Since the polarization in the optical system of the telescope causes the light of the star, even before passing through the polaroid, to become partially polarized, the obtained data indicate that our instrument had only a negligible effect on the obtained relative intensity distribution in the spectra of objects with low polarization, which includes the moon if it is photographed not close to the quadratures.

9. Thus, the principal conclusion of our spectrophotometric and spectro-colorimetric investigations of the lunar surface is that the color contrasts of the outermost crust of the moon are very small, although they can be detected by a large number of measurements of the color of each individual object. The spectral differences of lunar objects are not more noticeable than the colorimetric differences and are expressed only by minor changes in the slope of the spectral curves.

BIBLIOGRAPHY

1. Aller, L.Kh.: Astrophysics (Astrofizika). Moscow, Vol.I, Izd. Inostr. Lit., 1955.
2. Barabashov, N.P.: Comments on the Determination of the Color of Light-Reflecting Surfaces (Zamechaniye ob opredelenii tsveta otrazhayushchikh svet poverkhnostey). Tsirk. Astron. Observatorii Khar'kov. Univ., No.15, 1956.
3. Yezerskiy, V.I. and Fedorets, V.A.: On the Problem of Color Contrasts of the Lunar Surface (K voprosu o tsvetovykh kontrastakh lunnoy poverkhnosti). Tsirk. Astron. Observatorii Khar'kov. Univ., No.15, 1956.
4. Lipskiy, Yu.N.: Polarization-Spectrophotometric Method of Investigating Light Scattered by Dull Surfaces (Polyarizatsionno-spektrofotometricheskiy metod issledovaniya sveta, rasseyannogo matovymi poverkhnostyami). Vestnik Mosk. Gos. Univ., No.9, 1954.
5. Lipskiy, Yu.N.: Effect of Polarization Properties of a Dispersing Medium on the Results of Spectrophotometric Investigations (Vliyaniye polyariza-tsionnykh osobennostey dispergiruyushchey sredy na rezul'taty spektrofoto-metricheskikh issledovaniy). Astron. Tsirk. No.155, 1954.
6. Lipskiy, Yu.N.: Dependence of Equivalent Widths of Coronal Lines on the Degree of Polarization of the Continuous Spectrum of the Corona (Zavisimost' ekvivalentnykh shirin koronal'nykh liniy ot stepeni polyarizatsii nepre-ryvnogo spektra korony). Astron. Zh., Vol.35, No.4, 1958.
7. Teyfel', V.G.: Spectrophotometry of the Lunar Surface. Part II: Catalog of Normal Color Indices of Lunar Surface Areas (Spektrofotometriya poverkhnosti Luny. II Katalog normal'nykh pokazateley tsveta : chastkov lunnoy pover-khnosti). Trudy Sekt. Astrobotan., Vol.8, Alma-Ata, Izd. Akad. Nauk KazSSR, 1960.
8. Teyfel', V.G.: Normal Color Indices of Lunar Surface Areas (O normal'nykh pokazatelyakh tsveta uchastkov lunnoy poverkhnosti). Astron. Tsirk., No.192, 1958.

CERTAIN CONSIDERATIONS ON THE CONDITION OF THE
LUNAR SURFACE

V.G.Teyfel'

In almost all colorimetric investigations of the moon, we note that with an increase of the brightness of the lunar details their color index increases, i.e., the lighter objects appear more reddish. Spectrophotometric investigations by the author (Bibl.5, 6) led to the same result.

One of the reports (Bibl.5) contains a calculation for the theoretical correlation between color and brightness of the details of the lunar surface, assuming the presence of a certain discrete cover superposed on the subjacent surface. Depending on the color and brightness of the cover and the subjacent surface, there is a variation in the curvature and slope of the curves of color index versus logarithm of relative intensity (brightness) of the objects. It was demonstrated there that the theoretical curves agree with the observational data.
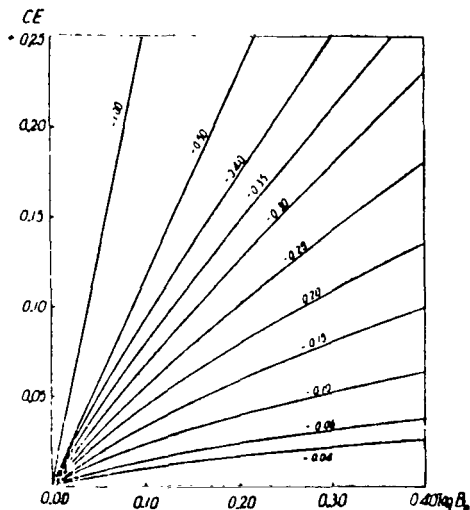

Fig.1

If we extend the curves (Bibl.5) into the region of $B_0 > 1$, i.e., if we change over to objects that are lighter and more reddish than the reference area of the lunar surface, then we can compare the theoretical curves with the results of observations cited in our other report (Bibl.6).

The theoretical curves, prolonged into the indicated region, are shown in Fig.1. Let us compare the graphs of the correlation between color and brightness of lunar objects in this report (Bibl.6) and the theoretical curves. It is quite obvious that, for all studied regions of the lunar surface, this dependence of color excess CE on log I which, in first approximation, is charac-

terized by a straight line, can be satisfactorily presented by either one of the theoretical curves in Fig.1 (i.e., by these or other values of the parameter k). Figure 1 clearly shows that the theoretical curves have the greatest curvature near zero, to which the "subjacent" surface corresponds. The absence of a noticeable curvature on the graphs (Bibl.6) apparently indicates that, at /166 such an interpretation of the observational data, all investigated objects - including the reference object - lie to one side from the zero point of the theoretical curve, i.e., not one of the investigated areas of the moon can be taken as the "subjacent" surface.

The agreement of the observations and the theoretical curves in our case can in no way be considered a confirmation of the theoretical calculations of the scheme of the outer layer of the moon in the form of a subsurface and discrete cover. Such a scheme does not correspond to modern data on the structure of the lunar surface and is taken only as the simplest scheme for calculating the relationships of color and brightness. Nevertheless, the same calculations can be used also for another, more realistic scheme. We will make an attempt to define the possible and impossible causes for the dependence of the color on the brightness of lunar surface details.

At present, the most popular hypothesis is that we do not observe the lunar rocks themselves but only their surface which has been worked and altered as a result of various external (exogenous) influences: from ultraviolet and cosmic radiation to meteorites. Most of the Soviet investigators agree that the main role in the change of properties of the lunar surface is played by meteorites whose collision with the lunar surface is accompanied by explosions that lead to the formation either of vast amounts of dust or of porous cinder whose optical and physical properties differ from the original surface. The latter theory would elegantly explain the absence of major color contrasts and the low heat conductivity of the outermost layer of the moon.

However, it is impossible to explain the existence of the interdependence of color and brightness on the lunar surface by the effect of meteorites. During the time of existence of the lunar crust [even during the last stage of formation, according to A.V.Khabakov (Bibl.7)] it was bombarded by meteorites to the same extent over all its parts. There is no doubt that the uniform meteor impacts led to a uniform distribution of the products of such impacts over the entire lunar surface and thus could not be accompanied by the formation of light and dark, variously colored, areas on the moon.

On the other hand, some observations point toward the possibility that the regular increase in color index with increase in reflectance is a characteristic of the petrographic composition of lunar rocks. Although, on earth, basic and ultrabasic magnetic rocks are characterized by a dark or greenish color whereas acidic magmatic rocks are lighter and more reddish, it is impossible to detect any noticeable correlation between color and brightness of various rock types, as was shown in comparisons made by N.N.Sytinskaya (Bibl.3). Therefore, the interrelation of color and brightness of the lunar surface areas can be explained, in all probability, as follows: Before formation of the belt of lunar seas, the entire crust of the moon consisted mainly of light reddish, possibly acidic, rocks. During the formation of the seas, the eruption of dark lava, at places of gigantic collapses of the lunar crust, flooded the remains of the crust,

fusing with them. This led to the formation of light patches and streaks on the present surface of the lunar seas. This is how V.V.Sharonov explains the origins of the ghost craters on the surface of the maria (Bibl.9). Depending on the degree of disintegration of the light substance of the crust, the result of fusion of the dark lava with the light substance was the appearance of patches with different reflectivity, different color, and different polarizing capacity which also correlates with the brightness of the objects, as demon- /167 strated in the investigations by N.N.Sytinskaya (Bibl.4) and V.P.Dzhapiashvili (Bibl.1). If the lava, just as the earth's basic rocks, had a greenish hue (in comparison with acidic rocks), then the dependence of color on brightness would be exactly as it is observed on the moon. Thus, the color-to-brightness ratio has to do with internal (endogenous) processes on the moon.

If we assume that the fusion of the light and dark substance in the seas occurred without appreciable change in the physical properties of the sub- stances, then our calculations of the theoretical ratio of color to brightness can be applied without change to such a process, considering that s is the por- tion of light substance per unit surface of a given lunar area. As indicated before (Bibl.6), the color-to-brightness ratio is most distinct in the maria, i.e., exactly where the processes of fusion of leucocratic and melanocratic rocks occurred most frequently. On the continents these processes could not take place half as often, and mainly occurred during lava eruption from craters. In the region of the remains of small seas of an early period in the continental zone, almost hidden by younger craters and mountain formations, the processes were somewhat different but also could have led to a similar relationship be- tween color and brightness.

The effect of meteorites (regardless of the type of its manifestation, formation of a dust layer or porous cinder) should lower the gradient of the color-to-brightness ratio, while simultaneously reducing the difference in color and brightness between the seas and continental regions. Thus, the ob- served dependence of color on brightness no longer pertains to the original lunar surface but is a combination of the actual dependence of color on bright- ness, due to the fusion of different lunar rocks and the superposition of pro- ducts resulting from the churning of the lunar surface by meteorites.

We will attempt to make a rough estimate on whether the observed optical properties of the lunar surface might be a consequence of reworking of earth- type rocks under the effect of exogenous factors. Since we do not know the mechanism of such reworking, we will introduce certain simplifying assumptions in the calculation.

Let us assume that the continents and mountainous regions on the moon con- sist of acidic rocks and the seas of melanocratic basic rocks.

We will stipulate that the substance obtained upon reworking by meteorites can be represented as a combination of the original rock and a certain addition- al substance. The relative quantity of the original rock per unit surface will be denoted, in this case, by f and the additional substance, by (1-f). As opti- cal characteristics of the terrestrial and lunar rocks, we will take the bright- ness coefficient o and the color excess relative to the sun D. We will consider as known the values of the brightness coefficient and of the color excess for

the lunar maria (ρ_M and D_M), for the continents (ρ_c and D_c), for the earth's acidic magmatic rocks (ρ_k and D_k), and for the basic and ultrabasic magmatic rocks (ρ_0 and D_0). Then, the values to be determined will be: the relative portion of the original rock in the reworked outer layer of the lunar surface (f), the brightness coefficient, and the color excess of the additional substance (ρ_x and D_x).

Let us now set up the following equations:

The brightness coefficient of a region of the lunar surface can be represented as

$$\rho_L = \rho_T \cdot f + \rho_x (1 - f), \tag{1}$$

where ρ_L is the brightness coefficient of the lunar surface and ρ_T is the /168 brightness coefficient of the terrestrial rocks which, according to our assumption, should yield – after reworking – the same optical effect as the observed lunar surface,

and

$$\rho_L = \rho_M \quad \text{at} \quad \rho_T = \rho_0$$

$$\rho_L = \rho_c \quad \text{at} \quad \rho_T = \rho_k.$$

To express the color excess, we will use eq.(12) from our other paper (Bibl.5). This formula, with the notations accepted here, will read

$$C_L = C_\odot \frac{\rho_{x\lambda_1}(1-f) + \rho_{T\lambda_1} f}{\rho_{x\lambda_2}(1-f) + \rho_{T\lambda_2} f}, \tag{2}$$

where C_L is the color index of the lunar surface, $C_\odot$ is the color index of the sun in nonlogarithmic form, and $\lambda_1 \lambda_2$ are the wavelengths at which the color index is calculated. We will transform the formula, dividing the numerator and denominator of the right-hand side by $\rho_{x\lambda_2}\rho_{T\lambda_2}$:

$$\frac{C_L}{C_\odot} = \frac{\dfrac{\rho_{x\lambda_1}}{\rho_{x\lambda_2}}(1-f)\dfrac{1}{\rho_{T\lambda_2}} + \dfrac{\rho_{T\lambda_1}}{\rho_{T\lambda_2}} \cdot \dfrac{1}{\rho_{x\lambda_2}} \cdot f}{\dfrac{1}{\rho_{T\lambda_2}}(1-f) + \dfrac{1}{\rho_{x\lambda_2}} \cdot f} \tag{3}$$

Further, on multiplying the numerator and denominator by $\rho_{T\lambda_2}$, we obtain

$$\frac{C_L}{C_\odot} = \frac{\dfrac{C_x}{C_\odot}(1-f) + \dfrac{C_T}{C_\odot}\dfrac{\rho_{T\lambda_2}}{\rho_{x\lambda_2}} f}{(1-f) + \dfrac{\rho_{T\lambda_2}}{\rho_{x\lambda_2}} f}. \tag{4}$$

The values of $\dfrac{C_L}{C_\odot}$, $\dfrac{C_T}{C_\odot}$, and $\dfrac{C_x}{C_\odot}$ are the color excesses of the objects relative to the sun, expressed in nonlogarithmic form. We will denote them, respectively, by D'_L, D'_T, and D'_x. Then, eq.(4) will take the form

$$D'_L = \frac{D'_x (1-f) + D'_T \frac{\rho_T}{\rho_x} f}{(1-f) + \frac{\rho_T}{\rho_x} f}$$

(5)

We will omit the indices λ_2, in view of the fact that the ratio of the brightness coefficients at this wavelength is equal to the ratio of the integral coefficients, since λ_2 is close to the effective wavelength of the visible spectrum region in which ρ is determined.

This yields equations for the brightness [eq.(1)] and the color [eq.(5)] of the lunar regions. Each of these equations can be written for the seas and continents of the moon, by substituting the corresponding values of ρ and D' into the equations. We must assume that, for both seas and continents, the introduced conditional quantities f and ρ_x are identical. In this case, we are justified to simultaneously solve the system of equations set up for the seas and continents. Such an assumption is not quite rigorous, if we take the hypothesis of meteoritic cinder on the lunar surface. However, not knowing the true processes on the lunar surface, we cannot make more definite assumptions as to the properties of the additional substances or derive even more complex /169 equations.

The paper by V.V.Sharonov (Bibl.8) gives the extreme and average values of ρ and D, for various groups of rocks. The values of ρ for lunar regions are taken from the paper by L.N.Radlova (Bibl.2). The values of D for lunar objects will be calculated on the basis of the data in our other report (Bibl.6), with consideration of the color excess common to the entire moon and determined by V.V.Sharonov, $D_{\bigcirc} = +0.^m33$.

First, we will perform calculations with the average values of the optical characteristics for each group of examined terrestrial rocks and lunar regions. These values are shown in Table 1.

TABLE 1

Group	$\bar{\rho}$	$\bar{D}$	$\bar{D}'$
Basic magmatic rocks	0.14	$-0.^m01$	1.00
Acidic magmatic rocks	0.24	$+0.^m39$	1.43
Moon – Maria	0.08	$+0.30$	1.32
Moon – Continents	0.13	$+0.35$	1.38

We will find the values of ρ_x and f from the following system of equations:

$$\begin{cases} 0.13 = 0.24 f + \rho_x (1-f) \\ 0.08 = 0.14 f + \rho_x (1-f) \end{cases}$$

(6)

195

This yields f = 0.5 and ρ_x = 0.02. To determine D'_x, it is necessary to substitute the values of D'_L, f, and $\frac{\rho_T}{\rho_x}$ into eq.(5). The solution of this equation for continents and acidic rocks leads to a value of D'_x = 0.68 or D_x = = -0.°31. For seas and basic rocks, we obtain D'_x = 3.56 or D_x = +1.°38. Obviously, the values differ greatly. Let us determine the result if, for the terrestrial rocks, we take the smallest values of ρ corresponding to the dispersion of brightness of terrestrial rocks, as calculated by V.V.Sharonov. These values are ρ_n = 0.09, ρ_k = 0.16. A system of equations analogous to that given earlier (Bibl.6) yields f = 0.7, ρ_x = 0.06. Then, at the average values of D'_0 and D'_k, we obtain D'_x = 0.94 or D_x = -0.°06 for the continents and D'_x = 2.5 or D_x = +1.°00 for the seas. The difference in D_x, as usual, remains substantial and indicates that one and the same additional substance cannot possibly be sufficient, relative to brightness and color properties, for reducing terrestrial acidic rocks to the optical properties of lunar continents or basic rocks to the optical properties of lunar seas. With respect to brightness properties, the reworking of terrestrial rocks, relative to the addition of some substance, can be reduced to a single-valued result for seas and continents; for obtaining the observed color characteristics, the reworking of terrestrial rocks, in the case of acidic rocks and continents, should tend to an increase in color excess, i.e., be equivalent to the addition of a greenish substance and, in the case of basic rocks and seas, should tend to the addition of a reddish substance.

This is difficult to correlate with any known form of exogenous influence on the lunar surface. It cannot be assumed that, on the continents, the cinder or dust formed on impact of meteorites should be appreciably greener (or bluer) than the original rocks, whereas in the seas the reverse should be true. Of /170 course, by the trial-and-error method one can find combinations of terrestrial basic and acidic rocks which would give color and brightness values close to those for the lunar surface, at identical values of ρ_x and D_x for seas and continents. However, this method is largely conditional since there is no justification to give preference to any type of combinations.

As stated previously, the calculations are quite rough and approximate, since the mechanisms of possible exogenous actions and physical processes are still unknown; nevertheless, the qualitative result will not be contradictory under other assumptions.

Apparently, the original lunar rocks which had not been subject to exogenous influences differ in their optical properties (in any case, in color) from terrestrial rocks in that a smaller diversity in color exists between the continental and sea regions. However, this does not necessarily mean a different petrographic composition of the primary lunar rocks. Their subsequent reworking under the effect of endogenous factors such as eruption, refusion, etc., could in itself lead to an averaging of the brightness-color properties. In this case, the effect of meteorites and other exogenous factors might result in a positive color excess with respect to the sun, i.e., the reddish hue characteristic for the entire moon, even for its most greenish and bluish areas.

The above statements permit the following conclusions:

1. The original lunar surface, which had not been subject to exogenous influences, later in the lunar history possessed smoothed brightness–color properties, differing from those of terrestrial magmatic rocks.

2. The rocks of an early lunar period might have been similar in optical properties to terrestrial acidic and basic magmatic rocks, but later underwent extensive reworking by endogenous processes, which is indicated in particular by the observed color–brightness dependence of the lunar objects and by its comparison with theoretical calculations.

3. The effect of meteorites and other exogenous factors led to a further reduction in the brightness–color contrast and to the formation of a reddish hue, characteristic for the entire lunar surface.

These conclusions, just as most other attempts to explain the observed optical properties of the lunar surface, only constitute working hypotheses, which will have to be checked by further observations.

BIBLIOGRAPHY

1. Dzhapiashvili, V.P.: Byul. Abastuman. Astrofiz. Observatorii, No.21, 1957.
2. Radlova, L.N.: Astron. Zh., No.20, Issue 5–6, 1943.
3. Sytinskaya, N.N.: Uch. Zap. Leningr. Gos. Univ., No.190, Issue 29, 1957.
4. Sytinskaya, N.N.: Astron. Tsirk. Akad. Nauk SSSR, No.168, 1956.
5. Teyfel', V.G.: Trudy Sekt. Astrobotan., Vol.7, Alma–Ata, Izd. Akad. Nauk KazSSR, 1959.
6. Teyfel', V.G.: Trudy Sekt. Astrobotan., Vol.8, Alma–Ata, Izd. Akad. Nauk KazSSR, 1960.
7. Khabakov, A.V.: Basic Problems of the Developmental History of the Lunar Surface (O osnovnykh voprosakh istorii razvitiya poverkhnosti Luny). Moscow, Geografgiz, 1948.
8. Sharonov, V.V.: Astron. Zh., No.31, Issue 5, 1954.
9. Sharonov, V.V.: Nauchn. Byul. Leningr. Gos. Univ., No.30, Issue 3–4, 1952.

V.G.Teyfel'

In 1955 – 1956, using the Bredikhinskiy astrograph with an objective UV prism (c = 13°), the author photographed the spectra of certain asteroids. The photographic plates used were Agfa Astro Panchromatisch, Agfa Isopan ISS, and Agfa Spektral Rot Rapid. Calibration was performed by photographing the spectra of α Lyrae through different diaphragms. Unfortunately, many negatives proved unsuitable for analysis for the following reasons:

To obtain the spectrogram of an asteroid weaker than 6.5, an exposure of at least 1.5 – 2.5 hrs is needed. During this time the plate is severely fogged by the background of the sky. To shorten the exposure, it is necessary to photograph very narrow spectra. At the small dispersion of the objective prism, such spectra cannot be measured on the microphotometer with sufficient accuracy. On certain negatives, the spectra of the asteroid were superposed on the spectra of some star or were very faint.

Therefore, it was necessary to eliminate from a detailed analysis the spectrograms of Metita, Pallada, Julia, Bamberga, and Amphitrida. The spectrograms of Vesta, for which the greatest number of negatives were obtained in 1956, and the spectrograms of the asteroid Eunomia which was sufficiently bright in 1955, were analyzed.

(4)Vesta

Twenty-four spectrograms of Vesta were obtained in April–June 1956 at exposures from 15 to 60 min. In July 1956, I.D.Kupo made several attempts to photograph the spectrum of Vesta with an objective prism producing a large dispersion (ω = 20°) on Ilford FP4 plates at an exposure of 30 – 60 min; however, at that time the brightness of Vesta dimmed, and the spectra were underexposed.

For a spectrophotometric tie-in of the extremely few stars on the negatives with the spectra of Vesta, we selected those most suitable in spectral class and closest in brightness to the investigated asteroid (Table 1).

The stellar magnitudes of the spectral class are given in conformity with the HD (Henry Draper) catalogue.

All spectrograms were measured on an MF-4 recording microphotometer. After the conventional conversion of blackening to intensities, the spectrophotometric gradients of Vesta were calculated relative to comparison stars. We found that the spectrophotometric gradient of Vesta can be reliably obtained in the spectrum region of λ = 380 – 500 mμ. At larger values of λ, it is difficult to /172 draw the line of the gradient (straight line). This is apparently due to the characteristics of the reflection of solar rays inherent to Vesta itself, since

TABLE 1

HD	BD	m_V	m_{pg}	S_p
129655	$-1°2891$	$7.^m17$	$7.^m27$	A 2
128461	$-3°3649$	7. 05	7. 61	G0
122106	$-2°3768$	6. 3	6. 72	F 5

the gradient of a star of class Go, relative to a star of class A2, for the same negatives is reliably determined in the range of $\lambda = 380 - 600$ mµ.

Table 2 shows the dates of observation, exposure (τ), value of the spectrophotometric gradient of Vesta relative to a star A2 (g_{VA}) and relative to a star Go (g_{VG}), and the spectrophotometric gradient of a star Go relative to a star A2 (g_{GA}).

TABLE 2

No. of Negative	Date (April 1956)	τ	g_{VA}	g_{VG}	g_{GA}
			+	+	+
V 3	8 — 9	60^m	1.31	—	—
V 4	9 — 10	45	1.59	0.35	1.24
V 5	10 — 11	60	1.77	0.48	1.29
V 6	11 — 12	40	1.63	0.48	1.15
V 7	12 — 13	45	1.68	0.39	1.29
V 8	13 — 14	30	1.84	0.37	1.47
V10	17 — 18	20	2.07	—	—
V11	18 — 19	15	1.84	0.27	1.57

The mean values of the relative spectrophotometric gradients of Vesta are as follows: $\overline{g}_{VA} = +1.73 \pm 0.07$; $\overline{g}_{VG} = +0.39 \pm 0.04$.

In the spectrum region of $\lambda > 500$ mµ, the gradient of Vesta relative to a star of class A2 is approximately equal to zero. As indicated by the data in Table 2, the variations in the gradient of Vesta and of a star Go relative to a star A2, from night to night, occur approximately in the same limits and in the same direction; therefore, it is impossible to attribute the variations in the gradient of Vesta to actual changes in its color.

Seven spectrograms of Vesta with exposures of 15 min, at 15-min intervals between exposures, were taken on one negative on June 13 - 14, 1956. This was done to define the possible short-period changes in color of the asteroid. The spectrophotometric gradient was determined relative to a star of class F5, the only suitable comparison star on this negative.

Table 3 shows the values of the gradient (g_{VF}) and the corresponding exposure intervals (T) for universal time.

TABLE 3

No. of Negative	T	g_{VF}
1	$16^h17^m - 16^h32^m$	1.57
2	16 45 — 17 00	1.38
3	17 15 — 17 30	1.10
4	17 45 — 18 00	1.08
5	18 15 — 18 30	0.76
6	18 45 — 19 00	1.43
7	19 15 — 19 30	0.81

As indicated by the data in Table 3, the gradient of Vesta shows a gradual but significant decrease with time. Only one spectrum (No.6) yields a value of g_{VF} which contrasts sharply with the main sequence.
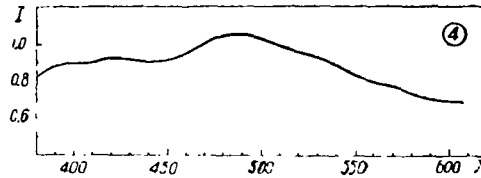

Fig.1

Unfortunately, this series of spectrograms remained the only series and it is not possible to repeat photographing; in addition, the absence of other comparison stars on the negative makes it impossible to check the result and to detect the cause for the change in gradient. Since the conditions of photographing and developing in this case were exactly the same, the systematic drop in the gradient might be attributed to the sequential superposition of the background of the sky. But the last two spectrograms speak more against than for this effect. In view of the scarcity of data, there is no assurance that the decrease in gradient is caused by a change in color of Vesta during its rotation. However, the fact is interesting that the time of the decrease in gradient is close to half the vibration period of the brightness of Vesta (Bibl.1) and accordingly of its color (Bibl.2).

From the four best spectrograms we plotted the spectral curve of Vesta relative to a star of class Go. Table 4 contains the values of the relative monochromatic intensities (I_λ) and the standard deviation (σ). The spectral curve of Vesta is shown in Fig.1.

As is apparent from the data in Table 4 and the curve, the spectrum of Vesta is characterized by a maximum intensity close to $\lambda = 480$ mu and by a drop in intensity toward the violet and especially toward the red end of the spectrum.

Let us now compare our results with previous investigations of Vesta. Only three reports (Bibl.2, 3, 4) have been devoted to a spectrophotometric study of

minor planets. One of these (Bibl.2) contains no spectral curves of asteroids and only a qualitative comparison of microphotograms of the spectra of asteroids and other celestial objects.

TABLE 4

λ	I_λ	σ	λ	I_λ	σ
380 mμ	0.80	$\pm$ 0.12	500 mμ	1.00	$\pm$ 0.00
390	0.90	0.11	510	0.97	0.07
400	0.88	0.04	520	0.93	0.07
410	0.89	0.04	530	0.92	0.06
420	0.92	0.02	540	0.88	0.04
430	0.89	0.03	550	0.83	0.04
440	0.89	0.04	560	0.78	0.02
450	0.90	0.04	570	0.77	0.03
460	0.93	0.04	580	0.71	0.01
470	1.00	0.08	590	0.70	0.04
480	1.04	0.07	600	0.69	0.04
490	1.01	0.04	610	0.68	0.06

In 1933, A.N.Deych (Bibl.3) at Pulkovo, using the same Bredikhinskiy astrograph with a UV prism, found in one observation that the spectrophotometric /174 gradient of Vesta in the range λ = 360 – 500 mμ, relative to a star of class F8–Go, was equal to 1.5. This value of the gradient differs from ours. A gradient close to the indicated one was obtained in our observations relative to a star of class A2.

Johnson (Bibl.4), in 1934, obtained seven spectrograms of Vesta on a Clark refractor with a prism having a refracting angle of $3°$. A comparison with stars of classes F8–Go led to appreciably different relative intensity distribution curves in the spectrum of Vesta even for spectrograms obtained in one and the same night, so that it was impossible to plot an average spectral curve of Vesta. The color index of Vesta varied by more than $1^m.0$; Johnson considers that the changes in the color of Vesta have to do with the change in its brightness.

We can compare our results with the determinations of the color indices of asteroids. Based on the observations by Ye.V.Sandakova (Bibl.5) the color index of Vesta is equal to CI_v = +$0^m.67 \pm 0^m.10$ (1950, n = 1); CI_v = +$0^m.70 \pm 0^m.05$ (1951, n = 3); n is the number of observations.

In calculating, on the basis of our observations, the color excess of Vesta relative to stars of the classes A2 and Go, we obtain the color index of Vesta as CI_v = +$0^m.69 \pm 0^m.05$ (for an A2 star, n = 6); CI_v = +$0^m.56$ (for a Go star, n = 4).

As we see, the first value of the color index virtually coincides with that obtained by Ye.V.Sandakova. The difference of the second value can be explained by an inaccuracy of the photometric data in the HD catalogue, according to which the color indices of the comparison stars were determined.

<u>(15)Eunomia</u>

In October 1955, we obtained four spectrograms of this asteroid with exposures up to 2 hrs. Two of the negatives were suitable for analysis.

The comparison stars were those given in Table 5.

TABLE 5

HD	BD	m_v	m_{pg}	S_p
17605	+36°569	6.^{m}63	7.^{m}19	GO
17249	+35°554	8. 1	8. 1	AO

The spectrophotometric gradient of the asteroid in the $\lambda = 400 - 520$ mu range was determined with respect to an Ao star.

TABLE 6

Date (October 1955)	τ	g_{EA}	g_{GA}
11—12	1^h27^m	+ 1.38	+ 1.61
16—17	2^h00^m	1.65	1.38

The gradient of a star of class Go with respect to a star of class Ao is given in the last column. The variations in the gradients of Eunomia and the

Fig.2

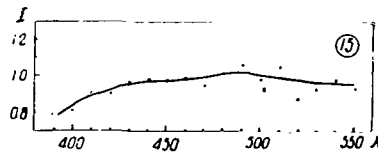star are almost identical, although opposite in sign. The spectral curve of <u>/175</u> Eunomia with respect to a star of class Go is plotted on the basis of two observations with an uncertainty (Fig.2). However, in any case this curve differs from the spectral curve of Vesta by an appreciably smaller intensity drop in the yellow spectrum.

The color index of Eunomia with respect to both comparison stars is almost

identical: $CI_E = +0.^{m}57 \pm 0.^{m}02$ (with respect to the Ao star); $CI_E = +0.^{m}54 \pm 0.^{m}02$ (with respect to the Go star).

According to the observations by Recht (Bibl.6, 7), the color index of Eunomia is

$$CI_E = + 0.^{m}56.$$

The agreement of the results is very good, although it might be accidental.

BIBLIOGRAPHY

1. Groeneveld, I. and Kuiper, G.: Astrophys. J., Vol.120, No.2, 1954.
2. Bobrovnikoff, N.T.: The Spectra of Minor Planets. Lick Obs. Bull., No.14, 1929.
3. Deych, A.M.: Spectrophotometry of Vesta (Spektrofotometriya Vesty). Tsirk. Glav. Astron. Observatorii v Pulkove, No.25, 1939.
4. Johnson, W.A.: Spectrophotometric Study of Three Asteroids. Bull. Harvard Coll. Observ., No.911, 1939.
5. Sandakova, Ye.V.: Determination of the Color Index of Asteroids (Opredeleniye pokazateley tsveta malykh planet). Astron. Tsirk., No.163, 1955.
6. Recht, A.W.: Magnitudes and Colour Indices of Asteroids. Astron. J., Vol.44, No.25, 1934.
7. Putilin, I.I.: Minor Planets (Malyye planety). Moscow, Gostekhizdat, 1953.

Ya.A.Teyfel'

In 1956 – 1958, the Observatory of the Astrobotany Sector obtained several spectrograms of Uranus (Fig.1) on a meniscus telescope AZT-7 with a slit spectrograph ASP-9. This article gives the results of preliminary investigations of Uranus with respect to the spectrograms, forming the beginning of a planned regular spectrophotometric study of the atmosphere of giant planets.

The spectrograms were recorded on Agfa Spektral Rot Rapid plates at a slit width of 0.100 mm. The negatives were calibrated by the conventional method, using an echelon; the light source was the star α Canis Majoris. The spectrophotometric scale was recorded on each negative. Analysis was carried out on the basis of the monochromatic characteristic curves plotted with consideration of the selectivity of the echelon. For spectrophotometric correlation of the plate with the spectrum of Uranus, we photographed the spectrum of a comparison star of an early spectral class which at the moment of photographing was at a zenith distance close to the zenith distance of the planet.

The best of the spectrograms of Uranus were selected for analysis (Table 1).

TABLE 1

No. of Negative	Date	Time of Photographing (Universal)
P 4	12 – 13 Oct 1956	Not recorded
P 24	9 — 10 Feb 1957	$19^h30^m — 20^h00^m$
P 38	25 – 26 Jan 1958	18 31 — 19 01
P 39	26 – 27 " 1958	17 55 — 18 20
P 40	27 – 28 " 1958	17 55 — 18 20
P 42	11 – 12 Feb 1958	17 35 — 18 00

Continuous Spectrum

In studying the continuous spectrum of Uranus, we were only able to analyze two spectrograms (P24 and P42) since, on all other negatives, the blackening of the spectra of Uranus and the comparison stars differed too much, i.e., they had to be analyzed on different segments of the characteristic which, as is known, is undesirable.

The spectrograms of Uranus were rated on a recording microphotometer MF-4. The microphotometer tracings were analyzed just as those for Saturn (Bibl.1). /177 The final spectral curves were plotted from the values

$$I_\lambda = \frac{I_\lambda'}{I'_{500}},$$

where I_λ' is the intensity of Uranus with respect to the intensity of the reference object at the wavelength λ; I_{500}' is the same for $\lambda = 500$ mμ, i.e., the intensity at $\lambda = 500$ mμ was taken as equal to unity, as is conventional in planetary spectrophotometry. Since the negatives P24 and P42 were obtained in differ-
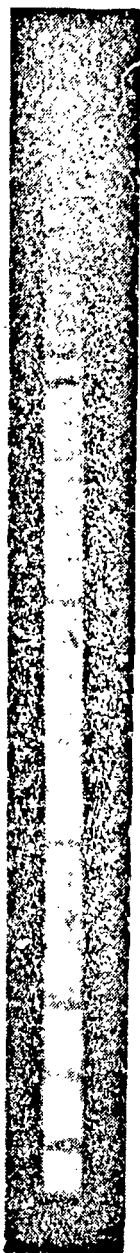

Fig.1

ent years, the comparison stars on them were different; on the negative P24, β Leonis and on the negative P42, γ Geminorum. Table 2 shows the intensity

205

distribution in the spectrum of Uranus with respect to these comparison stars.

The spectrum of Uranus was transected by several wide absorption bands of methane, which have an appreciable effect on the apparent color of the planet. Therefore, it was necessary to distinguish the apparent color index of Uranus (CI_a) from the true (CI_t). The apparent color index of Uranus is always less than the true index, since the presence of absorption bands in the red spectrum region makes the planet appear bluer than it would be from the energy distribution in its continuous spectrum. Thus, the true color index must be calculated from the continuous spectrum, and the apparent color index must be determined from the spectral curve plotted with allowance for the absorption bands.

TABLE 2

$\lambda m\mu$	P 24	P 42	$\lambda m\mu$	P 24	P 42
390	0.305	0.359	510	1.048	1.010
400	0.442	0.451	520	1.320	1.110
410	0.508	0.543	530	1.400	1.180
420	0.550	0.562	540	1.500	1.260
430	0.556	0.588	550	1.600	1.310
440	0.646	0.699	560	1.690	1.350
450	0.835	0.794	570	1.740	1.390
460	0.913	0.872	580	1.770	1.410
470	0.955	0.912	580	1.780	1.420
480	0.995	0.955	600	1.770	1.410
490	1.010	0.977	610	1.750	1.740
500	1.000	1.000	620	1.710	1.380

The intensity distribution in the spectrum of Uranus yields its color excess relative to the comparison star (CE_p), from which then the color index is calculated:

$$CI_p = CE_p + CI_s,$$

where CI_p is the color index of the planet, and CI_s is the color index of the star. It is common to consider the usual color index as the intensity ratio of spectrum regions of an object, having wavelengths of 440 and 550 mμ expressed in stellar magnitudes. To avoid random errors, the intensities were determined on the basis of the areas of the spectral curve, in small segments close to the wavelengths indicated above: 430 - 450 mμ and 540 - 560 mμ. The color indices of the comparison stars were taken from Kulikovskiy (Bibl.2): β Leonis A3 CI = = +0.06; γ Geminorum Al CI =+0.10.

For a better accounting of the effect of the absorption bands, the color indices of Uranus were calculated also in several wider wavelength ranges: 420 - 460 mμ and 536 - 576 mμ (Table 3).

The data in Table 3 indicate that the difference between the color indices

of Uranus in 1957 and 1958 is quite substantial. It is difficult to say just how real this difference is. We note only that the atmospheric transparency could not have had a significant effect on the results, since Uranus and the comparison star were photographed almost simultaneously and at near zenith distances (Table 4).

TABLE 3

$\lambda m\mu$	540—560 430—450	536 - 576 420—460
No. of Negative		
CI_t P 24	$+1.^m00$	$+1.^m01$
P 42	$+0.75$	$+0.77$
ΔCI_p	$+0.25$	$+0.24$
CI_* 24	$+0.64$	$+0.46$
42	$+0.42$	$+0.40$
ΔCI_s	$+0.22$	$+0.06$

TABLE 4

No. of Negative	Object	Z	ΔM
P 24	Uranus	31°	
	β Leonis	31	0.00
P 42	γ Geminorum	33	
	Uranus	26	0.08

In Table 4, Z is the zenith distance and ΔM is the difference in air masses. The value of ΔM in the second case is too small to cause the observed difference in the color indices.

G.A.Tikhov previously established (Bibl.3) that the true color of Uranus is close to the color of stars of class G5 (CI = $+1.^m0$). The apparent color index found by Kuiper (Bibl.4) is equal to $+0.^m50$. The photoelectric color indices (apparent) were determined by Giclas (Bibl.5) as the ratio of brightness of Uranus at wavelengths of 455 and 525 mu: 1950, $+0.^m372$; 1951, $+0.^m373$; 1952, $+0.^m364$.

The value of Giclas' color index, which is lower than that obtained by us, can be attributed to the fact that more closely adjacent spectrum regions were recorded.

Thus, despite marked variations, our data on the color index of Uranus do not contradict the results of previous investigations.

The profiles of the absorption bands of methane CH_4 6190, 5970, 5760, and 5430 Å were measured and plotted for all the spectrograms of Uranus indicated in Table 1. Since the absorption bands are very intense, we found it convenient
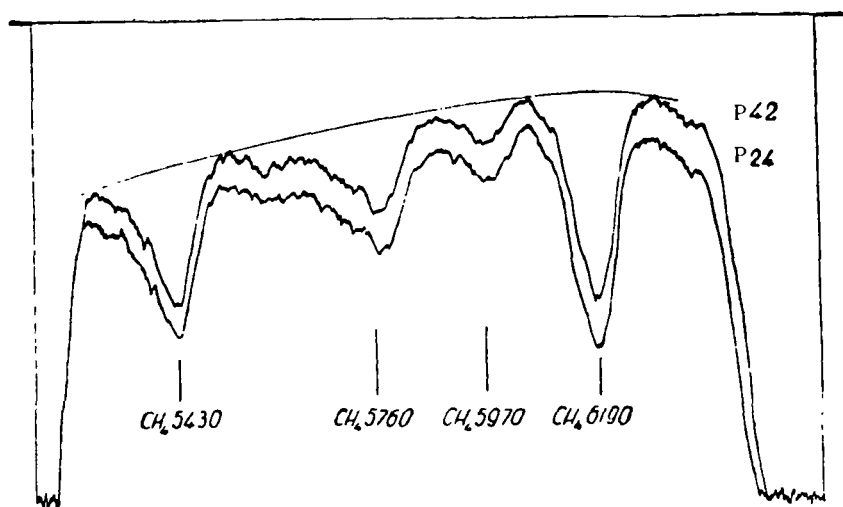
Fig.2

to measure them on the recording MF-4. The tracings gave very smooth curves, on which plotting and rating the profiles presented no difficulty (Fig.2). The

TABLE 5

CH₄ λ No. of Negative	5130Å	5760Å	5970Å	6190Å
P 4	73 0	113.2	31.4	112.2
P 24	71.8	121.0	50.6	136.2
P 38	72.3	140.2	34.5	108.0
P 39	65.5	112.3	35.4	118.3
P 40	58.9	113.2	35.2	106.0
P 42	59.8	97.4	29.3	114.0
$\overline{W}$	66.9	116.2	36.0	115.9

final result was obtained in the form of curves for $\dfrac{I_b}{I_c}$ as a function of n; /179

I_b is the intensity inside the band, I_c is the intensity of the continuous spectrum, n is the reading of the linear scale (along the dispersion). Next, we calculated the equivalent widths of the absorption bands in linear units, which

Fig.3

were then converted to angstroms by multiplication by the mean value of the dispersion for a given band. Table 5 shows the equivalent widths of the bands for each negative W and their mean values $\overline{W}$.

Fig.4

To determine whether an application of the mean value of the dispersion introduces a substantial error into the data on the equivalent bandwidths, for
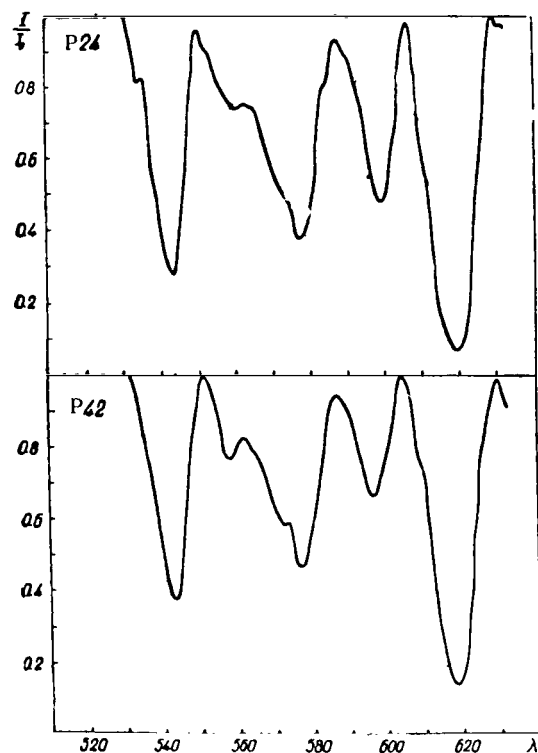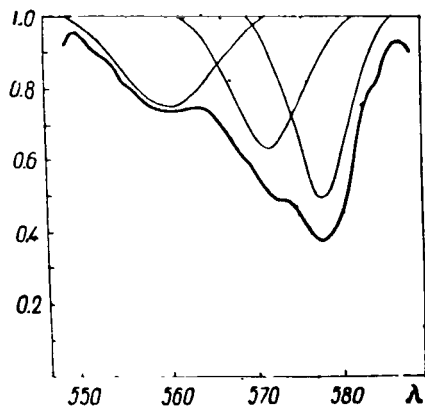
negative P24 and P42, we plotted the profiles of the bands at one wavelength scale (Fig.3) and calculated the equivalent widths with accurate allowance for the dispersion (Table 6).

As we see, the difference between the equivalent widths, calculated with accurate allowance for the dispersion and from the mean values, is negligible and is expressed by a deviation ΛW of not more than 4.4 Å, i.e., in the worst cases not more than 3%.

TABLE 6

No. of Negative	P 24		P 42	
λ	W′	ΔW	W′	ЛW
5430Å	74.2Å	+2.4Å	60.8Å	+1.0Å
5760	120.3	−0.7	97.1	−0.3
5970	52.9	·;2.3	31.3	+2.0
6190	131.8	−4 4	114 2	−0.2

It should be mentioned that the observed absorption bands are actually the result of a superposition of several fluctuating bands; this is especially noticeable in the band $CH_4 5970$ Å which can be divided into three and more components. Figure 4 shows such an approximate separation of this band.

Since the absorption bands of methane in the visible spectrum region are not observed in the laboratory, an analysis of the profiles of the bands and their change in the spectra of giant planets is of considerable interest and will be the object of further investigations.

BIBLIOGRAPHY

1. Teyfel', V.G. and Teyfel', Ya. A.: Experience in Spectrophotometry of Saturn (Opyt spektrofotometrii Saturna). Trudy Sekt. Astrobotan., Vol.7, Alma-Ata, Izd. Akad. Nauk KazSSR, 1959.
2. Kulikovskiy, P.G.: Handbook for the Amateur Astronomer (Spravochnik astronoma-lyubitelya). Moscow, Gosud. Tekh.-Teoret. Izd., 1953.
3. Tikhov, G.A.: Principal Works (Osnovnyye trudy). Vol.2, Alma-Ata, Izd. Akad. Nauk KazSSR, 1955.
4. Keyper (Kuiper), D.: Atmosphere of the Earth and Planets (Atmosfery Zemli i planet). Moscow, Izd. Inostr. Lit., 1951.
5. Giclas, H.L.: Astron. J., Vol.59, No.3 (1215), pp.128-131, 1954.

Yu.V.Glagolevskiy

For the investigation, six stars were selected from the list given by Babcock (Bibl.1). The spectra were photographed with the Bredikhinskiy astrograph, having an objective prism with a refraction angle of $13° 45'$. This prism gives spectra with the following dispersion in various spectrum regions:

Line	H_a	H_γ	H_δ	H_ϵ	H_ζ	H_η	H_θ	H_ι	H_χ
Dispersion, Å/mm	204	140	115	95	90	85	80	77	74

Broadening of the spectra during long exposure was obtained by retarding the clock drive and, during short exposure, by stopping the clock drive and using the diurnal motion of the star itself.

As photographic material, we mainly used Ilford H.P.Z. plates and, in certain cases, Agfa Astro-Platten Panchromatisch. On the Ilford H.P.Z. plates the lines were rather coarse-grained, so that the faint lines were not photometered. To plot the characteristic curves, we photographed spectra of the
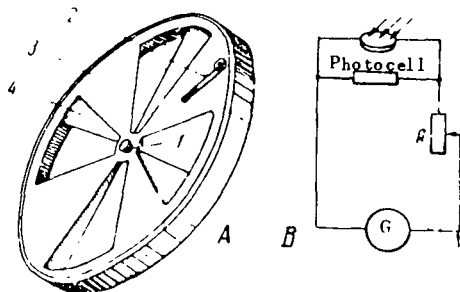
Fig.1   Diagram for Determining the Transmission
of the Diaphragm
A - Diaphragm; B - Circuit

stars ~ Aquilae (m = 0.89, A7V), α Lyrae (m = 0.14, AoV), and α Canis Majoris (m = -1.58, AIV). The difference in altitudes of the investigated stars and the comparison star during photographing did not exceed $3°$; therefore, the transparency of the atmosphere was not taken into account. This should not lead to excessive errors, since the spectra of the investigated stars were photographed for photometering the hydrogen lines whereas the spectra of the comparison stars were photographed only for plotting the characteristic curves.

The diaphragm for obtaining the scale had nine transmission steps; however,

the use of six steps proved sufficient since the points, from which the charac-
teristic curves were plotted, were spread properly.

The diaphragm was constructed in the following manner: In the aluminum
disk 4, we made four holes in the form of sectors (Fig.1,A); to this disk we
attached another similar disk which could be rotated about the axis 1. The
pawl 2 stopped the rotatable disk 3 at nine different positions, from full   /182
opening of the sectors to a certain minimal opening. To reduce absorption ef-
fects in the prism, diametrically opposed slots of the diaphragm were oriented
parallel to the refracting angle of the prism, whereas the other two slots were
perpendicular. The diaphragm was checked as to its transmission by means of a
selenium photocell installed where the plate holder goes. During the investiga-
tion, the telescope was pointed at the zenith at noon on a clear, cloudless day.
The photoelectric current was recorded by a mirror galvanometer, connected in
aperiodic operation (Fig.1,B). The sensitivity of the circuit could be changed
by a variable resistance R. The root-mean-square error in determining the
transmission was 1.5%, which is completely permissible for photometric work.
The logs of transmission log I of the diaphragm were as follows:

No. of Diaphragm	1	2	3	4	5	6	7	8	9	10
log I	0.000	0.265*	0.456	0.575*	0.643	0.744*	0.806	0.860*	0.906	1.220*

* The asterisks denote the position of the diaphragms at which
the spectra for the characteristic curves were obtained.

When converting the photographic density into intensity we used the method
of compound characteristics. The latter were plotted for each hydrogen line up
to H_{12} inclusive, based on the intensity minima. Over these lines, we then
plotted the curves based on the continuous spectra which were shifted parallel
to the abscissa until they coincided with the other curves. Thus, the compound
characteristics encompassed a much greater density range than each separately;
furthermore, this method is equivalent to using 12 diaphragms.

TABLE 1

Star	α (1950)	δ (1950)	m	Sp	Magnetic Field Strength (Bibl. 1)	Number of Observations
710	$2^h23^m37^s$	$-15°\ 34'$	$5.^m8$	A2p	$-1070--2970$ (±250)	3
36 Eridani	3 57 47	-21 09	4. 7	A0p	$+1360$ (±700)	3
μ Leporis	5 10 41	-16 16	3 3	A0p	$+620$ (±250)	3
β Coronae Borealis	15 25 36	$+29$ 17	5. 7	F0p	$+2670-90$ (±150)	5
52 Herculis	16 47 46	$+46$ 04	4. 9	A2p	$+2780$ (±300)	5
γ Equulei	21 07 55	$+9$ 56	4. 8	F0p	$+760+2750$ (±110)	3

The spectral lines (hydrogen) were photometered with the MF-2 microphotometer every 0.01 mm and, in certain cases, every 0.005 mm (through half-divisions of the drum). The lines Hη – H$_F$ were photometered from a point 30 – 40 Å from the center of the line, in order to definitely include the wings of the line (i.e., 1.5 – 2 times farther than the wings coincide with the continuous spectrum); beginning with H$_\epsilon$, the spectrum was photometered continuously.

For a preliminary investigation, we photographed the spectra of the six stars shown in Table 1.

The astrograph was focused on the middle portion of the spectrum so that the lines H$_\beta$ – H$_F$ were in focus. The lines of shorter wavelengths were then no longer noticeable at the focus. Figure 1,a shows the chromatic curve of the objective of the Bredikhinskiy astrograph, while the horizontal heavy line shows the position of the photographic plate. In such a position, the greatest wavelength range was found without noticeable distortion.
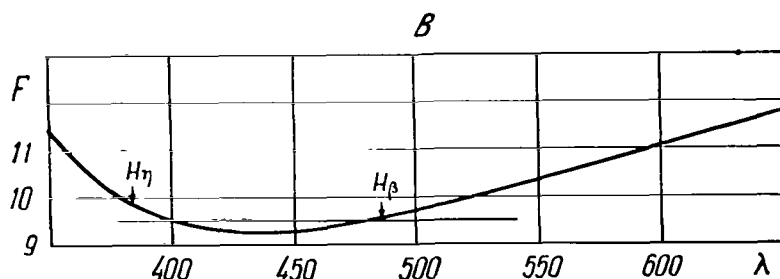
Fig.1a   Chromatic Curve of Objective

Figure 2 shows the profiles of the hydrogen lines of magnetic stars. The number of spectra used for plotting these profiles is indicated in Table 1 in the last column. The ordinate gives the logarithms of the brightness ratio of different points of the line to the continuous spectra. In Fig.2, no lines are drawn through the points for μ Leporis, but their scattering gives an idea as to the accuracy of the results. This scattering is due mainly to the considerable graininess of the photographic plates.

We found that the intensity of the hydrogen lines of the investigated magnetic stars is appreciably weaker than that of the lines of the comparison stars. Therefore, it became of interest to determine the spectral type of these stars, based on three characteristics: depth and equivalent width of the hydrogen lines and the K (Ca II) lines. To plot these characteristics as a function of the spectral class we photographed the spectra of the following stars: η Aurigae (B3V), β Persei (B8V), α Lyrae (AoV), θ Leonis (AIV), α Canis Majoris (A2V), δ Ursae Majoris (A3V), α Cephei (A7P), α Aquilae (A7V), δ Cassiopeiae (A5V), and σ Ceti (F5V). The depth of the hydrogen lines, in percent of brightness of the continuous spectrum of the comparison stars, is shown in Table 3 and the equivalent widths, in Table 4. The corresponding values of these quantities for magnetic stars are indicated in Tables 5 and 6. On the basis of Table 3, we plotted the graphs for the dependence of depth of the spectral lines H$_\beta$ – H$_\epsilon$ on the
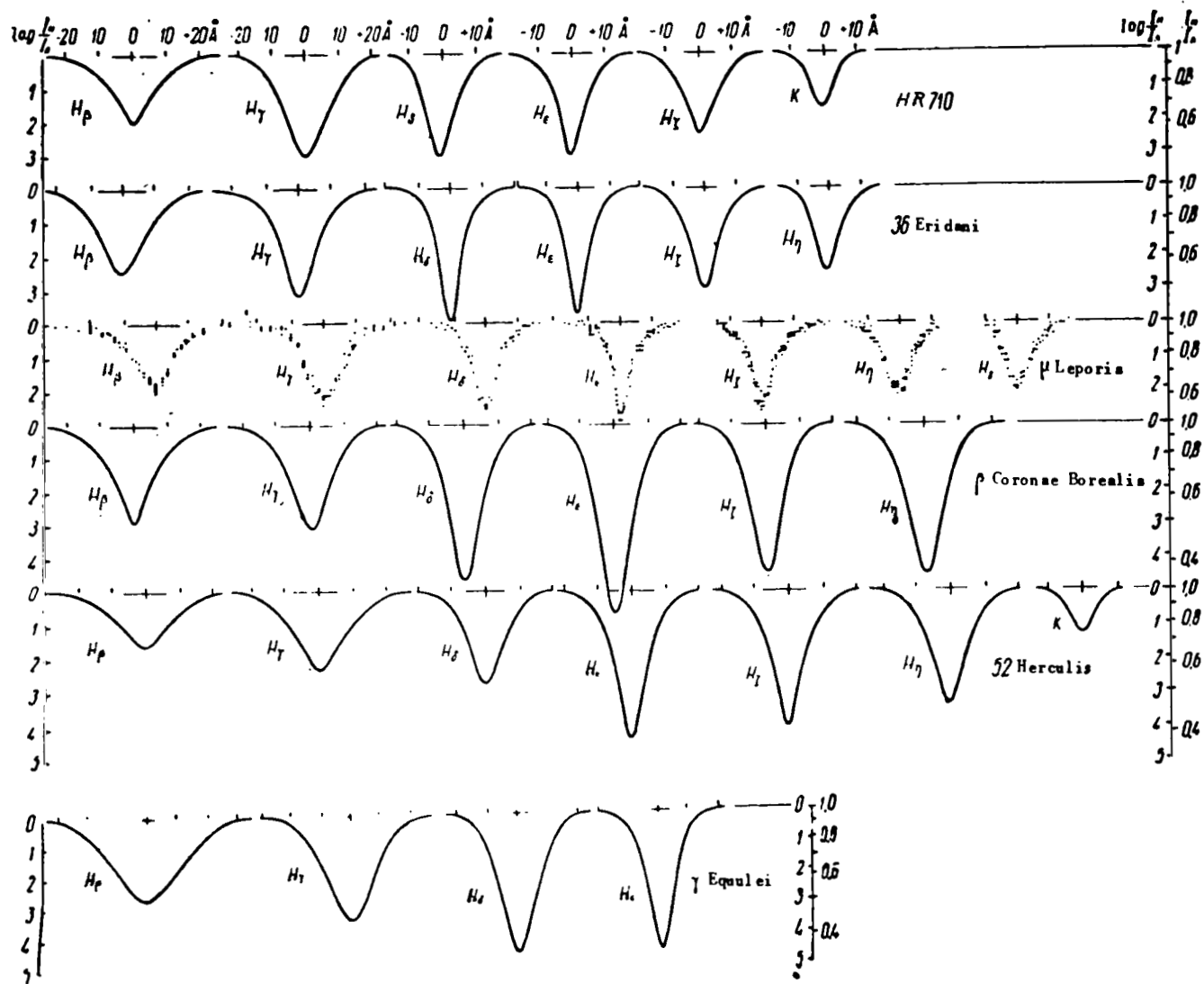
Fig.2 Profiles of the Lines of Magnetic Stars

spectral class (Fig.3,A). From these graphs, we determined the spectral classes of the magnetic stars based on the depth of the lines; these are shown in the next to the last column of Table 5. The column Sp gives the spectra from the
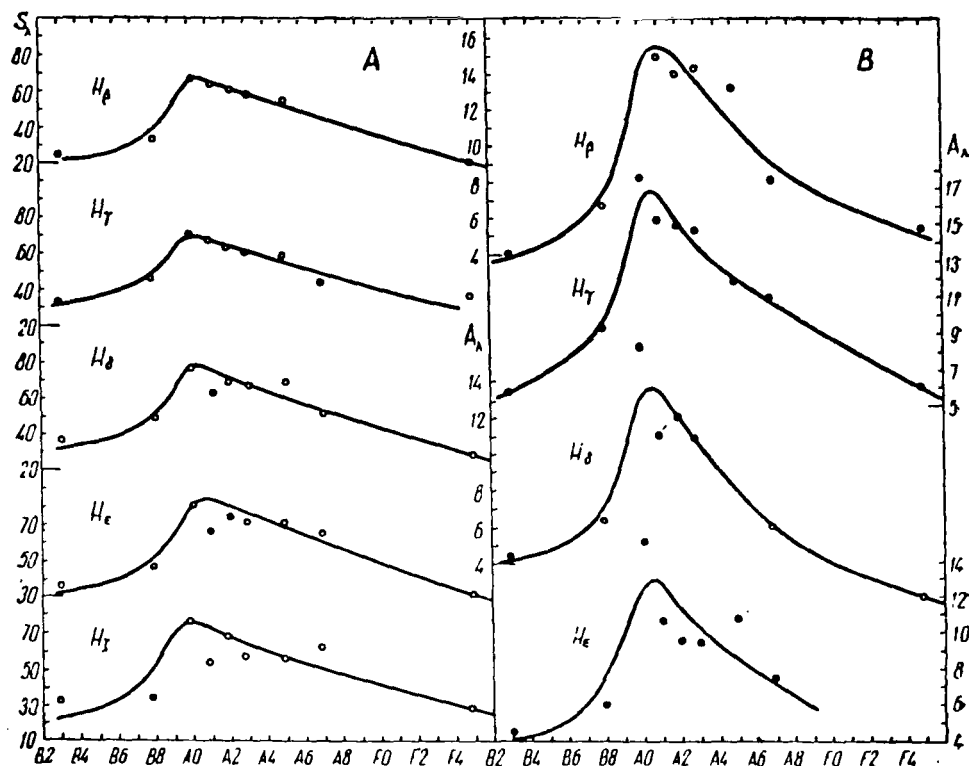
Fig.3 Graphs for Determining the Spectral Classes of
Stars Based on Hydrogen Lines
A – Dependence of the depth of the lines – spectrum for
stars of the main sequence; B – Dependence of equivalent
width – spectrum for the same stars

TABLE 2

Star	Line Depth						
	Sp	H_β	H_γ	H_δ	H_ϵ	H_ξ	k
τ Aur	B3V	25%	34%	38%	36%	32%	6%
β Per	B8V	34	47	50	48	38	5
α Lyr	A0V	68	72	78	81	80	17
θ Leo	A1V	64	68	64	67	57	9
α CMa	A2V	60	65	70	74	72	16
δ UMa	A3V	59	61	58	72	62	23
δ Cas	A5V	56	60	70	72	60	40
α Aql	A7V	30	45	53	67	64	47
α Cet	F5V	22	38	30	32	30	72

TABLE 3

| Star | Equivalent Line Width | | | | |
	H_β	H_γ	H_δ	H_ϵ	k
η Aur	4.1	5.6	4.5	4.5	0.1
β Per	6.8	9.0	6.4	6.0	0.1
α Lyr	—	17.4	16.0	15.0	0.4
θ Leo	15 0	15.0	11.1	10.7	0.5
α CMa	14.1	14.8	12.1	9.6	0.8
δ UMa	14.4	14.4	11.1	9.5	1.7
δ Cas	8 2	11.7	—	10.8	3.2
α Aql	8.2	10.8	6.1	7.6	2.9
σ Cet	5 4	6.0	2.2	—	5.2

TABLE 4

Star	H_β	H_γ	H_δ	H_ϵ	H_ζ	H_η	H_θ	H_ι	$H_\varkappa$	H_λ	Sp	$Sp(H)$	$Sp(k)$
HR 710	37 %	50 %	51 %	51 %	46 %	40 %	38 %	31 %	18 %	—	A2	A9	A2
36 Eri	43	52	60	60	51	44	35	21	18	15 %	A0	A7	A7
μ Lep	35	39	43	46	44	36	36	26	15	9	A0	F1	A7
β CrB	44	51	65	72	69	65	55	40	26	--	F0	A5	±
52 Her	32	42	46	63	61	54	35	32	25	20	A2	A8	A1
γ Equ	40	46	55	64	64	37	37	26	25	—	F0	A7	A6

TABLE 5

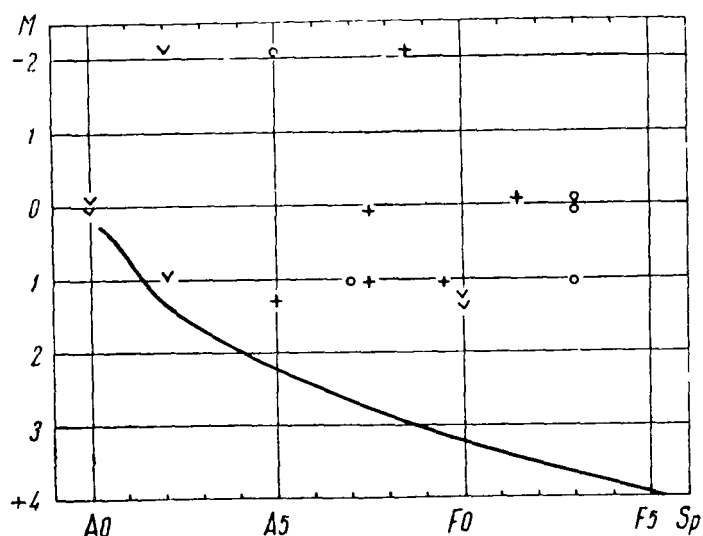| Star	H_β	H_γ	H_δ	H_ϵ	H_ζ	H_η	H_θ	H_ι	$H_\varkappa$	H_λ	Sp	$Sp(H)$	$Sp(k)$
HR 710	8 3	8.1	5.2	5.6	5.6	6.2	4.6	1.8	1.2	—	A2	F0	A7
36 Eri	9.5	8.0	6.1	6.1	6.1	5.4	4.4	3.2	2.0	1.0	A0	A8	F3
μ Lep	6.6	6.0	4.8	4.6	4.8	4.5	3.4	2.4	1.2	0.8	A0	F2	F3
β CrB	—	10.0	9.2	9.2	8.4	6.2	4.1	2.0	2.0	—	F0	A5	—
52 Her	8.0	7.7	8.0	7.1	5.6	5.9	4 0	2.8	1.8	—	A2	A9	A5
γ Equ	9.1	7.3	9 6	8.0	7.6	7.6	6.8	5.8	2.0	—	F0	A8	F3

Fig.4   Spectrum-Versus Luminosity for Magnetic Stars

catalogues, i.e., those generally used, and the last column contains the spectra obtained on the basis of the depths of the K lines (Ca II). The spectral classes with respect to hydrogen were obtained from five lines. Analogously, on the basis of Table 4 and Fig.3,B we determined the spectral classes of magnetic stars based on the equivalent widths of hydrogen lines and K lines, which are shown in the next to the last and in the last columns of Table 6. A comparison of the spectral classes obtained by both methods with respect to hydrogen, shows that they virtually coincide.

The difference between the spectral classes obtained by us and those given in the catalogues is quite interesting. For β Coronae Borealis and γ Equulei the spectrum is earlier and for the others, later. This fact (see below) can be explained by the latter having a high luminosity.

Unfortunately, no exact parallaxes are known for magnetic stars, and their luminosities cannot be reliably obtained. Table 7 shows the trigonometric /185 parallaxes π" of the investigated stars, taken from Schlesinger's catalogue (Bibl.4) and the absolute visual magnitudes M. For γ Equ, Schlesinger's catalogue does not give π"; hence, we took it from Bechvarzh's catalogue which, unfortunately, does not indicate the method by which this parallax was determined nor the error. Figure 4 shows the data of Table 7, where the curve depicts the

TABLE 6

Star	m	π''	M
HR 710	5.84	0.011±9	+1.05
36 Eri	4.69	0.012±12	+0.08
μ Lep	3.3	0.021±8	−0.08
β CrB	3.72	0.033±5	+1.30
52 Her	4.9	0.001±8	−2.10
γ Equ	4.76	0.018	+1.04

main sequence, plotted on the basis of Table 2 in the paper by P.P.Parenago and A.G.Mosevich (Bibl.5). In this diagram, the asterisks denote the relation /187 between M and the spectrum cited in the catalogues, the crosses give the relation with the hydrogen spectrum, and the circles pertain to the K lines (Ca II). Despite the inaccuracy of the absolute magnitudes and the great difference in spectral classes determined by different methods, the investigated magnetic stars nevertheless show a tendency to be located above the main sequence. We plotted an analogous graph for another 15 magnetic stars, for which we found the parallaxes or absolute magnitudes in the literature. In this case, almost all points lay above the main sequence. Unfortunately, all these magnitudes were rather inaccurate. Nevertheless, the character of the hydrogen lines and the above facts lead to the assumption that the magnetic stars apparently have a higher luminosity than stars of the main sequence.

When changing from H to lines with a higher quantum number, we approach ever closer to optically thin layers. Therefore, to determine the number of

atoms N_2H of hydrogen over 1 cm^2 of the stellar surface (Bibl.2), we can use the following formula:

$$W_\lambda = \frac{\pi e^2}{m c^2} \cdot \lambda^2 \cdot f \cdot N_2 H,$$

or

$$\log N_2 H = 17.053 + \log W_\lambda \; [m\text{\AA}] - 2 \; \log \lambda \; [\text{\AA}] - \log f, \tag{1}$$

where W_λ is the equivalent line width in milliangstroms, λ is the wavelength of the line in angstroms, and f is the force of the oscillators. N_2H is determined in the following manner: From our measured equivalent widths W, we first calculate log N_2H from eq.(1), using a purely formal method. Further, we plot the graph of log N_2H as a function of the quantum number n of the line. On this graph, log N_2H increases on changing to higher terms of the series and thus to optically thin layers, whereas the curve asymptotically approaches a certain limit showing the true value of the number of hydrogen atoms per 1 cm^2 of stellar surface. Because of the Stark effect, the lines are so blurred that the curve does not reach the limit and, at a certain value n, again begins to descend. Therefore, this method yields only the lower boundary of the number of atoms. We can approach the true value if we extend the left-hand part of the graph as a smooth line, by means of a French curve, as indicated in Fig.5 (broken line). This will approximately reproduce that portion of the graph which would be obtained in the absence of the Stark effect and of other factors that distort the true values of the equivalent line widths.

TABLE 7

Line, n	λ	f [2]
H_β 4	4861	$1.19 \cdot 10^{-1}$
H_γ 5	4310	$4.47 \cdot 10^{-2}$
H_δ 6	4102	$2.21 \cdot 10^{-2}$
H_ϵ 7	3970	$1.27 \cdot 10^{-2}$
H_ζ 8	3889	$8.04 \cdot 10^{-3}$
H_η 9	3835	$5.43 \cdot 10^{-3}$
H_θ 10	3798	$3.85 \cdot 10^{-3}$
H_ι 11	3771	$2.84 \cdot 10^{-3}$
H_κ 12	3750	$2.15 \cdot 10^{-3}$
H_λ 13	3734	$1.67 \cdot 10^{-3}$

Table 7 shows the wavelengths and force of the oscillators (f) for the /188 measured lines. Table 8 lists the names of the stars for which we determined N_2H and the values of log N_2H in columns 2 - 11 determined from eq.(1). Based on the data in these columns, we plotted the curve in Fig.5. Column 12 of Table 8 gives the values of log N_2H^*, determined from the ordinates of the peaks of the curves in this diagram; column 13 contains the values of log N_2H^{**}, determined from the ordinates of the horizontal segment of the smooth curve, which had been extended by means of a French curve.

To estimate the reliability of the results obtained with our instrument, we plotted (on the graph of Fig.5) the logarithms of N_2H for the spectrum of

Sirius (crosses) obtained by us and those obtained by Gunter (circles) (Bibl.3).
As is apparent, up to n = 9 the curves osculate, after which they diverge because
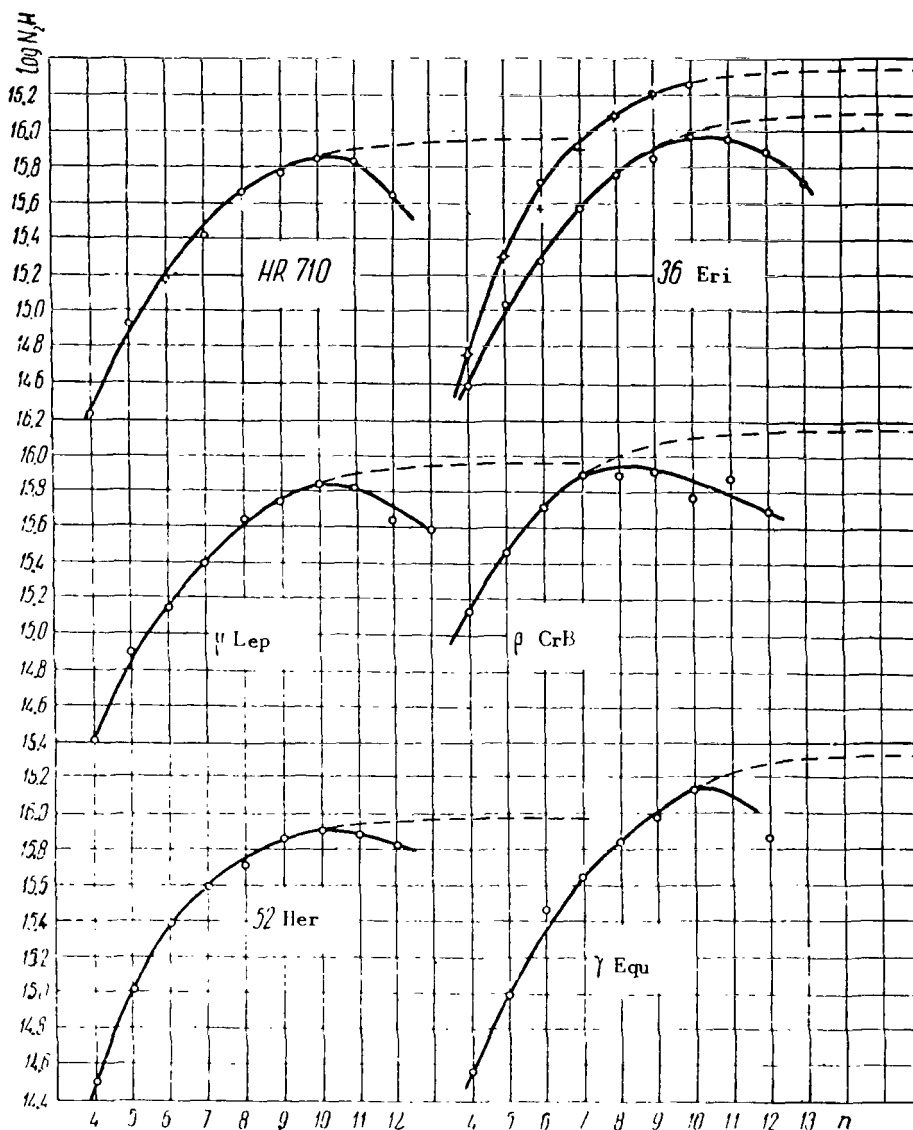
Fig.5   Graph for Determining log N_2H

of the fact that our spectrum in the shorter wavelengths was out of focus;   /189
however, if we continue the left-hand portion of the graph by the described
method, then the values of log N_2H in both cases will coincide satisfactorily.

Figure 6 gives the values of log N_2H, measured by Gunter for the spectra
of main-sequence stars (solid circles) and C-stars (hollow circles). The re-
sults of our measurements (crosses) are also entered. As is apparent, the num-
ber of hydrogen atoms per 1 cm^2 surface of the magnetic stars is less than for

TABLE 8

Star	log N₂H (accd. to eq. (1))										log N_2H^*	log N_2H^{**}
	H_β	H_γ	H_δ	H_ϵ	H_ξ	H_η	H_θ	H_ι	H	H_λ		
HR 710	14.523	15.039	15.199	15.498	15.716	15.892	15.971	15.703	15.653	—	15.96	16.13
36 Eri	14.581	15.032	15.269	15.536	15.754	15.832	15.951	15.953	15.874	15.687	15.97	16.10
μ Lep	14.423	14.907	15.163	15.413	15.648	15.754	15.840	15.828	15.653	15.590	15.84	15.96
β CrB	—	15.129	15.447	15.714	15.892	15.892	15.921	15.749	15.874	15.687	15.94	16.16
52 Her	14.506	15.016	15.386	15.600	15.718	15.870	15.910	15.894	15.828	—	15.91	15.99
γ Equ	14.563	14.992	15.465	15.653	15.848	15.980	16.141	16.211	15.874	—	16.18	16.33

Fig.6   log N₂H versus Spectrum
The solid circles are stars of the
main sequence; hollow circles are
C-stars; crosses are magnetic stars

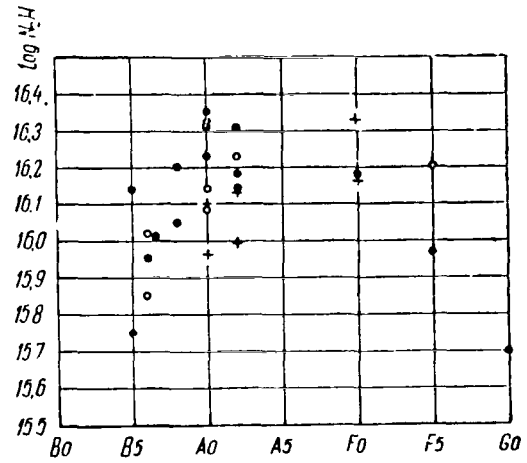main-sequence stars and C-stars of the corresponding spectral classes. The more shallow curves in Fig.5 for magnetic curves, in comparison with Sirius, indicate a more rapid intensity drop of the hydrogen lines, which can be explained by the weaker effects of pressure.

The resultant values of log N_2H are underestimated since eq.(1) is valid only for optically thin layers, which can be approached using sufficiently high terms of the Balmer series. Furthermore, the lines are blurred due to various instrument errors and due to the presence of the Stark effect. The upper boundary of log N_2H could be obtained from the H_α line, which, unfortunately, on our spectra is not at the focus.

Thus, summing up the above statements, we can note that: 1) The investigated magnetic stars have narrow hydrogen lines, mainly of a smaller equivalent width in comparison with the lines of main-sequence stars; 2) the stars 36 Eri, HR 710, μ Lep, and 52 Her, based on equivalent width and depth of the hydrogen lines, have a later spectral class than is indicated in the catalogues, /190 whereas ε CrB and ν Equ have an earlier class; 3) the spectral classes with respect to the K lines (Ca II) obtained on the basis of Tables 5 and 6 are mainly later; 4) an analysis of the dependence of the spectrum on the luminosity of the hydrogen spectrum indicates that the investigated magnetic stars probably belong to stars of a higher luminosity than the main sequence; 5) in comparison with Sirius, the examined stars have lower pressure effects and lower values of log N_2H.

BIBLIOGRAPHY

1. Babcock, H.W. and Cowling, T.G.: Monthly Notices, Vol.113, No.3, 1953.
2. Voigt, H.: Z. Astrophys., Vol.31, p.48, 1952.
3. Gunter, S.: Z. Astrophys., Vol.7, p.106, 1933.
4. Schlesinger, F.: The Photographic Determinations of Stellar Parallaxes Made with the Yerkes Refractor. Astrophys. J., Nos.32-34, 1910-1911.
5. Parenago, P.P. and Mosevich, A.G.: Trudy GAISh., Vol.20, Moscow, Izd. Moskov. Univ., 1951.

Yu.V.Glagolevskiy

It is common knowledge that the problem of the luminosity of stars is of extreme importance. In many cases, it is necessary to know whether a star belongs to the main sequence or some other branch of the spectrum-luminosity diagram. In particular, this must be known when studying the physical state of stars, their chemical composition, temperature, and structure of the atmosphere. In connection with this, we attempted to determine the position of magnetic stars on the diagram, since this problem is still unsolved.

In our previous work (Bibl.1) we pointed out the fact that the hydrogen lines of certain magnetic stars are weaker than that of main sequence stars of the same spectral class. The same holds true for a number of other stars, which we subjected to a preliminary study. These were the following stars: 52 Her, HD 173650, HD 192913, HR 710, 36 Eri, and μ Lep (Table 1). Stars 21 Aql and

TABLE 1

Star	Sp	Sp_K	Sp_H		Star	Sp	Sp_K	Sp_H	
52 Her	A2p	A1	A8	In depth	γ Equ	F0p	A9	A6	In depth
		A5	A8	In width			A5	F5	In width
HD 188041	F0p	A5	A9	•	HR 710	A2p	A2	A9	•
		A7	A9				A7	A9	
HD 173650	A0p	—	B8	•	36 Eri	A0p	A7	A6	•
		—	B7	•			F3	A8	•
21 Aql	B8	—	ö8	•	μ Lep	A0p	A7	F0	•
		—	B7	•			F3	F1	•
HD 193913	A0p	—	B4	•	β CrB	F0p	—	A5	•
		—	B4	•			—	A5	•

Note: Sp-Spectroscopic type; Sp_K-spectrum relative to CaII; Sp_H-spectrum relative to hydrogen.

γ Equ show, with respect to hydrogen, the same spectrum, which is ascribed to it. An opposite effect in comparison with the first six stars is shown only by HD 188041, whose spectrum was earlier by two classifications which of course is within the limits of the errors, and β CrB whose spectrum is earlier by five classifications. We can add α² CVn to our list of stars having weak hydrogen /192 lines. According to work (Bibl.2) this star has weak hydrogen lines owing to its smaller quantity (in comparison with the usual) per unit volume of atmosphere.

Thus, we can say that the hydrogen lines, for some of the studied magnetic stars, are weak and in approximately half of them, have a normal intensity. It

was pointed out earlier (Bibl.1) that for five (of the six) studied magnetic stars, the number of absorbing hydrogen atoms over 1 cm^2 of the stellar surface is apparently slightly diminished in comparison with main-sequence stars. It was also indicated that, for these stars, the effects of pressure are less manifest than for αCMa belonging to the main sequence.

All this makes us assume that magnetic stars mainly have properties of stars lying above the main sequence.

The problem of the luminosity of magnetic stars could have been solved easiest in the presence of trigonometric parallaxes. However, of the 25 parallaxes found in catalogues of Schlesinger (Bibl.3) and Jenkins (Bibl.4), only 10 have an accuracy of more than 30% (Table 2). Nevertheless, the values of the absolute magnitudes obtained on the basis of the parallaxes in Table 1 can give

TABLE 2

№	Star	Coordinates 1950				m	Sp	π''	M
1	HR 710	$2^h23^m37^s$	$-15°34'$			5,8	A2p	0,011± 9	+1,1 S [1]
2	HD 19445	3 5	28	+26	9	8,0	F6	0,021 ÷ 6	+4,6 J [2]
3	36 Ery	3 57	47	−24	9	4,7	A0p	0,012 ± 12	+0,1 S
4	16 Ory	5 6	34	+ 9	46	5,4	F2	0,006 ± 10	−0,7 J
5	μ Lep	5 10	41	−16	16	3,3	A0p	0,021 ± 7	−0,1 S
6	HD 60414,5	7 31	30	−14	25	5,1	M3ep	0,008 ± 8	0 S
7	30 UMa	10 20	33	+65	49	4,9	A0p	0,040 ± 11	+2,0 J
8	17 ComA	12 26	25	+26	11	5,4	A0p	0,019 ± 6	+1,8 S
9	γ Vir	12 39	7	− 1	10	2,9	F0p	0,106 ± 6	+2,2 J
10	α² CVn	12 53	42	+38	35	2,9	A0p	0,025 ± 5	−0,1 S
11	78 Vir	13 31	35	+ 3	55	4,4	A2p	0,018 ± 5	+1,2 S
12	μ LibA	14 46	34	−13	56	5,4	A4p	0,014 ± 8	− 1,1 S
13	β CrB	15 25	46	+29	17	3,7	E0p	0,033 ± 5	+1,3 S
14	ω Oph	16 29	10	−21	21	4,6	A7p	0,030 ± 9	+2,0 J
15	45 Her	16 45	19	+ 5	20	5,3	A0p	0,009 ± 5	+0,1 J
16	52 Her	16 47	46	+46	4	4,9	A p	0,004 ± 8	2,1 S
17	21 Aql	19 11	11	+ 2	20	5,1	B8	0,005 ± 6	−1,9 S
18	RR Lyr	19 23	52	+42	41	7−8	F	0,009 ± 5	−2,7 J
19	51 Sqr	19 33	00	−24	50	5,7	F	0,012 ± 9	+1,1 J
20	HD 187474	19 48	27	−40	1	5,4	A0p	0,015 ± 10	+1,3 J
21	θ¹ Mic	21 17	34	−41	1	4,9	A2p	0,008 ± 9	− 0,6 J
22	AG Peq	21 48	37	+12	23	7,6	Bcp	0,007 ± 11	+1,8 S
23	VV Cep	21 55	14	+63	23	5	M2e	0,001 ± 7	+0,3 S
24	i Phe	23 32	23	−42	54	4,8	A2p	0,001 ± 8	−5,9 S
25	108 Aqr	23 48	46	−19	11	A0p	A0p	0,018 ± 10	+1,5 J

[1] S = from Schlesinger's catalogue (Bibl.3).
[2] J = from Jenkins' catalogue (Bibl.4).

a general picture of the distribution of the magnetic stars on the spectrum-luminosity diagram, since we are not interested in the position that a particular star occupies. This diagram is shown in Fig.1,A. The black dot designates absolute magnitudes M, which were calculated from parallaxes having an accuracy higher than 30% and the white dots, below 30%. The dots lie mainly above the main sequence. The black dots which are below the main sequence belong to /193 17 ComA, 30 U Ma, and HD 19445. It should be noted that the deviation of M for

these stars from the main sequence is within the limits of errors in determining their parallaxes.

A similar diagram, shown in Fig.1,B, was plotted from the data of Table 3, in which spectral parallaxes and the corresponding absolute magnitudes of certain magnetic stars are given. The material for this Table was taken from
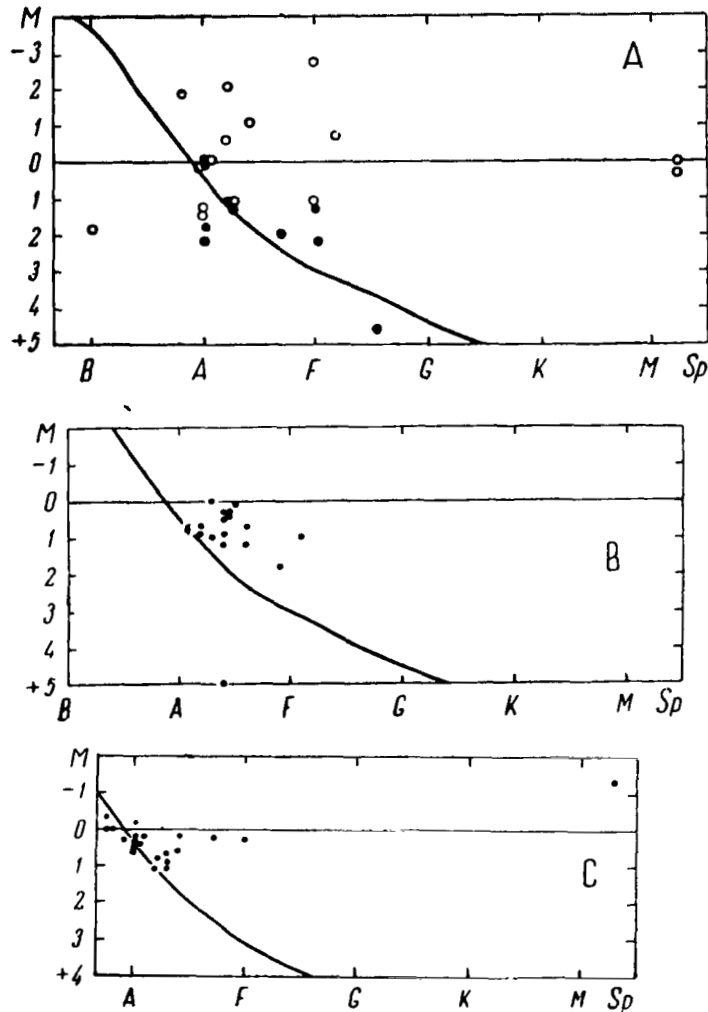
Fig.1   Spectrum of Magnetic Stars as a Function of
Absolute Magnitude
A - Obtained from trigonometric parallaxes; B - Obtained
from spectral parallaxes; C - Obtained from
P.P.Parenago's catalogue

the catalogue of spectral stellar parallaxes (Bibl.5). The general picture is analogous to the preceding, except that the dots lie closer together (the dots lying below the main sequence belong to a white dwarf). Here, doubts may arise as to the reality of the spectral parallaxes, in view of the fact that they were

determined on the basis of the relative intensity of lines SrII, TiII, FeII, ScII, CrII, YII, CaII, certain of which demonstrate an anomalous intensity /194 in individual stars. However, the coincidence of the spectral absolute magnitudes with respect to their arrangement on the diagram with the trigonometric magnitudes confirms their existence and also shows that the relative intensities of the line pairs used are completely normal. Apparently, the lines with an explicitly amplified intensity were not used by Adams (Bibl.5), since they are listed as anomalous in the annotation.

TABLE 3

Star	Coordinate 1950	m	Sp	M	π''
HD 10783	1^h43^m $4^s \pm 8°18'$	6.6	A3sp	1.0	0.003
HD 19445	3 5 28 +26 9	8.0	A4sp	5.0	0.025
68 Tau	4 22 36 +17 49	4.2	A4s	1.2	0.025
16 Ory	5 6 34 + 9 46	5.4	A9s	1.8	0.019
WY Gem	6 8 54 +23 14	7.4	M3ep	—0.8	0.002
15 Cnc	8 10 3 +29 48	5.9	A2sp	0.9	0.010
3 Hya	8 33 2 — 7 48	5.6	A4sp	0.9	0.011
49 Cnc	8 42 2 + 0 16	5.6	A4sp	0.5	0.010
μ LibA	14 46 34 —13 56	5.8	A4sp	0.3	0.008
33 Lib	15 26 45 —17 16	7.2	F1p	1.0	0.006
ω Oph	16 29 10 —21 21	4.6	A6s	1.2	0.021
52 Her	16 47 46 +46 4	4.9	A4sp	0.3	0.012
HD 171586	18 33 8 + 4 54	6.7	A4sp	0.8	0.007
10 Aql	18 56 29 +13 50	5.9	A6sp	0.7	0.009
HD 188041	19 50 42 — 3 15	5.6	A5sp	0.1	0.008
HD 192913	20 14 23 +27 37	6.7	A2sp	0.7	0.006

TABLE 4

Star	Coordinate 1950	m	Sp	M
43 Cas	$1^h38^m36^s +67°47'$	5.5	A0p	+0.4
HD 10783	1 43 4 + 8 18	6.6	A3p	+0.7
HD 11187	1 48 10 +54 40	7 1	A0p	—0 2
21 Per	2 54 15 +31 44	5.2	A0p	+0 2
41 Tau	4 3 32 +27 28	5.3	A0p	+0.2
68 Tau	4 22 36 +17 49	4.2	A2	+1.1
μ Leo	5 10 41 — 16 16	3.3	A0p	—1.3
HD 45677	6 25 59 —13 1	7.5	B2e	—2.2
3 Hya	8 33 2 — 7 48	5 6	A2p	+1.1
49 Cnc	8 42 2 +10 16	5.6	A4p	+0.6
k Cnc	9 5 2 +10 52	5.1	B8p	0.0
1 Cen	12 37 10 —39 43	4.8	B8p	+0.3
γ Vir	12 39 7 — 1 10	2.9	F0p	+0.2
HD 125248	14 15 52 —18 29	5.7	A0p	+0.6
i CrB	15 59 26 +29 59	4.9	A0p	+0.2
HD 171586	18 33 8 + 4 54	6 7	A2p	+0.8
10 Aql	18 56 29 +13 50	5.9	A3p	+0.9
HD 188041	19 50 42 — 3 15	5.6	F0p	+0.3
HD 192913	20 14 3 +27 37	6.6	A0p	+0.5
β Scl	23 30 18 —38 6	4.5	B9p	+0.3

Finally, Fig.1,C is a graph plotted on the basis of the data from Table 4. The material for it was taken from the catalogue of P.P.Parenago at the Shternberg State Astronomical Institute (GAISh). The pattern is again analogous to the preceding one but less clearly expressed.

We obtain the same result when using trigonometric parallaxes and spectral classes, which we determined with respect to hydrogen lines and lines of ionized calcium (with respect to line depth and equivalent width), taken from Table 1. Figure 2,A shows a diagram with the abscissa giving the spectral class de termined from the equivalent broadening of the hydrogen lines (black dots) and /195
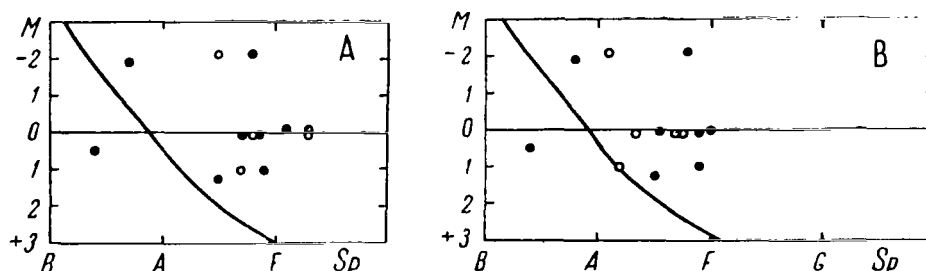

Fig.2 Spectrum of Magnetic Stars as a Function
of Absolute Magnitude
A – Obtained from trigonometric parallaxes. Dark dots:
spectral class, determined with respect to equivalent
broadening of hydrogen lines (Bibl.1). Light dots: with
respect to equivalent broadening of CaII lines (Bibl.1);
B – Obtained from trigonometric parallaxes. Dark dots:
spectral class, determined with respect to depth of
hydrogen lines (Bibl.1). Light dots: with respect to
depth of CaII lines (Bibl.1)

equivalent broadening of the lines of ionized calcium (light dots). On the ordinate, the trigonometric parallaxes from Table 2 are laid off. A similar diagram is shown in Fig.2,B, but here we used spectral classes determined from the depth of these lines (as in the preceding case, black dots pertain to hydrogen and light dots to the lines of ionized calcium). There is no detectable difference between the spectrum-luminosity curve relative to hydrogen and the spectrum-luminosity curve relative to the CaII lines, compared to our preliminary investigation. All these data, in our opinion, justify a classification of magnetic stars with a certain sequence located somewhat higher than the main sequence. However, we were unsuccessful in an attempt to find a correlation between the deviations of our spectral classes and the difference in absolute magnitudes of magnetic stars and the main sequence. This indicates that the effect of luminosity plays a negligible role in reducing the intensity of the hydrogen lines. This could be expected, since the sequence of magnetic stars is apparently located only slightly higher than the main sequence. For lack of observational data, it is difficult to define the true reason for the decrease in intensity of the hydrogen lines of certain magnetic stars.

The author wishes to thank G.A.Starikova who transmitted the necessary data

from the catalogues from GAISh.

BIBLIOGRAPHY

1. Glagolevskiy, Yu.V.: Spectrophotometry of Magnetic Stars (Spektrofoto-
    metriya magnitnykh zvezd). Trudy Sekt. Astrobotan., Vol.VIII, Alma-Ata,
    Izd. Akad. Nauk KazSSR, 1960.
2. Tai, N.: MN, Vol.100, p.94, 1939.
3. Schlesinger, F.: General Catalogue of Stellar Parallaxes. Yale Univ.
    Observ., 1935.
4. Jenkins, L.: General Catalogue of Trigonometric Stellar Parallaxes, 1952.
5. Adams, Walter S.: The Spectroscopic Absolute Magnitudes and Parallaxes of
    4179 Stars. Contributions from the Mount Wilson Observ., No.511, 1935.
6. Babcock, H.W.: Magnetic Fields of the A-Type Stars. Astron. J., Vol.128,
    No.2, 1958.
7. Babcock, H.W.: Remarks on Stellar Magnetism. Publ. Astron. Soc. Pacific,
    Vol.59, p.112, 1947.

I.D.Kupo

1. Results and Problems of Investigating χ Ophiuchi

The star χ Ophiuchi still figures in the catalogues of Flemsted and Johnson published at the beginning of the 19th Century. However, as far as the author knows its variability was first suspected by Guldt at Uranometria, Argentina. In 1873, Guldt assigned to it a mean visual magnitude of $4^m.6$; however, in comparing with the data of various observers, he concluded that the star is probably variable. Thus, Argelander (1855) and Hays gave it a magnitude of 6^m, while Yarnell in 1865 estimated its magnitude as $4^m.5$. In the Revised Harvard Photometry, the stellar magnitude of χ Oph is given as $4^m.85$.

Since the 1870's, there have been eleven series of observations of the brightness of this star, which differed widely both with respect to the number of estimates (from 1 to 120) and to the method, including visual estimates, Pickering observations with a meridian photometer, and photographic data. In 1949, Ashbrook published a review of these observations, reducing them to the visual Harvard system (Bibl.15) on the basis of which he drew a conclusion about very slow, discontinuous changes in brightness and the inexpediency of systematic observations of the star.

For some unknown reason, Ashbrook in his review did not use the material of the American Association of Variable Star Observers AAVSO (Bibl.16), which included 83 estimates of brightness obtained during the period from June 28, 1946 to January 13, 1947.

The observations of AAVSO, carried out in some kind of strange photometric system, are nevertheless of considerable interest in connection with the fact that on some nights there are several estimates of stellar brightness, frequently made by one and the same observer. From our point of view, of special interest is the fact that, in three cases, the estimates of a single night differ by a magnitude of $0^m.5$ and of three nights by $0^m.3$, which is difficult to ascribe to observation errors since the latter, in experienced observers, generally do not exceed $0^m.10 - 0^m.15$.

Beginning in the 1950's Cousins in South Africa has been searching for new variable stars in the southern sky (Bibl.17, 18). The observations are being carried out by the Fabry method with a standard error of one measurement of $0^m.012$. The star χ Oph, which is included in this program, showed a fluctuation in brightness of an amplitude of $4^m.32 - 4^m.45$.

According to the reviewed data, in the second edition of the General Catalogue of Variable Stars (Bibl.1) the stars are designated as novalike.

Based on its elements of proper motion, χ Oph belongs to the Scorpius-Centaurus association (Bibl.19). The absolute magnitude of the star was deter-

mined by several methods. Blaauw, from an analysis of the proper motions of the stars of the Sco-Cen cluster obtained a value of $M_{v1s} + A_v = -1\overset{m}{.}45$ (Bibl.20). Assuming, according to Blaauw (Bibl.19), a visual interstellar absorption of $A_v = 1\overset{m}{.}9$, we find $M_{v1s} = -3\overset{m}{.}35$.

Ramsey, on the basis of spectral observations, obtained $M_{v1s} = -2\overset{m}{.}5$ (Bibl.21, 22). However, Stebbins, Huffer, and Whitford obtained a mean absolute visual magnitude of stars of class B3 of $2\overset{m}{.}2$ (Bibl.23). It is known that emission stars are always somewhat brighter than stars of the same subclass containing only absorption lines, since the latter value more closely corresponds to the data by Blaauw and Ramsey. Finally, if we take the value of the spectral parallax from the Yale Catalogue (Bibl.24) $\pi = 0''.005$ and the visual stellar magnitude $3\overset{m}{.}3$ corrected for interstellar absorption according to Duke (Bibl.21), we obtain $M_{v1s} = -3\overset{m}{.}2$ which is in good agreement with the above data.

The average value of the first, second, and fourth determinations of the absolute brightness is $-3\overset{m}{.}0$, which means that the star certainly lies on the main sequence in the spectrum-luminosity diagram. The new classification of the spectrum of χ Oph B3 V-pe, cited in the second edition of the General Catalogue of Variable Stars (Bibl.1) is in complete agreement with what has been said. From this viewpoint, the classification by Slettebak and Howard of B2 IV-p is completely unfounded (Bibl.25).

In 1896, Campbell and Albrecht discovered a bright double emission for H_λ (Bibl.26). Measurements of the radial velocity, performed by these authors and by Burns and Wright in 1896 and 1902, showed changes in radial velocity of the star within limits from -10 to +22 km/sec. Observations in 1925 (Bibl.27) confirmed the variability of the radial velocity of the star. Furthermore, on August 13 two spectrograms taken an hour apart showed a change in radial velocity by 9 km/sec. Unfortunately, the accuracy of determining the radial velocities is not indicated in that report, but it can be imagined that such a value exceeds the error.

The measurement of radial velocities becomes rather difficult at the complex line structure in the spectra of Be stars. Furthermore, the results in many respects depend on the selected method of measurement. Since the general appearance of typical spectral lines of Be stars represents emission superposed on a broad absorption line, which in turn is divided into two components (violet V and red R) by narrow and sharp absorptions, the measurement of radial velocities is performed by three methods:

   a) By sighting the thread on the outer ends of the wings of the broad absorption line which, on averaging the result, characterizes the absorption of the center of this line that pertains to the reversing layer of the star.

   b) By sighting the filament on the core of the emission components V and R, which will give information on the rotation of the emitting zone.

   c) By sighting the filament on the sharp central absorption line.

The last method, which is most convenient for accurate sighting was used in the above-mentioned investigations. This method yields the difference in the radial velocities of the central absorption layer and emission zone of the star.

In the great majority of Be stars there are changes in the relative intensity of the hydrogen emission components V/R, these changes always being associated with a shift in central absorption, i.e., apparently, in radial velocity. When the central absorption line is shifted toward the short-wave end, the intensity of the violet component V will decrease while the intensity of R increases, and vice versa. That we are actually dealing here with radial velocity and not /198 with geometric "filling" of the absorption line by intensified emission is confirmed, according to Curtiss (Bibl.28) by the lateral shift of the emission line as a whole, almost by the same value. Thus, the value of V/R is a convenient characteristic for the changes in radial velocity, measured from the central absorption.

Cleminshaw (Bibl.29), on the basis of 113 spectrograms taken in 1913 and 1923 - 1934, constructed the radial velocity curves for χ Oph from the emission lines of hydrogen and FeII and from the helium absorption lines. He found that:

a) The radial velocities with respect to all elements show a definite fluctuation with amplitude, exceeding 20 km/sec, with a highly doubtful indication of a 10-year periodicity for H and FeII. He I showed no periodicity.

b) The average radial velocities with respect to lines of different elements do not coincide and fluctuate from +8 km/sec for FeII to -15 km/sec for helium triplets; the average velocity with respect to the hydrogen lines is -1 km/sec.

c) A curious fact is the divergence of radial velocities for triplets and singlets of He. For the former, the average radial velocity is equal to 15 km/sec, whereas for singlets it is +7 km/sec; in addition, the radial velocity curve of singlets lags about one year behind the triplets. The physical principle of this phenomenon has not yet been established.

d) The radial velocity curve with respect to helium is not in phase with those for H and FeII.

e) Brief changes in radial velocity, possibly of an irregular character, are observed.

An examination of the curves given in the paper by Cleminshaw raises considerable doubt as to the reality of any period of variation in radial velocities. One could say that this is due to the relatively brief observation period, but this series is the longest and most systematic of all, so that it is impossible to supplement it by other observations. Therefore, at this stage it might be best to assume irregular velocity fluctuations of the star.

In 1952, Burbidge investigated two diffraction spectra of high dispersion of the star χ Oph, obtained for the visible and near-infrared regions. The measurements of the shifts of the emission components for lines of the Balmer and Paschen series, and the lines FeII and OI, give close values of radial ve-

locities, corresponding to -15.1 (average for all H lines), to -12.8, and to -18.5 km/sec. The average velocity based on the absorption lines of helium is doubtfully estimated as -19.2 km/sec. Unfortunately, in Burbidge's work which was performed with a high degree of accuracy, only one observation was actually used, which makes it impossible to compare it with Cleminshaw's work cited above. The method used by Burbidge in determining radial velocities yields an indirect characteristic of the shift in central absorption relative to the emission line; therefore, it is of interest to define whether the coincidence of the radial velocities for the lines of various elements is a law common to the average of numerous observations (in contrast to the data obtained by Cleminshaw for the shift of the emission line as a whole) or a random phenomenon. The former assumption, from our point of view, is more probable. Apparently, emission and both types of absorption lines have their own autonomous laws of shifts. Consequently, the divergence in phases between the radial velocity curves of H and FeII on one hand and HeI on the other, indicated in Cleminshaw's work, is not surprising. Actually, the former were obtained for the geometric center of the emission lines, whereas the curve for HeI pertained to broad   /199 absorption lines of the reversing layer, usually for stars of the B class. The expressed hypothesis is in agreement with the results obtained by Hynek (see Bibl.30) who, in the spectrum of ω Per, found independent changes of radial velocities for all three types of lines.

The spectrum of χ Oph also showed CaII lines of interstellar origin. Adams observed a splitting of the H and K lines of CaII into two components, with a shift of -11.1 and -27.5 km/sec. He suggested that this was due to the fact that the light of the star on its way to earth passes through two clouds of interstellar calcium having different velocities with respect to the line of sight (Bibl.31).

The work of Burbidge (Bibl.32) touched upon another interesting problem concerning the type of rotation of χ Oph. As is known, the considerable widths of the absorption lines of the reversing layer, observed in Be stars (with the exception of the hydrogen lines), are usually explained by the rapid rotation of these stars. Doubling of the emission lines is caused by rotation. It is evident that, with a random arrangement of the axes of rotation of stars in space, these effects will be manifested differently depending on the magnitude of the radial components of the velocity of rotation, vsini. Thus, the width of the absorption lines of a Be star serves as a characteristic of the inclination of its axis to the line of sight. Based on this viewpoint, the concepts of "pole-on stars" and "shell-stars" have been introduced. Stars which have single emission lines of hydrogen as well as moderate sharpness of the absorption lines of the reversing layer are referred by Slettebak to "pole-on stars" (Bibl.33). The hydrogen absorption lines cannot serve as a characteristic of the velocity of rotation since their broadening is mainly due to the Stark effect rather than to rotation.

The problem as to which of the indicated types one should refer a particular star is not of scholastic importance. If one holds to the most widespread hypothesis of a "gaseous ring", meaning that the shell is not spherical but greatly elongated in the equatorial plane of Be stars with almost zero thickness at the poles, then the degree of inclination of the axis will indicate the extent of which the shell can affect the stellar spectrum. The usefulness of this

indication for interpreting the spectrum and its changes is obvious.

The spectrum of χ Oph, as indicated by several authors (Bibl.34, 35) has unusually narrow hydrogen emission lines. Apparently, this was the basis used by Slettebak for referring the star to the type "pole-on stars", which is a designation rather firmly entrenched in the literature. However, as long ago as 1932 McLaughlin, basing his investigation on spectra of moderate dispersion, detected doubling of the bright lines Hγ, Hδ, Hε (Bibl.36).

Slettebak, in comparing the observed profile of the lines HeI 4026 with those calculated for various radial velocities, obtained a value for the radial component of the velocity of rotation of the star of vsini = 115 km/sec (Bibl.37, 25) which, at an average velocity of rotation of Be stars of 300 to 400 km/sec, corresponds to an inclination of the axis of χ Oph to the line of sight of 15 - 20°, i.e., a fully perceptible value.

Burbidge investigated the degree of separation of the emission components V and R, for lines of various elements (Bibl.32). He found that the average distance of the components from the Balmer and Paschen lines is equal to 110 km/sec, at satisfactory internal agreement of individual measurements. For hydrogen, this yields a value of vsini = 55 km/sec. This value, with respect to the emission lines FeII and OI, is equal to 70 and 42 km/sec, respectively. These figures indicate a stratification of the elements in the stellar atmosphere; if the angular velocity of rotation of the star retains its value also for the outer layers, then the FeII lines will obviously occur in deeper portions of the emission zone than the hydrogen lines and still deeper than the oxygen lines. /200

The first to draw attention of observers to the anomalies of the spectrum of χ Oph was King, who reported that "one line is bright and the absorption lines are doubled". Fleming (Bibl.39) in 1890 noted a bright Hε in the spectrum of the star and that, as a whole, the spectrum was similar to that of δ and μ Cen. In 1895, Campbell reported that, according to the observations at Mt. Hamilton, the Hγ line shows strong emission (Bibl.40). In 1896 Campbell and Albrecht, as already mentioned, discovered doubling of the bright Hγ line (Bibl.26). Separation of the components on June 30, 1896, reached 1.37 Å and on July 1, 1.53 Å (Bibl.41). Further observations by Fleming and by Cannon showed that Hβ, Hγ, Hδ, Hε, and Hζ are fine emission lines superposed on broad absorption lines (Bibl.42, 43) and that there are other emission lines in the spectrum (Bibl.44). Later, a number of authors [McLaughlin, Struve and Swings, Merrill (Bibl.36, 45, 46)] established that most of the nonhydrogen emission lines belonged to ionized iron. The presence of very broad MgII emission lines 4481 was also established (Bibl.47, 45). Of the absorption lines, according to Struve (Bibl.45), singlets and triplets of neutral helium and also a series of weak lines belonging to OII, CII, SiIII are observed with certainty. In the infrared portion of the spectrum, the emission of CaII and of OI has been detected (Bibl.32, 38, 48). Struve (Bibl.45) gave the width of the emission lines of hydrogen, FeII and MgII as

Line	$H\beta$	$H\gamma$	$H\delta$	FeII	MgII
Width of line	3 Å	2.6 Å	2.3 Å	4.1 Å	5.7 Å

Since the width of the emission lines is proportional to the velocity of rotation, we can draw the following conclusions, again using the law of the constancy of the moment of rotation:

1. The emission of MgII occurs in lower portions of the emission zone than that of FeII and hydrogen;
2. The hydrogen lines occur at various heights of the emission zone, the lines with a lower excitation potential coming from deeper layers.

This leads us to a very important question: It is a fact that the known dependence of the width of emission lines on the ionization potential of Wolf-Rayet stars is manifested precisely in the above sense: The greater the ionization potential, the narrower will be the emission bands of the corresponding ions. However, an interpretation of this phenomenon proposed by Mensel and Bils (Aller, Astrophysics, Vol.II, p.183) leads to completely contradictory conclusions. Mensel and Bils consider that gases in the envelopes of Wolf-Rayet stars move outward at an accelerated rate and that the width of the bands is caused by the Doppler effect. In this case, the ions with a higher ionization potential are located in deeper layers of the envelope, a conclusion completely contradicting that cited above for the case of Be stars. This means that either the laws of the distribution of atoms in the stellar atmosphere are contradictory for cases of excitation and ionization, or one of the explanations is false. Thus, for Wolf-Rayet stars we can obtain the opposite results if we ascribe a negative velocity gradient to the atmosphere. As for the Be stars, to make the facts agree we would have to reject rotation as the exclusive (or at least the predominant) factor of line broadening.

Let us examine separately the characteristics of the behavior of lines of various elements.

a) Hydrogen

In 1932 Merrill, Humason, and Burwell noted that, whereas the lines from Hγ to Hδ show a visual emission intensity decreasing with an increase in the number of the line, the ultraviolet lines from Hζ to Hk are observed in absorption and are very weak (Bibl.49). Cleminshaw detected a change in the widths of emission lines of hydrogen (Bibl.29). The curve of the width of Hβ, plotted on the basis of 107 measurements connected at mean annual points, showed good agreement with the mean annual curve of radial velocities. The widths of Hγ and Hδ show only negligible changes. The meaning of the changes of the curve of Hβ is this: The greater the approach velocity obtained from the shift of hydrogen emission, the narrower will be the emission at Hβ. It is assumed that a physical explanation for this fact can be given only on the assumption of a change in effective height of the emission layer of Hβ in the atmosphere, at a positive velocity gradient. In this connection, it would be of interest to check the indicated correlation for short-term fluctuations of the line width and radial velocities for both individual lines and the average for a given element.

The Be stars show two types of changes in lines:

233

a) A change in relative intensity of the emission components V/R.

b) A change in emission intensity with respect to the continuous spectrum E/C.

Most observers [McLaughlin (Bibl.36, 50), Ashbrook (Bibl.51)] note that the ratio V/R for χ Oph changes extensively, but rarely is greater than unity, whereas the total intensity of emission shows no noticeable changes. True, these conclusions are obtained on the basis of individual evaluations. Quantitative data on equivalent widths may lead to a radical revision of these statements. However, reference is made here to the interesting fact noted by McLaughlin (Bibl.36) that in many (it is not known, of course, whether in all) stars of the Be type with a variable total emission E/C, the violet component of the emission line is more intense. If this characteristic should have the character of a law, whose physical meaning is still vague, there will be no reason to expect a change in E/C for χ Oph.

As already stated, at an appropriate dispersion the emission lines will double. However, McLaughlin who worked with a moderate dispersion (Bibl.36) noted that Hγ is even resolved into three emission components. We must assume that the third component occurs sporadically, since no other observers have noted it.

Burbidge, using the Hiltner photograph of May 13, 1951 (dispersion 4.8 Å/mm) detected a third emission component for Hβ (Bibl.32). This was located midway between the normal components V and R, and the intensity was approximately equal to V at a shift of −15.8 km/sec, which closely corresponded to the mean velocity based on the Balmer and Paschen lines on the same negative, equal to −15.1 km/sec. No third component was observed in higher members of the series. Hα was so wide that it was impossible to distinguish any structure. Burbidge considered that the third component could occur in portions of the envelope where the Balmer decrement was steeper than in the usual emission zone. However, such an assumption can be confirmed only by discovering the third component in Hα. The sporadic occurrence of the third component of emission in Hγ, which is not always simultaneous with the manifestation of this characteristic in Hβ, evidently complicates matters even more.

Burbidge, on a diffraction infrared spectrum with a dispersion of 17 Å/mm, was the first to resolve the lines of the Paschen series into two components (Bibl.32). Their separation did not differ from that for lines of the Balmer series. Both for the Balmer and the Paschen lines, the red component of emission was somewhat more intense than the violet, which is in good agreement with the above results by McLaughlin.

b) Oxygen

Of the oxygen lines in the spectra of Be stars, we observed λ 8446 Å ($3^3P - 3^3S$) and λ 7774 ($3^5P - 3^5S$); their behavior is an interesting point. It was found that λ 8446 Å emits much more readily than OI 7774. On the other hand, the absorption of λ 7774 Å in the spectrum of star envelopes is appreciably more intense than λ 8446 Å. Rather frequently, OI 8446 is observed in

emission whereas λ 7774 Å gives an absorption line. Hence, it is obvious that the behavior of these lines is an independent indicator of the classification of stars with respect to the two above types. Actually, the absorption of OI 7774 will be stronger in "shell-stars". This means, if OI 8446 is observed in emission and OI 7774 in absorption, the star can be considered a "shell-star". If both lines give emission (of course, unequal in intensity), we can conclude that the axis of the star is inclined only little to the line of sight.

What is the physical principle underlying these phenomena? It is known that, in shells of large radius where the dilution of radiation is sufficiently great, the absorption lines with metastable levels are more intense than lines whose lower level is ordinary. This is understandable because of the fact that in a field of diluted radiation and in the presence of relatively little excitation, the ordinary levels will be rapidly discharged by successive transitions, whereas at the metastable levels the electrons will accumulate, leading to an overpopulation. This explains the outwardly abnormal behavior of the lines TiII, MgII, He in certain spectra. The lower level of λ 7774 Å 3^5S is partially metastable so that, in the spectra of "shell-stars", this line should be more intense. As for the emission at λ 8446 Å, Bowen proposed a mechanism of resonance absorption for its explanation (Bibl.52, 53). The essence of this is as follows: The transition OI $2^3P - 3^3D$ gives a wavelength of 1025.766 Å, whereas the wavelength of Lβ is 1025.717 Å. If the emission at Lβ is intense, resonance absorption will cause the population of the level 3^3D_n of oxygen to increase. Reverse transitions $3^3D - 3^3P$ will yield emission λ 11287 Å and will lead to an overpopulation of 3^3P, the upper level for emission λ 8446 Å. For a graphic explanation of this mechanism, we are showing Grotrian's diagram for OI (Bibl.53) in Fig.1.
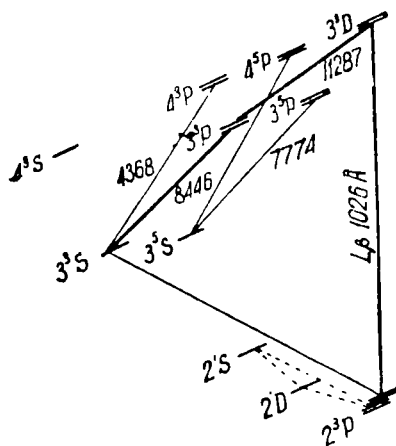
Fig.1

Thus, the appearance of emission at λ 8446 Å characterizes the intensity of emission at Lβ. Since the behavior of the Balmer series should resemble the behavior of the Lyman series, we can expect a correlation between the intensity of the Balmer lines and the intensity of λ 8446 Å. This dependence, which is especially well defined for Hβ, is actually observed. Only apparently, the relative intensity of Lβ is appreciably higher than that of Hβ.

Bowen's mechanism could be checked if it were possible to observe the infra-red line λ 11287 Å.

The oxygen line in the spectrum of χ Oph was observed by Hiltner (Bibl.48), Slettebak (Bibl.38), and Burbidge (Bibl.32). Emission at λ 7774 Å is very weak in conformity with Bowen's mechanism and with the available information on the inclination of the axis of rotation of χ Oph. As we see, the effect of the shell is little noticeable.

As mentioned before, Burbidge was able to resolve λ 8446 into two components based on the degree of separation, of which the emission zone of OI apparently is more remote from the star than the emission zone of hydrogen. It should be noted that this does not fit into the above-indicated scheme of stratification in relation to the excitation coefficient, since the latter is smaller for OI than for hydrogen. The red component of OI 8446 is much more intense than the violet, unlike the H and FeII lines for which V/R is only slightly less than unity. This fact has not yet been explained. Possibly, it has to do with an analogous structure in the Lyman series, but the physical picture of this conformity is extremely difficult to present.

c) Iron

The emission lines of ionized iron are characteristic of the spectrum of χ Oph, second in intensity after the hydrogen lines. They are also resolved into two components, of which the red is only somewhat more intense than the violet. One anomaly is observed (Bibl.45): of the two weak lines FeII 4523 [b^{4}F$^1_3$ − α^{4}D$^1_2$] and FeII 4508 [b^{4}F$^1_2$ − α^{4}D$^1_1$], the first is more intense, whereas in the laboratory spectrum the opposite is true.
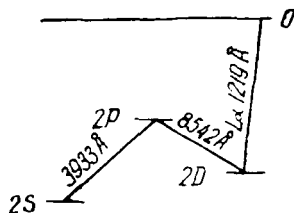
Fig.2

On the basis of preliminary data obtained as the result of spectrophoto-metry of several Be stars, Butler (Bibl.54) suspected a proportionality of the emission of FeII to the intensity of the emission at Hα. It is of interest to check this fact for stars with a variable intensity of emission. Anticipating the result, we can state right here that our data for χ Oph permit no final conclusions.

d) Calcium

The question of the presence of CaII in χ Oph is disputable. According to

various authors (Bibl.31, 29, 32), the ultraviolet doublet H and K of CaII, which is observed in absorption, has an interstellar origin. It has not been established whether the infrared emission triplet of CaII (λ 8662, 8542, 8498 Å), which is often encountered in Be stars along with absorption at H and K is observed in χ Oph, since the lines of the triplet are close to the very intense lines of the Paschen hydrogen series.

Wyse proposed a mechanism for the coexistence of ultraviolet absorption /204 and infrared emission of the ion CaII in stellar atmospheres (Bibl.55). His explanation yields Fig.2, taken from his paper.

The state $3d^2D$ is metastable, and in order for emission to occur some other transition should exist besides $4p^2P$ which reduces the population of the metastable level. Wyse believes that ionization from the ^2D level, produced by Lα whose energy is only slightly greater than the ionization energy of CaII from this state, represents such a transition.

Comparing this mechanism with that proposed by Bowen for oxygen, it seems that the behavior of the infrared emission of OI and CaII permits an evaluation, in particular, of the Lyman decrement Lα:Lβ. The enormous magnitude of this quantity, and especially its changes, is obvious.

A number of authors (Bibl.23, 56, 57) made photoelectric determinations of the color of χ Oph; none of these were made separately but always together with other stars. The results are given below.

Stebbins (Bibl.23)			Schilt and Jackson (Bibl.56)			Oosterhoff (Bibl.57)		
$C\cdot I$	n	E	$C\cdot I$	n	E	$C\cdot I$	n	E
$-0.^m02$	—	$+0.^m17$	$-0.^m01$	7	$+0.^m20$	$0.^m00$	3	$+0.^m19$

Here C·I and E are the color index and color excess, reduced to the system of Stebbins, Huffer, and Whitford (Bibl.23). The effects of the wavelengths of Stebbins' system are λ 4260 and 4770 Å; n is the number of observations from which the result given in the Table was obtained.

Thus, in Stebbins' system the color index of χ Oph is close to zero with a good internal consistency of the results. This is contradicted by the results of Tsoi Dai O (Bibl.2) who determined the absolute spectrophotometric gradient of the star for the region λ 3650 – 4650 Å. He obtained $\phi_1 = 1.51 \pm 0.16$, which leads to a noticeable positive color index. Correction for selected interstellar absorption reduced the gradient to only 1.14, i.e., to a value corresponding to the gradient of α Lyr(Ao). Obviously, the abnormally red color of χ Oph cannot be explained by external causes. Furthermore, χ Oph remains one of the reddest stars among those investigated by Tsoi Dai O, being somewhat inferior only to χ^2 Ori[*].

---

[*] For footnote see following page.

The Balmer discontinuity of χ Oph, found by the above author, proved to be equal to -0.03 ± 0.01. In the list by Tsoi Dai O, only three stars out of forty of the investigated objects of classes Be and B show a negative value of discontinuity. Two of them belong to class B0e, one of them is the well-known γ Cas and the third star is χ Ophiuchus.

The increase in intensity beyond the limits of the Balmer series points toward the existence of either a rather dense envelope or an intense continuous emission that distorts the ultraviolet spectrum of the star. /205

The presence of continuous emission in the spectrum of χ Oph, just as in γ Cas, was detected by Ch'ing Sung Yu in 1927 (Bibl.58), who noted the relation between the intensity of this emission and the intensity of emission at H^a and its absence or extreme weakness in stars with brightness $H\alpha$ and absorption in the remaining hydrogen lines. There was a change in the intensity of continuous emission in the spectrum of star f' Cyg, which occurred parallel to the changes suffered by the emission at Hβ. Ch'ing Sung Yu confirmed that the intensity of the continuous emission increases from the last visible Balmer line to the boundary of the series, after which it begins to drop off according to the law ν^{-3}. Its maximal value in χ Oph is about 22% of the intensity of the continuous spectrum at the given point (Bibl.59). Karpov (Bibl.60), in studying the hydrogen emission of B0 – B5 stars, detected a rise in intensity of the continuous spectrum at the boundary of the Balmer series, which correlates with the intensity of the emission lines. This phenomenon was detected only for stars earlier than B4e. Burbidge also noted continuous emission in the spectra of certain Be stars (Bibl.33). One gains the impression that this phenomenon is rather frequent in stars of the Be class. True, we cannot say for certain what the interrelation might be between the excess continuous emission in the ultraviolet of Be stars and the phenomenon which bears the same name and has been the main concern of researchers on late variable dwarfs.

Polarization in the integrated light of χ Oph was detected by Hall and Mikesell (Bibl.61) and van Smith (Bibl.62). In the first case, polarization was found to be 0.4% (based on two observations) and in the second case 1.8%, i.e., negligibly small in both cases. The question concerning the changes of this value remains open in view of the sparse material.

e) Resumé

All of the observational material pertaining to the star χ Ophiuchus known to the author was examined in the present Chapter. Summing up, we emphasized

---

* If this is the case, the absolute magnitude cited at the beginning of the Chapter is overestimated since it was determined on the assumption that the entire color excess is due to interstellar absorption. However, even an overestimation by one magnitude, produced if only half of the observed color excess is explained by interstellar causes, will still be within the dispersion of absolute magnitudes for the given subclass, which according to Parenago (Bibl.3) reaches ±0ᵐ.5. Consequently, the conclusion that the star belongs to the main sequence still holds.

certain characteristics of the star which require particular attention.

1. χ Ophiuchus is a star of the main sequence with a variable brightness, radial velocity, and – apparently – color.

2. The radial velocities obtained from the absorption lines of the reversing layer, emission component, and central absorption are different in value and, probably, in character of changes.

3. A difference is observed in the behavior of singlets and triplets of helium, which is expressed both in the difference of the mean values of v_r and in the shift of the phases of the radial velocity curves.

4. The curve of the changes in widths of the emission line of Hβ quite accurately osculates the radial velocity curve obtained from the hydrogen lines, whereas neither Hγ nor Hδ show such conformity.

5. A third component of the emission for Hβ and Hγ occurs sporadically. Unfortunately, it is not known whether this takes place in both lines simultaneously or independently.

6. The red component of the emission is somewhat brighter than the violet. An exception is the line OI 8446, for which this ratio is much greater.

7. The emission lines in the spectrum of χ Oph are very narrow. Although the star is not a typical "pole-on star", the effect of the shell on its   /206 spectrum is comparatively small, which follows from the absence of absorption at OI 7774 Å.

8. χ Oph is distinguished by intensive reddening, caused by the physical peculiarities of the star.

9. The negative value of the Balmer discontinuity indicates the possible presence of nonthermal continuous emission in the ultraviolet spectrum of the star.

10. Polarization of the integrated light of χ Oph is negligibly small.

The numerous observations bear a nonsystematic character. However, the resultant characteristics do show that the star is a highly interesting object for further investigations of an observational (with spectrophotometric inclination) as well as of a theoretical nature.

2. Methodics

The observations of χ Ophiuchus at the Astrobotany Sector were started in the summer of 1956. However, because of the great diversity of the negative material used, these data were not used in the final analysis. The material presented here was obtained from the beginning of May to August 1957. The observations were carried out on every clear moonless night, using the permissible hours of the selenian period. However, as a consequence of the extraordinarily

unfavorable and unusual summer at Alma-Ata, observations could be carried out only on 28 nights. To define the short-term changes in the spectrum of the star, photographs were taken every 30 min up to eight times per night. The observations were carried out by means of the Bredikhinskiy astrograph (D = 170 mm, F = 80 cm) and an objective prism $\omega = 17°$. As negative material we used Agfa Isopan ISS plates. The chromaticity curve of the Bredikhinskiy astrograph made it impossible to obtain a focal photograph over the entire length of the spectrum. Because of lack of time, it was also impossible to take photographs with a variable focus. Therefore, we selected a focus of 9.5 which yielded good definition of the spectrum up to about 5500 Å. Only relative measurements were possible in the longer-wave region of the spectrum under such conditions.

The negatives were calibrated by means of diaphragms attached to the telescope objective; beginning with the negative χ 25, a cruciform diaphragm with sectors of variable cross section was used. The photometric scales were obtained with respect to the star α Lyr on each observation night. The exposure, in fixing the scale, was approximately 1/10 that of the exposure in photographing the investigated region. However, according to data by G.A.Tikhov (Bibl.4), who investigated Agfa Isopan plates, such a divergence yields no more than a 12% error in the slope of the characteristic curves. When doubling the exposure time, no noticeable deviation from the reciprocity law was observed. Thus, this shortcoming of the method is not too serious.

The photographs taken in one night were obtained on sections of the same plate; on one negative was printed the scale, calculated such that the total exposure time of the scale-carrying negative was approximately equal to the exposure time of other negatives on which up to three photographs of the investigated region were obtained.

For standardization, the spectrum of α Lyr with the same diaphragm and <u>/207</u> the same exposure as that used for the investigated region was printed on each plate.

This made it possible to calculate the atmospheric attenuation of light which, when comparing α Lyr with stars in the region of χ Oph, is very substantial.

Along with the objective-prism spectra on the mirror-lens telescope AZT-7 with an ASP-9 slit spectrograph (dispersion 140 Å/mm for Hγ), we obtained one spectrogram of the star χ Oph on each of the eight nights. The dispersion of the slit and the objective-prism spectrograms coincided in accuracy. The purpose of simultaneous observations of the star by the methods of slit and prism spectrography was:

a) To obtain the Balmer decrement Hα:Hβ, which is impossible to do from prism spectra because of the chromatic aberration of the optical system of the Bredikhinskiy astrograph.

b) To compare the results of photometry of the lines: the profiles and equivalent width obtained with a prism and the slit spectrograph, used as a criterion for the significance of the data obtained by the first method.

The spectrograms were measured by a recording microphotometer MF-4 with × 7 magnification. For photometry of the lines, the spectra were rated on an MF-2 photoelectric microphotometer. On the spectrum, the slit of the micro- photometer cut out an area of 1 Å width in the region of the Hβ line. Points were also taken every 1 Å.

In all, for measuring the continuous spectrum we selected 126 spectrograms, on which, including the comparison star and α Lyr standard, we analyzed 331 spectra. For photometry of the lines, we used 120 spectra.

The conversion of blackening to intensity was done from the monochromaticity characteristics plotted every 100 Å. Curves similar in slope and position were interconnected. The spectra were analyzed alternately on the basis of 17 – 18 characteristic curves.

3. Investigation of the Continuous Spectra of χ Ophiuchi

The continuous spectrum is the basic characteristic of emission of a star. Its energy distribution is determined by physical conditions in the star and thus makes it possible to determine these conditions. Determination of the energy distribution in the stellar spectrum in absolute energy units is usually based on correlating the investigated spectrum with a well-calibrated terrest- rial source, which is a cumbersome task. For a number of problems of practical astrophysics, such as mass statistical investigations of the emission of stars or studies of the changes in the spectra of variables, etc., it is completely sufficient to know the spectral energy distribution of the investigated object with respect to that of a selected reference object. Such relative spectro- photometry is presently used in the majority of astrophysical work. Further- more, if, as comparison star, we select an object for which absolute measure- ments are available (for example, α Lyr), then it is not difficult to change to the absolute energy distribution in the spectrum of the investigated star.

Thus, in relative spectrophotometric work, the directly measured quantity is $\log \dfrac{I_{*\lambda}}{I_{\cap\lambda}}$, i.e., the logarithm of the ratio of monochromatic intensities of the investigated and comparison stars. Observations have shown that, in sufficiently large spectral ranges, this value is a linear function of the wave number $1/\lambda$. This has made it possible to introduce the concept of a relative spectrophotometric gradient for the numerical characteristic of continuous spectra, determined from the correlation

$$\Delta\Phi = -2.303 \frac{d\log\frac{I_*}{I_0}}{d\,1/\lambda} = -2.303\cdot H \tag{1}$$

and to then geometrically designate the tangent to the angle of inclination of the indicated line. Since, in spectral ranges up to a length of 1000 Å, the stellar emission is satisfactorily characterized by Planck's law,

$$I(\lambda, T) = \frac{C_1}{\lambda^5 (e^{C_2/\lambda T_c} - 1)} \tag{2}$$

then the spectrophotometric gradient has a single-valued connectivity with the so-called spectrophotometric temperature of the star

$$\Delta\Phi = \frac{C_2}{T_*}(1 - e^{-C_2/\lambda T_*}) - \frac{C_2}{T_0}(1 - e^{-C_2/\lambda T_0}),\qquad(3)$$

where T_* and T_0 designate, respectively, the temperatures of the investigated and comparison stars. The concept of temperature is purely formal here, since it serves only as a numerical characteristic of the energy distribution in the examined spectral range and has a physical meaning only in the case of black-body radiation of a star. The quantity

$$\Phi = \frac{C_2}{T}(1 - e^{-C_2/\lambda T})\qquad(4)$$

is known as the absolute spectrophotometric gradient. It is obvious from eq.(3) that, if the relative spectrophotometric gradient of the investigated star is determined from observation and if the absolute gradient of the comparison star is known, it is not difficult to determine the absolute gradient and temperature of the investigated object.

The comparison star in our work was HD 148898 ($m_{phot} = 4\overset{m}{.}85$; $m_{vis} = 4\overset{m}{.}57$, F0). Its spectrum was recorded on the plate simultaneously with the spectrum of χ Oph, which is one of the basic advantages of prism observations. Because of only a small difference in zenith distances of both objects, a calculation of the atmospheric attenuation of light was superfluous.

The relative spectrophotometric gradient of χ Oph was determined in the usual manner. Conditional equations of the type

$$\Delta\log I_\lambda = \frac{1}{\gamma}H + a\qquad(5)$$

were set up for 28 wavelengths, which were solved by the method of least squares.

Along with the gradients, we determined the standard deviation of the observed relative energy distribution in the spectrum of the star from a dependence of the type of eq.(5)

$$\varepsilon = \pm\sqrt{\frac{\overline{\varphi^2(1/\lambda)}}{n-1}},\qquad(6)$$

where $\varphi(1/\lambda) = 1/\lambda\,H + \alpha - \Lambda\log I$. This quantity characterizes the gradient /209 determinations.

The absolute gradient of the comparison star was determined by correlating it with the spectrum of ~ Lyr. For this purpose, we determined the relative gradient of HD 148898 with respect to α Lyr from each negative and then calculated the atmospheric attenuation of light by the method described elsewhere (Bibl.5); from the resultant corrected values for individual nights, we obtained the mean value of the relative gradient for the comparison star. The dispersion
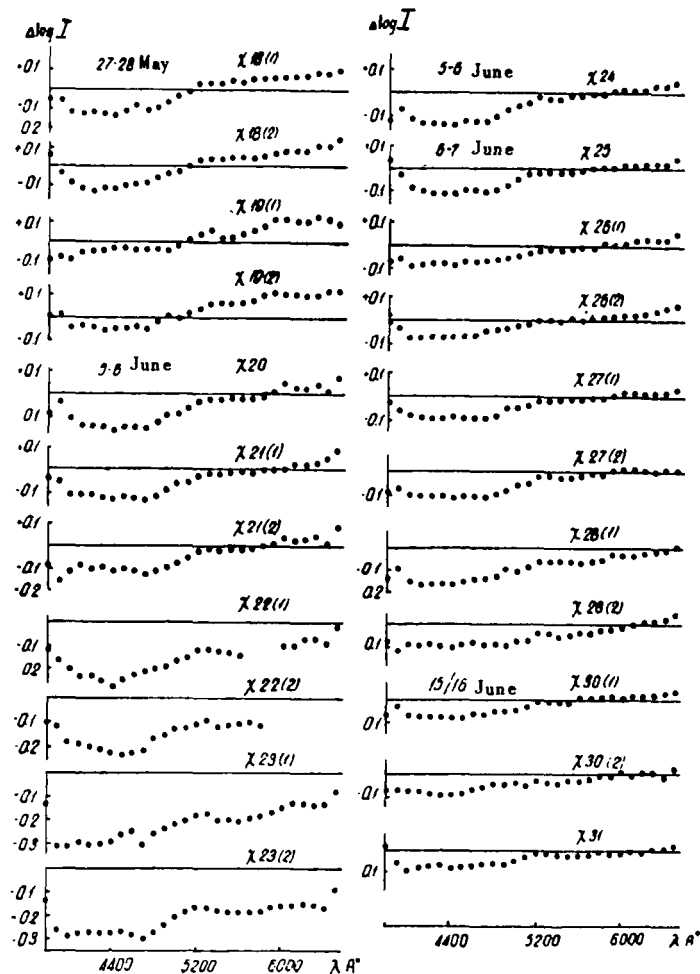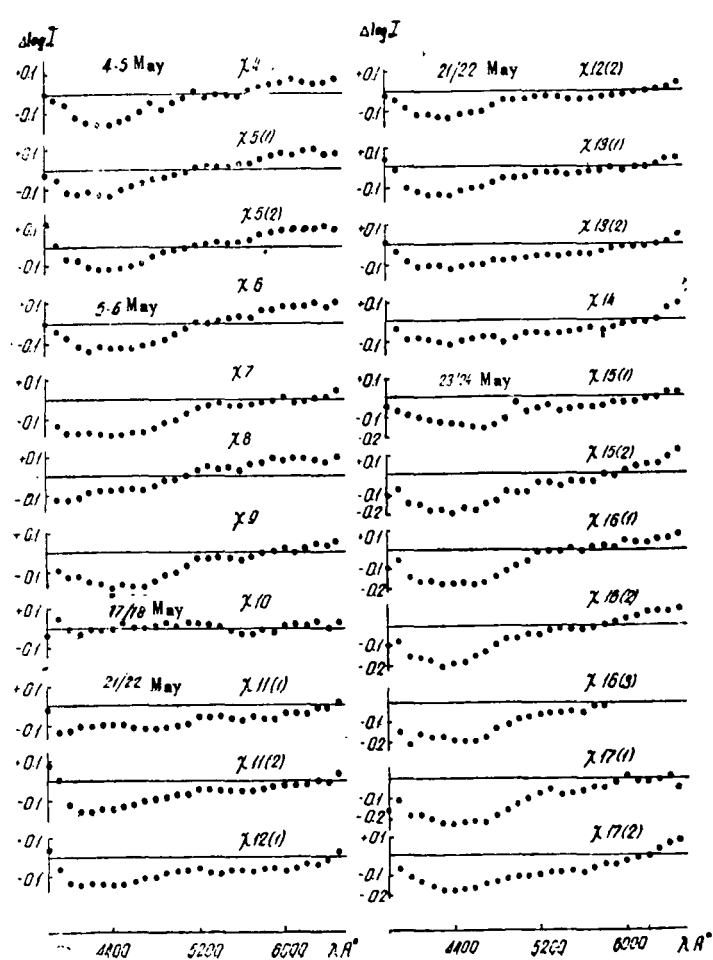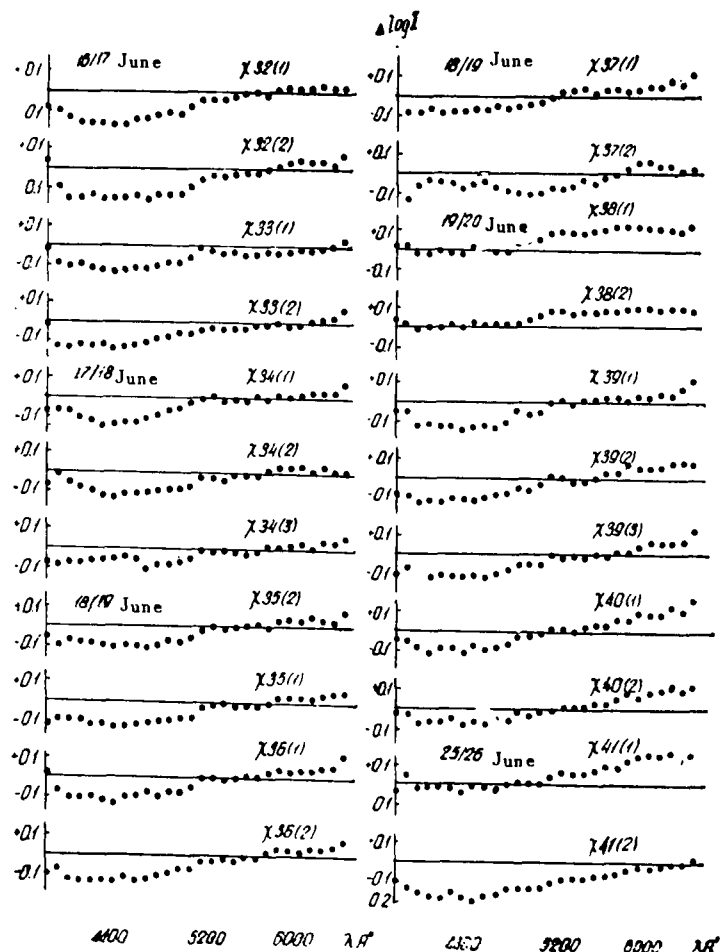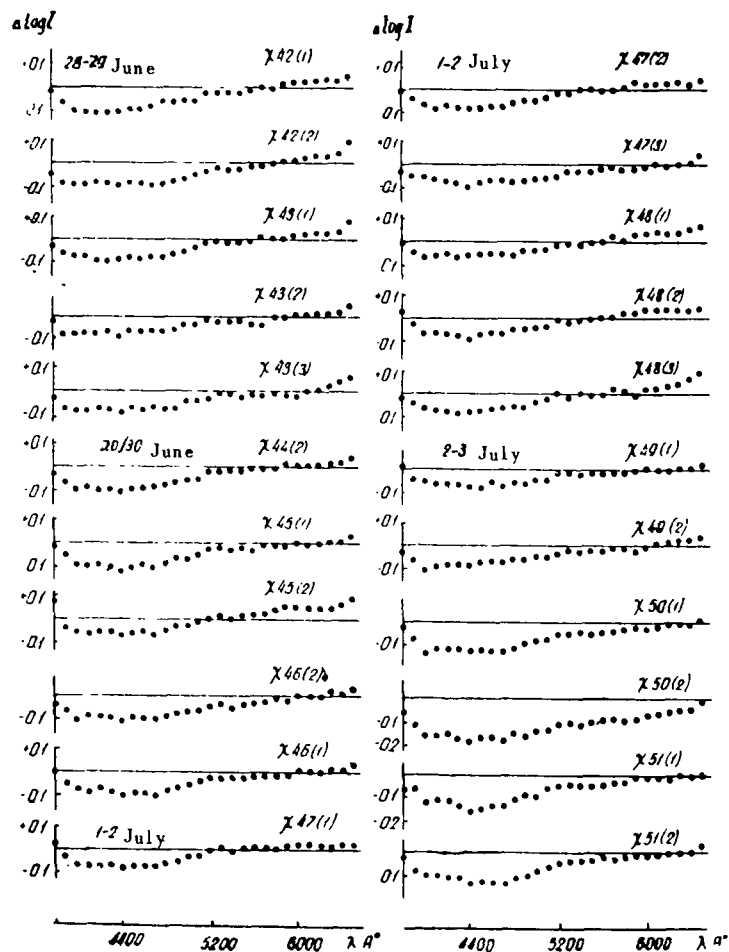
TABLE 1 /213

Negative	$I \cdot D$ 2435 ...	Φ_1 3800 - 4400	T_1 10^{-3}	Φ_2 4500 - 5200	T_2 10^{-3}	Φ_3 5300 - 6500	T_3 10^{-3}
1	2	3	4	5	6	7	8
χ4	963,3368	0,86	20,3	2,69	5,4	1,85	8,2
χ5 (1)	3660	1,86	11,0	2,39	6,1	1,86	8,1
χ5 (2)	3750	0,58	∞	2,47	5,9	1,88	8,0
χ6	964,3354	1,15	13,5	2,51	5,8	1,95	7,7
χ7	3660	1,74	8,4	2,59	5,6	1,66	9,4
χ8	3938	2,00	7,3	2,27	6,4	1,60	9,8
χ9	4257	1,25	12,2	2,57	5,7	1,84	8,2
χ10	976,2743	1,77	8,2	1,58	9,5	1,38	12,0
χ11 (1)	980,2813	1,81	8,0	1,67	8,9	1,65	9,4
χ11 (2)	3083	0,52	∞	2,14	6,8	1,70	9,1
χ12 (1)	3361	0,98	16,7	2,13	6,8	1,76	8,7
χ12 (2)	3604	1,29	11,7	2,38	6,1	1,62	9,6
χ13 (1)	3778	0,81	22,4	2,21	6,6	1,74	8,8
χ13 (2)	4014	1,18	13,1	1,88	7,8	1,89	8,0
χ14	4201	1,54	9,6	1,74	8,5	2,11	7,1
χ15 (1)	982,2632	1,43	10,4	2,38	6,1	1,76	8,7
χ15 (2)	2882	1,18	13,1	2,60	5,6	2,30	6,4
χ16 (1)	3160	1,28	11,8	2,84	5,1	1,78	8,6
χ16 (2)	3396	1,19	13,0	2,73	5,3	2,06	7,2
χ16 (3)	3611	1,90	7,7	2,76	5,3	1,08	18,0
χ17 (1)	3833	1,07	14,9	2,80	5,2	1,69	9,2
χ17 (2)	4042	1,13	13,8	2,05	7,1	2,22	6,7
χ18 (1)	986,2972	1,45	10,2	2,53	5,8	1,72	8,9
χ18 (2)	3194	0,97	17,0	2,54	5,7	1,84	8,2
χ19 (1)	3528	1,97	7,4	2,04	7,2	1,91	7,9
χ19 (2)	3750	1,47	10,1	2,34	6,2	1,69	9,2
χ20	995,2118	1,26	12,1	2,69	5,4	1,98	7,6
χ21 (1)	2458	1,35	11,1	2,39	6,1	1,93	7,8
χ21 (2)	2688	1,89	7,7	1,94	7,6	1,87	8,1
χ22 (1)	2917	0,88	19,6	2,66	5,5	1,86	8,1
χ22 (2)	3104	0,95	17,5	3,01	—	1,20	14,8
χ23 (1)	3313	1,26	12,1	2,40	6,0	2,10	7,1
χ23 (2)	3528	1,27	12,0	2,73	5,3	1,71	9,0
χ24	3729	1,67	8,8	2,60	5,6	1,81	8,4
χ25	996,2035	0,72	28,0	2,65	5,5	1,71	9,0
χ26 (1)	2333	1,64	8,9	2,29	6,3	1,74	8,8
χ26 (2)	2570	1,29	11,7	2,50	5,8	1,73	8,9
χ27 (1)	2785	1,35	11,1	2,65	5,5	1,65	9,4
χ27 (2)	2986	1,51	9,8	2,71	5,4	1,61	9,7
χ28 (1)	3194	1,38	10,8	2,59	5,6	1,72	8,9
χ28 (2)	3389	1,73	8,5	2,07	7,1	2,00	7,5
	2436...						
.χ30 (1)	005,1917	1,61	9,1	2,44	6,0	1,57	10,1
χ30 (2)	2167	1,61	9,1	2,24	6,5	1,65	9,4
χ31	2375	1,30	11,6	2,33	6,2	1,48	10,9
χ32 (1)	006,1979	1,29	11,7	2,69	5,4	1,84	8,2
χ32 (2)	2188	0,79	23,4	2,50	5,8	1,96	7,7
χ33 (1)	2417	1,21	12,7	2,73	5,3	1,54	10,3
χ33 (2)	2604	1,26	12,1	2,62	5,6	1,75	8,8
χ34 (1)	007,2222	1,21	12,7	2,90	5,0	1,64	9,5
χ34 (2)	2431	1,18	13,1	2,47	5,9	1,53	10,4
χ34 (3)	2722	1,91	7,6	1,94	7,6	1,75	8,8
χ35 (1)	008,1847	1,70	8,6	2,44	6,0	1,73	8,9
χ35 (2)	2042	1,59	9,3	2,38	6,1	1,67	9,3
χ36 (1)	2250	0,93	18,0	2,45	5,9	1,90	7,9
χ36 (2)	2451	1,52	9,7	2,55	5,7	1,94	7,7
χ37 (1)	2674	1,03	15,6	2,23	6,5	1,75	8,8
χ38 (1)	009,1875	1,64	8,9	2,50	5,8	1,41	11,6
χ38 (2)	2083	1,69	8,6	2,31	6,3	1,47	11,0
χ39 (1)	2285	1,15	13,5	2,86	5,1	1,84	8,2
χ39 (2)	2521	1,64	8,9	2,68	5,4	1,95	7,7
χ39 (3)	2729	1,61	9,1	2,70	5,4	2,07	7,2

TABLE 1 (cont'd)

/214

1	2	3	4	5	6	7	8
χ40 (1)	009.2924	1.49	9.9	2.63	5.5	2.23	6.6
χ40 (2)	3132	1.48	10.0	2.42	6.0	2.12	7.0
χ41 (1)	015.1764	1.69	8.7	2.19	6.6	2.10	7.1
χ41 (2)	2007	1.35	11.1	2.40	6.0	1.98	7.6
χ42 (1)	018.1806	1.09	14.5	2.38	6.1	1.88	8.0
χ42 (2)	2014	1.63	9.0	2.37	6.1	2.08	7.2
χ43 (1)	2292	1.31	11.5	2.47	5.9	1.81	8.4
χ43 (2)	2500	1.43	10.4	2.27	6.4	1.76	8.7
χ43 (3)	2708	1.45	10.2	2.28	6.3	1.78	8.6
χ44 (2)	019.2146	1.32	11.4	2.48	5.9	1.67	9.3
χ45 (1)	2340	1.06	15.0	2.55	5.7	1.61	9.5
χ45 (2)	2542	0.95	17.5	2.49	5.8	1.82	8.3
χ46 (1)	2750	1.11	14.2	2.56	5.7	1.67	9.3
χ46 (2)	2951	1.36	11.0	2.30	6.3	1.85	8.2
χ47 (1)	021.1910	1.14	13.7	2.51	5.8	1.44	11.3
χ47 (2)	2139	1.30	11.6	2.47	5.9	1.65	9.4
χ47 (3)	2340	1.35	11.1	2.04	7.2	1.69	9.2
χ48 (1)	2590	1.45	10.2	2.15	6.8	1.81	8.4
χ48 (2)	2750	1.07	14.9	2.39	6.1	1.68	9.2
χ48 (3)	2944	1.30	11.6	2.53	5.8	1.87	8.1
χ49 (1)	022.1736	1.20	12.8	2.25	6.5	1.53	10.4
χ49 (2)	1938	1.42	10.5	2.22	6.5	1.74	8.8
χ50 (1)	2160	1.12	14.0	2.53	5.8	1.70	9.1
χ50 (2)	2317	0.97	17.0	2.42	6.0	1.89	8.0
χ51 (1)	2542	1.23	12.4	2.59	5.6	1.70	9.1
χ51 (2)	2743	1.13	13.8	2.63	5.5	1.62	9.6
χ51 (3)	2944	1.09	14.5	2.78	5.2	1.65	9.4
χ52	024.1757	1.78	8.2	2.16	7.1	1.60	9.8
χ53 (1)	1993	1.40	10.6	2.17	6.7	1.55	10.2
χ53 (2)	2215	1.67	8.8	2.29	6.3	1.77	8.6
χ54 (1)	2361	1.27	11.9	2.81	5.2	1.62	9.6
χ54 (2)	2625	1.42	10.5	2.45	5.9	1.62	9.6
χ55 (1)	2785	1.61	8.9	2.00	7.3	1.62	9.6
χ55 (2)	2958	1.47	10.1	2.31	6.3	1.46	11.1
χ56 (1)	040.1556	1.49	9.9	2.44	6.0	1.73	8.9
χ56 (2)	1792	1.85	7.9	2.16	6.7	1.82	8.3
χ58 (1)	043.1611	1.77	8.2	2.05	7.1	1.67	9.3
χ58 (2)	1868	1.47	10.1	2.59	5.6	1.82	8.3
χ59 (1)	2097	1.30	11.6	2.50	5.8	1.77	8.6
χ59 (2)	2313	1.51	9.8	2.51	5.8	1.66	9.4
χ60 (1)	044.1590	1.41	10.6	2.09	7.0	1.64	9.5
χ60 (2)	1833	1.42	10.5	2.62	5.6	1.77	8.6
χ61 (1)	2063	1.22	12.5	2.51	5.8	1.87	8.1
χ61 (2)	2292	1.16	13.4	2.57	5.7	1.92	7.8
χ63 (1)	C46.1576	1.26	12.1	2.51	5.8	1.80	8.4
χ63 (2)	1806	1.29	11.7	2.51	5.8	1.95	7.7
χ64 (1)	1889	1.48	10.0	2.16	6.7	1.92	7.8
χ64 (2)	2014	1.59	9.2	1.96	7.5	2.26	6.5
χ65	2229	1.81	8.0	3.28	—	1.55	10.2
χ66 (1)	049.1646	1.23	12.4	2.55	5.7	1.82	8.3
χ66 (2)	1847	1.37	10.9	2.65	5.5	1.70	9.1
χ67 (1)	2104	1.29	11.7	1.91	7.7	1.92	7.8
χ67 (2)	2278	0.91	18.6	1.89	7.8	1.96	7.7
χ68 (1)	2472	2.04	7.1	1.68	8.9	1.86	8.1
χ68 (2)	2625	—	—	1.69	8.8	1.74	8.8
χ70 (1)	053.1771	1.35	11.1	2.40	6.1	1.39	11.9
χ70 (2)	1917	1.55	9.5	2.56	5.7	1.77	8.6
χ71 (1)	2118	0.37	∞	2.38	6.1	1.53	10.4
χ71 (2)	2222	0.00	∞	2.31	6.3	1.54	10.3
χ72 (1)	2340	0.34	∞	2.35	6.2	1.97	7.6
χ72 (2)	2472	0.69	∞	2.39	6.1	1.79	8.5

of its values for different nights characterizes the upper limit of accuracy of our gradient determination. Actually, the photographs of α Lyr and the region of χ Oph, in which HD 148898 is found, were not taken simultaneously; α Lyr was photographed with a diaphragm. An extensive difference of zenith distances and the incomplete calculation of atmospheric attenuation due to inconstancy of the atmospheric transparency greatly reduced the estimated accuracy of the work. All these factors were excluded when determining the gradients of χ Oph. Thus, the accuracy of determining the gradients of the investigated star is appreciably higher than the value given below. However, even this value is not too high and, in any case, does not throw doubt on the constancy of the comparison star.

For HD 148898, we had to determine two values of the spectrophotometric gradient: the photographic value for the portion $\lambda\lambda$ 3800 – 5200 Å and the visual value for the $\lambda\lambda$ 5300 – 6500 Å range. The absolute gradient of α Lyr has been determined by many authors, since it is not difficult to obtain the absolute gradient of the comparison star. We took the values of the gradient of γ Lyr given by L.V.Mirzoyan for the range $\lambda\lambda$ 3700 – 4600 Å (Bibl.6), as ϕ_1 = 1.14 and by O.A.Mel'nikov for the photo-visual range $\lambda\lambda$ 4220 – 7190 Å (Bibl.7), as ϕ_2 = = 1.19. With these values, we obtained the absolute gradients of HD 148898 for the photographic and visual regions

$$\Phi_1 = 1.68 \pm 0.18; \quad \Phi_2 = 1.24 \pm 0.11.$$

The first value corresponds nicely to the absolute photographic gradient determined by Barbier and Chalonge for stars of class Fo, namely, ϕ_1 = 1.70 (Bibl.8).

For determining the limits of the spectral range characterized by one value of the gradient and for graphically representing the spectrum of the investigated star, we plotted the curves of the relative energy distribution in the spectrum of χ Oph with respect to HD 148898 (Fig.3). An examination of the curves showed primarily that the spectrum of χ Oph must be represented by three values of the gradient: violet ($\lambda\lambda$ 3800 – 4400 Å), blue ($\lambda\lambda$ 4500 – 5200 Å), and red ($\lambda\lambda$ 5300 – – 6500 Å), which in the photographic range of the spectrum represents, in a manner of speaking, a trough of variable depth. Secondly, it is obvious that the energy distribution and the brightness of the star basically vary from night to night as well as within the same night of observation. The quantitative characteristic of the changes in the energy distribution is given by the absolute gradients ϕ_1, ϕ_2, ϕ_3, corresponding to the above spectrum ranges and presented in Table 3. The first column of the Table gives the number of the negative, the second column the time of observation in I.D., followed by the gradients and the corresponding values of the spectrophotometric temperatures.

As we see, the changes in the gradients appreciably exceed the errors /215 of observation. Therefore, although there is no reason to doubt the reality of these variations, it was of interest to reveal the character of changes in the gradients from night to night. For this purpose we obtained the probability-weighted average of all observations for each night from the formula

$$\Delta\bar{\Phi} = \frac{\Sigma \frac{1}{\varepsilon} \Delta\Phi}{\Sigma \frac{1}{\varepsilon}}, \tag{7}$$

where ϵ was determined by eq.(6).

The resultant values of Φ are represented in Fig.4. Along the abscissa in this diagram are plotted the times of observation in I.D. A study of Fig.4 shows the well-defined "mirror-image" dependence between the diurnal changes of Φ_1 and Φ_2. With increasing Φ_1, Φ_2 decreases and vice versa. The individual
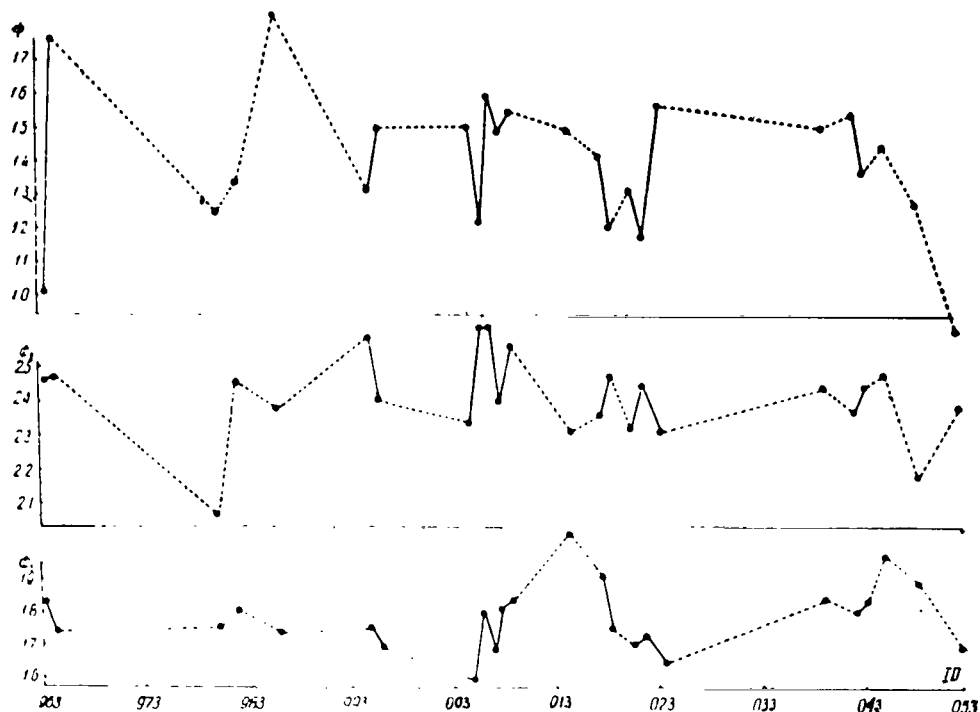
Fig.4 Curves of Changes in Absolute Spectrophotometric Gradients
Each point is a probability-weighted average, obtained
from observations of one night

disturbances do not cast doubt on the character of the correlation. In the second half of the observation period, Φ_3 shows diurnal changes that run parallel to the curve Φ_2.

The mirror-image dependence of the gradients of Φ_1 and Φ_2 is only a numerical depiction of the trough of variable depth in the photographic range of the spectrum, observed on the curves of Fig.3. Its minimum, according to our data, is in the range $\lambda\lambda$ $4300 - 4400$ Å. This raises the question as to the reliability with which our relative measurements indicate its location in the spectrum. If the absolute energy distribution in the stellar spectrum were known, it /216 would be easy to accurately define the position of all possible details on the curve. In relative measurements, the measured position will be displaced relative to the true position, depending on the temperature of the comparison star. It is not difficult to see that, if the comparison star is a hot star (for example, a star of class Ao), then any trough in the photographic region of the

spectrum of the investigated star, occurring on the descending branch of the /217
Planck curve (which approximately characterizes the energy distribution in the
comparison spectrum), will be shifted toward the short waves on the relative
spectral curve. Conversely, in the case of a low-temperature comparison spec-
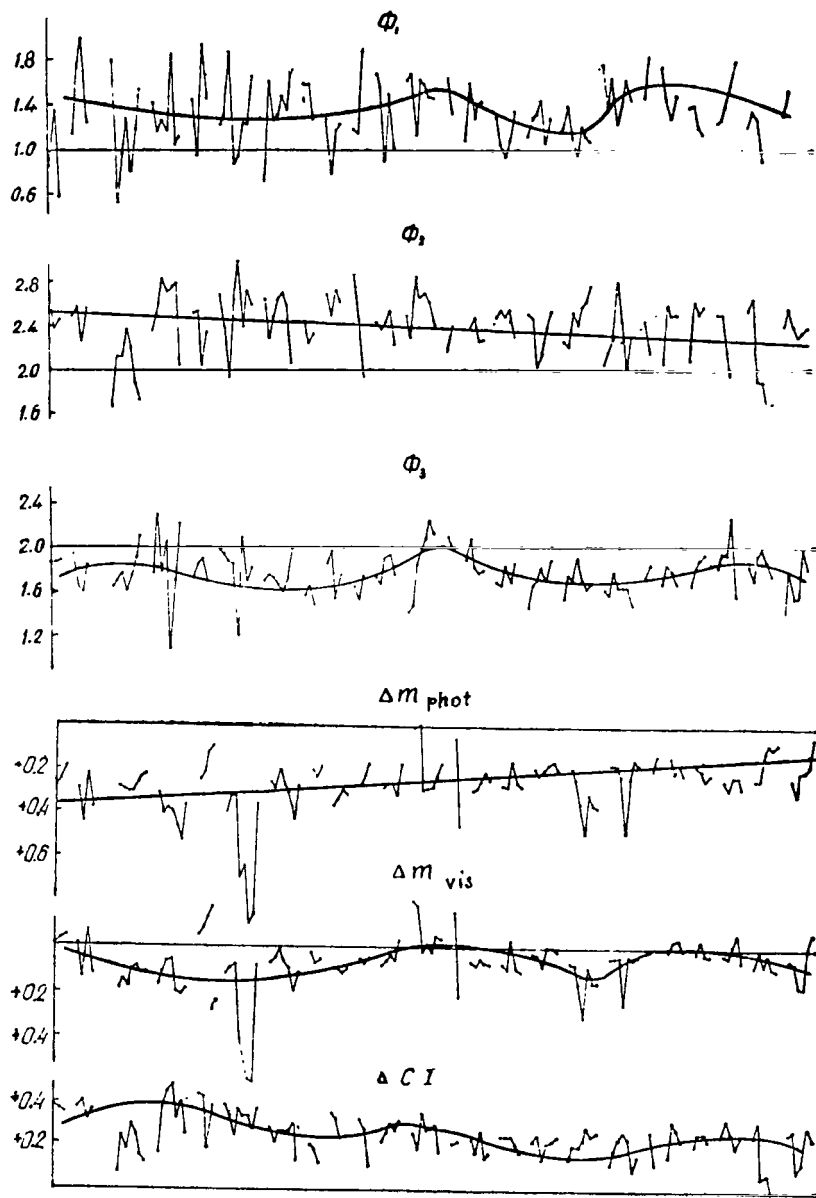trum, the measured value of the minimum will be shifted toward the red portion

Fig.5 Curves of Changes in Absolute Spectrophotometric
Gradients, Brightness, and Color of χ Ophiuchi
Observations of one night are connected by a broken line.
The smooth curve indicates the long-period character of
the changes of the indicated quantities.

of the spectrum. Consequently, the best comparison spectrum in relative spectro-photometric work is one for which the maximum of the Planck curve is located in the investigated spectral region. Of course, this discussion only makes sense under the assumption that the emission of normal stars, selected as comparison stars, obeys the laws of black-body radiation; it is known that this occurs in limited spectral regions.

At the spectrophotometric temperature ascribed to stars of the early sub-classes of class F, the maximum of the Planck curve is situated in the photographic range of the spectrum. This makes stars of these types the most convenient comparison objects when working in the photographic region. This advantage of stars of the class Fo over the traditional Ao stars is also demonstrated by the fact that, in the former, the hydrogen lines are not as intense so that the merging of the line wings begins at shorter waves than for Ao stars, for which a distinct depression of the continuous spectrum begins to be manifest at λ 4000 Å.

Thus, since the comparison star selected in this work belongs to the class Fo, the position of the depression in the photographic portion of the spectrum is determined more or less correctly.

Figure 5 shows the changes in the gradients of Φ taken from Table 3. On the abscissa, a variable time scale is laid off. The observations of one night are connected by a broken line and individual nights of observation are separated by a constant interval, regardless of how much time had elapsed. Of course, such a scale distorts the exact slope of the curve of long-period variations but cannot affect the overall slope and, furthermore, is convenient for comparing individual characteristics as well as for a graphic presentation of both short- and long-period variations on a single curve. The diagram shows the mentioned mirror dependence also for individual variations in the gradients Φ_1 and Φ_2 during the night, which constitutes a control of the reliability of determining short-period variations of the gradient. Judging by Fig.4, the obtained mean value of Φ_1 coincides well with the value of the gradient $\Phi_1 = 1.51$, given by Tsoi Dai O (Bibl.2).

The value of $\wedge \log I$ obtained by analyzing the microphotograms is related to the difference of monochromatic stellar magnitudes of the investigated and comparison star by the evident dependence $\wedge m = -2.5 \wedge \log I$. Thus, the obtained data permit plotting the monochromatic curves of stellar brightness. These curves show a gradual change of slope with wavelength, and the integrated curves with respect to the photographic and visual ranges satisfactorily reflect the general contours of the individual curves. Therefore, the monochromatic brightness was graphically integrated in the ranges $\lambda\lambda$ 3800 – 4800 Å and $\lambda\lambda$ 4500 – – 6500 Å, and the brightness curves for photographic and visual rays were plotted. Reduction to the international photometric system was not done. In addition, the value of $\wedge C.I. = \wedge m_{4300} - \wedge m_{6500}$, which is the difference of the special color indices of χ Oph and the comparison star, was determined. The /220 three lower curves in Fig.5 show the changes of $\wedge m_{phot}$, $\wedge m_{vis}$, and $\wedge C.I.$ The numerical values are given in Table 2.

A comparison of the six curves in Fig.5 leads to interesting conclusions.

TABLE 2

2435. *I. D.*	Δm_{phot}	Δm_{vis}	$\Delta C. I.$
1	2	3	4
963,3368	+0,28	0.00	+0,38
3660	25	—0,03	36
3750	19	04	35
964,3354	29	01	37
3660	44	+0,14	40
3938	22	—0,07	32
4257	37	+0,13	36
980,2813	28	19	07
3083	29	15	24
3361	30	18	18
3604	30	11	29
3778	26	09	24
4014	24	12	15
4201	22	12	12
982,2632	31	17	16
2882	40	11	37
3160	38	07	44
3396	39	06	47
3611	46	21	32
3833	52	22	39
4042	36	19	25
986,2972	25	—0,05	43
3194	21	08	42
3528	12	13	19
3750	09	18	38
995,2118	40	+0,12	38
2458	32	10	33
2688	32	08	24
2917	69	42	36
3104	64	—	33
3313	90	61	33
3528	86	62	27
3729	36	08	36
996,2035	26	07	27
2333	28	05	21
2570	20	01	26
2785	27	07	26
2986	31	10	26
3194	43	20	30
3389	27	12	13
2436.			
005,1917	20	03	20
2167	23	08	18
2375	18	06	12
006,1979	36	10	35
2188	33	10	32
2417	29	12	23
2604	31	10	24
007,2222	27	06	32
2431	22	07	27
2722	17	05	10
008,1847	23	08	22
2042	26	06	26
2250	26	04	30
2451	31	06	27
2674	17	—0,03	31
009,1875	00	21	25
2083	—0,01	18	18
2285	+0,29	+0,02	34
2521	28	—0,01	27
2729	27	+0,02	28
2924	23	—0,05	29

TABLE 2 (cont'd) /219

1	2	3	4
C09.3132	+0.17	−0.04	+0.17
015.1764	05	16	21
2007	45	+0.23	22
018.1706	29	07	23
2014	28	08	17
2292	25	06	27
2500	21	07	14
2708	24	08	16
019.2146	27	08	24
2340	28	10	21
2542	16	−0.03	24
2750	26	+0.10	21
2951	27	11	17
021.1910	19	03	22
2139	22	04	25
2340	20	09	14
2590	17	00	21
2750	16	00	22
2944	20	02	24
022.1736	19	07	14
1938	24	08	20
2160	35	17	20
2347	48	32	23
2542	31	09	28
2743	35	16	25
2944	37	16	26
024.1757	17	05	12
1993	17	05	18
2215	22	04	23
2361	48	26	26
2625	23	01	24
2785	15	05	09
2958	17	04	15
040.1556	19	00	27
1792	13	00	12
043.1611	14	+0.01	15
1868	21	−0.03	31
2097	17	04	28
2313	22	00	23
014.1590	17	+0.02	21
1833	19	−0.03	26
2063	24	+0.03	26
2292	22	03	23
046.1576	21	03	25
1806	28	04	32
1889	22	−0.01	26
2014	22	06	20
2229	28	+0.06	25
019.1646	24	08	35
1847	24	02	31
2104	11	07	06
2278	08	03	07
2472	09	08	−0.03
2625	07	09	03
053.1771	24	05	+0.26
1917	30	06	27
2118	20	17	08
2222	19	17	12
2340	17	−0.01	29
2472	04	07	24

1. Both short- and long-period variations are observed on all curves.

2. The short-period variations occurring during the night are greater and more frequent for the gradients than for the brightness. The short-period variations of the gradients Φ_1 and Φ_2 show a mirror dependence. For photographic and visual brightness, the closely similar variations do not always accurately match, resulting in fluctuations of the color index which, on some nights, reach $0^m.2$ of the stellar magnitude. No dependence was observed between short-period variations of brightness and gradients.

3. The slope of the long-period curves for the variations in the gradients Φ_1 and Φ_2 does not exhibit the mirror dependence noted for the short-period variations. The curve of Φ_2 has a distinct tendency toward a decrease. During the time of observation, the mean value of the gradient dropped by 0.3. The curves of the variations in Φ_1 and Φ_3 have an undulatory character.

4. The long-period slope of the brightness curves also shows no similarity. The photographic brightness during the observation period increases steadily, being $0^m.12$ greater at the end than at the start of the observations. The curves of Δm_{vis} and $\Delta C.I.$ again have an undulatory slope.

5. Whereas no relation between variations of the same characteristics for different regions of the spectrum is observed, the variations in brightness and in gradients are very similar. A decrease in the gradient Φ_2 is accompanied by an increase in photographic brightness; the waves on the curves of Φ_1 and of the visual brightness coincide in time, while the curve of the long-period variations of the color index is a mirror image of the curve for Φ_3, but at a lower amplitude. Such coincidence of the curve slopes can be due either to a physical interrelation of the characteristics or to systematic errors during their determination. However, in our case systematic errors cannot cause the observed correlations. Actually, the only source of systematic errors are the characteristics themselves, consisting in either an underestimation or overestimation of their slope. However, in this case the curves of the physical characteristics, referring to one spectral region, would show optimum coincidence, so that the correlation between Δm_{vis} and Φ_1 in the absence of such a relation for Δm_{phot} and Φ_1 would be absolutely unexplainable. The coincidence of the obtained values of the absolute gradients for HD 148898 and of the average for χ Oph with the data given by other authors also precludes the assumption of systematic errors. However, let us again examine the dependence between Δm_{phot} and Φ_2. Since both characteristics pertain approximately to one spectral range, the systematic overestimation of the slope of the characteristic curves could qualitatively create a dependence of the observed type. Let us make a quantitative evaluation.

Let the difference of the densities of the investigated star and comparison star at a wavelength of $\lambda_1 - \Delta D_1$ be $\lambda_2 - \Delta D_2$. Then the corresponding relative intensities are

$$\log \frac{I_1}{I_{01}} = \frac{\Delta D_1}{\gamma_1} \; ; \log \frac{I_2}{I_{02}} = \frac{\Delta D_2}{\gamma_2} ,$$

where γ_i are the contrast factors of the corresponding monochromatic character-

istic curves.

Let an error Λ be permitted in the slope of the characteristic curves.
Then, the measured values of the relative intensities will be

$$\log \frac{I'_1}{I'_{01}} = \frac{\Delta D_1}{\gamma_1 + \Delta \gamma_1}, \; \log \frac{I'_2}{I'_{02}} = \frac{\Delta D_2}{\gamma_2 + \Delta \gamma_2}.$$

Thus, on obtaining the relative intensities we permit the error

$$\log \frac{I'_i}{I'_{0i}} : \log \frac{I_i}{I_{0i}} = \frac{\gamma_i}{\gamma_i + \Delta \gamma_i} = \frac{1}{1 + \Delta \gamma_i / \gamma_i}.$$

It is not difficult to understand that if, as a result of errors in γ, one value of the gradient is replaced by another (erroneous) one, then we will have, in the spectral region under consideration,

$$\frac{\Delta \gamma_i}{\gamma_i} = \text{const}.$$

Consequently,

$$\log \frac{I'_i}{I'_{0i}} : \log \frac{I_i}{I_{0i}} = c. \tag{8}$$

Designating the erroneous value of the gradient by $\Lambda \Phi' = 2.303\, H$, we can write:

$$\log \frac{I'(\lambda)}{I'_0(\lambda)} = \frac{1}{\lambda} H' + A'.$$

Solving the last equation by the method of least squares, we find

$$H' = \frac{n \sum \frac{1}{\lambda} \Delta \log I'(\lambda) - \sum 1/\lambda \sum \Delta \log I'(\lambda)}{n \sum 1/\lambda^2 - (\sum 1/\lambda)^2} =$$
$$= \frac{c \left[n \sum \frac{1}{\lambda} \Delta \log I(\lambda) - \sum 1/\lambda \sum \Delta \log I(\lambda) \right]}{n \sum 1/\lambda^2 - (\sum 1/\lambda)^2} = cH. \tag{9}$$

If we assume that, at the start of observations, the characteristic curves were properly constructed and the proper value of the gradient was obtained, whereas later the error increased systematically, having stipulated by the end of the observation period an error which gave the value of H', we can determine the value of c. We thus found c = 0.70. This value corresponds to an error in the contrast factor of 45%, which is hardly possible specifically in view of the systematic increase of $\Lambda \gamma$.

Let us examine what change in brightness might cause such an error. Assuming that, at the start of observations, the brightness Λm was determined properly, then on the basis of our observations we can write

$$\Delta m = - 2.5 \log \int_{\lambda_1}^{\lambda_2} e^{1/\lambda \Delta \Phi + A} \, d\lambda = 0.^m 15,$$

255

since, at the start of the observation period, the average brightness of the star in the $\lambda\lambda$ 4500 – 5200 Å range (the integration limits correspond to the spectral range in which the gradient Φ_2 was determined) was equal to $0^m.15$.

At the end of the observation period, we obtained an erroneous value which, based on the above statements, can be presented as

$$\Delta m' = -2.5 \log \int_{\lambda_1}^{\lambda_2} e^{c\,(1/\lambda\Delta\Phi\,+\,A)} \; d\lambda.$$ (10)

The integral (10) is expanded in a series

$$\Delta m' = -2.5 \log \left\{ -e^{cA} \left[-\frac{e^{c\,\Delta\Phi\,1/\lambda}}{1/\lambda} + c\Delta\Phi \left(\ln 1/\lambda + \frac{c\,\Delta\Phi\,1\lambda}{1\cdot1!} + \right.\right.\right.$$
$$\left.\left.\left. + \frac{(c\,\Delta\Phi\,1/\lambda)^2}{2\cdot2!} + \dots \right) \right] \right\}.$$

After substituting the numerical values, we obtain $\Delta m' = 0^m.11$, i.e., the errors in plotting the characteristic curves might cause a fictitious change in brightness during the observations, not exceeding $0^m.04$. The observed change of brightness is three times greater. Thus, the assumption of systematic errors does not explain the quantitative dependence between Δm_{phot} and the gradient Φ_2.

Thus, rejecting the assumption of systematic errors, we are forced to acknowledge physical interrelations between the said characteristics.

Thus, a change in photographic brightness is associated with a functional relation with a change of Φ_2 $\delta\Delta m_{phot} = \varphi(\delta\Phi_2)$.

On the basis of the above, there are two other dependencies pertaining to long-period variations $\delta\Delta m_{vis} = \psi(\delta\Phi_1)$ and $\delta\Delta C.I. = \omega(\delta\Phi_3)$. Then, on the basis of determining the color index we can write[*]

$$\varphi(\delta\Phi_2) - \psi(\delta\Phi_1) = \omega(\delta\Phi_3)$$ (11)

Thus, the variations in the three values of the gradient of χ Oph are associated with a functional dependence of the type of eq.(11), whose analytic expression can be obtained from an analysis of the curves of brightness and gradients. For such work, the data of many years will be needed. If the dependence (11) is not sporadic, which future observations would show, then its analytic expression will be an important criterion for the authenticity of projected models of the stellar atmosphere.

4. Certain Characteristics of the Emission Spectrum of χ Ophiuchi

Provided that the investigations of the continuous spectrum in the above

---

[*] The curve for the color index given in Table 4 and the color index determined by the dependence $\Delta C.I. = \Delta m_{phot} - \Delta m_{vis}$ have the same long-period variation.

sense do not lose in accuracy because of low dispersion and are performed more reliably with prism instruments than with slit types, the situation will be worse when dealing with a line spectrum. Atmospheric turbulence and guiding defects will distort the line profile, actually determining its width. However, these factors should have the same effect on all lines. Thus, if a comparison of various spectrograms shows that, at constant width or sharpness of a given line, another line changes or disappears, the above assumptions must be considered facts. In other respects, only statistical investigations are possible. Nevertheless, the equivalent line widths, determined from the prism spectra, are obtained with sufficient reliability. This was proved by Shapley and Payne /223 in 1922 (Bibl.63) and is confirmed by our comparisons of the equivalent widths, determined from simultaneous slit and prism spectra which coincided within the limits of the observation errors. A small dispersion, according to L.V.Mirzoyan (Bibl.9) also introduces no substantial distortions into the determinable values of the equivalent widths.

The determination of the equivalent widths, as usual, was carried out in two stages: We plotted the profiles of all hydrogen lines in residual intensities $r_\lambda = I_\lambda / I_{\lambda_0}$, where I_λ is the intensity at a given point of the line and I_{λ_0} at the corresponding wavelength of the continuous spectrum; we then determined the area of this profile, expressed as the width of an equal-area portion of the continuous spectrum.

The profiles of the lines, as was found during the work, vary greatly. Along with the usual structure of Be emission, the structure of P Cygni bounded
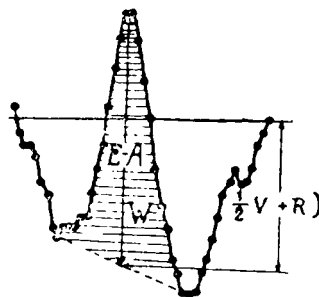
Fig.6

by the red R and violet V absorption components was repeatedly observed, especially in the Hγ lines which do not always appear simultaneously in all lines. A change in the width of the wings of the absorption line was noted. All this does not permit us to correct the profile of the absorption line for distortion by emission or to determine the true value of the equivalent width. We determined the area of that portion of the line which is above the mean level of the absorption components (Fig.6). This method is no less erroneous than the conventional method of "constructing" the absorption line for known variable profiles, and it is convenient since it precludes the effect of errors in drawing the continuous spectrum to the size of the equivalent width. In addition to the equivalent widths, for statistical purposes we determined the quantities E – A

TABLE 3

/224/

I.D 2435...	H₃			H₇			H₅			H₆		
	W Bred. Astr.	AZT-7	S	W	E-A	S	W	E-A	S	W	E-A	S
1	2	3	4	5	6	7	8	9	10	11	12	13
962.3285	5.5	5.4	9.0	2.0	0,27	6.0	0.8	0.16	5.2	0,8	0.15	5,0
4097	5.5		8.5	2.0	30	7.4						
963.3368	5.3		8.3	1.8	28	6.8						
3660	5.0		8.3	1.4	26	4.5	0.6	0.14	4.6			
3750	5.4	6.0	9.9	1.5	24	5.8						
964.3354	6.3		8.7	1.5	26	5.2						
3660	6.0		8.0									
3938	4.9		8.5									
4257	4.0		8.5	1.5	26	6.0	1.1	0.23	5.0			
980.2813	7.8		5.0	1.6	28	5.2	0.6	0.16	3.7			
3083	6.7		10.6	1.0	20	5.2	0.4	0.11	4.1			
3361	6.1		5.9	2.1	43	5.4	0.9	0.22	3.3			
3604	4.6		12.0	2.0	27	6.6						
982.2682	4.7		9.0	1.4	34	4.2	0.8	0.34	2.3			
2882	4.1		7.2	1.6	27	6.6						
3160	6.0		10.8	1.9	36	4.2	0.6	0.15	4.8			
3396	5.6		9.7	1.9	41	4.9						
3611	7.4	6.8	9.0	1.9	30	5.6						
986.2972	10.6		8.0	1.0	22	4.9	0.5	0.14	3.5	0.5	0.13	3.5
3194	4.4		7.6	0.7	28	4.2	0.4	0.10	4.8			
3528	3.1		8.6	0.9	13	7.7						
3750	5.2		11.0	0.7	16	4.9						
995.2118	5.7		10.8	0.9	14	8.4	0.5	0.11	5.2	0.6	0.12	5,5
2458	6.2		10.2	1.5	20	7.4						
2688	5.2		9.1	2.3	32	7.4	0.5	·0.22	2.0			
2917	4.4		9.5	1.5	26	6.0				0.3	0.12	3.2
3104	4.5		10.0	1.7	27	6.2	0.3	0.10	2.8	0.7	0.18	3.0
3313	5.0		9.6	1.3	0.24	5.8						
3528	6.5	6.8	11.2	1.0	26	3.8						
3729	4.2		12.0	0.9	18	5.6	0.8	0.18	3.2			
996.2035	5.0		10.3	1.0	18	5.4	0.6	6.13	5.9			
2333	4.3		9.4	1.4	22	7.0						
2570	4.5		7.5	1.0	26	2.8						
2785	4.2		9.4	1.6	23	7.4						
2986	4.2		12.2									
3194	4.6		11.2	0.6	?	4.9						
3389	3.8		11.8	1.8	28	5.6						
2436...												
005.1917	4.6		10.0									
2167	2.8		6.0	0.7	19	2.4						
2375	2.9		9.0	1.6	27	4.8	1.1	0.24	5.5			
006.1979	4.0		6.9	0.4	15	6.3				0.3	0.09	3.5
2188	4.4		8.8	0.9	20	4.2				0.2	0.08	3.5
2417	4.2		13.2									
2604	3.6		9.0									
007.2222	4.6		7.6	1.0	16	8.4						
2431	4.8		5.3	0.8	19	4.9						
2722	3.6		5.0							0.4	0.13	4.0
008.1847	4.0		9.2	0.7	14	6.4				0.3	0.10	4.0
2042	4.0		10.0									
2250	3.8		8.8	1.2	18	6.6	0.3	0.14	2.1	0.5	0.15	3.5
2451	3.6		9.0	0.9	13	6.3						
2674	4.0		9.6	0.8	14	6.6	0.3	0.14	3.0	0.3	0.12	2.6
009.1875	7.8		7.9									
2083	7.4		6.7	1.5	22	8.0						
2285	4.9		11.0									
2521	4.0		9.0									

TABLE 3 (cont'd)

/225

1	2	3	4	5	6	7	8	9	10	11	12	13
009.2729	3.6		10.2									
2924	3.3		10.0	1.0	0.19	6.0						
2436 . . .												
015.1764	3.6		8.0	1.1	16	8.4						
2007	4.4		9.0	2.2	22	10.5						
018 1806	5.9		8.4	1.3	27	4.2	0.8	0.16	5.5			
2014	5.3		9.2							1.0	0.20	4.0
2292	4.4		5.3	1.8	28	7.0	1.3	0.32	4.7			
2500	5.2		9.2	1.3	24	6.0	1.1	0.22	6.0			
2708	4.8		10.7	1.8	24	9.0						
019.2146	5.4		8.9	1.3	20	7.6	1.1	0.30	3.0	0.7	0.15	4.5
2340	6.2		8.6	1.9	28	7.7	0.9	0.18	5.3	0.6	0.21	2.0
2542	6.1		9.7	2.1	32	6.0				0.2	0.08	4.0
2750	6.2		12.5	1.3	18	8.4						
021.1910	4.7		8.4				0.5	0.16	2.7	0.3	0.10	4.3
2139	3.0		8.0	1.2	16	7.1						
2340	3.4		12.3									
2590	4.3		10.5	1.2	23	5.6	0.5	0.12	4.7			
2750	2.4		7.0									
2944	2.4		10.7									
022.1736	3.9		10.4	1.0	21	4.2						
1938	4.0		8.2	1.2	17	8.1				0.4	0.14	2.5
2160	4.8		9.2							0.4	0.12	3.2
2347	4.3		9.0	1.6	21	9.1						
2542	5.1		8.3	1.8	30	5.7						
2743	4.8	4.8	8.7									
024.1757	3.6		9.0									
1993	4.0		7.9									
2215	2.4		9.6									
2361	2.8		8.6									
2625	3.5		10.8									
2785	4.9		14.0									
040.1556	3.3		13.5									
043.1611	3.0		9.5	1.4	0.16	7.0						
1868	4.2		10.0	1.2	16	7.7						
2097	3.6		11.5									
2312	3.9		10.0									
044.1590	3.0		7.8									
1833	3.3		9.6									
2062	3.1		8.0									
2292	4.8	4.4	12.7				0.6	0.10	7.5			
2507	4.2		11.0									
046.1576	4.2		9.8	1.0	14	7.0	0.6	0.15	5.2			
1806	3.7		11.0	1.6	20	9.1	0.4	0.18	1.7			
1889	5.8		8.8									
2014	7.2		15.3	2.1	28	6.1						
2229	8.2		11.8							0.7	0.12	8.0
049.1646	5.2		10.3	1.2	16	7.9						
1847	4.1		12.0	1.2	16	10.5						
2104	4.4		11.7	1.9	33	5.4	0.6	0.15	3.6			
2278	4.0		10.0	1.8	37	3.5						
2472	5.8		11.8									
053.1528	8.6	6.8	12.7									
1771	4.7		8.9									
1917	4.5		14.8									
2118	5.0		9.4	2.0	26	7.7						
2222	3.8		11.4	1.8	32	5.2						
2340	4.2		14.4	1.6	0.22	7.7						
2472	4.8		10.0	1.6	25	5.6						

(intensity of central emission above the mean level of the absorption components) and the half-width of emission lines s, the smallest reliably determinable value. Figure 6 shows the profile of the H line obtained from negative χ5, in which all determinable values are entered. The results of the determinations are shown in Table 3. The second column gives the equivalent width of Hβ, determined from prism observations; the third column shows the same based on slit spectrograms; the fourth column contains the half-width of Hβ in angstrom. The Table also gives the equivalent width of the emission component, the values of E − A, and the value of s for the lines of Hγ, Hδ, and Hε. As indicated, noticeable changes occur only in the equivalent widths of the line Hβ, whereas for Hγ, Hδ, Hε the changes are very small. This is in agreement with the conclusions by Curtiss (Bibl.28) who considers that the line variations increase with decreasing line number. This dependence is characteristic for all lines: The narrower the emission line, the greater is its intensity, which is especially noticeable on lines of high numbers. The marked increase in E − A always is accompanied by a distinct narrowing of the emission component. We plotted E − A as a function of s. The position of the points in the diagram indicates that the values of E − A predominate and frequently are associated with corresponding half- /226 width values. The curve of the frequency of deviations from the mean value of E − A, plotted for the H line, had the slope of two superposed Gaussian curves. The maxima of these curves correspond to E − A = 0.26 and E − A = 0.16 on our intensity scale. These values correspond to half-widths of 5 − 6 Å and 7 − 8 Å. It is impossible to ascribe an absolute value to the latter owing to observational errors; for this reason, they are given only for illustration of the statistical dependence. Thus, the E − A tends to assume one of two discrete values, with the deviation from these values caused partially by observational errors and partially by random fluctuations characteristic for any physical process. For the lines Hδ and Hε, the material was insufficient for a statistical investigation, but available data indicate that their E − A is close to 0.12, fluctuating only about this value. Thus, we gain the impression that E − A is one of the most constant characteristics of the spectrum of χ Oph. However, on the profiles, and even on the negatives, we note an extensive change in intensity of the portion of the line lying above the continuous spectrum. Comparing this with the constancy of the emission level of E − A, it can be concluded that the change in line intensity above the level of the continuous spectrum is due to the fact that the line is swamped more or less in the continuous spectrum.

The equivalent widths shown in Table 3 were used for determining the Balmer decrement. For this purpose, they were reduced to the intensity of the continuous spectrum of Hβ by multiplying the equivalent widths by the ratio of the measured intensities of the continuous spectrum for the investigated line and Hβ. Table 4 shows the Balmer decrement determined in this manner, with the equivalent widths of Hβ taken as unity.

The obtained Balmer decrement varies greatly. Nevertheless, it is of interest to compare this with the data of other authors. For χ Oph there is only one determination of the decrement, made by Cannon on the basis of visual estimates of the line intensities: Hβ:Hγ:Hδ:Hε = 1.00:0.29:0.14:0.14 (Bibl.42).

Rojasa and Herman, in determining the decrements for Be stars, found an extensive variation from star to star. In their list, the decrements for early Be stars vary within the limits from Hβ:Hγ:Hδ:Hε = 1.00:0.35:0.15:0.05 to

TABLE 4

I. D. 2435 . . .	H β	H γ	H δ	H ε
1	2	3	4	5
962.3285	1.00	0.29	0.11	0.08
4097	1.00	0.32		
963.3368	1.00	0.25		
3660	1.00	0.22	0.08	
3750	1.00	0.23		
964.3354	1.00	0.21		
4257	1.00	0.29	0.18	
980.2813	1.00	0.21	0.08	
3083	1.00	0.15	0.06	
3361	1.00	0.26	0.10	
3604	1.00	0.29		
982.2632	1.00	0.27	0.17	
2882	1.00	0.33		
3160	1.00	0.32	0.12	
3396	1.00	0.33		
3611	1.00	0.23		
986.2972	1.00	0.11	0.06	0.05
3194	1.00	0.16		
3528	1.00	0.20	0.08	
3750	1.00	0.10		
995.2118	1.00	0.11	0.06	0.05
2458	1.00	0.18		
2688	1.00	0.32	0.06	
2917	1.00	0.23		0.04
3104	1.00	0.27	0.04	0.08
3313	1.00	0.17		
3528	1.00	0.10		
3729	1.00	0.15		
996.2035	1.00	0.12	0.10	
2333	1.00	0.22	0.09	
2570	1.00	0.14		
2785	1.00	0.27		
3194	1.00	0.11		
3389	1.00	0.41		
2436 . .				
005.2167	1.00	0.22		
2375	1.00	0.33	0.22	
006.1979	1.00	0.10		0.06
2188	1.00	0.23		0.04
007.2222	1.00	0.20		
2431	1.00	0.15		0.06
008.1847	1.00	0.14		0.06
2550	1.00	0.26	0.06	0.09
2451	1.00	0.22		
2674	1.00	0.16	0.06	0.04
009.2083	1.00	0.18		
2924	1.00	0.24		
015.1764	1.00	0.22		
2007	1.00	0.40		
018.1806	1.00	0.18	0.10	
2014	1.00			0.13
2292	1.00	0.35	0.24	
2500	1.00	0.21	0.17	
2708	1.00	0.29		
019.2146	1.00	0.21	0.15	0.08
2340	1.00	0.26	0.12	0.07
2542	1.00	0.31		0.02
2750	1.00	0.19		
021.1910	1.00		0.07	0.05
2139	1.00	0.26		
2590	1.00	0.19	0.10	

TABLE 4 (cont'd)   /228

1	2	3	4	5
022.1736	1.00	0.16		
1938	1.00	0.20		0.08
2160	1.00			0.07
2347	1.00	0.24		
2542	1.00	0.23		
043.1611	1.00	0.38		
1868	1.00	0.22		
044.2063	1.00		0.14	
046.1576	1.00	0.16	0.10	
1806	1.00	0.29	0.07	
2014	1.00	0.24		0.13
049.1646	1.00	0.22		
1847	1.00	0.27		
2104	1.00	0.38	0.08	
2278	1.00	0.30		
053.2118	1.00	0.34		
2222	1.00	0.42		
2340	1.00	0.31		
2470	1.00	0.27		

$H\beta:H\gamma:H\delta:H\epsilon = 1.00:0.67:0.53:0.22$ (Bibl.64).

Our data are rather close to these values, although the curvature of the decrement $H\beta:H\gamma$ in our case is usually greater. We should note that the above-described method of determining the equivalent widths can only reduce the curvature of the decrement. The following is also interesting. If, on the basis of the data in Table 4, we define the average value of the decrement, it will be found that $H\beta:H\gamma:H\delta:H\epsilon = 1.00:0.24:0.10:0.07$. Adding here the average value of $H\alpha:H\beta$, which is obtained from the slit spectrograms but is rather uncertain since the line $H\alpha$ is at the spectral sensitivity limit of the plate, we find $H\alpha:H\beta:H\gamma:H\delta:H\epsilon = 5.66:1.00:0.24:0.10:0.27$, which is very close to the theoretical value of the decrement obtained by V.V.Sobolev on the basis of the theory of moving shells for an electron temperature of the shell of $T_e = 20,000°C$ and a parameter $x = 1.0$ (Bibl.10). Unfortunately, the shell theory cannot explain many characteristics of a star, so that we cannot use this coincidence for a physical interpretation.

Figure 7 shows the curves of the long-period variation of the equivalent widths $W_{H\beta} E - A_{H\gamma}$, the depth of the absorption components $\frac{V + R}{2}$ for the $H\gamma$ line measured from the profiles of the Balmer decrement $H\gamma/H\beta$, and the photographic and monochromatic brightness for wavelengths of λ 4400 and λ 4900 Å. The points were obtained as a result of averaging the data of one night. The long-period variation of the curve $E - A_{H\lambda}$ is a mirror image of the curve $W_{H\beta}$. Of considerable interest is a comparison of the last five curves.

The above-mentioned swamping of the lines by the continuous spectrum seemed to indicate that this is caused by a change in level of the continuous spectrum, i.e., a variation in brightness. However, in such a case the change in bright-

ness should be accompanied by a change in depth of the absorption lines. A comparison of the short-period variation of brightness and depth of the absorption components actually showed such a tendency. This was manifested in the short-period variation of the curves in Fig.7. The curve of the Balmer decrement also
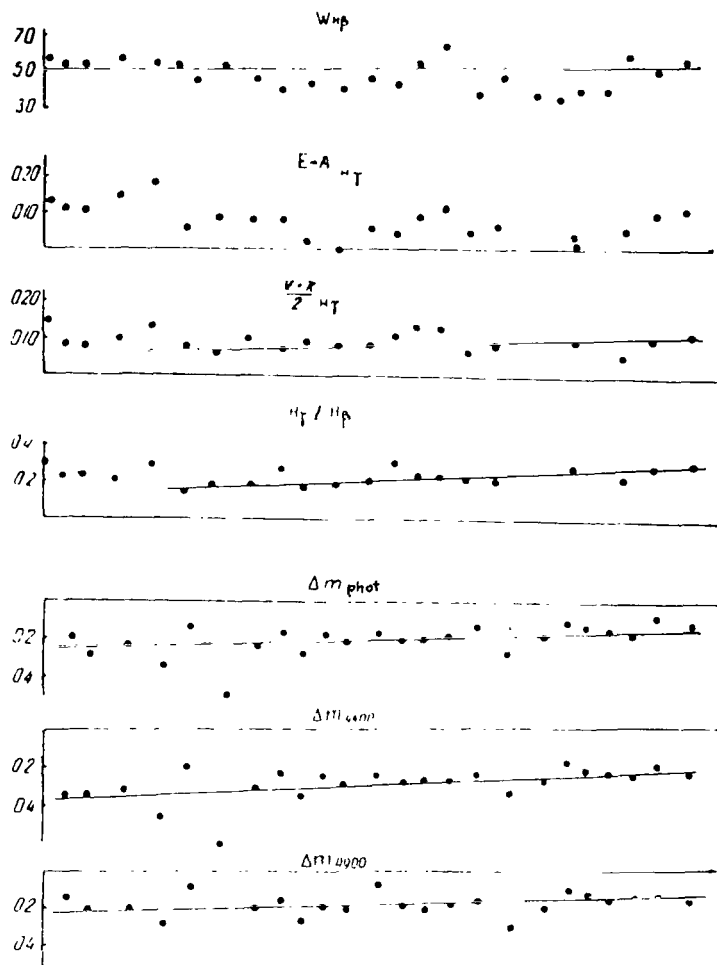

Fig.7

showed a systematic increase during the period of observation. This is not difficult to understand. Actually, the equivalent width of Hβ was determined for the line segment lying above the continuous spectrum. Here, Hγ is independent of the level of the continuous spectrum. However, neither Hβ nor Hγ show a systematic decrease or increase of equivalent widths during the observation. This means that we are here dealing with the relative energy distribution in the continuous spectrum of the star. It is known that the photographic brightness increases, but that Hβ is on the very edge of the photographic range. Therefore, if this increase in the region of Hγ is greater than in that of Hβ, then on reducing the equivalent width of Hγ to the continuous spectrum for Hβ

263

$$E_{H\gamma} = W_{H\gamma} \frac{I_{0H\gamma}}{I_{0H\beta}},$$

the value of $E_{H\gamma}$ becomes greater and the decrement increases. The curves of the monochromatic brightness in Fig.7 actually show the expected difference.

It should be mentioned that the average intensity of the Hβ line above /229 the level of the continuous spectrum during the observation period decreased somewhat. Quantitatively, this drop is satisfactorily explained by a rise in the level of the continuous spectrum in the region of the line by about 0ᵐ1 of stellar magnitude and by "filling up" of the wings of the emission line. Simultaneously with this, a certain broadening of the Hβ line was observed, which is difficult to explain.

Thus, from an analysis of the emission spectrum of χ Oph we established, by a completely independent method, a systematic increase of brightness in the photographic range of the spectrum, as it was found in the preceding Section. This serves as a control for the reliability of the above data.

On examining the profiles, we note still another interesting fact. In four cases, a second emission component, shifted toward the short-wave end, was manifested for Hγ. The shift varied from 21 to 13 Å.

Only in one case, on June 5 - 6, was the violet component of emission for Hβ observed together with the second component Hγ. Their shift relative to /230 the normal position was 23 Å for Hβ and 18 Å for Hγ, whereas the intensities were respectively 0.3 and 0.5 of the intensity of the normal component. The shifts are approximately proportional to the wavelengths, which support the assumption of a Doppler nature of the phenomenon.

In this case the position of the shifted components indicates the approach of gaseous masses toward the earth, with the components traveling at a velocity of the order of 1000 km/sec.

The most interesting finding was that, during this night for $2\frac{1}{2}$ hrs before appearance of the described components, a pronounced weakening of stellar brightness in all rays of the spectrum began and extended to 0ᵐ6. This phenomenon lasted about two hours; by the time the shifted emission components were noted, the brightness had again reached its normal value. If this is interpreted from the most logical assumption of an ejection of gaseous masses, it might be possible to make a rough estimate as to the radius of the emission zone of the star.

The ejected cloud was opaque and, on screening some portion of the star, weakened in brightness. By the time the cloud reached the emission zone, it had expanded and become transparent in the visible portion of the spectrum. The fact that the emission components did not appear immediately on weakening of the brightness but somewhat later would indicate that the emission zone is at a certain distance from the star. Taking the start of brightness attenuation as the instant of ejection and the radius of the star as equal to 5 solar radii and considering the velocity of motion of the cloud to be constant, we find

$$R_e \simeq 2 R_*,$$

where R_e is the altitude of the average level of the emission zone in the atmosphere of χ Oph. This value exceeds by a factor of 3 that given by A.A.Boyarchuk for the average altitude of emission zones in Be stars (Bibl.11) and corresponds to the value given by M. and G.Burbidge for the emission zone of χ Oph (Bibl.65). Nevertheless, it must be remembered that our estimate is very rough.

In conclusion, we note that during all observations the violet absorption component was usually more intense than the red and only in individual cases did we observe V/R < 1.

5. Discussion of Results

First, we will attempt to give a physical interpretation of the noted phenomenon and will compare the main regularities discussed in the preceding Sections.

1. A systematic increase in brightness in the photographic region of the spectrum occurs simultaneously with an increase in the spectrophotometric temperature T_2. This is accompanied by deepening of the absorption lines but does not change the emission lines.

2. A comparison of the curve of the violet gradient Φ_1 with the curve of the equivalent widths of $H\beta$, indicates satisfactory agreement in the character of their variations.

3. The short-period variations of the gradients Φ_1 and Φ_2 show a mirror-image dependence, whereas the long-period variations have a different character.

4. Changes in m_{vi} and Φ_1 occur simultaneously so that, on increasing the temperature T_1, the visual brightness of the star decreases.

5. The short-period variations of brightness and temperature are not related.   /231

6. There is a functional dependence between variations of the three values of the gradient.

7. Powerful processes, causing the ejection of matter at velocities of the order of 1000 km/sec, occur in the star.

8. At a distance of the order of 2 R_* from the surface of the photosphere there is an effective emission zone in the star envelope.

9. The intensity of the emission lines above the average level of the absorption components tends to keep a constant value.

The most important of the above regularities, for our viewpoint, is the first. This phenomenon is most distinctly expressed and is indicated by many characteristics. It can be physically interpreted if we assume that, during the observation, the liberation of additional energy under the photosphere of the star is systematically enhanced. That this liberation occurs below the reversing

layer is clear from the deepening of the absorption lines. To prove that it also occurs below the photosphere a simple calculation is sufficient: It is known that thick shells, an extended photosphere, etc. greatly distort the spectral distribution in stellar emission, reducing its similarity with black-body radiation. If, in the stellar atmosphere, the optical thickness τ for frequencies of the continuous spectrum does not vary gradually but in marked discontinuities, changing from $\tau < 1$ to a value $\tau \gg 1$ at a minor variation in radius, the deviation of stellar radiation from black-body radiation would play a role only in the region of the limiting frequencies of the spectral series, such as takes place in normal atmospheres. Thus, we can consider that the "black" portion of stellar radiation is created by the photosphere layers with $\tau > 1$, whereas the atmosphere and the processes occurring in it cause diverse deviations. Let us examine whether the relation between the variations of the gradient Φ_2 and brightness (whose character cannot be explained by the shell) obeys the laws of black-body radiation. We will write the well-known formula, derived for black-body radiation,

$$M_{phot} = -0.72 - 5\log R + \frac{36700}{T} + x, \tag{12}$$

where M is the absolute stellar magnitude, R is the radius, and T is the temperature of the star. This formula indicates that an increase in temperature is accompanied by an increase in luminosity of the star. It is evident that, for this star,

$$\Delta M = \Delta m.$$

Therefore, from eq.(12) it follows that $m_1 - m_2 = \dfrac{36,700}{T_1} - \dfrac{36,700}{T_2}$

where the subscripts denote two times of observation. If, for the times 1 and 2, we take the start and end of the observation period, then, having determined from the variation curve of Φ_2 the values of $(\Phi_2)_1$ $(\Phi_2)_2$ and the corresponding temperatures, we can determine the degree of brightness variation of the star under the assumption that the variations in brightness and temperature obey the laws of black-body radiation. At the observed increase in temperature $(T_2)_2 - (T_2)_1 = 800°C$, a change in brightness of $\Delta m = 0^m.08$ would occur. Actually, a value of $\Delta m = 0^m.10 - 0^m.12$ was observed.

The good agreement of the results demonstrates that the photographic change in brightness had a thermal character and that, consequently, the liberation of additional energy occurred under the photosphere.

The photosphere converts radiation of any nature into thermal radiation, whose temperature corresponds to the temperature of the photosphere. Table 3 /232 indicates that the value of T_2 varies within limits of 5000 to 8000°C. Hence, we can conclude that χ Oph does not have a photosphere of class B as would be expected of classes G - F. If we eliminate speculation from this, it is difficult to explain why the low-temperature radiation rather than the hot (violet) radiation exhibits the "black-body" nature.

The rise in the spectral curve of χ Oph starts from λ 4400 Å toward the short-wave end. Beginning with this wavelength, the main role in the spectral

curve is no longer played by low-temperature radiation but by an extremely variable radiation whose gradient indicates temperatures varying from 8000 degrees to infinity. The changes in the gradient Φ_1 show no relation with the photographic brightness, whereas the relation with the visual brightness has an inverse sense, i.e., with an increase in temperature the brightness decreases. It was pointed out above that the gradient of Φ_1 is similar in its changes to the curve of the ultraviolet excess. All this, in combination with the encountered values $T = \infty$, indicates the nonthermal nature of this radiation. Nonthermal radiation, whose intensity apparently increases greatly in the ultraviolet, may create conditions of ionization and excitation in the stellar atmosphere, corresponding to its classification. Below, we will discuss the problem of the intense ultraviolet in the spectrum of the intermediate star. Here, we will note that our assumption explains the above spectral dependence of the gradients Φ_1 and Φ_2. Somewhere in the region of λ 4300 Å there are two types of radiation of a different spectral distribution and different physical nature. If, at some instant, there is an increase in temperature T_2 (decrease in Φ_2), then the maximum of the Planck curve is shifted toward the short-wave end. If the spectral distribution of the nonthermal radiation remains constant, then the addition of energy leads to a flattening of the slope of the spectral curve in the violet portion of the spectrum, i.e., to an apparent drop in temperature T_1 (increase in Φ_1). The same may take place on any change in the intensity of the nonthermal radiation at constant thermal radiation. If both types of radiation change dissimilarly but in the same direction, the mirror dependence may become weak or disappear altogether, as was actually observed (see Fig.3).

The spectral distribution in nonthermal radiation does not remain constant. Therefore, its effect on the long-wave region of the spectrum is not always cut off at the same wavelength. This is apparently due to some physical causes underlying the nonthermal radiation and acting at a certain instant of time. Therefore, aside from the fact that the curve of the long-period variations of Φ_1 should show a certain general increase with a decrease of the curve of Φ_2, it cannot have its conventional structural features which would have to affect the character of the changes in Φ_2. Such a disparity is completely understandable. The drop in intensity on the Planck function occurs slowly, whereas in nonthermal radiation the function $I(\lambda)$ may be steeper. This could explain the absence of a correlation between the long-period variations of the gradients Φ_1 and Φ_2.

We have no data that could explain the dependence between Φ_1 and m_{vis}. The sense of these correlations is that, with an increase in intensity of the ultraviolet and nonthermal radiation in the photographic range of the spectrum characterized by the gradient Φ_1, the visual brightness decreases while the spectrophotometric temperature in the red spectrum region increases. Changes of such a character could be caused by the following mechanism: If a star is surrounded by a stationary envelope, as follows from the data by A.A.Boyarchuk (Bibl.11) /233 and is confirmed by our observations, then the increment of the ultraviolet radiation and consequently of the radiation pressure should lead to broadening, which means a decrease of the envelope density. The luminosity of the envelope will decrease and, since the role of the envelope shows mainly in the long-wave region of the spectrum, the visual brightness of the star will also decrease. On the other hand, V.G.Gorbatskiy (Bibl.12) showed that a weakening of the effect of the envelope leads to an increase in the spectrophotometric temperature T_3.

This picture agrees qualitatively with the observational data. A corresponding analytical expression for the functional relation of the change in gradients could confirm this, but there are too few observations available to establish this relation.
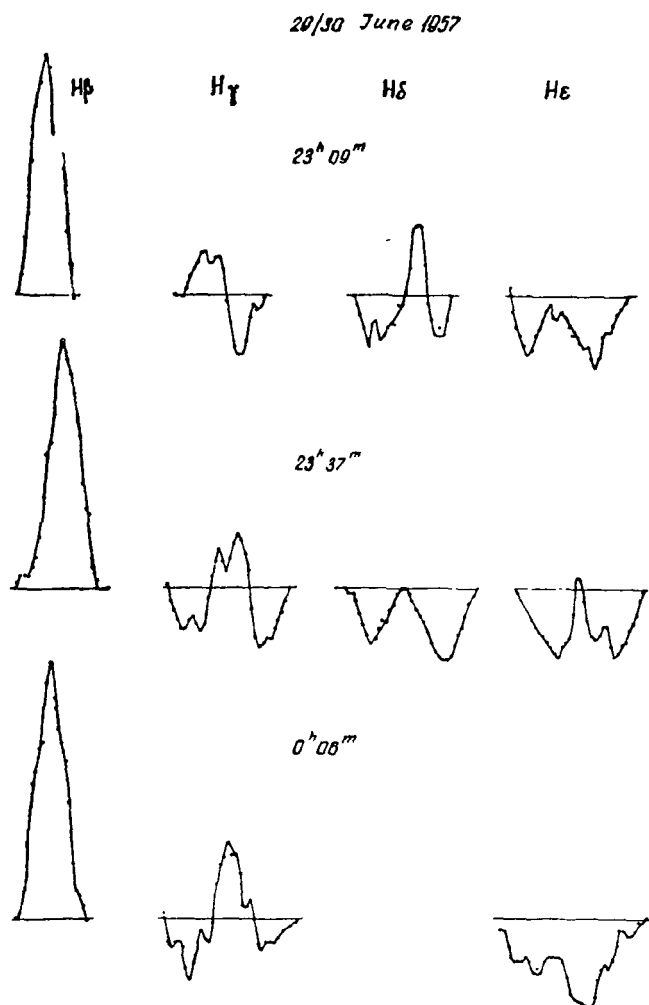

Fig.8 Changes in the Profiles of Hydrogen Lines during
the Observation Period of June 29-30

In conformity with the theory by V.A.Ambartsumyan (ыbl.13), concerning the different altitudes at which liberation of energy can occur in the stellar atmosphere, we assume that the nature of the process causing the changes in thermal and in nonthermal radiation of the star is the same. When the process is not sufficiently intense and liberation of energy occurs under the photo- /234 sphere, variations in the thermal radiation of the star will occur. When this liberation occurs in the atmosphere or in the envelope, there will be an increase in the intensity of nonthermal radiation equivalent to the width of the emission lines, a change in the spectral distribution of the nonthermal radiation, etc.

Based on this hypothesis, we must conclude that, during the observations, the intensity of the atmospheric liberation of energy changed irregularly, whereas the intensity of the process of the release of energy under the photosphere increased continuously. From time to time ejection of matter, not associated with the energy carrier of nonthermal radiation, from the surface of the star takes place.

It was mentioned that the increment in nonthermal radiation is associated with an increase in the equivalent width of the emission lines. It is difficult to say what physical mechanism is operating here. Let us return to the changes in the spectrum of χ Oph, observed on the night of June 29-30, 1957 (Fig.8). The line variations shown in the diagram were accompanied by a marked increase in intensity of the ultraviolet which, on the last photograph, had a value greater than all previously observed increases. The excitation mechanism is unclear, but apparently it acted in the stratified hydrogen envelope where the atoms in states of lower excitation potential are close to the surface of the star; obviously, an agent moving at a velocity common for ejection of matter in stellar atmospheres is involved here, i.e., traveling at several hundreds of kilometers per second. This character of the stratification of the envelope is in agreement with the data by O.Struve on the width of hydrogen emission lines (Bibl.45).

On this basis, we can assume that the intensification of the Hβ and Hγ lines took place before start of our observations.

The hypothesis of a star of an intermediate spectral class with a stratified hydrogen envelope and intense variable nonthermal emission does not explain all the regularities in the spectrum of χ Oph enumerated at the beginning of the Section. The purpose of the work reported here was not to construct the model of a star but to obtain the largest possible amount of systematic observational data. Therefore, the interpretation proposed here should furnish a convenient working hypothesis for further detailed observations. It is suggested to subject χ Oph, just as other bright Be stars, to continuous spectral and photoelectric observations for a period of several years. No doubt, this would shed light on the nature of the changes occurring in them.

BIBLIOGRAPHY

1. Kukarkin, B.V., Parenago, P.P., Kholpov, P.N., and Yefremov, Yu.I.: General Catalogue of Variable Stars (Obshchiy Katalog peremennykh zvezd). No.1, Moscow, Izd. Akad. Nauk SSSR, 1958.
2. Tsoi Dai O.: Astron. Zh., Vol.33, No.4, 1956.
3. Parenago, P.P.: Course on Stellar Astronomy (Kurs zvezdnoy astronomii). Moscow, Gos. Izd. Tekhn.-Teor. Lit., 1954.
4. Tikhov, G.A.: Principles of Visual and Photographic Photometry (Osnovy vizual'noy i fotograficheskoy fotometrii). Alma-Ata, Izd. Akad. Nauk KazSSR, 1950.
5. Kupo, I.D.: Trudy Sekt. Astrobotan., Vol.8, Alma-Ata, Izd. Akad. Nauk KazSSR, 1960.
6. Mirzoyan, L.V.: Soobshch. Byurakansk. Observ., Yerevan, Izd. Akad. Nauk

ArmSSR, No.16, 1955.

7. Mel'nikov, O.A.: Variable Stars (Peremennyye zvezdy). Moscow, Izd. Akad.
    Nauk SSSR, Vol.10, No.6, 1956.

8. Aller, L.Kh.: Astrophysics Part I (Astrofizika, T.1). Moscow, Izd. Inostr.
    Lit., 1955.

9. Mirzoyan, L.V.: Soobshch. Byurakansk. Observ., No.7, Yerevan, Izd. Akad. /235
    Nauk ArmSSR, 1951.

10. Sobolev, V.V.: Moving Envelopes of Stars (Dvizhushchiyesya obolochki zvezd).
    Leningrad, Izd. Len. Gos. Univ., 1947.

11. Boyarchuk, A.A.: Emission-Line Stars (Étoiles à raies d'émission). Papers
    of the Liège Symposium, p.159, 1958.

12. Gorbatskiy, V.G.: Astron. Zh., Vol.26, No.5, 1949.

13. Ambartsumyan, V.A.: Soobshch. Byurakansk. Observ., No.13, Yerevan, Izd.
    Akad. Nauk ArmSSR, 1954.

14. Gordon, I.M.: Tr. Khar'kov. Astron. Observatorii, Vol.12, Khar'kov, Izd.
    Khar'kov. Gos. Univ., 1957.

15. Ashbrook, J.: P.A., Vol.57, No.3, p.111, 1949.

16. Mayall: AAVSO HQR, Nos.2-3, 1946-1947.

17. Cousins, A.: Observatory, Vol.72, pp.867, 87, 1952.

18. Cousins, A.: MN ASSA, Vol.11, No.1, p.9, 1952.

19. Blaauw, A., Morgan, W., and Bertiau, F.: Astrophys. J., Vol.121, No.2,
    p.557, 1955.

20. Blaauw, A.: Gron. Publ., No.52, 1946.

21. Duke, D.: Astrophys. J., Vol.113, No.1, p.100, 1951.

22. Ramsey: Astrophys. J., Vol.111, p.434, 1950.

23. Stebbins, Huffer, and Whitford: Astrophys. J., Vol.91, p.20, 1940.

24. - Yale Catalogue of Parallaxes.

25. Slettebak, A. and Howard, R.: Astrophys. J., Vol.121, No.1, p.102, 1955.

26. Campbell, W. and Albrecht, S.: Lick Obs. Bull., Vol.5, p.174, 1908-1910.

27. Campbell, W.: Lick Obs. Bull., Vol.16, 1928.

28. Curtiss, R.: Publ. Obs. Univ. Mich., Vol.4, p.12, 1932.

29. Cleminshaw, C.I.: Astrophys. J., Vol.83, No.5, p.487, 1936.

30. Hynek, J.: Pers. Contr., No.14, 1940.

31. Adams, W.: Astrophys. J., Vol.97, p.105, 1943.

32. Burbidge, E.M.: Astrophys. J., Vol.115, No.3, p.418, 1952.

33. Burbidge, E.M. and Burbidge, G.R.: Astrophys. J., Vol.118, p.252, 1953.

34. Struve, O.: Astrophys. J., Vol.73, p.94, 1931.

35. Struve, O.: Astrophys. J., Vol.78, p.2, 1933.

36. McLaughlin, D.B.: Publ. Obs. Univ. Mich., Vol.4, p.12, 1932.

37. Slettebak, A.: Astrophys. J., Vol.110, No.3, p.508, 1949.

38. Slettebak, A.: Astrophys. J., Vol.113, No.2, p.436, 1951.

39. Fleming: Astron. Nachr., Vol.126, p.163, 1891.

40. Campbell: Astrophys. J.: Vol.2, p.177, 1895.

41. Merrill, P.W.: Lick Obs. Bull., Vol.7, p.162, 1912-1913.

42. Cannon, A.: Harvard College Obs. Annals, Vol.56, p.71, 1912.

43. Pickering, E.C.: Harvard College Obs. Circ., No.98, 1905.

44. Fleming: Harvard College Obs. Annals, Vol.56, p.181, 1912.

45. Struve, O. and Swings, P.: Astrophys. J., Vol.75, p.161, 1932.

46. Merrill, P.W.: Astrophys. J., Vol.65, p.286, 1927.

47. Struve, O.: Die Sterne, Vol.12, p.1, 1932.

48. Hiltner, W.A.: Astrophys. J., Vol.105, No.1, p.212, 1947.

49. Merrill, P., Humason, and Burwell, C.: Astrophys. J., Vol.76, p.156, 1932.
50. McLaughlin, D.B.: Publ. AAS, Vol.7, p.93, 1932.
51. Ashbrook, J.: P.A., Vol.50, No.1, p.30, 1942.
52. Bowen: Publ. Astron. Soc. Pacific, Vol.59, p.196, 1947.
53. Keenan, P.C. and Hynek, J.A.: Astrophys. J., Vol.111, p.1, 1950.
54. Butler, H.E.: Emission-Line Stars (Étoiles à raies d'émission). Papers of
      Liège Symposium, p.193, 1958.
55. Wyse: Publ. Astron. Soc. Pacific, Vol.53, p.184, 1941.
56. Schilt, J. and Jackson, C.: Astronom. J., Vol.56, No.8, p.224, 1952.
57. Oosterhoff: Bull. Astron. Inst. Neth., Vol.11, No.425, p.299, 1951.
58. Ch'ing Sung Yu: Publ. Astron. Soc. Pacific, Vol.39, p.112, 1927.
59. Ch'ing Sung Yu: Lick Obs. Bull., Vol.15, p.1, 1930-1932.
60. Karpov, B.G.: Lick Obs. Bull., Vol.16, pp.457, 159, 1933.
61. Hall, J.S. and Mikesell, A.H.: Publ. US Naval Obs., Vol.17, No.1, Ser.2,
      1950.
62. van Smith, E.P.: Astrophys. J., Vol.124, No.1, p.43, 1956.
63. Shapley, H. and Payne, C.: Harvard Bulletins, Vol.28, 1922.
64. Rojasa, H. and Herman, R.: Emission-Line Stars (Étoiles à raies d'émis-
      sion). Papers of the Liège Symposium, p.198, 1958.
65. Burbidge, E.M. and Burbidge, G.R.: Astrophys. J., Vol.122, No.1, p.89,
      1955.

METHOD FOR CALCULATING ATMOSPHERIC TRANSPARENCY IN DETERMINATIONS OF SPECTROPHOTOMETRIC GRADIENTS

I.D.Kupo

The attenuation of light in the earth's atmosphere affects both the general level of brightness and the relative energy distribution in its spectrum. This necessitates its calculation when solving photometric and spectrophotometric problems. An exact computation is rather cumbersome; therefore, most observers resort to simplifications, assuming that the transparency is the same over the entire sky, that it does not change during the time of observation, and that on the average it is constant for a given point on the earth. Atmospheric transparency is calculated by Bouguer's method and, in spectrophotometric work, is usually computed for each wavelength separately. In this case, Bouguer's law can be written in the form

$$-\frac{I_{z\lambda}}{I_{0\lambda}} = p_\lambda{}^{M(z)-1} \quad , \tag{1}$$

where $I_{0\lambda}$ is the intensity at the wavelength λ when the star is at the zenith; $I_{z\lambda}$ is the same for a zenith distance z; p_λ is the transmission coefficient at the wavelength λ; M(z) is the atmospheric mass. By observing the star at different zenith distances, we can find p_λ and $I_{0\lambda}$ from eq.(1). It is obvious that this process is tedious if repeated for a number of wavelengths. Nevertheless, this is the conventional procedure.

In our work, we greatly facilitated this problem. In determining the gradients we did not use the values of $I_{0\lambda}$ but only the zenith value of the spectrophotometric gradient. Let us write Bouguer's law separately for both photometered objects (in our case HD 148898 and α Lyr). Then,

$$\Delta \log I_{z\lambda}{}^{*-\alpha\,Lyr} = \log I^*_{z\lambda} - \log I_{z\lambda}{}^{\alpha\,Lyr} = \log I^*_{0\lambda} - \log I_{0\lambda}{}^{\alpha\,Lyr} +$$
$$+ \log p_\lambda [M(z_*) - M(z_{\alpha\,Lyr})] . \tag{2}$$

However, the value of $\Delta \log I$ is correlated with the gradient by

$$\Delta \log I_\lambda = \frac{1}{\lambda} \quad H + a,$$

where H is proportional to the gradient and a is a constant. Then,

$$\frac{1}{\lambda} H = \frac{1}{\lambda} H_0 + A + g\,p_\lambda \Delta M(z) . \tag{3}$$

Here, H_0 is the unknown zenith gradient, and A is a new constant:

$$A = a_0 - a. \tag{4}$$

However, a = $\Delta \log I$ for $\frac{1}{\lambda}$ = 0.

Consequently, the value of a depends on the brightness difference of the compared stars, a_0 is the zenith value of this difference, and a is the same, distorted by the atmosphere effect. It is evident that if the brighter star is located at a shorter zenith distance, we have $a > a_0$, and if the latter is the comparison star, we can write, again using Bouguer's law,

$$a = a_0 - \log p_\infty \cdot \Delta M(z). \tag{5}$$

From eqs.(4) and (5) we obtain

$$A = \log p_\infty \cdot \Delta M(z), \tag{6}$$

after which eq.(3) can be rewritten in the form

$$\frac{1}{\lambda} H = \frac{1}{\lambda} H_0 + \Delta M(z) \cdot \log p_\lambda + \Delta M(z) \log p_\infty . \tag{7}$$

We do not know the value of p_∞, but we can indicate its extreme limits. Assuming that, for $\lambda = \infty$, the atmosphere is transparent, $p_\lambda = 1$, then

$$\frac{1}{\lambda} H = \frac{1}{\lambda} H_0 + \Delta M(z) \log p_\lambda . \tag{8}$$

On the other hand, we can assume that $p_\infty = p_\lambda$, i.e., that the transparency for an infinite wavelength is the same as for the selected wavelength in the spectral region under consideration. In such a case, eq.(7) will take the form

$$\frac{1}{\lambda_c} H = \frac{1}{\lambda_c} H_0 + 2 \Delta M(z) \log p_{\lambda_c} , \tag{9}$$

where λ_c is some kind of fixed wavelength.

Thus, eq.(7) can be presented in the form

$$\frac{1}{\lambda_c} H = \frac{1}{\lambda_c} H_0 + n \Delta M(z) \log p_{\lambda_c} , \tag{10}$$

where $2 \geq n \geq 1$.

On solving eq.(10) by the method of least squares, we obtain

$$\log p_{\lambda_c} = \frac{K \Sigma n \Delta M H_z - \Sigma H_z \cdot \Sigma n \Delta M}{K \Sigma (n \Delta M)^2 - (\Sigma n \Delta M)^2} ;$$

$$H_0 = \frac{\Sigma (n \Delta M)^2 \cdot \Sigma H_z - \Sigma n \Delta M \cdot \Sigma n \Delta M H_z}{K \Sigma (n \Delta M)^2 - (\Sigma n \Delta M)^2} ,$$

where k is the number of equations.

As we see, the second expression does not depend on the value n. Consequently, the zenith value of the gradient in this method is free of any assumptions.

In determining the quantity log p_{λ_c}, the value n enters so that the above method can be used only for deriving the limits within which the transmission coefficient is located.

If, at a fixed wavelength, we take one corresponding to the mean frequency of the spectral interval

$$\left(\overline{\frac{1}{\lambda}}\right) = \frac{1}{2}\left(\frac{1}{\lambda_1} + \frac{1}{\lambda_2}\right),$$

then the equality (10), in final form, is rewritten as

$$H = H_0 + \frac{n}{\left(\overline{\frac{1}{\lambda}}\right)}\, \Delta M(z) \log \overline{p_\lambda},$$ (11)

where

$$\overline{p_\lambda} = \sqrt{p_{\lambda_1} \cdot p_{\lambda_2}}.$$

Of course, the proposed method of calculating the atmospheric transparency cannot be used if the transmission coefficient of the atmosphere is wanted, but in our opinion it has a number of advantages in determining the spectrophotometric gradients. First, the method is less cumbersome since all values entering into eq.(11) are determined beforehand for other purposes and it remains only to solve this equation. Second, instead of plotting the values of log I, which are weighted with random errors, a certain average value for a given region, i.e., in this case the gradient, is laid off on the ordinate of Bouguer's diagram in accordance with Bouguer's method. Finally, reliable plotting of Bouguer's line requires observations at sufficiently spaced zenith distances. This is difficult to achieve when a region with a small declination is observed. In our case, in observing the region of χ Oph, the maximal Δz reached during the night did not exceed 11°. If, along with stars of such a region, an object is observed which rapidly changes its zenith distance, the change in the difference of atmospheric masses – at appropriate selection of the observation time – may yield an appreciably higher value. A combination of the observations of the region χ Oph and α Lyr will yield a change of ΔM during the course of the night, almost twice the maximal permissible change of M.

It is obvious that, in the above method, the dependence log $p_\lambda \sim \frac{1}{\lambda}$ is postulated for a limited spectral region. This assumption is approximately valid since, without such proportionality, it would be impossible to observe changes in the value of the gradient in a given spectrum region; the strong camber of the spectral curve would not permit its expression by one gradient value.

This method of calculating atmospheric transparency is identical at least for that portion of the celestial dome where both compared regions are located. This is one of the simplifications of the problem mentioned at the beginning of this Section.

This method of calculating atmospheric transparency was used in our work (Bibl.1). The investigated region of χ Oph was photographed repeatedly (up to 8 times) during the night. The spectrum of α Lyr was imprinted on each negative.

The relative spectrophotometric gradient of the star HD 148898, which served as comparison star when spectrophotometering χ Oph, was determined on each photograph with respect to α Lyr. For nights during which more than four gradients were obtained, eq.(11) was solved by the method of least squares, and the value of the zenith distance was obtained. We also calculated the values of $\bar{p}_\lambda$ for the boundary conditions n = 2 and n = 1. Since the gradients of the comparison star were determined for two regions of the spectrum λλ 3800 – 5200 Å and λλ 5300 – 6500 Å, the values of p_λ were also obtained for the wavelengths λ 4500 Å and λ 5900 Å. The results of the calculation for p_{4500} are shown in Table 1. For $\bar{p}_{5900}$ only the average value, obtained from the data of six nights of observation, is given:

$$\overline{p_{5900}} = 0.80\,(n=2);\ 0.65\ (n=1)$$

TABLE 1

Date 1957	21/22 March	23/24 March	27/28 March	5/6 June	6/7 June	18/19 June	19/20 June	28/29 June	29/30 June	4/5 July	2/3 August	Average
$\overline{p}_{4500}$	0.69	0.74	0.81	0.70	0.78	0.81	0.84	0.60	0.83	0.66	0.63	0.74
	0.47	0.55	0.66	0.50	0.62	0.65	0.71	0.36	0.69	0.44	0.40	0.55

Thus, both the average and the individual values of $\bar{p}_\lambda$, found on the assumption of n = 2, are in satisfactory agreement with the data of other transparency determinations. There also is agreement between these results and the daytime determinations of transparency, made by V.S.Sokolova for the Kamenskiy Plateau (Bibl.2). Apparently, the formal value of p_∞ can be considered as approximately equal to p_λ, and for an incidental approximate evaluation of the transmission coefficient we can use eq.(9).

In plotting Bouguer's lines it was noted that, first, they represent a straight line only up to an atmospheric mass difference not exceeding $\Delta M = 2$ and that, second, the curvature produced at large values of ΔM is convex toward the abscissa. The first fact indicates an inconstancy of transparency during the observations, which is a serious shortcoming of the astroclimate of the Observatory. The second fact leads to a curious conclusion: Since $\Delta M > 2$ was usually reached after midnight, the impression is gained that the character of the break in Bouguer's line indicates a deterioration of atmospheric transparency during the second half of the night. The available material does not permit a final conclusion. The question arises whether this phenomenon is caused by temporary midnight disturbances, which become stabilized during the course of the night or which, conversely, progress to the predawn hours. These questions require further study. In any case, the noted effect contradicts the usual concept of the variation of transparency during the night; although we cannot insist on its reality owing to the lack of material, we thought it useful to call the attention of observers to this finding.

BIBLIOGRAPHY

1. Kupo, I.D.: Spectrophotometric Investigation of χ Ophiuchi (Spektrofoto-
   metricheskoye issledovaniye χ Zmeyenostsa). Trudy Sekt. Astrobotan.,
   Vol.8, Alma-Ata, Izd. Akad. Nauk KazSSR, 1960.
2. Sokolova, V.S.: Investigation of the Astroclimate in the Region of Alma-Ata
   (Issledovaniye astroklimata v rayone g. Alma-Aty). Vestn. Akad. Nauk
   KazSSR, No.8 (41), 1948.

COMPARISON OF THE TELLURIC LINES OF O_2 AT DIFFERENT HEIGHTS ABOVE SEA LEVEL

L.G.Kuznetsova

Investigations of the oxygen content in the earth's atmosphere have been carried out at the Astrobotany Sector of the Kazakh Academy of Sciences since 1955 (Bibl.1). Their purpose was to determine the dependence of the oxygen content in the atmosphere on the seasons of the year, the subjacent surface, and on the height of the locality above sea level, and for other reasons.

In 1955 - 1956, A.K.Suslov made systematic observations of the telluric lines of O_2 at Alma-Ata. As a result, he was able to define the annual variation in intensity of the telluric lines of O_2 for Alma-Ata with a maximum in July.

The observations of 1955 - 1956 at Alma-Ata, Ashkhabad, Vannovskiy, and Temir-Tau in Gornaya Shoriya indicated that the telluric lines of O_2 depend on the subjacent surface of the geographic point, on the seasons of the year, on changes in the type of macrocirculation in the atmosphere, etc.

In 1958, the author in collaboration with A.K.Suslov, carried out investigations to demonstrate the dependence of the intensity of telluric lines of O_2 on the height above sea level. The observations were made simultaneously at heights of 850 and 3060 m above sea level (a difference in altitude of 2210 m). The results of this work are given below.

1. Description of Instruments

The observations were performed simultaneously at two localities:

1) Observatory of the Astrobotany Sector at Alma-Ata ($\lambda = 5^h 7^m 42^s.46$; $\varphi = 43° 14' 47"$; H = 850 m above sea level). The observer was L.G.Kuznetsova.

2) Observatory of GAISh (Shternberg State Astronomical Institute) at Dzhaylyau (Zailiyskiy Alatau, region of Lake Alma-Ata) ($\lambda = 5^h 9^m$; $\varphi = 43° 4'$; H = 3060 m above sea level). The observer was A.K.Suslov.

At the former site, a diffraction telespectrograph 2, described elsewhere (Bibl.1), was used.

The diffraction grating of the spectrograph had 5600 lines per centimeter. The objective of the camera was a Tessar apochromatic lens with an aperture ratio of 1:10 and a focal length of 46 cm. The objective of the collimator had a focal length of 40 cm. In front of the slit an objective (No.52000, 12 × 10, London, Rapid Rectilinear) was attached, which projected the image of the sun onto the slit of the collimator.

The spectrum of the center of the solar disk at the third order with a dispersion of 7.077 ± 0.042 Å/mm was investigated. The resolution was $\frac{\lambda}{\Delta\lambda}$ = = 6288 (Fig.1).
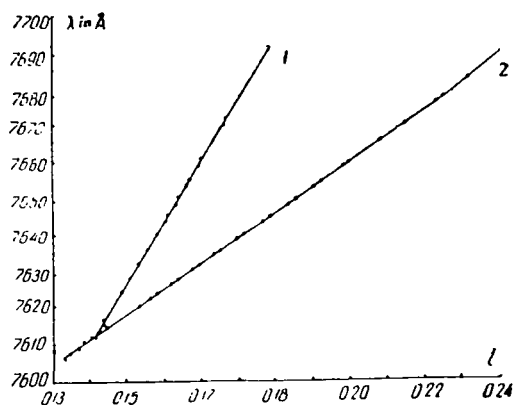

Fig.1 Dispersion Curves
(Numbers of the lines correspond to the numbers
of the spectrograph on all diagrams)

The dispersion curve was plotted from the photometric segment of the band A.

At the second observation site, a diffraction spectrograph 1, described elsewhere (Bibl.2), was used.

The objective of the camera was a calloptate with an aperture ratio of 1:7.7 and a focal length of 19 cm (E.Krauss, Paris, No.70831). The focal length
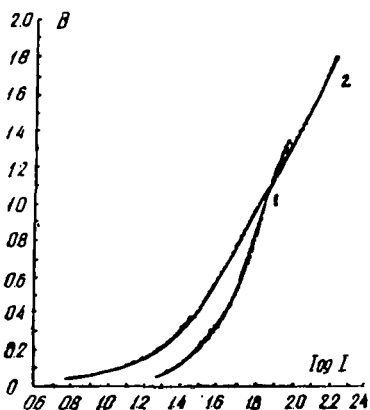
Fig.2 Characteristic Curves

278

of the collimator objective was 21 cm and the lens diameter, 2.5 cm.

The spectrograph was used as a nebular type, using a method analogous to that given elsewhere (Bibl.1). A third-order spectrum with a dispersion of 16.63 ± 0.18 Å/mm was investigated.

At both sites, the telluric line of O_2 with a wavelength of $\lambda = 7620$; 995 Å was spectrographed.

2. Work-Up of the Negatives

The scale of a step wedge was imprinted on each negative. At the first observation site, we used a quartz step wedge No.550193 which we calibrated on the MF-2 microphotometer with a red filter through which the sun was spectrographed.

At the second site, we used a step wedge No.510003 from the ISP-51-M spectrograph belonging to the GAISh. The data of field transmission are taken
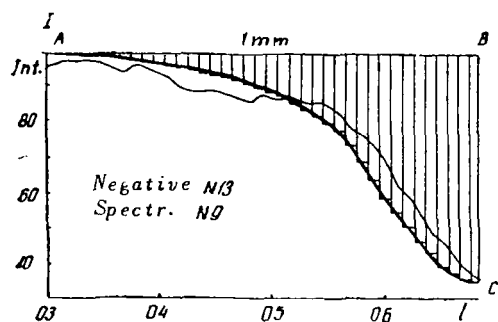

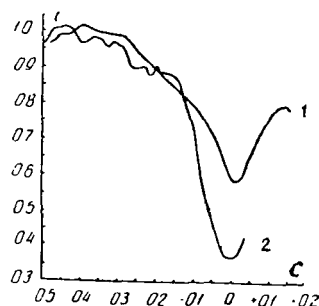Fig.3 Profile of O_2 Lines and Averaged Curve

Fig.4 Profiles of O_2 Lines

from the description. The first field of the step wedge No.550193 has a transmission coefficient of 2.0, the second, 1.82; third, 1.59; fourth, 1.42; fifth, 1.27; sixth, 1.1; seventh, 0.93; eighth, 0.76.

The step wedge No.510003 had the following transmission coefficients: first field, 2.0; second, 1.8; third, 1.63; fourth, 1.46; fifth, 1.28; sixth, 1.1; seventh, 0.93; and eighth, 0.76.

At the first site, an extrafocal image of the sun, obtained by using one back lens of the objective, was used when photographing the scale. The front lens was unscrewed. The characteristic curves were plotted for the spectral region between the investigated line and the main series (Fig.2).

The negatives were analyzed on the MF-2 microphotometer. The measured values of the density from the characteristic curves were converted to intensity

logarithms. The profiles of the oxygen lines were plotted from the obtained values. From these points we plotted the average curve, from which we recorded the values every 0.01 mm (0.07 Å) (Fig.3).

The equivalent width of the investigated oxygen lines was determined by <u>/242</u> the conventional method. Table 1 shows the equivalent widths of the oxygen lines investigated at the indicated two observation sites.
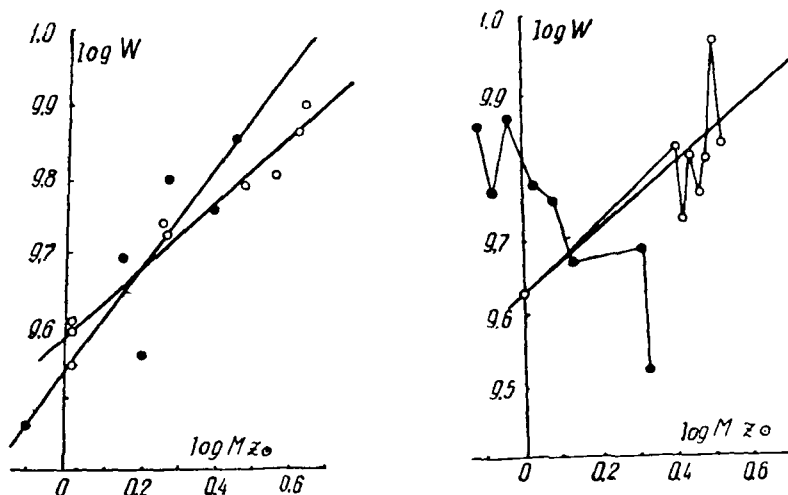
Figs.5, 6 Values of the Equivalent Widths of O₂ Lines
The dark circles are for Alma-Ata and the light circles for
the Observatory GAISh at Zailiyskiy Alatau

The intensity of the telluric lines of oxygen was compared with respect to 21 values of the equivalent widths of lines obtained at coinciding instants of time, with the difference in time of photographing not exceeding 10 min. Most often this difference was from 2 - 7 min.

The intensity of the telluric lines of O₂ at both sites is shown in Figs.5 and 6.

Having calculated the logarithms of the air masses log $M(Z_\odot)$ and reduced <u>/244</u> them to sea level (based on the Tables by N.M.Shtaude) and also the logarithms of the equivalent widths of O₂ lines log W, we plotted the curve (Fig.6). For all observation sites, we obtained the average straight lines characterizing the variation in intensity of the telluric lines of O₂ with a change in air mass.

The logarithms of the values of the equivalent widths of O₂ lines for log $M(Z_\odot)$ = 0.5 were taken by days for comparison. On the basis of this Table, we obtained the arithmetic mean values of log W for Alma-Ata and the Observatory of GAISh at Dzhaylyau. We have

$$W_A = 0.673 \ A; \quad W_D = 0.748 Å; \quad \Delta W = W_D - W_A = 0.075 Å .$$

Thus, the equivalent width of the O₂ lines formed by the atmospheric layer

TABLE 1

/243

VALUES OF EQUIVALENT LINE WIDTHS OBTAINED AT ALMA–ATA (850 m ABOVE SEA LEVEL) AND AT THE OBSERVATORY GAISh (ZAILIYSKIY ALATAU, 3060 m ABOVE SEA LEVEL)

| Date 1958 | log $M(Z_\odot)$ | Equivalent Line Width | | Date 1958 | log $M(Z_\odot)$ | Equivalent Line Width | |
| | | Alma-Ata log W | Observatory GAISh log W | | | Alma-Ata log W | Observatory GAISh log W |
1	2	3	4	1	2	3	4
24 July	0,430		9,462	27 July	0,399	9,748	9,681
	0,340		9,505		0,289	9,643	
	0,287		9,462		0,270	9,732	
	0,284		9,505		0,149		9,813
	0,246		9,462		0,094		9,756
	0,179		9,505		0,059		9,491
	0,150		9,477		−0,062		9,556
	0,155		9,568		−0,089		9,380
	0,036		9,415		−0,125		9,230
	0,013		9,663		−0,104		9,544
	−0,030		9,568	28 July	0,944	0,041	
	−0,061		9,398		0,891	0,017	
	0,056	9,531			0,554		9,944
	0,054	9,556			0,579	9,934	
	−0,078	9,602			0,425	9,880	
	−0,087		9,518		0,380	9,806	
	−0,112		9,531		0,290	9,672	
	−0,118		9,447		0,035		9,633
	0,285	9,806			−0,028		9,633
	0,301	9,771			−0,005	9,633	
	0,310	9,839		30 July	0,809	9,954	
	0,468	9,857			0,572	9,857	
	0,581	9,732			0,441		9,903
	0,779	9,991			0,554	9,851	
	0,866	0,009			0,502	9,857	
25 July	0,024		9,613		0,333		9,716
	0,023		9,653		0,419	9,845	
	−0,051		9,544		0,352	9,813	
	−0,111		9,431		0,215		9,699
	−0,112		9,580		0,175	9,756	
26 July	0,476	9,778			0,160		9,477
	0,205		9,518		−0,090		9,415
	0,167		9,681		−0,114		9,462
	0,286	9,690			−0,003	9,724	
	0,234	9,602			0,297	9,732	
	0,105		9,602		0,399	9,799	
	0,093		9,556		0,507	9,863	
	0,065		9,580		0,515	9,897	
	0,003		9,544		0,554	9,892	
	−0,095		9,518		0,581	9,903	
	−0,116		9,491		0,616	9,903	
	−0,124		9,544		0,640	9,903	
	−0,006	9,568		31 July	0,121		9,663
	−0,006	9,580			0,073		9,748
	−0,124		9,544		0,021		9,771
	−0,117		9,672		−0,045		9,863
	−0,117		9,602		−0,085		9,763
	−0,117		9,643		−0,005	9,623	
	0,112		9,740		−0,124		9,851
27 July	0,665	9,914			0,406	9,819	
	0,630	9,903			0,424	9,724	
	0,505		9,934		0,313		9,681
	0,611	9,778			0,442	9,813	
	0,594	9,851			0,329		9,518
	0,538	9,623			0,462	9,756	
	0,491	9,813			0,481	9,806	

TABLE 1 (cont'd)

1	2	3	4	1	2	3	4
31 July	0.506	9.968		15 Aug.	0.209		9.556
	0.530	9.826			0.266	9.724	
1 Aug.	0.392		9.839		0.143		9.690
	0.323		9.839		0.257	9.740	
	0.217		6.663		−0.105		9.462
	0.049		9.663		0.015	9.602	
	−0.121		9.491		0.016	9.544	
	−0.022		9.518		0.016	9.591	
14 Aug.	0.408		9.875	17 Aug.	0.550		9.826
	0.392		9.756		0.459		9.756
	0.269		9.699		0.283		9.681
	0.153		9.690		0.175		9.623
	−0.107		9.556	18 Aug.	0.592		9.939
	0.224		9.653		0.464		9.792
15 Aug.	0.636	9.903			0.282		9.672
	0.619	9.869			0.167		9.580
	0.449		9.857		−0.087		9.568
	0.562	9.806		19 Aug.	0.592		9.919
	0.476	9.792			0.465		9.813
	0.391	9.755	9.756		0.383		9.763
	0.269		9.799				

over the Observatory of GAISh at Dzhaylyau (Zailiyskiy Alatau) was 0.075 Å greater than that over Alma-Ata, despite the fact that the latter lies 210 m lower than the Observatory of GAISh at Dzhaylyau. It is useful to mention here the results of the investigations by A.K.Suslov in 1955 - 1956, although his observation sites did not differ that greatly in altitudes. There is more oxygen at Alma-Ata (850 m above sea level) than at Vannovskiy (610 m above sea level) than at Temir-Tau in Gornaya Shoriya (471 m above sea level) and at Ashkhabad (234 m above sea level). But there is less oxygen at Vannovskiy than at Ashkhabad.

Probably the subjacent surface of a given locality has a greater effect on the oxygen content at various geographic points than its height above sea level.

BIBLIOGRAPHY

1. Suslov, A.K.: Method and Certain Results of Spectrophotometry of Telluric Lines of O_2 (Metodika i nekotoryye rezul'taty spektrofotometrii telluricheskikh liniy O_2). Trudy Sekt. Astrobotan., Vol.VII, Alma-Ata, Izd. Akad. Nauk KazSSR, 1959.
2. Tikhomirov, V.S.: Seasonal Variations of Certain Reflective Properties of Plants and the Problem of Vegetation on Mars (Sezonnyye izmeneniya nekotorykh otrazhatel'nykh svoystv rasteniy i vopros o rastitel'nosti na Marse). Alma-Ata, Izd. Akad. Nauk KazSSR, 1951.
3. Shtaude, N.M.: A Method of Processing Spectrograms of the Self-Emission of Plants (K metodike obrabotki spektrogramm samoizlucheniya rasteniy). Trudy Sekt. Astrobotan., Vol.I, Alma-Ata, Izd. Akad. Nauk KazSSR, 1953.

BACK SCATTERING OF TWILIGHT AT ARBITRARY POINTS OF THE SKY

M.P.Perevertun

The totality of our knowledge on the troposphere, stratosphere, and ionosphere indicates that in the earth's atmosphere, beginning with the ground layers and ending with the atomic region, there are powerful movements of air masses, electric discharges of colossal force, and widely fluctuating temperature and pressure changes. Therefore, it is completely inadequate to study the atmosphere at one or several points of the earth no matter how efficient might be the facilities used for this purpose.

The atmosphere of the earth must be studied as a whole, using simple and accessible means of observations, which permit organizing a dense network of stations over a large portion of the USSR territory so as to obtain diurnal data on the physical state of the stratosphere and ionosphere. Of all indirect methods, the twilight method is optimum in this respect. A broad network of twilight stations will permit studying the structure of the stratosphere and lower layers of the ionosphere and to define its variations with changes in latitude and longitude of the observation sites. Such information will help to establish the interrelation and interdependence of meteorological phenomena with processes in the stratosphere and ionosphere. Practical experience has shown that the twilight method gives results that agree well with results obtained from rockets and artificial earth satellite launchings.

All this obliges Soviet scientists to develop and elaborate the twilight theory as well as to improve and design new apparatus for ensuring a successful twilight service. Further development of the twilight theory as a whole is intimately connected with working out a theory for calculating the secondary and higher orders of light scattering. Various papers by Soviet scientists have been devoted to this problem.

For a rigorous solution of the problem of calculating back scattering in twilight phenomena, the mode of calculation of the primary brightness of twilight at any point of the sky must be known. The twilight theory developed in the classical work by Academician V.G.Fesenkov and the numerous papers by N.M.Shtaude permit calculating the theoretical values of the primary brightness of twilight for the entire sky.

N.M.Shtaude, having laid the foundation of the general twilight theory and using the values of the primary brightness of the twilight sky as basis, gave a general formula for the magnitude of back scattering:

$$I_{11} = \frac{1}{C_1} \int_0^\infty BK\eta^M \, dr, \qquad (1)$$

where

$$C_1 = 2\pi \int_0^\pi f(\alpha) \sin \alpha \, d\alpha , \tag{2}$$

Here, η^M is a factor allowing for absorption along the line of sight; K is the optical density; B is the value of the double integral equal to

$$B = \int_0^{2\pi} dA \int_0^{v(A)} I_1 \sin v \, f(\alpha) \, dv , \tag{3}$$

where A is the azimuth; I_1 is the primary brightness of the ray; v is the angle of elevation above the horizon, i.e., the zenith distance of the influencing direction; $f(\alpha)$ is the scattering indicatrix.

Equation (1) permits a theoretical determination of back scattering at any point of the sky. However, a direct determination of the value of I_{II} by this formula requires extremely cumbersome calculations, since here the value of the primary brightness at a sufficiently large number of points along the line of sight must be known. This forced researchers to look for the limiting values of the unknown quantity I_{II}.

For the zenith, N.M.Shtaude found that

$$I_{II} = \frac{B_0}{C_1}(1 - p) , \tag{4}$$

where

$$B_0 = \int_0^{2\pi} dA \int_0^{\frac{\pi}{2}} I_1 f(v) \sin d v , \tag{5}$$

since, for the zenith, $\alpha = v$; p is the transmission coefficient at the observation site, and C_1 is the former value of the constant in eq.(1).

However, further development and elaboration of the theory of calculating the back scattering for the entire sky requires a determination of I_{II} for any direction of the line of sight. We made an attempt to define the limiting value of I_{II} for any point of the twilight sky.

In eq.(1), let us replace the factor η^M, which allows for absorption along the line of sight, by a value equal to

$$\eta^M = e^{-\theta_0 \widehat{b}(z_0)} \cdot e^{\theta \widehat{b}(z)} \tag{6}$$

and use a new integration variable $\widehat{}$.

From a determination of the generalized secant and the optical mass, we will obtain

$$\frac{dr}{dh} = \widehat{b}(z) , \tag{7}$$

$$d\theta = - k dh . \tag{8}$$

Hence,

$$kdr = k\widehat{b}(z)\,dh = -\widehat{b}(z)\,d\theta.$$

Substituting the values of η^M and kdr into eq.(1) will yield

$$I_{\parallel} = \frac{B_0}{C_1} \int_0^\theta e^{-\theta_0\widehat{b}(z_0)}\, e^{\theta\widehat{b}(z)}\,\widehat{b}(z)\,d\theta. \tag{9}$$

Since b(z) varies extremely slowly with any change in the value of z, i.e., $\widehat{b}(z_0) \cong \widehat{b}(z)$, the value of the integral (9) is easily taken in final form, so that

$$I_{\parallel} = \frac{B_0}{C_1}\left[1 - p\,\widehat{b}(z_0)\right]. \tag{10}$$

Based on eq.(10) we calculated, for every 10° of the solar vertical, the brightness of back scattering of the light of the twilight sky I_{II} at two wavelengths $\lambda_1 = 420$ mu and $\lambda_2 = 512$ mu for 6°, 7°, and 8° of solar depression.

To facilitate the calculations, we set up Tables for the values of $p^{\widehat{b}(z_0)}$ and Tables of their logarithms also for two wavelengths, $\lambda_1 = 420$ mu and $\lambda_2 = 512$ mu.

The value of B_0 entering into eq.(10) was calculated by the method of quadratures

$$B_0 = \int_0^{2\pi} dA \int_0^{\frac{\pi}{2}} W\,dv, \tag{11}$$

where $W = I_I \sin v\, f(\alpha)$.

The working formula for calculating W has the form

$$\log W = \log I_1 + \log \sin v + \log f(\alpha). \tag{12}$$

In calculating the values of W, we used the Rayleigh scattering indicatrix $f(\alpha)$:

$$f(\alpha) = 1 + \cos^2 \alpha, \tag{13}$$

since the values of the ratios I_{II}/I_I for Rayleigh and Rocar indicatrices showed only a negligible divergence, lying within the error of the calculation:

	Rocar	Rayleigh
z	$\dfrac{I_{II}}{I_I}$	$\dfrac{I_{II}}{I_I}$
94°	0.23	0.21
98°	0.62	0.61

The scattering angle α, made by a line passing through the point on which

285

the back-scattered light is incident and the line passing through the point which is the center of the back-scattering wave was calculated by the formula

$$\cos\alpha = \cos z_0 \cos v + \sin z_0 \sin v \cos A, \tag{14}$$

where z_0 is the zenith distance of the point at which the value of the back $\underline{/248}$ scattering is determined; v is the zenith distance of the effective point; A is the azimuth.

TABLE 1

$\xi_{\odot} = 96°$

v	m_{II}	
	λ_1	λ_2
0	—4.59	—5.89
2	—4.64	—5.89
5	—4.60	—5.79
10	—4.49	—5.53
20	—4.18	—5.14
30	—3.93	—4.78
40	—3.70	—4.53
50	—3.53	—4.34
60	—3.41	—4.17
70	—3.27	—4.00
80	—3.17	—3.91
90	—3.11	—3.84
100	—3.11	—3.82
110	—3.13	—3.86

TABLE 2

$\xi_{\odot} = 97°$

v	m_{II}	
	λ_1	λ_2
0	—3.51	—4.84
2	—3.53	—4.92
5	—3.51	—4.76
10	—3.73	—4.51
20	—3.09	—4.06
30	—2.80	—3.71
40	—2.60	—3.43
50	—2.41	—3.24
60	—2.25	—3.05
70	—2.09	—2.89
80	—1.98	—2.74
90	—1.88	—2.69
100	—1.93	—2.71
110	—2.00	—2.72
120	—2.11	—2.85
130	—2.23	—3.05
140	—2.42	—3.27
150	—2.62	—3.54
160	—2.92	—3.91
170	—3.37	—4.47
175	—3.51	—4.76
178	—3.53	—4.92
180	—3.51	—4.34

TABLE 3

$\xi_{\odot} = 98°$

v	m_{I}	
	λ_1	λ_2
0	—2.33	—3.73
2	—2.31	—3.62
5	—2.30	—3.60
10	—2.19	—3.46
20	—1.88	—2.62
30	—1.62	—2.62
40	—1.40	—2.38
50	—1.22	—2.19
60	—1.06	—1.95
70	—0.93	—1.78
80	—0.77	—1.62

TABLE 3 (cont'd)

$\xi_{\odot} = 98°$

v	m_{I}	
	λ_1	λ_2
90	—0.66	—1.52
100	—0.72	—1.56
110	—0.85	—1.66
120	—0.96	—1.82
130	—1.14	—2.05
140	—1.34	—2.23
150	—1.58	—2.53
160	—1.86	—2.88
170	—2.18	—3.46
175	—2.30	—3.60
178	—2.31	—3.62
180	—2.33	—3.73

286

In determining W, the scattering angles α were calculated at the solar vertical every 10° of elevation above the horizon and every 30° with respect to azimuth for the points $v = 0^\circ$, 2°, 5°, 10°, 20°, 30°, 40°, 60°, 70°, 90° at zenith distances of the sun equal to 96°, 97°, and 98°.

To check the degree of symmetry of I_{II} for the light and shaded sides of /249 the sky, we additionally calculated α and W for $v = 110^\circ$, 140°, 160°, 170°, 175°, 178°, and 180°.

The values of the back scattering brightness of light of the twilight sky I_{II}, calculated by eq.(10), are shown in Tables 1, 2, and 3, expressed in stellar magnitudes with square degrees.

An analysis of the results shows that the values of the light side of the twilight sky exhibit almost the same variation as the dark side. The difference does not exceed $6 - 8\%$ of the average values of m_{II}. Therefore, for all practical purposes we can consider the value of back scattering m_{II} to be symmetrical relative to the zenith for the entire sky. This opens broad possibilities for calculating the theoretical brightnesses of twilight with allowance for back scattering in any direction of the line of sight.

BIBLIOGRAPHY

1. Fesenkov, V.G.: Structure of the Atmosphere (O stroyenii atmosfery). Tr. Gl. Rossiyskoy Astrofiz. Observatorii, Vol.2, Moscow, 1923.
2. Fesenkov, V.G.: On the Problem of Investigating the Stratosphere by Photometric Analysis of Twilight (K voprosu issledovaniya stratosfery putem fotometricheskogo analiza sumerek). Trudy Vses. Konf. Izuch. Stratosf., Moscow, 1935.
3. Shtaude, N.M.: General Formula for Sky Brightness; Bemporad Function and its Value in Atmospheric Optics (Obshchaya formula yarkosti neba; funktsiya bemporad i yeye znacheniye v atmosfernoy optike). Izv. Akad. Nauk KazSSR, Ser. Astron. Fiz., No.32, Issue 2, 1946.
4. Shtaude, N.M.: Twilight Method of Investigating the Stratosphere (Sumerechnyy metod issledovaniya stratosfery). Izv. Akad. Nauk SSSR, Ser. Geogr. Geofiz., Vol.XIII, No.4, 1949.
5. Shtaude, N.M.: Back Scattering at Twilight, in Various Structures of the Atmosphere (Vtorichnoye rasseyaniye vo vremya sumerek pri raznykh stroyeniyakh atmosfery). Dokl. Akad. Nauk SSSR, Vol.LXIV, No.6, Moscow, 1949.
6. Perevertun, M.P.: New Possibilities of the Twilight Method in Determining the Temperature of the Stratosphere and Ionosphere; Brightness of the Twilight Sky at the Solar Vertical with Consideration of Back Scattering (Novyye vozmozhnosti sumerechnogo metoda v opredelenii temperatury stratosfery i ionosfery; yarkost' sumerechnogo neba v vertikale Solntsa s uchetom vtorichnogo rasseyaniya). Trudy Sekt. Astrobotan., Vol.VII, Alma-Ata, Izd. Akad. Nauk KazSSR, 1959.

A.K.Suslov

1. C.Flammarion's Contribution to Propagating Natural-Science Knowledge

It has presently become necessary to study in detail the role of the French scientist C.Flammarion in the matter of spreading knowledge about astronomy in general and the problem of life in the universe in particular, and to give it an objective evaluation. This is necessitated, first, by the rapid development of astrobotany which raises the question of vegetation on Mars as an integrable part of the general question of astrobiology, to which C.Flammarion devoted a considerable portion of his life. Many problems that he raised were solved scientifically by Soviet scientists who continued and developed certain aspects of his theory of life in the universe. Second, numerous scientists had a tendency, on one hand, to distort the theory of C.Flammarion concerning life on other worlds by quoting at random from his individual works and, on the other hand, to draw a parallel between the thus falsified theory and certain basic premises of the science of life on other celestial bodies – astrobiology (Bibl.1, 2, 3). Therefore, it is necessary to shed light on this problem and to show what we have accepted from Flammarion's theories and what we are rejecting, to prevent the later possible vulgarization of the teachings of Flammarion and to free his hypotheses from idealistic and metaphysical aspects by defining what is most basic and scientific in order not to lapse into eclecticism. Third, the publication of many science-fiction books on astronomy, which are quite diverse and often poorly edited, together with the lack of any good popular book encompassing as much of astronomy as possible, necessitated the translation of the recently published new edition "Astronomie Populaire" by C.Flammarion (Bibl.18).

Below, I will briefly describe the ceremony of placing a memorial plaque on Flammarion's home (Bibl.4).

October 27, 1955 marked the ceremony of unveiling the memorial plaque placed on the wall of the house No.16 on Rue Cassini, in the XIV District opposite the Paris Observatory, on the corner of Observatory Lane, the house in which C.Flammarion lived for more than 50 years (at first the entire year, then beginning in 1833, at those periods when he was not at his Observatory at Juvisy). Here, he wrote his "Astronomie Populaire" which was published somewhat earlier than the Review "Astronomy" (1882), immediately before the founding of the French   /251 Astronomical Society. In his address at this ceremony, the vice chairman of the Paris Municipality mentioned that among those gathered were many students of C.Flammarion, members of the Council of the French Astronomical Society. They were all well-known astronomers and famous scientists. The speaker further said, "For sixteen years C.Flammarion directed the Academy of Youth – an aid society and a seminar center. His scientific and social cognition has been outlined before; kindness, for him, was a natural second aspect of science and thinking. For C.Flammarion, just as for an Athenian philosopher, it holds true that a man of science cannot help but spread modesty at the same time, which constitutes an expression of knowledge in a world of morals" (underlining is the author's).

Flammarion's book "Astronomie Populaire" was translated into many languages and was distributed throughout the world. Imbued with the cosmic beauty which the sight of infinity opened before him, he wanted to make accessible to many what had been the privilege of a few. He always believed in progress and in the future.

Professor A.Danjon in his speech pointed out the success of the first publications of C.Flammarion "The Multiplicity of Inhabitable Worlds" and "The Wonders of the Sky". These works were translated into all languages. Under the patronage of C.Flammarion, scientific societies were founded even in countries where there were few followers of astronomy. A.Danjon cited Emil Borel who stated that C.Flammarion did more than many generations of teachers to propagate science and to determine vocations (underlining is the author's) and also Poincaré who rendered just due to the scientist who was at the same time a poet, and a poet who was at the same time a scientist (underlining is the author's).

A.Danjon concluded his speech, "Flammarion was constitutionally unable to distort science, to weaken it in order to make it more easily absorbed, to proclaim knowledge without making it vulgar — such was the slogan of his entire life. For three quarters of a century there has not been a single astronomer whose vocation has not been aroused by the call of C.Flammarion."

In his address, the mayor of the XIV District said: "Children now are avidly reading science fiction, but C.Flammarion has revealed to the children of my generation that reality by far exceeds any product of human imagination. This is why I am convinced that the new edition of his remarkable work 'Astronomie Populaire' will attract our young people to these lofty truths."

This description of the commemoration for C.Flammarion (Bibl.4) reveals the respect of the French community for the scientist, for his enormous contribution to popularizing astronomy by democratizing this science and bringing it to the masses, by converting it from a cabinet-type "aristocratic" science to a popular science. This original intention of C.Flammarion was realized only in the USSR and in countries of the Peoples' Democracy where a network of peoples' Observatories is being constructed. C.Flammarion's creation of the French Astronomical Society and his book "Astronomie Populaire" are of importance not only for the French people but also for young students the world over, who are founding astronomical societies in all countries, and for the unification of astronomers into the International Astronomical Union. Many of us have become, or are becoming, astronomers under the impact of the stimulating book "Astro- /252 nomie Populaire". To write such a book it is not enough to be a specialist in the field and a teacher. At the same time, one must be a poet. The traditions of C.Flammarion were to a certain extent continued by the Russian poet V.Ya. Bryusov, but his poems did not become as widespread as the works of C.Flammarion. Furthermore, V.Ya.Bryusov, despite his encyclopedic knowledge, was not a professional astronomer, and he did not set out to propagate astronomical knowledge. The writers and astronomers of the USSR have every opportunity for creating Soviet works that will not be inferior, in their stimulating effect on the reader, to Flammarion's books. The foundation for this has already been laid by members of the Astrobotany Sector, concerning life on other planets, and by the great achievements of Soviet scientists and engineers who have created the first artificial earth satellites.

2. Flammarion's Hypotheses on Life on Other Planets and Critical Evaluation

Some scientists, carried away by the criticism of the negative aspects of C.Flammarion's theory negate his entire writings and especially his concept on life throughout the universe (Bibl.1): "These thinkers attack this question from a materialistic position. However, the idea of inhabitability of other planets has been shared also by outspoken idealists. This concept has become especially popular as a result of the activity of the idealist and spiritualist C.Flammarion." At the II Congress of the All-Union Astronomical and Geodetic Society in Leningrad, this statement by V.G.Fesenkov met with objections by a number of scientists. It is impossible to agree that Flammarion is only a mystic and spiritualist for us; he remains this only to very few individuals. For the overwhelming majority he is an outstanding propagandist of astronomical knowledge, and many do not even know of his metaphysical ideas. One cannot reject the basic progressive opinions of the scientist because of the fact that he also might have had some other incorrect opinions. We do not reject Newton's laws merely because of the fact that, at the end of his life, he wrote an interpretation of the Apocalypse. The diverse opinions on Flammarion, written during various years, reduce to that C.Flammarion was widely known as the author of popular science books on astronomy and science-fiction novels. He also investigated Mars, the moon, and double stars. He wrote a number of papers on meteorology and physics (Bibl.16, 17, 19). In addition to popular science books, Flammarion wrote many books of a philosophical nature, in which he professed himself an enemy of materialism and an advocate of mysticism and spiritualism (Bibl.17). V.G.Fesenkov (Bibl.1) writes, "With such an ideological objective it is natural to assume, despite common sense, that there are intelligent beings on each planet, on each cosmic body of any significance. Let us take, for example, our moon ..." Let us also quote the remarks by Flammarion himself (loc. cit): "In any case there is a high probability that lunar life began earlier than life on earth and is actually in decline. The activity there is no longer as it had been at some previous time. This world is apparently in a state of silence and tranquility, an example as no other world can give it. This is an indisputable phenomenon! However, this silence, which abounds in the lunar world and is /253 so mysteriously manifest when observing, through the telescope, the still landscape illuminated by the night, evidences the relative tranquility of this celestial body which once was so restless, but by no means evidences its death. Probably, lunar life is on the decline but it presumably has not yet vanished altogether; perhaps the last remnants of lunar mankind still exist there on the floor and velvety plain of Plato, in the undulating valley of Huygens, or on the shores of the Mare Serenitatis, contemplating the earth and asking themselves how a planet so stormy as ours and blanketed with clouds can be inhabited by delicate and intelligent beings."

Obviously, Flammarion did not base his theories on an ideological objective postulating the obligatoriness of life on the moon, but on the inadequate observational data of that time, which certainly could not prove the presence of living beings on the moon. The absence of an atmosphere on the moon was proved only recently. The theory of the origin and evolution of the moon is still in the process of development. Consequently, during the time of Flammarion there was absolutely nothing known about conditions on the moon in the remote past, but it was also impossible to reject summarily an earlier biogenesis there.

Nevertheless, Flammarion is cautious in describing lunar life and, if he admits it at all, then only as close to extinction owing to the continued deterioration of physical conditions. On page 519 of his book, Flammarion writes that we will not necessarily become extinct, since we cannot possibly define the limits of the power of nature. This optimistic concept is supplemented by the theorem of the unlimited power of man over nature, of man's reasoning and technical know-how which make use of the most diverse laws of nature.

Flammarion asserts that life is at the upper limit of development of nature. "Whether we inhabit Jupiter now or this evening or tomorrow is of little importance to the all-encompassing philosophy of Nature! Life is the end purpose of its formation (Bibl.3), just as life was the end purpose of the formation of the earth. This is the main thing. A moment, an hour means nothing" (Bibl.5). In the area of inorganic nature the "end purpose" is the upper limit of motion, the apex of this motion. On the other hand, Marxism teaches that "in nature nowhere is there a realized, desired purpose ..." (Bibl.6). "Purposes are generated by an objective world and are deemed to be accessible" (Bibl.7). Since nature exists eternally, as Flammarion himself notes, then it is completely unimportant whether life arises on a given celestial body earlier or later; what is important is that it does originate at some point during the evolution of the celestial body. At present it is known that a number of celestial bodies are developing without passing through the stage of being populated by living creatures, but in Flammarion's time even his own concept of life was not distinctly formulated, and F.Engels' formulation was not known at all to many bourgeois scientists. Flammarion's position that life develops, without end in space and in time, is confirmed here on our planet. The distribution of microorganisms is extremely widespread and there seems no reason why life on earth should end in the foreseeable future. The realization of space flights means that, within the rocket, bacteria could survive which, landing on other planets, could adapt to its conditions. F.Engels also asserted that life originates first at one point of /254 the universe and then at another. Thus, there is neither mysticism nor metaphysics in C.Flammarion's attitude toward the question of life on other planets. However, Flammarion greatly exaggerated the adaptive capability of living organisms to hostile environmental conditions. The main point in his teachings was the stipulation of development in time and space and the postulate of the infinity of the universe in time and space, which inflicted the greatest blow on idealism and metaphysics. The critics of Flammarion, who were unfamiliar with his dialectic approach to natural phenomena, did not know how to separate his eclectic philosophy from scientific concepts and thus themselves lapsed into electicism.

3. Evaluation of C.Flammarion by Russian and Soviet Scientists

Besides the statements made above (Bibl.1), nowhere in the literature did I find such negative opinions of Flammarion. Many pointed out that he was at the same time a classical writer, a fine poet, a philosopher-thinker, a meteorologist, and a daring balloonist. E.Puyshe spoke about Flammarion: "He compelled us to acknowledge and love astronomy, one of the most beautiful sciences ..." (Bibl.8). S.P.Glazenap asserted that "The first works of C.Flammarion appeared in print when most astronomers considered it beneath their dignity to popularize this science" (Bibl.9). "C.Flammarion belonged to the same type of

scientists as J.Herschel, Fr.Arago, Cl.Bernard who all considered it their duty to serve the masses, reporting to them about their discoveries and about the discoveries of others in a form accessible to all. Flammarion should be a text-book for any popularizer of astronomy, despite his foreign, and sometimes hostile ideology", wrote S.V.Shcherbakov (Bibl.10). The ideological errors of Flammarion in his popular books are so naive and in such contrast with the basic scientific background, that they are received by the Soviet reader as pure fancy and not in need of any special exposure. For example, in one place he populates Mars with the souls of people who died on earth (Bibl.11). A.V.Vinogradov wrote: "His world outlook is, so to speak, patched together from many individual, diverse, purely randomly selected scraps of contradictory idealistic and naively materialistic views taken from all possible systems, beginning with antiquity" (Bibl.12). But in no way should we forget that Flammarion was a great artist and stylist, a wonderful popularizer who always knew how to give an account of difficult, abstract, and, at first glance, dry questions in a simple and fascinating manner. Although Flammarion was not an atheist himself, he objectively played a major role in propagandizing scientific atheism by popularizing the achievements of contemporary science, the more so as he attracted his readers away from religion while not frightening them away by naked materialism. Flammarion knew how to spread his knowledge where superstition and prejudice reigned (Bibl.13). "... Living astronomy, a study of the conditions of life in the universe, is the most attractive aspect of astronomy", wrote Flammarion in his autobiography. Since childhood he had studied butterflies and, beginning in 1881, he investigated leaf and blossom formation of the chestnut tree and studied the effect of constant temperature on oaks, finding that, under such conditions, the tree retained its foliage the entire year. Flammarion literally worshipped astronomy as the science of the living universe.

Thus, all scientists agree in a positive evaluation with respect to /255 the activity of C.Flammarion as a popularizer of science, while at the same time unanimously rejecting his false ideology. Not only Soviet scientists support such an opinion, but also the Russian scientists of the end of the last century.

4. Multiplicity of Inhabitable Worlds

To judge Flammarion's book "The Multiplicity of Inhabitable Worlds", we must examine the historical background of its publication. Only then will we be able to say whether this book played a negative or positive role. Before its publication in France and other countries, there were many books devoted to life in the universe. These books frequently were not written by expert astronomers but simply by lovers of sensation and easy profit who used the ignorance and gullibility of the reader. The matter went so far that certain writers asserted that they had seen flying people and other living creatures on the moon and other planets. Others wrote that such things had been seen by some of the outstanding astronomers of that time, for example, by Herschel who had the most powerful reflectors. Herschel then had great difficulty proving that he had not seen any creatures and had not made any statements to the journalists to this effect. The most unthinkable and fantastic fabrications were published by their authors as "popular science" where the so-called latest word in science was cited, which was frequently taken as truth by the credulous public. This was the background against which Flammarion's book appeared, written in beautiful language contain-

ing all the latest information on planets and on the possibility of life on them. The author preached the power of nature in its endless forward stride, in its development in time and space up to the very highest form – that of living creatures on planets. However, also dialectical materialism teaches that nature endlessly develops in space and time, that it is infinitely diverse in its forms, and that its power is inherent in this. That portion of matter which assumed an intellectual form and manifests itself in human thought and technology gradually becomes predominant over other elemental forces of nature, detecting its laws, utilizing them, and thus subduing them. In the cosmos, there is nothing supernatural, nothing that could stand above social and natural laws. "If we imagine worlds that could be inhabited, we immediately conclude that, since they are capable of supporting life, they must necessarily be inhabited. If we imagine worlds that could not be inhabited, we will just as promptly attempt to disprove support of life and thus come to think that such worlds are actually uninhabitable", wrote Flammarion (Bibl.15, p.85). Before one can argue against life on a given planet, one must prove first that its physical environment does not meet the requirements that constitute the biological laws for the genesis and development of organisms. The opponents of astrobiology proceed in the opposite direction. They doubt the inhabitability of worlds capable of supporting life and speak for or against inhabitability only when the absence of life is antagonistic to the laws controlling the universe and life. Certain authors (Bibl.14) believe that direct proof of dead matter is more important than observations of living matter or appearance of life from great distances. Both statements of the problem ultimately lead to the truth. The difference is /256 that the method of astrobiology, despite its errors and individual delusions, will more rapidly lead to the truth, whereas the opposite method of proof is tedious and circuitous and shelves solution of the problem until interplanetary or even interstellar and intergalactic travel will be possible. Even then, this will not yield a general solution of the problem of life in the universe, since the uninvestigated portion of space will always be immeasurably greater than the investigated segment, leaving sufficient room for skepticism. During Flammarion's time, the philosophical belief in the existence of a multitude of populated worlds was not supported by astronomical observations of Mars and other planets. Hence, it is obvious that the crux of the matter does not lie in the ideological aspects but in physical conditions, for example, in the presence of air on the moon, which was the prerequisite for Flammarion's conjecture on the possibility of life (Bibl.15, p.21). At a given stage of evolution, the highest form of matter are intelligent beings; before this, matter must proceed to develop everywhere where physical conditions permit. Laplace asserted that by analogy, on other planets as on earth, solar radiation will cause the development of animals and plants. Today we know that a simple analogy is insufficient. It is necessary to take into account the totality of all physical conditions generating life on planets, in order to judge the properties of living creatures. At the time of Flammarion, the essential features of the moon were already known, which postponed the answer to the question on inhabitability (Bibl.15, p.59). The care with which Flammarion spoke about inhabitability, completely rejecting life on the sun and stars, is characteristic. Speaking about the insignificance of the instant of time for the origin of worlds and life on them (Bibl.15, p.90), Flammarion refuted the theory of the creation of the world and its end. He fought against geocentrism, asserting that the earth has no advantage over any other planet (Bibl.15, p.93). He attributed great significance to the role of external environment and physical conditions necessary for the origin of life

293

(Bibl.15, p.100). Flammarion closely approached the dialectic laws of the universal interrelation and causality of events, the unity and struggle of opposites (Bibl.15, p.114). The term "goal" to him meant something higher to which the development of matter from a lower state unconsciously strives. Not knowing the true physical conditions of the atmosphere of Jupiter, Flammarion did not insist on its inhabitability, leaving this to depend directly on natural conditions, meaning that, as in the case of the moon, the physical conditions rather than a preconceived notion would be primary (Bibl.15, p.132). A comparison of the statements by C.Flammarion (Bibl.15, p.140) with those by V.G.Fesenkov (Bibl.1) shows that both authors agree that life is not an exceptional phenomenon in the universe and that living matter is just as natural a form of matter as any other.

The social views of Flammarion are characterized by the fact that he was well aware of the injustice of the bourgeois structure (Bibl.15, p.135). He believed that, on any planet, mankind in time will reach such a perfect state that freedom of action will only lead to good (Bibl.15, p.215), i.e., will lead to Communism.

We have shown here that Flammarion clearly understood the law of dialectics (Bibl.15, pp.147, 194). He considered the philosophical theory of the multiplicity of inhabitable worlds as a truly scientific problem and did not associate it with any religious teaching (Bibl.15, p.257). The most important shortcoming in the teachings of Flammarion was his contribution of teleology. Flammarion was led astray by the circumstance that, during development of matter from lower to higher, matter which is conscious of itself is the highest form of matter at the given stage of its development. The main virtue of his /257 teachings is the recognition of the eternity and infinity of matter. He considers nature primary, life as dependent on the natural environmental conditions, and the problem of its presence on planets as solved on the basis of practical experience.

BIBLIOGRAPHY

1. Fesenkov, V.G.: Physical Conditions and Possibility of Life on Mars (O fizicheskikh usloviyakh i vozmozhnosti zhizni na Marse). Vopr. filosofii, No.3, 1954.
2. Fesenkov, V.G.: Materialism and Idealism in Astronomy (Materializm i idealizm v astronomii). Vestn. Akad. Nauk KazSSR, No.6, 1955.
3. Suslov, A.K.: On the Philosophical Substantiation of the Problem of Extraterrestrial Life (O filosofskom obosnovanii problemy zhizni vne Zemli). Trudy Sekt. Astrobotan., Vol.V, Alma-Ata, Izd. Akad. Nauk KazSSR, 1957.
4. - Astronomiya, Vol.XI, 1955.
5. Flammarion, C.: Heavenly Worlds (Les terres du ciel). p.621, 1884.
6. Marx, K., and Engels, F.: Sochineniya, Vol.XIV.
7. Lenin, V.I.: Philosophical Notes (Filosofskiye tetradi). Moscow, 1934.
8. Puyshe, E.: Camille Flammarion (Kamill Flammarion). Meteorol. Vestn., No.8, 1925.
9. Glazenap, S.P.: Camille Flammarion (Kamill Flammarion). Izv. Russk. Astron. Obshches., No.1, Issue XXVI, 1926.

10. Shcherbakov, S.V.: Camille Flammarion in the Estimation of Russian Amateur Astronomers and Scientists of the 1890's (Kamill Flammarion v otsenke russkikh astronomov-lyubiteley i uchenykh 90-godov XIX v). Russk. Astron. Kalendar', No.XXXVI, 1933.

11. Klements, D.: On the Problem of Extraterrestrial Life (K voprosu o vozmozhnosti zhizni vne nashey planety). Nauch. Oboz., No.26, 1896.

12. Vinogradov, A.V.: The Creativity of C.Flammarion from the Point of View of the Soviet Reader (Tvorchestvo K.Flammariona s tochki zreniya sovetskogo chitatelya). Mirovedeniye, Vol.XXIV, 1935.

13. Goryainov, G.: Memories of the Teacher Camille Flammarion (Pamyati uchitelya Kamilla Flammariona). Russk. Astron. Kalendar', Vol.XXIX, 1925.

14. Oparin, A.I. and Fesenkov, V.G.: Life in the Universe (Zhizn' vo Vselennoy). Moscow, Izd. Akad. Nauk SSSR, 1956.

15. Flammarion, C.: Multiplicity of Inhabitable Worlds (Mnogochislennost' obitayemykh mirov).

16. — Entsiklop. Slovar', Vol.3, Moscow, 1955.

17. — Bol'shaya Sovets. Entsiklop., Vol.7, Moscow, 1936.

18. — Astronomie Populaire Camille Flammarion, 1955.

19. — Bol'shaya Sovets. Entsiklop., Vol.45, Moscow, 1956.

PROBLEMS OF ASTROBIOLOGY AT THE INTERNATIONAL SYMPOSIUM ON THE PROBLEM OF THE ORIGIN OF LIFE ON EARTH

N.I.Suvorov

In recent years, there has been a lively discussion concerning the possibility and distribution of life in the universe. The problems under discussion have been treated in special and popular science literature, both Soviet (Bibl.8, 10, 11) and foreign (Bibl.17, 18). The problem of the inhabitability of the planet Mars has attracted particular attention, since considerable factual material has been accumulated concerning the presence of plant life on this celestial body. Various opinions have been expressed concerning the origin and evolutionary level of life on other planets. Two basic astrobiological trends have been determined in biology and planetary astronomy.

In the astrobiological school of G.A.Tikhov, generalization of the facts and ideas about cosmic life is based on the principles of Michurin's biology. In the evolution of stellar systems, there has been a period of relatively stable energy conditions during which chemical motion is able to reach its highest level, namely, the formation of proteins. If the surface of a planet is endowed with conditions permitting the development of proteins in a colloidal state, then, at a certain level of chemical motion, there inevitably will be a dialectic transitional jump of this motion to a higher biological stage. The simplest forms of life can arise from the most complex inert substances, namely, proteins. Apparently, at first a living substance was formed which was similar to a protoplasmic mass, from which individuals (coacervates) became isolated. The simplest living creatures became widespread in various environmental habitats and developed different types of metabolism. Life, at an early stage, took on a species form of existence. Numerous species populated the entire surface of the planet, forming the biosphere (lithosphere, hydrosphere, and atmosphere).

From the most general point of view, life in the universe is a completely regular and widespread phenomenon. During the evolution of life, at a particular level of development, biological movement changes to social. Intelligent social creatures, capable of working, appear which become self-cognizant and aware of the surrounding world and able to transform nature and society. Thus, the propagation of rational life in the universe is admitted (Bibl.6).

Such concepts are being developed by astronomers of the USA and biologists of China and are finding support by scientists of other countries where astrobiological investigations are in progress (Bibl.3). For example, American astronomers (Harlow, Shapley, and others) reckon in the Milky Way system, i.e., in our Galaxy, about 10 billion stellar systems in which life is assumed on the planets.

The astrophysical school of V.G.Fesenkov is developing opposite opinions. Theoretically, on the basis of the philosophical premises of dialectical materialism, the existence of sufficiently diverse life is assumed in an infinite universe. However, in specific regions of the universe, for example in a given

galaxy, life is considered to be a very rare phenomenon. Here, V.G.Fesenkov and A.I.Oparin (Bibl.12) cautiously suggest, on the basis of their mathematical calculations, that "only in one case in a million will we find a planetary system on which there can be organic life in any form" (Bibl.13, p.13). Many tens of millions of stellar systems are considered to be unsuitable for the origin of life, based on a number of features, mainly the instability of energy conditions.

Certain astronomers, dragging into modern science the old figment of geocentrism, arbitrarily interpret the concept of progressive evolution of matter, which is especially important in the philosophy of dialectical materialism. The highest forms of existence of matter – chemical, biological, and social movements – can only occur on planets. It would seem entirely logical to consider the planetary period of cosmic evolution to be more progressive than the initial period of stellar evolution, when intra-atomic processes of the development of elementary material forms prevailed. However, the Soviet astronomer Yu.G.Perel' asserts that the theory of the progressive character of planetary development of the stellar system is a "doubtful attempt of applying the laws of the development of society to the development of nature" (Bibl.5, p.800). Denying the applicability of the concept of progressive development to studies on the cosmic phenomena of nature, Yu.G.Perel' rejects (without proof) one of the most important premises of Marxist dialectics on the universality of the progressive development of matter on the basis of the struggle of internal contradictions. Yu.G.Perel', in this case, arbitrarily interprets the well-known postulate by F.Engels concerning the eternal cycle of matter, "in which the time of the highest development, the time of organic life and, even more so, the time of the life of creatures who are cognizant of themselves and of nature is just as scantily measured as is the space within which life and self-consciousness exist" (Bibl.66, p.20). This statement by F.Engels, in the opinion of Yu.G.Perel', so to speak confirms the hypothesis defended by the school of V.G. Fesenkov, that the origination of the combination of environmental conditions necessary for the origin of life "is not a frequent event in nature" (Bibl.5, p.798). Actually, in the introduction to "Dialectics of Nature" F.Engels asserts the idea of the regular occurrence and ineradicableness of life in the universe: "We have the certainty that matter, in all its transformations, remains eternally one and the same, that not one of its attributes can ever be lost and that therefore with the same inescapable necessity with which it will some time annihilate its terminal flower – the thinking mind – on earth, it will have to generate it again somewhere in some other place at some other time" (Bibl.16, p.21). Thus, the attempts of the astronomers of V.G.Fesenkov's school to prove the exclusiveness of life on earth and its extreme rarity in the universe in no way agrees with the philosophy of dialectical materialism, although they assert in every way possible that this problem is independent of philosophy.

Astrobiologists consider a number of the planets of our solar system inhabitable, mainly Mars and Venus. In connection with this, a spirited dis- cussion arose between scientists of different opinions on the question of plant life on Mars. The conditions for the creation of life on Mars, according to the paleobotanical hypothesis of G.A.Tikhov (Bibl.7, 9), were favorable in the remote past. As the environment for life on this planet deteriorated (cooling, drying, thinning of the atmosphere) progressive biological evolution was stepped up. Highly developed organisms are best adapted and best adapt to requirements

of the ambient medium. At present, the green-blue part of the Martian surface is covered by biologically highly developed plants. The assumption, made by certain astronomers, that Mars is populated only by lower organisms does not stand up to scientific criticism. Life could not have originated on Mars at a late period of evolution of its surface, when conditions were too harsh, specifically when considering that the conditions for biogenesis were much more favorable in the past. To believe that life on Mars developed in the remote past and then became more simple, would mean to agree with the theory of retrograde evolution which is not recognized in materialistic biology.

Therefore, to substantiate his position of negating the habitability of Mars, V.G.Fesenkov hypothesized that the surface of this planet was without water from the very beginning. Such a hypothesis is founded on very hypothetical cosmogonic considerations. It is assumed that, because of its relatively small mass, Mars lost its light gases, including hydrogen, at an early stage. Hence, "it would follow that, if at present there is extremely little water on Mars, there is no reason to assume that conditions were much different in the past epochs of existence of this planet" (Bibl.13, p.7).

This cosmogonic hypothesis connects with the problem of the origin of life on earth. It is entirely logical that certain astrobiological problems were raised at the International Symposium on the Problem of the Origin of Life on Earth, held in Moscow on August 1957.

The paper by V.G.Fesenkov on the original state of the earth postulated the theory of a separation of juvenile water from the bowels of the earth as the planet hardened. A primeval ocean, enriched with dissolved migrating chemical elements was created. "Without the presence of such a medium, organic life could not arise ... . On a planet such as Mars, where there never were any open water bodies, a medium necessary for the generation of organic matter could not be created" (Bibl.14, p.14).

Such an assertion, typical for the astrophysical school of V.G.Fesenkov, came under justified criticism, mainly from biologists. The Soviet biologist R.P.Berg in his report "Certain Conditions for the Development of Life on Earth", stated that life could arise not only in the ocean but also on continents (Bibl.4, p.48). It should be mentioned that most biologists consider the continental and coastal shallows to be the most favorable medium for the formation of colloidal proteins and the development of metabolism. At the Symposium, this point of view was supported by J.Bernal (England). Calling the process of the formation of life "biopoiesis", he and other scientists attribute great significance to the adsorption of molecules in the "probiotic broth" on mineral particles, most frequently clays, which is considered to be the second stage of biopoiesis. The optimum conditions for the occurrence of this process "probably existed only in nitrogenous soils, in submerged mud flats, on dry land, or /261 in alternately dry and moist land as, for example, in tidal estuaries" (Bibl.1, p.32). Conventional biologists, for example, V.R.Vil'yams (Bibl.2), have long ago stipulated the theory of the origin of life in moist loose layers on the surface of continents or in shallow basins (Bibl.15).

Consequently, from the biological viewpoint, the presence of oceanic masses of water on a given planet is not a prerequisite for life to arise. In Michurin's

298

biology, the basic law of life is the continuous interrelation of living
creatures with environmental conditions, accomplished in the metabolic process.
Under similar environmental conditions, the variability of organisms is relative-
ly weakly manifested and the evolutionary process is retarded. If there is an
exceptional amount of water on a planet (and we can imagine planets whose surface
is covered by one giant ocean over a long period of geological time), aquatic
life will not proceed far along the path of evolutionary development. On land,
the environmental conditions are more diverse and distinct, changing more quick-
ly; therefore, land life will always be on a higher evolutional stage than
aquatic life. The aquatic "reasoning" salamander of Karel Czapek is incompre-
hensible to the biologist. In the geological cycle of matter, land organisms
create, on the continental surface, soils and diverse substances, primarily
nitrogenous, which over the water cycle enter the World Ocean. Aquatic life is
unthinkable, isolated from life on land. The traditional theory of the emerg-
ence of animals and plants at the beginning of the Paleozoic onto land which,
before this, had been desert is quite untenable. The cradle of life is water,
but not necessarily oceanic. Evidently, the evolutional development of life
both on land and in water has been going on since the remote past, and both
main pathways of the evolution of species on earth were interrelated.

Thus, modern concepts on the origin of life on earth are intimately con-
nected with the actual biological theory and are far from the astrophysical
hypotheses of exceptional rarity of life in the universe.

BIBLIOGRAPHY

1. Bernal, Dzh.: Problem of Stages in Biopoiesis. In the Book: Origin of
   Life on Earth. Collection of Papers Presented at the International Sym-
   posium, 1957 (Problema stadiy v biopoeze. V kn.: Vozniknoveniye zhizni na
   Zemle. Sb. dokladov na Mezhdunarodnom soveshchanii 1957 g.). Moscow,
   Izd. Akad. Nauk SSSR, pp.24-39.
2. Vil'yams, V.R.: Collection of Works on Soil Science (Sobr. soch. Pochvo-
   vedeniye). Vol.6: Agriculture and the Principles of Soil Science (1927 –
   1938) [T.6: Zemledeliye s osnovami pochvovedeniya (1927-1938)]. Moscow,
   Sel'khozgiz, 1951.
3. – Foreign Comments on Astrobiology (Zarubezhnyye otkliki na astrobiologiyu).
   Trudy Sekt. Astrobotan., Vol.V, Alma-Ata, Izd. Akad. Nauk KazSSR, 1957.
4. Kriviskiy, A.S.: Problem of the Origin of Life on Earth (Problema proiskhozh-
   ·deniya zhizni na Zemle). International Symposium in Moscow (Mezhdunarodnyy
   simpozium v Moskve). Priroda, No.1, 1958.
5. Perel', Yu.G.: On the "Philosophical Substantiation" of a Single Problem
   (Po povodu "filosofskogo obosnovaniya" odnogo voprosa). Astron. Zh.,
   Vol.XXXV, No.5, 1958.
6. Suvorov, N.I.: Problem of Organic Evolution in Contemporary Studies of
   Planets (Problema organicheskoy evolyutsii v sovremennom planetovedenii).
   Trudy Sekt. Astrobotan., Vol.V, Alma-Ata, Izd. Akad. Nauk KazSSR, 1957.
7. Suvorov, N.I. and Parshina, Z.S.: Hypothesis on the Paleobotany of Mars
   (K gipoteze o paleobotanike Marsa). Vestn. Akad. Nauk KazSSR, No.4, 1954.
8. Suvorov, N.I.: Conference on the Problem of Predicting Conditions of Life
   on other Planets (Soveshchaniye po probleme prognozirovaniya usloviy zhizni

na drugikh planetakh). Vestn. Akad. Nauk KazSSR, No.2, 1957.

9. Tikhov, G.A.: Hypothesis on the Paleobotany of Mars and Venus (Gipoteza o paleobotanike Marsa i Venery). Vestn. Akad. Nauk KazSSR, No.1, 1953.

10. - Discussion of the Topic: Basic Achievements of the Astrobotany Sector and the Problem of the Possibility of Life on other Planets (September 25-27, 1952) [Diskussiya na temu: Osnovnyye dostizheniya Sektora astrobotaniki i vopros o vozmozhnosti zhizni na drugikh planetakh (25-27 sentyabrya 1952 g.)]. Trudy Sekt. Astrobotan., Vol.2, Alma-Ata, Izd. Akad. Nauk KazSSR, 1953.

11. - Material of the Conference on the Problem of the Possibility of Life on other Planets, Conducted by the Astrobotany Sector and the Leningrad Department of the All-Union Astronomo-Geodetic Society (LOVAGO) on February 23-25, 1953 [Materialy soveshchaniya po voprosu o vozmozhnosti zhizni na drugikh planetakh, provedennogo Sektorom astrobotaniki i Leningradskim otdeleniyem Vsesoyuznogo astronomo-geodezicheskogo obshchestva (LOVAGO) 23-25 fevralya 1953 g.]. Trudy Sekt. Astrobotan., Vol.4, Alma-Ata, Izd. Akad. Nauk KazSSR, 1955.

12. Oparin, A.I. and Fesenkov, V.G.: Life in the Universe (Zhizn' vo Vselennoy). Moscow, Izd. Akad. Nauk SSSR, 1956. /262

13. Fesenkov, V.G.: Origin of the Solar System and the Problem of Life in the Universe (Proiskhozhdeniye solnechnoy sistemy i problema zhizni vo Vselennoy). Vestn. Akad. Nauk KazSSR, No.2, 1956.

14. Fesenkov, V.G.: The Primary State of our Planet. In the Book: Origin of Life on Earth (Pervichnoye sostoyaniye nashey planety. V. kn.: Vozniknoveniye zhizni na Zemle). Collection of Papers Presented at the International Symposium, 1957 (Sb. dokladov na Mezhdunarodnom soveshchanii 1957 g.). Moscow, Izd. Akad. Nauk SSSR.

15. Kholodnyy, N.G.: Amidst Nature and in the Laboratory (Sredi prirody i v laboratorii). Moscow, Izd. Mosk. o-va ispytateley prirody, 1949.

16. Engels, F.: Dialectics of Nature (Dialektika prirody). Moscow, OGIZ-Gospolitizdat, 1941.

17. von Schmidt, Karl-Heinz: Life on Planets (Zum Leben auf den Planeten). Urania, No.1, pp.10-12, January 1957.

18. - Cosmos, Earth, and Man (Weltall, Erde, Mensch). Verlag Neues Leben, pp.105-107, 1957.

"The aeronautical and space activities of the United States shall be conducted so as to contribute . . . to the expansion of human knowledge of phenomena in the atmosphere and space. The Administration shall provide for the widest practicable and appropriate dissemination of information concerning its activities and the results thereof."

—NATIONAL AERONAUTICS AND SPACE ACT OF 1958

NASA SCIENTIFIC AND TECHNICAL PUBLICATIONS

TECHNICAL REPORTS: Scientific and technical information considered important, complete, and a lasting contribution to existing knowledge.

TECHNICAL NOTES: Information less broad in scope but nevertheless of importance as a contribution to existing knowledge.

TECHNICAL MEMORANDUMS: Information receiving limited distribution because of preliminary data, security classification, or other reasons.

CONTRACTOR REPORTS: Technical information generated in connection with a NASA contract or grant and released under NASA auspices.

TECHNICAL TRANSLATIONS: Information published in a foreign language considered to merit NASA distribution in English.

SPECIAL PUBLICATIONS: Information derived from or of value to NASA activities. Publications include conference proceedings, monographs, data compilations, handbooks, sourcebooks, and special bibliographies.

TECHNOLOGY UTILIZATION PUBLICATIONS: Information on technology used by NASA that may be of particular interest in commercial and other nonaerospace applications. Publications include Tech Briefs; Technology Utilization Reports and Notes; and Technology Surveys.

Details on the availability of these publications may be obtained from:

SCIENTIFIC AND TECHNICAL INFORMATION DIVISION

NATIONAL AERONAUTICS AND SPACE ADMINISTRATION

Washington, D.C. 20546